UNIVERSITAT DE BARCELONA

Elucidating variable disease severity of X-linked adrenoleukodystrophy through multiomics and metagenomics of gut microbiome

Lorenzo Torreni

UNIVERSITAT DE BARCELONA

“Elucidating variable disease severity of X-linked adrenoleukodystrophy through multiomics and metagenomics of gut microbiome”

Doctoral thesis dissertation presented by:

Lorenzo Torreni

to apply for the degree of doctor at the University of Barcelona

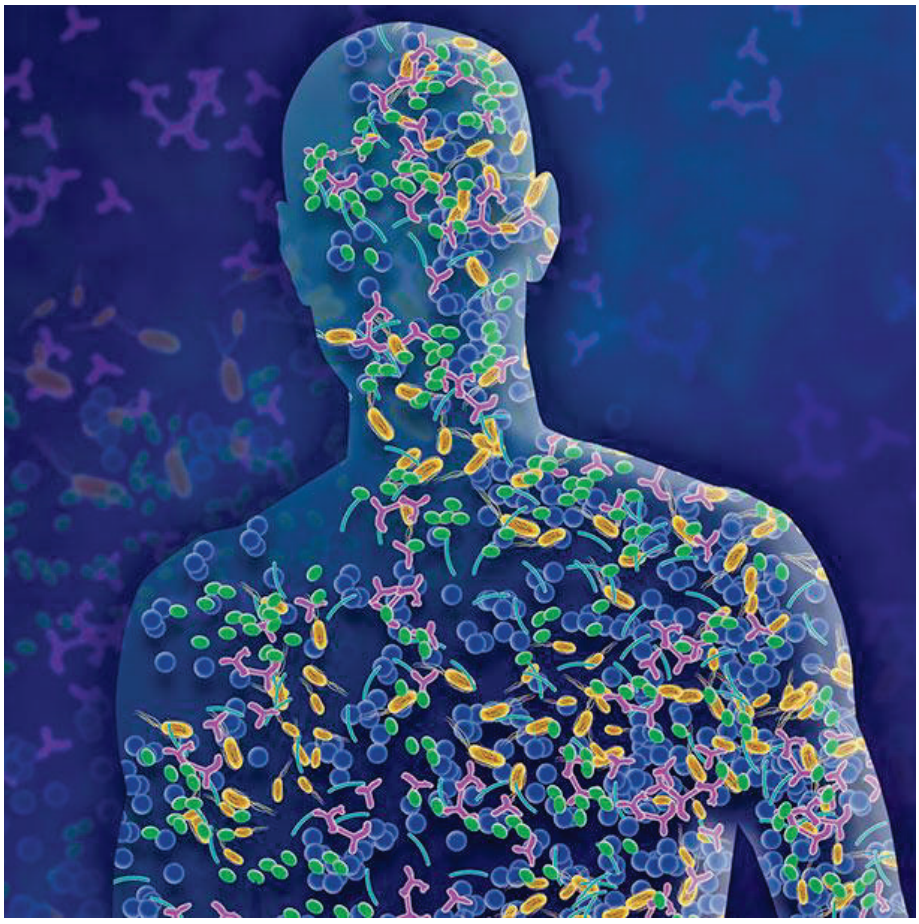

Biomedicine Doctoral Program

Biomedicine Doctoral Program

"Elucidating variable disease severity of X-linked adrenoleukodystrophy through multiomics and metagenomics of gut microbiome"

Doctoral thesis dissertation presented by:

Lorenzo Torreni

to apply for the degree of doctor at the University of Barcelona

This doctoral thesis has been conducted under the supervision of Dr. Stéphane Fourcade and Dr. Aurora Pujol Onofre at the Neurometabolic Diseases Laboratory of the Bellvitge Biomedical Research Institute (IDIBELL).

Dr. Stéphane Fourcade -Thesis Director

Dr. Aurora Pujol Onofre - Thesis Director

Dr. Carlos Casasnovas Pons -Tutor

Lorenzo Torreni – Doctoral student

Academic year 2023/2024

Alla mia famiglia…

…quella in cui sono nato,
… quella parte che ho perso,
… quella che ho trovato,
…quella che sarà.

ACKNOWLEDGMENTS

I thank Prof. Aurora Pujol for the opportunity to conduct this doctoral thesis in her laboratory.

Thanks to the thesis director Dr. Stephane Fourcade and my colleagues Montse and Agatha for the scientific and moral input received during these years, sharing with me, in addition to the room, joys and sorrows (not to mention those of statistics and R). Special thanks to Montse for the spontaneous and valuable Catalan lessons. Thanks to my tutor Carlos Casasnovas for the clinical and good humor input as well.

Thanks to all my lab colleagues (Ayelen, Cristina, Ivan, Juanjo, Laura, Mar, Tamara) for welcoming me, for their time and for their cooperation in the everyday life of the lab. I hope you don't send me the dietician's bill.

Thank you to my father, mother and grandmother for the education and deep sense of respect for work and colleagues that you have passed on to me. Sorry grandma for being away.

Thank you to Francesca, who left with me on this adventure abroad as my wonderful girlfriend, now my wonderful wife; thank you for your crucial support and continuous encouragement without which this milestone would not have been attainable. And then, joking aside, thanks also to my in-laws Mario and Maria Elena, for always taking an interest in me and helping us here in our Spanish home.

Thanks also to my fraternal friends, Andrea, Filippo, Mattia and Simone, who never let me miss their presence, even though they were far away and busy.

TABLE OF CONTENTS

ABBREVIATIONS AND ACRONYMS

ABC = ATP-binding cassette

ABCD1 = ATP-binding cassette transporter D1

AHCY = S-adenosyl-L-homocysteine hydrolase

Ala = alanine

ALDP = adrenoleukodystrophy protein

ALDRP= adrenoleukodystrophy-related protein

AMN = adrenomyeloneuropathy

Arg = arginine

Asn = asparagine

Asp = aspartate

ATP = Adenosine triphosphate

BBB = blood-brain barrier

BCAAs = Branched-Chain Amino Acids

BCATs = branched-chain amino transferases

BCKDH = branched-chain amino acid dehydrogenase

BCKDK = BCKDH kinase

CACT = mitochondrial carnitine: acylcarnitine translocase

cAMN = cerebral adrenoleukodystrophy-adrenomyeloneuropathy

CBS = Cystathionine beta synthase

ccALD = childhood cerebral adrenoleukodystrophy

ccf mtDNA = circulating cell-free mitochondrial DNA

cGAS-STING = cyclic GMP-AMP synthase (cGAS)-cyclic GMP AMP (cGAMP)-stimulator of interferon genes (STING)

CNS = central nervous system

CrAT = carnitine acetyltransferase

CrOT = carnitine octanoyltransferase

CSE = cystathionine γ-lyase

CSF = cerebrospinal fluid

Cys = cysteine

Cyst = cystine

DHCA = dihydroxycholestanoic acid

DHFR = Dihydrofolate reductase

DNA = deoxyribonucleic acid

DNMT = DNA methyltransferases

ER = endoplasmic reticulum

FAD = flavin adenine dinucleotide

FAs = fatty acids

FoxO = forkhead box protein O

GDF15 = growth differentiation factor 15

GFAP = glial fibrillary acidic protein

Gln = glycine

Glu = glutammate

GSH = glutathione

His = histidine

HSCT = hematopoietic stem cell transplantation

IEM = inborn errors of metabolism

Ile = isoleucine

IMM = inner mitochondrial membrane

iPSC = induced pluripotent stem cell

IQ = intelligence quotient

LCFA-CoA= Long-chain fatty acyl-CoA

LDs = lipid droplets

Leu = leucine

LPS = lipopolysaccharide

Lys = lysine

MAT = Methionine Adenosyltransferase

Met = methionine

MGBA = microbiota-gut-brain axis

mFAO = mitochondrial Fatty Acid Oxidation

MFGE8 = Milk Fat Globule EGF And Factor V/VIII Domain Containing

MIM = mitochondrial import complex

mtDNA = mitochondrial DNA

MRI = magnetic resonance imaging

MS = multiple sclerosis

MTHFD1 = Methylenetetrahydrofolate Dehydrogenase

MTHFR = methylene-THF-reductase

MTR = Methionine synthase

MTRR= Methionine Synthase Reductase

NAA = N-acetylaspartic acid

NAAG = N-acetylaspartylglutamate

NAD = nicotinamide adenine dinucleotide

NADP = nicotinamide adenine dinucleotide fosfato

NAWM = normal-appearing white matter

NfL = neurofilament light chain

NMDA = N-metil-D-aspartato

NPLR3 = nucleotide-binding domain, leucine-rich–containing family, pyrin domain–containing-3

NRF2/KEAP1 = Nuclear factor erythroid derived 2/kelch-like ECH-associated protein 1

OMM = outer mitochondrial membrane

OXPHOS = Oxidative Phosphorylation System

PBMCs = peripheral blood mononuclear cells

pFAO = peroxisomal Fatty Acid Oxidation

Phe = phenylalanine

PMPs = peroxisomal membrane proteins

PMP69 = peroxisomal membrane proteins 69

PMP70 = peroxisomal membrane proteins 70

Pro = proline

PUFA = polyunsaturated fatty acid

RNA = ribonucleic acid

ROS = reactive oxygen species

SAH = S-adenosyl homocysteine

SAM = S-adenosyl methionine

Ser = serine

SHMT = Serine Hydroxymethyltransferase

SOD = superoxide dismutase

Tau = taurine

TE = acyl-CoA thioesterase

THCA = trihydroxycholestanoic acid

TLR = toll like receptor

TMEM119= transmembrane protein 119

TOM = translocase of the outer membrane

TREM2= triggering receptor expressed on myeloid cells 2

Trp = tryptophan

TYMS = Thymidylate synthase

Tyr = tyrosine

UCHL1 = ubiquitin C-terminal hydrolase L1

Val = valine

VLCFA = very long-chain fatty acid

X-ALD = X-linked adrenoleukodystrophy

SUMMARY

X-linked adrenoleukodystrophy (X-ALD) is a rare and devastating neurodegenerative disorder characterized by inflammatory demyelination of the brain and/or axonal degeneration in the spinal cord. This arises from a loss-of-function mutation in the *ABCD1* gene, a peroxisomal transporter protein. Consequently, very long-chain fatty acids (VLCFAs) accumulate in tissues and plasma, serving as a pathognomonic biomarker for the disease. X-ALD manifests in three main phenotypes: childhood and adult cerebral X-ALD (ccALD and cAMN, respectively) and adrenomyeloneuropathy (AMN). Notably, these phenotypes can occur within a single family, suggesting a complex interplay of genetic, environmental, and stochastic factors influencing disease expressivity.

This thesis employed untargeted metabolomic analysis to identify a distinct metabolic signature within the normal-appearing white matter of X-ALD patient brains. Additionally, shotgun metagenomic analysis of fecal samples revealed bacterial adaptations indicative of environmental stress in X-ALD patients. These adaptations included an upregulation of pathways associated with redox metabolism, bacterial biofilm production, and lipopolysaccharide (LPS) modification. Furthermore, we observed perturbations in branched-chain amino acids, likely a consequence of gut microbiota dysbiosis. We quantified neuronal and glial biomarkers like neurofilament light chain (NfL), glial fibrillary acidic protein (GFAP), ubiquitin C-terminal hydrolase L1 (UCHL1), and TAU protein levels in both plasma and cerebrospinal fluid (CSF) across the different X-ALD phenotypes. Notably, NfL and GFAP exhibited significantly greater elevations in cerebral X-ALD compared to AMN patients in both fluids. Interestingly, NfL, but not GFAP, emerged as a potential predictive marker for patients at risk of conversion to the rapidly progressive cerebral form of the disease. Additionally, we observed a decrease in plasma methionine levels specifically in cerebral X-ALD patients, while levels remained unaltered in AMN patients. Importantly, methionine levels exhibited an inverse correlation with NfL levels specifically in the cerebral X-ALD cohort. Furthermore, this work confirmed the presence of two established hallmarks of X-ALD pathogenesis: mitochondrial dysfunction and inflammation. We observed

elevated levels of mitochondrial DNA (mtDNA) and GDF15, supporting these established features.

The findings presented in this thesis shed light on the potential significance of altered metabolite profiles in X-ALD pathogenesis, particularly their association with mitochondrial dysfunction, impaired myelinogenesis, and neuroinflammatory processes. We highlight the importance of plasma methionine as a readily accessible and measurable biomarker, especially in the context of cerebral inflammatory X-ALD. Additionally, this work proposes a novel hypothesis suggesting that gut microbiota dysbiosis may contribute to some of the metabolic alterations observed in X-ALD patients. Our human studies identified several disrupted homeostatic pathways, some of which may hold promise as potential therapeutic targets. This suggests the possibility of a multi-targeted therapeutic approach for X-ALD. Such an approach could combine medications to normalize amino acid levels, mitigate gut microbiota alterations, and potentially reduce intestinal inflammation, leading to synergistic and disease-modifying effects. Moreover, the assessment of plasma methionine levels holds significant promise as a valuable metric for monitoring disease activity and progression in clinical trials aimed at addressing demyelination in cerebral X-ALD patients.

INTRODUCTION -PART 1

1. Peroxisomes in health and diseases

1.1 Peroxisomes overview

Peroxisomes, ubiquitous single-membrane organelles ranging from 0.1 μm to 1 μm in diameter, are indispensable components of eukaryotic cells (Schluter et al., 2010). Devoid of DNA, these dynamic structures contain a granular matrix and a crystalline core, which suggest the presence of an intricate biochemical machinery (Schluter et al., 2010). Nearly seven decades ago, Rhodin (1954) first observed peroxisomes. However, their detailed characterization is attributed to De Duve and colleagues (De Duve and Baudhuin, 1966). Utilizing differential and density gradient centrifugation techniques, they identified the presence of the peroxide-degrading enzyme catalase, prompting the now-ubiquitous name "peroxisome" (De Duve and Baudhuin, 1966). Initially, the origin of peroxisomes was postulated to be endosymbiotic, similar to mitochondria, due to shared features like a protein import system and fission machinery (Lazarow and De Duve, 1976). However, current understanding favors the endoplasmic reticulum (ER) (Gabaldon et al., 2006; Schluter et al., 2006; van der Zand et al., 2012) and possibly mitochondria (Sugiura et al., 2017) as the source organelles for peroxisome biogenesis. Peroxisomes have emerged as critical metabolic hubs, orchestrating a diverse array of biochemical pathways essential for human health (Kumar et al., 2024; Wanders et al., 2016). These pathways encompass: (1) the biosynthesis of ether phospholipids, such as plasmalogens, which contribute to myelin sheath formation (Hajra and Bishop, 1982); (2) fatty acid α- and β-oxidation (Lazarow and De Duve, 1976); (3) bile acid synthesis; (4) the synthesis of docosahexaenoic acid (DHA), the predominant omega-3 long-chain polyunsaturated fatty acid found in human brain and eyes (Li J et al., 2021); (5) glyoxylate metabolism to glycine, which avoids the accumulation of the detrimental metabolite oxalate (Behnam et al., 2006) and (6) the metabolism of reactive oxygen species (ROS), particularly hydrogen peroxide (Kumar et al., 2024; Wanders et al., 2016).

1.2 The peroxisomes-mitochondria interplay in fatty acids β-oxidation

Beyond their intrinsic metabolic functions, peroxisomes engage in intricate communication with other organelles, including mitochondria, lysosomes, endoplasmic reticulum (ER), lipid droplets (LDs), and the cytosol (Shai et al., 2016). While interactions with LDs, ER, and lysosomes primarily focus on substrate acquisition for β-oxidation, the interplay with mitochondria is critical for channeling the end products of peroxisomal fatty acids β-oxidation (pFAO) (Poirier et al., 2006). In contrast to mitochondria, which are capable of complete oxidation of fatty acids to CO_2 and H_2O, peroxisomes are only able to chain-shorten fatty acids. The end products of peroxisomal beta-oxidation, including acetyl-CoA, propionyl-CoA, and medium-chain acyl-CoAs (figure 1A), require transport as free acids or carnitine esters to mitochondria for complete oxidation via the citric acid (KREBS) cycle (Poirier et al., 2006; Schrader et al., 2015; Wanders et al., 2016, 2023). The mitochondrial system handles the majority of dietary fatty acids, including long-chain palmitic, oleic, linoleic, and linolenic acids, whereas pristanic acid and very long-chain fatty acids (VLCFAs), particularly hexacosanoic acid (C26:0) (figure 1B) are solely processed by peroxisomes (Singh et al., 1984b; Wanders et al., 2016). Therefore, peroxisomes primarily degrade a specific set of minor FAs that escape mitochondrial processing. This degradation is crucial not for energy production, but to prevent the toxic effects of their accumulation. The pFAO system, therefore, is first and foremost a degradative machinery required for the oxidation of a range of FAs that cannot undergo β-oxidation in mitochondria as part of their homeostasis (Wanders et al., 2016). Furthermore, β-oxidation in peroxisomes generates NADH and continued β-oxidation necessitates the implementation of a mechanism for peroxisomal NADH reoxidation to NAD+. Specific NAD(H)-redox shuttles are now recognized to mediate this process (Wanders et al., 2016). However, NADH reoxidation to NAD+ relies on interaction with the cytosol and subsequent mitochondrial activity through the Oxidative Phosphorylation System (OXPHOS) (figure 1A) (Poirier et al., 2006; Wanders et al., 2016). The distinct physiological roles of pFAO and mitochondrial fatty acids β-oxidation (mFAO) systems are reflected in the contrasting clinical presentations associated with defects in each pathway. mFAO deficiencies present with cardiac abnormalities,

myopathy, fatigue, rhabdomyolysis, liver dysfunction, and neurological features. Conversely, pFAO defects typically manifest with much greater severity, including profound neurological abnormalities (Wanders et al., 2016).

1A

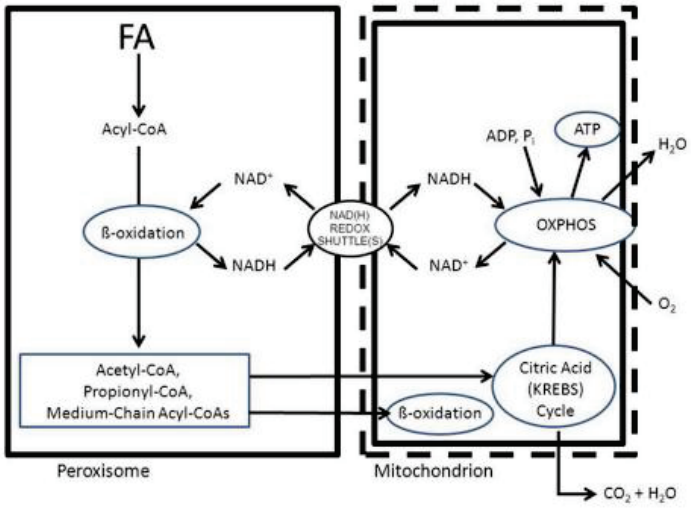

1B

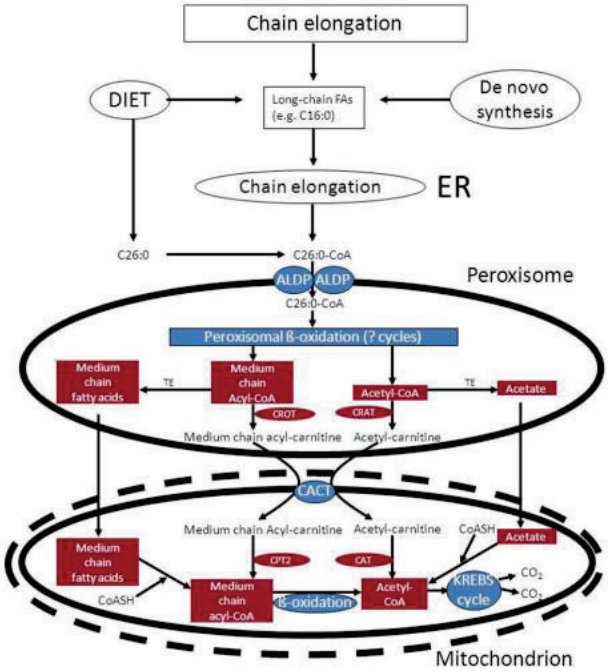

Figure 1A. Schematic diagram showing the functional interplay between peroxisomes and mitochondria in the beta-oxidation of fatty acids in peroxisomes. **Figure 1B.** Functional interplay between peroxisomes and mitochondria in the oxidation of C26:0. From Wanders et al., 2016.

1.3 Peroxisomal ABC transporters

Peroxisomal function necessitates the import of metabolites from the cytosol and the export of metabolic products across the peroxisomal membrane. Unlike low-molecular weight metabolites, peroxisomes appear impermeable to larger molecules such as nucleotides (NAD, NADH, NADP, NADPH), ATP, and both acylated and non-acylated CoA (Wanders et al., 2016, 2023).

Through the years, several integral peroxisomal membrane proteins (PMPs) with potential metabolite transporter function have been identified. The best-characterized PMPs belong to the ATP-binding cassette (ABC) protein family (Baker et al., 2015). ABC transporters constitute one of the largest superfamilies of conserved proteins from bacteria to mammals. Based on amino acid sequence and structural configuration, human ABC transporters are classified into seven subfamilies (A-G) encompassing a total of 48 transporters. ABC transporters of subfamily D include four proteins in mammals: ABCD1 (adrenoleukodystrophy protein, ALDP), ABCD2 (adrenoleukodystrophy-related protein, ALDRP), ABCD3 (70 kDa peroxisomal membrane protein, PMP70), and ABCD4 (peroxisomal membrane protein 69, PMP69) (Kawaguchi and Morita, 2016).

ABCD1, ABCD2, and ABCD3 localize to the peroxisomal membrane. ABCD4, initially identified through a homology search for ALDP and PMP70 sequences, was initially considered peroxisomal despite lacking a peroxisomal targeting signal (Shani et al., 1997). Recent studies have shown that ABCD4 resides in the endoplasmic reticulum and lysosomes, where its function is associated with cobalamin metabolism (Kashiwayama et al., 2009; Coelho et al., 2012; Kawaguchi and Morita, 2016).

These half-transporter proteins require dimerization for functionality, but likely exist primarily as tetramers. They exhibit overlapping yet specific substrate specificities, enabling the transport of various lipids into the peroxisomal matrix (figure 2) (Morita and Imanaka, 2012; Tawbeh et al., 2021; Baker et al., 2015).

.

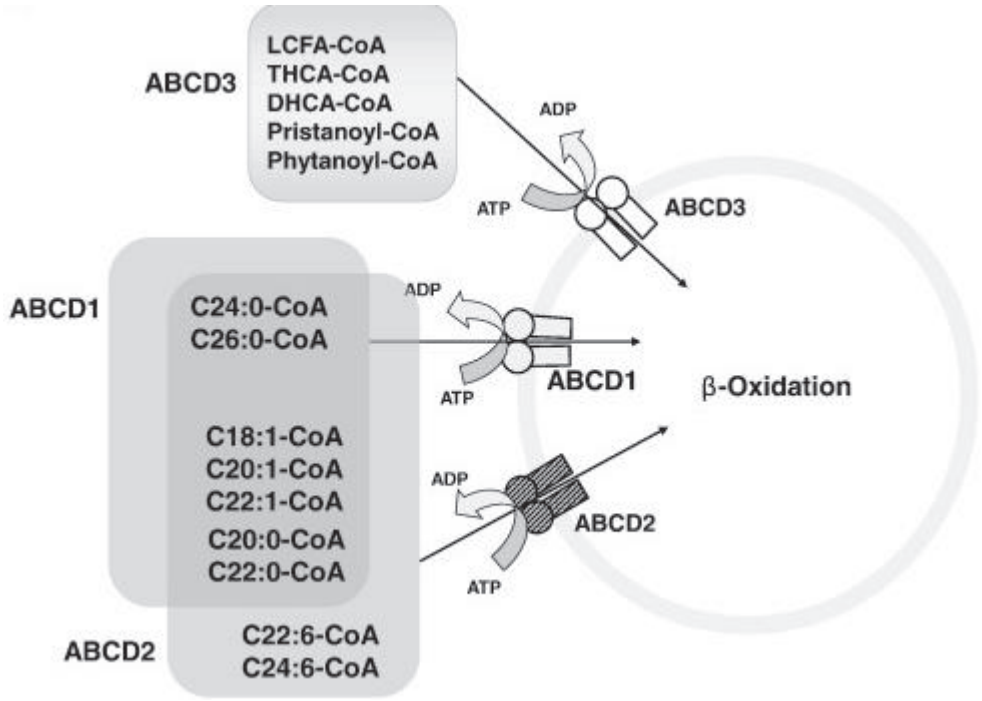

Figure 2. Function of ABC transporters on peroxisomal membranes

ABCD1 and ABCD2 have overlapping substrate specificities toward saturated and monounsaturated VLCFA-CoAs. However, ABCD1 has higher specificity to C24:0-CoA and C26:0-CoA than ABCD2. In contrast, ABCD2 has higher specificity for C22:0-CoA and C20:0-CoA than ABCD1. ABCD2, but not ABCD1, has an affinity for polyunsaturated VLCFA-CoA. ABCD3 is thought to be involved in the transport of LCFA-CoA, branched-chain acyl-CoA, THCA-CoA and DHCA-CoA. From Morita and Imanaka T, 2012

1.4 Peroxisomal disorders

The critical role of peroxisomes in human health and development is underscored by the existence of a spectrum of inborn errors of metabolism (IEMs) involving these organelles. These disorders manifest as impairments in one or more peroxisomal metabolic functions, impacting a multitude of organ systems. IEMs are broadly classified into peroxisome biogenesis disorders (PBDs) and single peroxisomal enzyme deficiencies (PEDs). PBDs, predominantly autosomal recessive, arise from mutations in any of the 14 PEX genes. These genes encode peroxins, proteins responsible for the import of peroxisomal

membrane and/or matrix proteins into the organelle (De base et al., 2020; Smith and Aitchison, 2013). PEDs, on the other hand, encompass defects in both peroxisomal matrix enzymes and membrane proteins involved in metabolite transport. Actually, much of our current understanding of peroxisomal functions stems from the phenotypic analysis of patients harboring mutations in genes encoding peroxisomal proteins (Table 1). Consequently, the biochemical and clinical consequences of each PED are dictated by the specific function of the affected protein within the peroxisome. Among PEDs, notable examples include defects in peroxisomal fatty acid α- and β-oxidation (Refsum disease and X-ALD), glyoxylate metabolism, ether-phospholipid biosynthesis (rhizomelic chondrodysplasia punctata – RCDP types 2, 3, and 4), bile acid synthesis, and catalase metabolism (extensively reviewed in Waterham et al., 2016). In Table 2 are showed some of the biochemical findings in deficiencies of peroxisomal fatty acid oxidation (Wanders et al., 2023). Interestingly, a pathognomonic feature in patients with PBD and peroxisomal β-oxidation dysfunction is the occurrence of lipid-laden macrophages in various tissues (Depreter M et al., 2003; Gilchrist KW et al., 1976), likely due to their inability to degrade very long-chain fatty acids (VLCFAs).While the clinical presentations of affected individuals vary based on the specific enzyme deficiency and its severity, these disorders are often characterized by severe neurological dysfunction and early mortality in many cases. This underscores the critical dependence of the nervous system on intact peroxisomal metabolism for its proper functioning (Wanders et al., 2016, 2023).

TABLE 1 - The single peroxisomal enzyme deficiencies and their underlying enzyme and gene defects. From Wanders et al., 2016

Metabolic pathway involved	Peroxisomal disorders	Enzyme deficiencies	Mutant gene
PEROXISOMAL BETA-OXIDATION			
	• X-linked adrenoleukodystrophy	ALDP	*ABCD1*
	• Acyl-CoA oxidase deficiency	ACOX1	*ACOX1*
	• D-bifunctional protein deficiency	DBP, MFE2, MFP2, D-PBE	*HSD17B4*
	• SCPx-deficiency	SCPx	*SCP2*
	• AMACR deficiency	AMACR	*AMACR*
	• PMP70-deficiency	PMP70	*ABCD3*
PLASMALOGEN BIOSYNTHESIS			
	• RCDP Type 2	DHAPAT/GNPAT	*GNPAT*
	• RCDP Type 3	ADHAPS/AGPS	*AGPS*
	• RCDP Type 4	Acyl-CoA reductase 1	*FAR1*
	• RCDP Type 5	PEX5L	*PEX5*
FATTY ACID ALPHA-OXIDATION			
	• Refsum disease	Phytanoyl-CoA hydroxylase	*PHYH*
BILE ACID SYNTHESIS			
	• BAAT-deficiency	BAAT	*BAAT*
GLYOXYLATE METABOLISM			
	• Hyperoxaluria Type 1	AGT	*AGXT*
ROS/RNS METABOLISM			
	• Acatalasaemia	Catalase	*CAT*

TABLE 2 - Biochemical findings in deficiencies of peroxisomal fatty acid oxidation. From Wanders et al., 2023.

Peroxisomal Disorder	OMIM	Gene	Peroxisomal Biomarkers (Blood)				
			VLCFA	Pristanic acid	Phytanic acid	DHCA/THCA	Plasmalogens
X-linked adrenoleukodystrophy	300100	*ABCD1*	↑	N	N	N	N
D-bifunctional protein deficiency	261515	*HSD17B4*	↑	↑	↑	↑	N
Acyl-CoA oxidase 1 deficiency	264470	*ACOX1*	↑	N	N	N	N
Acyl-CoA oxidase 2 deficiency	601641	*ACOX2*	N	N	N	↑	N
2-Methylacyl-CoA racemase deficiency	604489	*AMACR*	N	↑	↑	↑	N
ABCD3 (PMP70) deficiency	170995	*ABCD3*	N	?	?	↑	N
Sterol carrier protein X deficiency	613724	*SCP2*	N	↑	↑	↑	N
ACBD5 deficiency	616618	*ACBD5*	↑	N	N	N	N

Table legend: N = normal; ? = not determined.

2. X-linked adrenoleukodystrophy

2.1 A historical timeline of X-ALD discovery

The first documented case of X-ALD dates back to 1910, when Haberfeld and Spieler described a young boy with progressive visual impairment, school struggles, gait abnormalities, and hyperpigmentation – symptoms later recognized as hallmarks of the disease. The boy's condition rapidly deteriorated, leading to speech and motor difficulties, and he tragically passed away eight months later. Notably, he had an older brother who succumbed to a similar illness at the age of 8.5 years. The post-mortem neuropathological examination, conducted by Paul Schilder in 1924, revealed widespread involvement of the cerebral hemispheres with severe myelin loss, relatively preserved axons, and an accumulation of lymphocytes, fat-laden phagocytes, and glial cells (Schilder, 1924). Siemerling and Creutzfeldt (1923) described a similar case, but with the additional finding of adrenal gland involvement. Initially named Schilder's disease, the condition was later designated adrenoleukodystrophy (ALD) by Blaw in 1970.

Based on the family history, where only boys were affected, Fanconi et al. (1963) proposed that X-ALD was a genetic disorder inherited in an X-linked pattern. The 1970s witnessed significant advancements in X-ALD research. Powers and Schaumburg (1974) identified characteristic lamellar inclusions within the adrenal glands and brain macrophages of X-ALD patients. These inclusions were found to contain an unusually high proportion of very long-chain fatty acids (VLCFAs) with chain lengths ranging from C24 to C30. A few years later, a pivotal discovery was made by Igarashi et al. (1976) who demonstrated that these inclusions were enriched in cholesterol esterified with saturated VLCFAs. This finding led to the classification of X-ALD as a lipid storage disorder.

The identification of adult X-ALD patients by two independent groups in 1976 (Budka et al., 1976; Griffin et al., 1977) expanded the disease spectrum beyond childhood. In the 1980s, Moser et al. (1980, 1981) established that cultured skin fibroblasts and plasma from X-ALD patients displayed elevated levels of VLCFAs. This established VLCFA levels as a reliable diagnostic marker, a practice still in use today (Moser and Moser, 1999). Further studies by Singh et al. (1984b) revealed impaired VLCFA degradation

capacity in white blood cells and cultured skin fibroblasts from X-ALD patients. Additionally, Migeon et al. (1981) mapped the X-ALD gene to the Xq28 region, supporting the X-linked inheritance pattern proposed earlier (Fanconi et al., 1963).

The connection between X-ALD and peroxisomal disorders wasn't established until 1984 when Singh et al. demonstrated the inability of X-ALD patients to degrade VLCFAs, a process known to occur within peroxisomes (Singh et al., 1984a). Finally, in 1993, Mosser et al. achieved a breakthrough by identifying the X-ALD gene using positional cloning. This gene encodes a peroxisomal membrane ATP-binding cassette (ABC) transporter, initially named the ALDP protein and later designated ABCD1. This critical discovery paved the way for the development of mouse models in 1997 (Forss-Petter et al., 1997; Kobayashi et al., 1997; Lu et al., 1997) and the successful application of lentiviral-mediated gene therapy in 2009 (Cartier et al., 2009).

2.2 Epidemiology and molecular basis of X-ALD

X-ALD**,** classified under OMIM 300100, stands as the most prevalent peroxisomal disorder identified to date. It also holds the distinction of being the most common monogenic leukodystrophy, with an estimated birth incidence of approximately 1 in 14,700 individuals (Moser and Fatemi, 2018; Turk et al., 2020). Notably, there appears to be no significant variation in X-ALD prevalence across different geographic regions or ethnicities (Cappa et al., 2023).

The underlying cause of X-ALD lies in mutations affecting the *ABCD1* gene, located on the X chromosome at Xq28. Inheritance patterns suggest that roughly 95% of probands acquire a pathogenic variant of the *ABCD1* gene from a parent and at least 4% of X-ALD cases involve de novo pathogenic variants (Raymond et al., 2023). To date, researchers have identified over 2,552 distinct *ABCD1* mutations, with 759 classified as non-recurrent (www.x-ald.nl). The *ABCD1* gene encodes the ATP-binding cassette (ABC) half transporter known as ALDP (adrenoleukodystrophy protein) that resides on the peroxisomal membrane. Dysfunction in this transporter leads to a buildup of its preferred substrates, specifically VLCFAs, particularly C26:0. Fatty acids with chain lengths up to

16 carbons are synthesized within the cytosol by a multifunctional enzyme called fatty acid synthase (FAS). This process utilizes acetyl-CoA, malonyl-CoA, and NADPH to progressively lengthen fatty acids by two carbons at a time. The generation of VLCFAs occurs through further elongation of long-chain fatty acids, with elongases ELOVL6 (responsible for C18:0 to C22:0) and ELOVL1 (responsible for C24:0 to C26:0) playing a crucial role. Under normal conditions, ALDP facilitates the transport of C24:0/C26:0-CoA across the peroxisomal membrane. However, in X-ALD, a deficiency in ALDP not only disrupts peroxisomal VLCFA beta-oxidation but also leads to elevated cytosolic levels of C24:0/C26:0-CoA, which can then serve as substrates for further elongation by ELOVL1, exacerbating the overall VLCFA accumulation (Turk et al., 2020; Kemp et al., 2012, 2016) (figure 3).

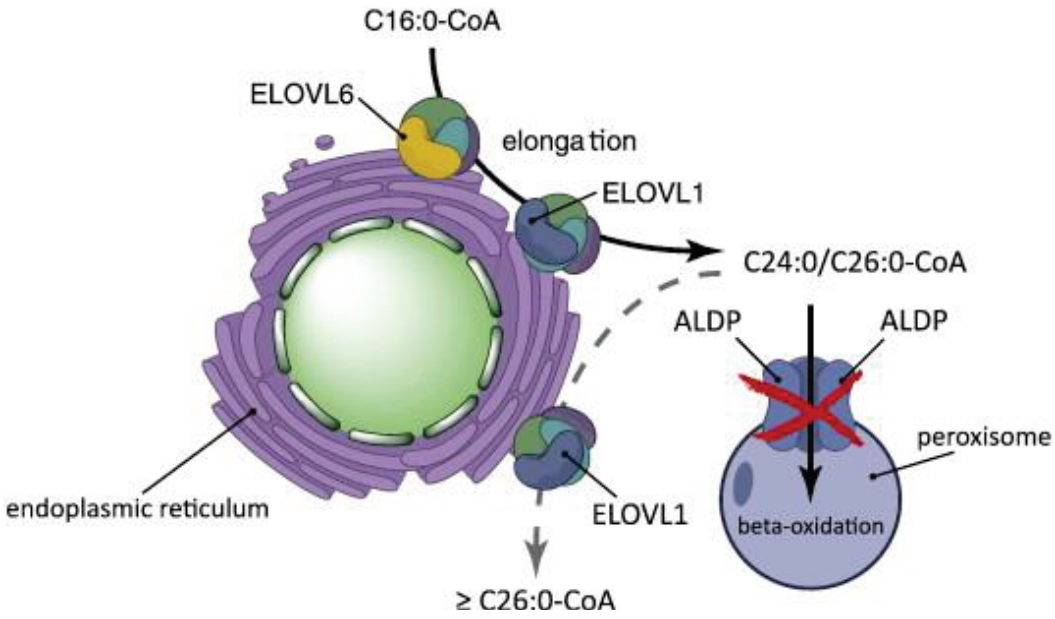

Figure 3: molecular mechanisms leading to the intracellular VLCFA accumulation in X-ALD patients. See the text for the detailed explanation. From Kemp et al., 2012.

The accumulation of VLCFA occurs in the plasma and various tissues, with the brain's white matter, spinal cord, adrenal cortex, and testicular Leydig cells being the most severely affected (Turk et al., 2020; Kemp et al., 2012,2016; Engelen et al., 2014; Ferrer

et al., 2010). *ABCD1* expression in the central nervous system is relatively low compared to other organs like heart, muscle, liver, kidney, and endocrine glands (Fouquet et al., 1997; Höftberger et al., 2007). Immunohistochemical analysis reveals the highest levels of ABCD1 in microglia, astrocytes, and epithelial cells. However, oligodendrocyte populations in the subcortical white matter and cerebellum exhibit variable ABCD1 expression, ranging from high to undetectable levels (Fouquet et al., 1997). Notably, most neuronal populations show minimal ABCD1 expression, with exceptions in the hypothalamus, basal nucleus of Meynert, periaqueductal grey matter, and locus coeruleus (Höftberger et al., 2007). Interestingly, cell populations and tissues like dorsal root ganglion with high proopiomelanocortin (POMC) expression, including the pituitary gland, adrenocortical cells, renal distal tubules, liver, and skin exhibit high levels of ABCD1 (Höftberger et al., 2007, 2010). Appreciable expressions of ABCD1 are also evident in the gastrointestinal system (figure 4) (www.proteinatlas.org, Thul et al, 2017)

Figure 4 **Expression of ABCD1 transporter at the brain and gastrointestinal level.** From www.proteinatlas.org

The precise mechanism linking VLCFA accumulation to the neurological deficits observed in X-ALD patients remains elusive. Several hypotheses have been proposed to explain VLCFA-induced cytotoxicity:

a) disruption of myelin sheaths: VLCFAs may accumulate within myelin components, such as the proteolipid protein (PLP). This accumulation, as proposed by Bizzozero et al. (1991), could destabilize and damage myelin sheaths;

b) immune response activation: VLCFAs might activate the immune response through CD1, an antigen-presenting protein. This protein can bind to self-lipid antigens, potentially triggering an autoimmune response against these antigens, as suggested by Ito et al. (2001);

c) cell death induction: VLCFAs could directly induce cell death of oligodendrocytes and astrocytes, vital cell types in the central nervous system. Hein et al. (2008) provided evidence supporting this hypothesis;

d) oxidative stress: VLCFAs may contribute to increased oxidative stress by promoting the generation of reactive oxygen species (ROS) and depleting glutathione (GSH), an important antioxidant molecule. This concept is supported by the work of Fourcade et al. (2008).

Furthermore, excessive VLCFA levels have been shown to decrease adrenocorticotropic hormone (ACTH)-stimulated cortisol release by human adrenocortical cells, potentially contributing to adrenal insufficiency observed in X-ALD patients (Whitcomb et al., 1988).

2.3 Clinical presentation

Although VLCFA accumulation begins in utero, both males and females with X-ALD are typically born without neurological impairments. They exhibit normal central and peripheral myelination and experience no developmental delays in early life. However, around the age of 3, the natural history of the disease can diverge dramatically. Three

major neurological manifestations are observable in X-ALD patients (Moser et al., 2001; Turk et al., 2020; Kemp et al., 2012,2016; Engelen et al., 2012,2014; Ferrer et al., 2010; Raymondet al., 2023):

a. cerebral adrenoleukodystrophy (ccALD): this form presents in approximately 35% of affected males. It is characterized by early onset (typically between 3 and 10 years old, with a peak incidence at 7 years) and a severe, unfavorable prognosis due to pronounced inflammatory and demyelinating processes in the cerebral white matter. Affected males often present with behavioral or learning difficulties, which may initially be misdiagnosed as attention-deficit/hyperactivity disorder. Seizures can also occur in some patients, with variable frequency. Disease progression can be rapid, leading to total disability within 6 months to 2 years.

b. adrenomyeloneuropathy (AMN): clinical manifestations of AMN typically appear after the age of 30 and progress over decades. Patients often experience sensory ataxia, characterized by impaired vibration sense. Other common symptoms include progressive spastic paraparesis (characterised by weakness and stiffness in the legs), leg pain, sphincter dysfunction, impotence and scalp hair loss (alopecia). The neurological symptoms arise from progressive damage to the spinal cord (degenerative axonopathy with Wallerian degeneration) and peripheral nerves (with lamellar or onion-layer lipid inclusions in Schwann cells and macrophages).

c. cerebral adrenoleukodystrophy-adrenomyeloneuropathy (cAMN): this combined form occurs in approximately 20% of affected males. It presents with an AMN-like clinical history that overlaps with cerebral complications. Patients exhibit the same histologic pattern of inflammatory demyelination observed in the childhood cerebral form of the disease.

In addition to the neurological manifestations, nearly 80% of male X-ALD patients will develop signs and symptoms of adrenocortical insufficiency. This can occur with or without neurological involvement (Addison-only patients).

Female carriers of the *ABCD1* mutation typically develop an AMN-like phenotype, usually in adulthood (rarely before the age of 40). These cases often present with mild signs of spinal cord dysfunction. Cerebral involvement and adrenocortical insufficiency are uncommon in females with X-ALD.

2.4 The diagnostic approach to the disease

Establishing a diagnosis of X-ALD involves a multi-modal approach, integrating various elements (Engelen et al., 2012,2022; Raymond et al., 2023):

a) biochemical analysis: measuring plasma VLCFA concentrations is the cornerstone of X-ALD diagnosis. Specifically, levels of hexacosanoic acid (C26:0), docosanoic acid (C22:0), and tetracosanoic acid (C24:0), along with their ratios (C26:0/C22:0 and C24:0/C22:0), are crucial biomarkers. If available, plasma C26:0-lysophosphatidylcholine (C26:0-lysoPC) measurement offers superior diagnostic accuracy. In the absence of C26:0-lysoPC testing, fasting plasma VLCFA levels (focusing on C26:0, C26:0/C22:0, and C24:0/C22:0 ratios) should be obtained. Notably, the biochemical phenotype of elevated plasma VLCFAs in X-ALD males exhibits 100% penetrance regardless of age. In February 2016, X-ALD was added to the Recommended Uniform Screening Panel (RUSP) in the USA. Outside the US, Taiwan initiated ALD newborn screening in November 2016 and a pilots are ongoing in Japan and Italy. From 1 October 2023, newborn boys in the Netherlands started to be screened for adrenoleukodystrophy (Salzman and Kemp, 2024). The biochemical analysis is complemented with other diagnostic techniques in order to differentiate X-ALD from other conditions (Table 3, from Raymond et al., 2023 for details) causing elevated plasma VLCFA levels.

TABLE 3 - List of genetic conditions with the relative gene affected and mode of inheritance causing increased plasma VLCFA levels. From Raymond et al., 2023

Gene	Disorder	Mode of inheritance
ABCD1	X-linked adrenoleukodystrophy	X-linked
ACBD5	Retinal dystrophy w/leukodystrophy (OMIM 618863)	Autosomal recessive
ACOX1	Acyl-coenzyme A oxidase deficiency (OMIM 264470)	Autosomal recessive
DNM1L	Lethal encephalopathy due to defective mitochondrial peroxisomal fission 1 (OMIM 614388)	Autosomal recessive or dominant
HSD17B4	D-bifunctional enzyme deficiency (OMIM 261515)	Autosomal recessive
PEX genes	Zellweger spectrum disorder	Autosomal recessive
SCP2	Leukoencephalopathy w/dystonia & motor neuropathy (OMIM 613724)	Autosomal recessive

b) Genetic testing: analyzing the *ABCD1* gene is considered the gold standard for confirming X-ALD. This test detects mutations responsible for the disease.

c) Neuroimaging: magnetic resonance imaging (MRI) is the gold standard for diagnosing cerebral ALD. The cerebral form of X-ALD manifests with a characteristic pattern of demyelination: it typically begins in the corpus callosum, where white matter fiber bundles are most densely packed, and progresses outward to the periventricular white matter. This initial demyelination transitions into a rapidly progressive inflammatory response, with blood-brain barrier disruption (becoming positive for gadolinium contrast enhancement, the sign of an active disease) and infiltration of mononuclear cells, predominantly macrophages containing myelin degradation products (Berger et al., 2014; Moser et al., 2001). The lesion typically progresses rapidly in a parieto-occipital (80% of

the cases) or fronto-parietal distribution (Berger et al., 2014). The MRI severity scoring system (Loes score), ranging from 0 (normal) to 34 (severely abnormal), allows for quantifying cerebral white matter lesions in X-ALD patients (Loes et al., 1994) (figure 5A, B).

d) Assessment of spinal cord involvement: MRI can be used to evaluate spinal cord involvement in patients with adrenomyeloneuropathy (AMN). Additionally, clinical outcome measures can be employed to assess walking function, such as the 6-minute walking test, and the Expanded Disability Status Scale (EDSS). The EDSS quantifies neurological disability on a scale of 0 (no disability) to 10 (death), with scores between 5 and 9.5 indicating varying degrees of impairment in walking. While abnormal white matter signals are frequently observed in the centrum ovale, pyramidal tracts (figure 5C), and internal capsules on MRI in AMN patients, the absence of gadolinium enhancement indicates an intact blood-brain barrier and the lack of an acute inflammatory process (Berger et al., 2014).

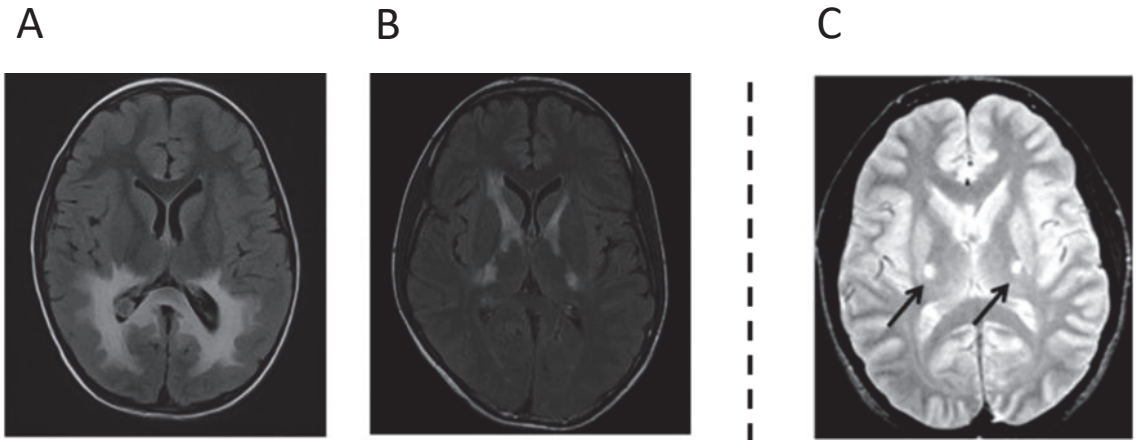

Figure 5: (A) Brain MRI (axial images) of a ccALD patient showing extensive demyelinating lesions (abnormally increased signal) in the splenium of the corpus callosum, the parieto-occipital white matter, the visual pathways as well as the medial geniculate bodies of auditory pathway and the posterior limbs of the internal capsules. (B) Brain MRI (axial images) showing abnormally increased signal involving the posterior and anterior limbs of the left and right internal capsule. From Kemp et al., 2012 (C) T2-weighted magnetic resonance (axial) image of the brain in an AMN patient. The arrows indicate the symmetric lesions in the corticospinal tract. From Powers et al., 2000.

2.5 Current Follow-Up and Treatment Landscape

While elevated VLCFA levels serve as a diagnostic marker for X-ALD, they don't adequately reflect disease severity or the likelihood of developing the cerebral form. Consequently, their clinical utility is limited to diagnosis (Engelen et al. 2012, 2022; Turk et al., 2020). Due to the limitations of VLCFA levels, the current approach to assessing disease severity and progression in X-ALD patients relies on a comprehensive follow-up protocol (figure 6). This protocol incorporates serial clinical evaluations, neuroimaging studies, and neurophysiological assessments scheduled according to the patient's age. All boys and men with X-ALD should undergo screening for cerebral ALD, regardless of the presence of neurological or cognitive symptoms. Even in the absence of symptoms, boys and men with characteristic confluent white matter abnormalities on brain MRI should be considered at risk for cerebral ALD, as these lesions may precede symptom onset. A baseline MRI scan is recommended at age 2 years. Between ages 2 and 12, male patients should be screened every 6 months. Thereafter, yearly screening is advised (Engelen et al., 2022).

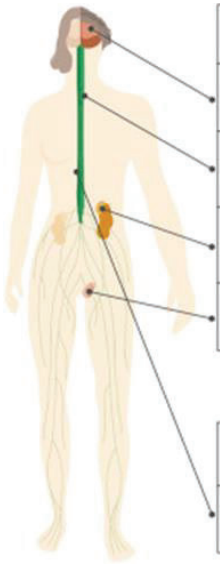

Male	Screening or diagnostic tool	Screening protocol	Treatment
Cerebral ALD	MRI	2 years old, baseline scan / 2–12 years old, every 6 months / >12 years old, yearly	HSCT or gene therapy
Myeloneuropathy	History and neurologic examination	>18 years old, only in parallel with any other testing	Supportive
Adrenal insufficiency	Morning fasted cortisol, ACTH, renin, electrolytes	0–6 months, start screening / 6 months–10 years old, every 3–6 months / >10 years old, yearly	Hormone replacement therapy
Gonadal insufficiency	Symptoms biomarkers: Testosterone, LH, FSH	No screening test if symptoms	Hormone replacement therapy

Female	Screening or diagnostic tool	Screening protocol	Treatment
Myeloneuropathy	History and neurologic examination	>18 years old	Supportive

Figure 6. Overview of the Management of Patients With X-ALD. From Engelen et al. 2022.

Studies by Moser et al. (2001) demonstrated that conventional dietary VLCFA restriction in X-ALD patients failed to significantly lower plasma C26:0 levels. Subsequent research has shed light on this phenomenon. Kemp et al. (2015) revealed that VLCFA accumulation in X-ALD arises from two sources: partial dietary absorption and, more importantly, endogenous synthesis through the elongation of long-chain and very long-chain fatty acids. Furthermore, they demonstrated that this elongation system appears to be upregulated, at least in fibroblasts from X-ALD patients (Kemp et al., 2015). This could explain the observed lack of C22:0 accumulation, and even slight reductions in some cases, in tissues and cells of X-ALD patients in spite of the fact that C22:0-CoA is an excellent substrate for ABCD1 (Wiesinger et al., 2013). These findings highlight the limitations of dietary VLCFA restriction as a sole therapeutic strategy in X-ALD and underscore the need to explore alternative approaches that target the endogenous synthesis of VLCFAs.

Currently, the only approved therapy with the potential to alter or slow the progression of the cerebral form, at least in children, is allogeneic hematopoietic stem cell transplantation (HSCT). HSCT should be considered for boys with early-stage disease (Loes score ≤ 9) and performance IQ ≥ 80. In boys with cerebral ALD a Loes score ≥ 10 at time of HSCT is associated with decreased survival and increased posttransplant neurodysfunction (Kirmse an Barron, 2022). In addition, a lentiviral-based autologous hematopoietic stem cell gene therapy agent, introducing a wild-type copy of the *ABCD1* gene into the patients' hematopoietic CD34+ stem cells ex vivo (Cartier et al., 2012), was granted FDA (www.fda.gov) accelerated approval to slow progression of neurologic dysfunction in male children aged 4-17 years with early, active cerebral ALD (Raymond et al., 2023). Dietary supplementation with Lorenzo oil may be considered in presymptomatic boys,but has insufficient evidence for reducing onset of cerebral disease (Kirmse and Barron, 2022). Leriglitazone is a novel synthetic orally bioavailable and selective PPAR gamma agonist with a potential first-in-class and best-in-class profile for CNS diseases (Rodríguez-Pascau et al., 2021; Pizcueta et al., 2023). The actions of PPARγ include crosstalk with several other important pathways involved in regulating systemic energy homeostasis. For example, PPARγ and the peroxisome proliferator-

activated receptor γ coactivator 1α (PGC-1α) play a key role in the co-regulation of mitochondrial oxidative metabolism induction (Pizcueta et al., 2023). In the CNS PPARγ plays a major role in neuroprotection by preventing neuroinflammation, regulates energy homeostasis, and regulates genes involved in fatty acids (FA) metabolism including genes for acetyl-CoA carboxylase, FA synthase, and carnitine palmitoyltransferase 1 (Pizcueta et al., 2023). Data from ADVANCE clinical trial (Köhler et al., 2023), in adult male patients with ALD, showed that leriglitazone reduces the progression of lesions and the development of progressive cALD. This is now supported by 24 week data from NEXUS trial (EUDRACT number 2019-000654-59), a phase 3 open-label clinical study in male pediatric patients with early stage cALD, showing a reduction in lesion progression comparable to Hematopoietic Stem Cell Transplantation (HSCT)-based approaches.

For the myeloneuropathy form, only supportive therapies are available with the aim to improve quality of life, maximize function, and reduce complications. This ideally involves multidisciplinary care by specialists in relevant fields like neuropsychologist for cognitive decline, urologists for neurogenic bladder and gastroenterologists for bowel function control (Raymond et al., 2023). Adrenal insufficiency, however, can be effectively managed with hormone (oral) replacement therapy (Engelen et al., 2022).

The narrow therapeutic window for HSCT in X-ALD with cerebral involvement underlines the critical need for a reliable prognostic biomarker (or combination of biomarkers). Unfortunately, no such biomarker currently exists to predict the natural history of X-ALD. The identification of a biomarker (or multiple biomarkers) would be a major breakthrough, allowing early identification of children in the pre-symptomatic or early symptomatic stages of cerebral X-ALD. This would allow timely intervention with HSCT, in ccALD patients, maximising therapeutic benefit but also avoiding unnecessary HSCT with its associated risks and the emotional burden on families faced with a diagnosis of X-ALD. In addition, the discovery of predictive and monitoring biomarkers would not only improve therapeutic decision-making in the context of HSCT, but also facilitate the design and development of new clinical trials, particularly for X-ALD with adrenomyeloneuropathy, for which effective therapies remain elusive.

2.6 X-ALD: modeling the disease

2.6.1 Fibroblasts

For decades, primary skin fibroblasts isolated from X-ALD patients have served as a cornerstone cellular model for the disease (Moser et al., 1980). In a landmark study by Moser et al. (1980), the presence of very long-chain fatty acid (VLCFA) accumulation was demonstrably replicated in these fibroblasts. This established the validity of the model for studying X-ALD, at least at the biochemical level. Since its inception, this model has become instrumental for a wide range of investigations, including:

- analyses of cellular lipid metabolism in X-ALD;

- diagnosis of X-ALD through detection of VLCFA accumulation;

- functional characterization of peroxisomal ATP-binding cassette transporters, particularly ABCD1;

- understanding the cellular consequences of ABCD1 deficiency;

- screening potential therapeutic compounds.

Undoubtedly, this readily accessible model has significantly advanced our understanding of X-ALD. However, its inherent limitation lies in the cellular origin: skin fibroblasts exhibit distinct gene expression patterns and functionalities compared to the neural, glial, and microglial cells.

2.6.2 Mouse models

While skin fibroblasts offer valuable insights into X-ALD biochemistry, they are inadequate for recapitulating the complex interplay between cell types in the central nervous system. To bridge this gap and investigate the function of peroxisomal ABC transporters and X-ALD pathogenesis within a living organism, researchers have turned to genetically modified mouse models. The year 1997 marked a significant milestone with the independent generation of three distinct X-ALD mouse models by different research groups, all achieved through *Abcd1* gene inactivation (Forss-Petter et al., 1997; Kobayashi et al., 1997; Lu et al., 1997). These *Abcd1* knockout mice faithfully replicate

the key biochemical feature of X-ALD: the accumulation of VLCFAs. However, their neurological phenotype deviates from the human condition. Unlike the characteristic cerebral demyelination and inflammation observed in ccALD/cAMN, these mice develop a late-onset, progressive neurodegenerative condition primarily affecting the spinal cord and sciatic nerves, with no signs of brain involvement. Around 18 months of age, they display an AMN-like phenotype, characterized by spastic paraparesis due to degeneration of corticospinal tracts. Notably, inflammation is observed in the spinal cord of old mice and includes microglia and astrocyte activation (Pujol et al., 2002) but inflammatory demyelination is absent in their brain (Pujol et al., 2002). While lacking the human cerebral phenotype, *Abcd1* knockout mice have proven instrumental in dissecting the pathophysiology of AMN (Fourcade et al., 2008, 2020; Galino et al., 2011; Launay et al., 2013, 2015, 2017, 2024; Lopez-Erauskin et al., 2012, 2013a, 2013b; Morato et al., 2013, 2015; Ranea-Robles et al., 2018; Parameswaran et al., 2022) and hold promise for screening potential therapeutic compounds.

Despite the phylogenetic proximity of mice to humans, the model fails to fully replicate the human brain X-ALD phenotype. Potential explanations for this discrepancy include species-specific differences in ABCD1-3 expression levels and potential functional redundancy between these transporters. Even *Abcd1/Abcd2* double-deficient mice exhibit a primarily spinal cord-restricted neuropathology, characterized by inflammatory T lymphocyte infiltration and sensory neuropathy due to ABCD2 contribution to the dorsal root ganglia. However, the onset of these defects is earlier (around 12 months) and more pronounced compared to single *Abcd1* knockouts, making them suitable preclinical models for testing disease-modifying drugs (Fourcade et al., 2020; Launay et al., 2017; Lopez-Erauskin et al., 2011; Mastroeni et al., 2009; Morato et al., 2013, 2015; Ranea-Robles et al., 2018). In contrast to *Abcd1* and *Abcd2* models, *Abcd3* knockout mice do not develop peripheral or central neurodegeneration, unlike the human condition with ABCD3 deficiency. Instead, they exhibit hepatomegaly associated with abnormal peroxisomal fatty acid metabolism, potentially serving as a suitable model for congenital bile acid synthesis defect type 5 (Ferdinandusse et al., 2015).

The lack of progression from the metabolic syndrome to cerebral demyelination and neuroinflammation in *Abcd1*-deficient mice underscores the potential role of modifier genes, epigenetic factors, environmental influences, or even stochastic events in triggering the cerebral forms of the disease beyond the loss of ABCD1 function.

Although the trigger(s) for the X-ALD cerebral form in humans is unknown, oxidative stress and inflammation have been proposed as inciting events (Fourcade et al., 2008; Singh and Pujol, 2010). Hashemi and colleagues (2023) proposed that a combination of oligodendrocyte oxidative stress (induced by a cuprizone diet, CPZ) with antigen-induced inflammatory demyelination (MOG-peptide EAE) would result in the formation of human X-ALD brain lesions. A cerebral phenotype was successfully generated in 8-week-old male *Abcd1*-null mice by employing a two-hit method that combined the CPZ and experimental autoimmune encephalomyelitis (EAE) models: MRI studies revealed T2 hyperintensities and post-gadolinium enhancement in the medial corpus callosum of mice; histological analysis of these lesions demonstrated features consistent with those observed in human lesions, including myelin phagocytosis, myelin loss, abundant microglial activation, T and B-cell infiltration, and astrogliosis (Hashemi et al., 2023).

2.6.3 Caenorhabditis elegans

In our recent investigation (Coppa et al., 2020), we established a nematode model of X-ALD by characterizing worms with a loss-of-function mutation in the *pmp-4* gene, the *C. elegans* orthologue of human *ABCD1*. While the *C. elegans* nervous system lacks myelin (El Bejjani and Hammarlund, 2012), precluding direct study of the infantile form of X-ALD (ccALD), *pmp-4* worms may represent a valuable model for the axonopathy observed in the adult form of the disease (Launay et al., 2024). This is supported by the fact that these mutants recapitulate key hallmarks of X-ALD, including: (i) accumulation of VLCFAs and disruption of mitochondrial redox homeostasis, and (ii) axonal damage leading to locomotor dysfunction.

2.6.4 Zebrafish

Another tool for studying X-ALD has been provided by the generation of a zebrafish (Danio rerio) *Abcd1* mutant model (Strachan et al., 2017). Importantly, *Abcd1* DNA and protein sequences are highly conserved in zebrafish, as are other key genes in lipid metabolism, including *Scd1* and *Elovl1* (Bhandari et al., 2016; Hsieh et al., 2003). The zebrafish X-ALD model not only recapitulates key aspects of X-ALD, but also manifests a motor phenotype in the first week of life.

2.6.5 Microglia

Microglia is increasingly recognized as important player in X-ALD pathogenesis, particularly regarding inflammatory processes. To further investigate its role, researchers have employed CRISPR/Cas9 gene editing technology to generate *Abcd1*-deficient and/or *Abcd2*-deficient microglia cell lines from the mouse BV-2 line (Raas et al., 2019). *Abcd1*$^{-}$ *Abcd2*$^{-/-}$ double knockout cells were created to circumvent potential masking effects caused by functional redundancy between these transporters. These novel cell lines exhibit the classic biochemical hallmarks of X-ALD, including elevated levels of saturated and monounsaturated VLCFAs. Interestingly, they also show increased levels of certain long-chain fatty acids (LCFAs) and polyunsaturated fatty acids (PUFAs). Additionally, similar to brain macrophages isolated from X-ALD patients (Schaumburg et al., 1974), these cells display whorled lipid inclusions, likely representing cholesterol esters of VLCFAs. This characteristic feature makes them particularly valuable for modeling the human disease. Further studies employing these cell lines, either alone or in co-culture with glial and/or neuronal cells, hold promise for new insights into the impact of *Abcd1/Abcd2* deficiencies on microglial function. They could also serve as a powerful tool for screening potential therapeutic compounds aimed at halting chronic inflammation in the brains of ccALD/cAMN patients.

2.6.6 iPSC

The advent of induced pluripotent stem cell (iPSC) technology has revolutionized disease modeling by offering the ability to study patient-derived cells carrying specific mutations

and exhibiting phenotypes that closely resemble human physiology (Trudler et al., 2021). This technology has been successfully applied to X-ALD, with several research groups generating iPSC lines from skin fibroblasts of both ccALD and AMN patients (Wang et al., 2012; Baarine et al., 2015; Son et al., 2017; Muffat et al., 2016; Jang et al., 2011, 2016). Importantly, upon differentiation into oligodendrocytes or astrocytes, these iPSCs exhibit increased VLCFA levels; this accumulation is more pronounced in ccALD-derived cells compared to AMN cells, while neurons show no significant VLCFA accumulation (Baarine et al., 2015). Furthermore, iPSC-derived astrocytes from X-ALD patients display pro-inflammatory features, with a severity-dependent correlation. The differentiation of microglia from iPSCs appears to be another promising avenue. These iPSC-derived microglia exhibit key characteristics of primary fetal and adult human microglia, including phagocytic and inflammatory capacity (Muffat et al., 2016). Additionally, iPSCs differentiated into brain microvascular endothelial cells from ccALD patients exhibit impaired blood-brain barrier (BBB) function, along with altered lipid metabolism and interferon activation (Lee et al., 2018). This model offers the potential to investigate a crucial factor in X-ALD brain pathogenesis. Collectively, these studies demonstrate the immense potential of iPSC-derived brain cells for studying X-ALD pathogenesis in unprecedented detail. This approach holds promise for identifying novel biomarkers, screening therapeutic molecules, and gaining deeper insights into intercellular communication within the brain through co-culture experiments.

3. X-ALD: beyond peroxisomes dysfunction

X-ALD is classified as a peroxisomal disease. Nevertheless, our group and others have contributed to highlighting different disease hallmarks that are not limited to strict peroxisomal function that are important for their pathophysiological and potentially therapeutic significance.

3.1 Redox dyshomeostasis

3.1.1 ROS: a double-edged sword

The term "reactive oxygen species" (ROS) encompasses a variety of molecules derived from molecular oxygen, a byproduct of aerobic life. These ROS are constantly generated and eliminated within the cells of all organisms that rely on oxygen. The major forms of ROS include free radicals like superoxide anion (O_2^{-}•), hydroxyl radical (OH•), alkoxyl radical (RO•), and peroxyl radical (ROO•), alongside non-radical forms like hydrogen peroxide (H_2O_2), ozone (O_3), and singlet molecular oxygen ($^1\Delta gO_2$). Two species, hydrogen peroxide (H_2O_2) and the superoxide anion radical (O_2·-), are key redox signalling agents generated under the control of growth factors and cytokines by more than 40 enzymes (Sies et al., 2017).

Interestingly, at low physiological levels (nanomolar range, known as "oxidative eustress"), ROS, particularly hydrogen peroxide (H_2O_2), act as important signaling molecules. They interact with specific cellular targets, influencing metabolic regulation and stress responses, ultimately promoting adaptation to a changing environment (Sies et al., 2020). However, when ROS production exceeds the cellular capacity for elimination, a state of "oxidative distress" ensues. This imbalance can lead to significant molecular damage and contribute to various pathologies; these disorders range from neurodegenerative diseases to metabolic disorders such as obesity or type 2 diabetes (Cross et al., 1987; Halliwell, 2006).

The mitochondrial electron transport chain (ETC), transmembrane NADPH oxidases (NOXs) and dual oxidases (DUOXI-II) are the primary source of ROS within the cell (Boveris et al., 1972; Halliwell, 2007; Jensen, 1966; Murphy, 2009). The level of ROS generated depends on the ETC's activity (see figure 7) (Sinenko et al., 2021; Murphy, 2009) and studies have identified eleven potential sites within the ETC where electron leakage can occur, leading to superoxide anion (O_2^{-}•) and ROS formation (Brand, 2016). While in vitro experiments suggest that complexes I (CI), II (CII), and III (CIII) are the main culprits (Goncalves et al., 2015), with CI and CIII playing a more prominent role *in*

vivo (Sena and Chandel, 2012; Chouchani et al., 2014), the specific contribution of each site remains an area of investigation. CI deposit ROS in the mitochondrial matrix, whereas CIII and glycerol 3-phosphate dehydrogenase release ROS into either the matrix or intermembrane space (Droge, 2002; Sena and Chandel, 2012; Bleier et al., 2015; Brand, 2016). Regarding the cytoplasm, transmembrane NOXs and DUOXI-II are the main contributors of ROS, generating $O2^{-}$ through the reduction of molecular oxygen. Cells possess a sophisticated antioxidant defense system to combat ROS and the superoxide dismutase (SOD) family plays a crucial role in this defense. The mitochondrial MnSOD (SOD2) and cytosolic/extracellular Cu/ZnSOD (SOD1 and ECSOD/SOD3) isoforms convert superoxide anions into oxygen and hydrogen peroxide. Subsequently, enzymes like glutathione peroxidase and catalase neutralize hydrogen peroxide, transforming it into water (Lubos et al., 2011; Dimauro et al., 2020). Furthermore, cellular signaling pathways involving transcription factors like NRF2/KEAP1, FoxO, and p53 act as sentinels, detecting oxidative stress and promoting the expression of antioxidant genes to maintain cellular homeostasis (Ward, 2017; Sinenko et al., 2021; Jena, 2023). ROS also play a role in regulating mitochondrial dynamics and stability, by influencing processes like mitochondrial fission, fusion, and autophagy. However, when the balance between ROS production and the antioxidant defense system is disrupted, oxidative stress can lead to mitochondrial dysfunction and ultimately, cell death through apoptosis. Therefore, ROS production within mitochondria is a complex phenomenon with both beneficial and detrimental consequences for cellular health. Understanding the intricate interplay between ROS generation, antioxidant defenses, and mitochondrial dynamics is crucial for developing therapeutic strategies to combat diseases associated with mitochondrial dysfunction (Willems et al., 2015; Ježek et al 2018; Geldon et al.,2021).

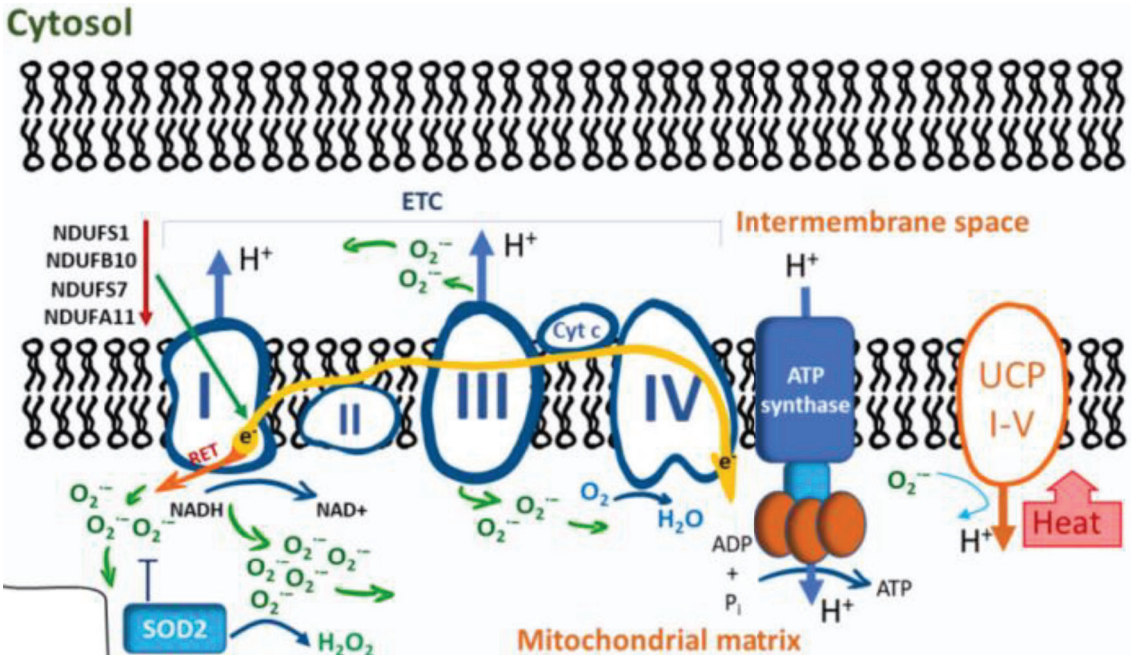

Figure 7. **Mitochondria: the OXPHOS system and ROS production**. From Sinenko et al., 2021.

3.1.2 The role of ROS in the pathophysiology of X-ALD

Peroxisomal diseases, and X-ALD in particular, are strongly linked to oxidative stress, a major contributor to their pathological progression (Galea et al., 2012; Singh and Pujol, 2010). Early evidence for this association in X-ALD emerged from studies demonstrating: a) a higher degree of LDL (low-density lipoprotein) oxidation in plasma from X-ALD patients compared to healthy controls (Di Biase et al., 2000); b) elevated expression of inducible nitric oxide synthase (iNOS), an enzyme able to generate the potent free radical nitric oxide, in astrocytes and microglia isolated from X-ALD patient brain tissue, but not in controls (Gilg et al., 2000).

The significance of oxidative damage in X-ALD was further solidified by its detection in various biological samples from patients. Elevated levels of oxidative stress markers were observed in plasma, erythrocytes, fibroblasts and lymphoblasts from X-ALD patients (Petrillo et al., 2013; Vargas et al., 2004, (Uto et al., 2008). In addition, studies have

shown evidence of oxidative stress in the adrenal cortex and brain sections of young X-ALD patients with the cerebral phenotype (Powers et al., 2005). Many oxidative markers such as manganese SOD (MnSOD), HO-1, lipid peroxidation 4-hydroxynonenal (4-HNE), malondialdehyde (MAL), and oxidized proteins (protein carbonyl) were found in the postmortem brains of patients with AMN and ccALD (Powers et al., 2005), and the immunoreactivities of these indexes are related to the degree of inflammation and myelin destruction (Powers et al., 2005; Vargas et al 2004;Yu J et al., 2022).

Intriguingly, research suggests a potential protective mechanism against oxidative stress in neurologically asymptomatic X-ALD cases. Studies have shown interesting results about:

a) total antioxidant status: this measure of the body's overall antioxidant capacity appears to be decreased only in neurologically symptomatic X-ALD patients, not in asymptomatic individuals (Deon et al., 2007). This suggests that asymptomatic patients may possess a yet-to-be-identified antioxidant defense mechanism that protects them from the detrimental effects of oxidative stress.

b) Oxidative stress in female carriers: female carriers of the X-ALD mutation, despite being asymptomatic, exhibit signs of oxidative stress, evident by increased lipid peroxidation products and decreased antioxidant reactivity in their plasma. However, their total antioxidant capacity remains unaltered (Deon et al., 2008). An additional layer of complexity arises from the lack of correlation observed between oxidative stress markers measured in plasma of female carriers with the levels of VLCFAs (Deon et al., 2008). However, it is important to note that limitations exist in the methods used to assess oxidative stress markers. These limitations, such as the non-quantitative nature of some assays and the lack of specificity of certain chemical reagents, could potentially obscure the true relationship between these markers and X-ALD (Halliwell and Whiteman, 2004).

Our research group employed sensitive techniques, such as gas chromatography/mass spectrometry, on 3.5-month-old Abcd1 null mice and discovered that oxidative stress is, in fact, an early event in X-ALD pathophysiology, particularly within the spinal cord

(Fourcade et al., 2008). This notion is further supported by the observation that fibroblasts and peripheral blood mononuclear cells (PBMCs) isolated from X-ALD patients exhibit a significant increase in specific biomarkers of oxidative damage. These biomarkers include:

- Glutamic semialdehyde (GSA) and aminoadipic semialdehyde (AASA) for protein carbonylation;

- Nε-(carboxymethyl)-lysine (CML) and Nε-(carboxyethyl)-lysine (CEL) for glycoxidation/lipoxidation;

- Nε- MDA-lysine (MDAL) for lipoxidation (Fourcade et al., 2008; Fourcade et al., 2010).

As *Abcd1* knockout mice reach 12 months of age, they accumulate even more oxidative damage products arising from various processes like metal-catalyzed oxidation and glycoxidation/lipoxidation (Fourcade et al., 2008). Interestingly, the severity of lipoxidative protein damage appears to correlate with the degree of VLCFA accumulation. This observation is further strengthened by studies using double knockout mice deficient in both *Abcd1* and *Abcd2* genes (Fourcade et al., 2010; Pujol et al., 2004). These mice exhibit a more aggressive disease course with a more severe neurodegenerative phenotype, characterized by axonal damage, behavioral abnormalities, and impaired peripheral nerve conduction (Ferrer et al., 2005; Pujol et al., 2004).

Our research has also revealed that *Abcd1*- mice suffer from impaired bioenergetic homeostasis, likely due to the oxidation of key enzymes involved in the glycolytic pathway and the Krebs cycle (Galino et al., 2011; Lopez-Erauskin et al., 2013b). This translates to decreased activity of pyruvate kinase, reduced levels of ATP and NADH, and diminished glutathione (GSH) pools (Galino et al., 2011).

Furthermore, a functional analysis of gene expression data from the spinal cord of X-ALD mice and the normal-appearing white matter (NAWM) of X-ALD patients revealed widespread dysregulation in genes associated with mitochondrial function. These genes are critical for components like the pyruvate and oxoglutarate dehydrogenase complexes, the TCA cycle, the OXPHOS system, and antioxidant defenses (Schluter et al., 2012).

VLCFA accumulation itself appears to be a driving force behind the redox imbalance observed in X-ALD. Excess C26:0 fatty acids have been shown to generate ROS in various cell types, including human fibroblasts (Fourcade et al., 2008; Fourcade et al., 2010), immortalized neuronal and oligodendrocyte cell lines (Baarine et al., 2012; Zarrouk et al., 2012), and even mitochondria and primary astrocytes isolated from both wild-type and *Abcd1*-deficient mice (Kruska et al., 2015).

In X-ALD fibroblasts, ROS generated by C26:0 can directly damage mitochondrial DNA (mtDNA) and impair the OXPHOS system. This damage, in turn, triggers further ROS production from electron transport chain complexes within the mitochondria (Lopez-Erauskin et al., 2013b). Collectively, this body of evidence strongly suggests that oxidative stress plays a pivotal role in X-ALD pathogenesis.

Recent findings from our group further emphasize the critical role of maintaining redox homeostasis in X-ALD. One study demonstrated that the NRF2 antioxidant response pathway is blunted in *Abcd1*$^{-}$ mice. However, oral administration of dimethyl fumarate, an NRF2 activator currently used in multiple sclerosis treatment, was able to restore this pathway's function (Ranea-Robles et al., 2018). Additionally, a phase II clinical trial in AMN patients showed that a combination antioxidant therapy was able to normalize several markers of inflammation and oxidative damage (Casasnovas et al., 2019).

3.2 Mitochondria impairment

3.2.1 Mitochondria in health and disease

Mitochondria, often dubbed the "powerhouses" of the cell, play a pivotal role in a vast array of biological processes, extending far beyond energy production (Chen et al., 2023). Nestled in the cellular cytoplasm, these elliptical organelles (Picard et al., 2011) are part of a network that is closely integrated with other cellular compartments, including the peroxisome (Schrader et al., 2015), and orchestrate the metabolism of carbohydrates, fats and amino acids, generating ATP via the electron transport chain and oxidative

phosphorylation. However, their role extends far beyond mere energy production; mitochondria safeguard cellular health in crucial ways, including (Osellame et al., 2012; Casanova et al, 2023; Harrington et al., 2023):

a) intracellular calcium regulation: mitochondria act as calcium reservoirs, releasing it when needed to activate essential cellular signals. Maintaining an optimal calcium balance is critical for diverse cellular functions, including muscle contraction, neurotransmission, and hormone secretion.

b) ROS management: as a byproduct of cellular respiration, mitochondria produce ROS. If not adequately controlled, these compounds can damage DNA, proteins, and lipids, leading to oxidative stress and contributing to chronic diseases. As already mentioned, mitochondria are equipped with antioxidant mechanisms to neutralize ROS and maintain cellular redox balance.

c) apoptosis: mitochondria play a key role in programmed cell death, an essential physiological process for eliminating damaged or infected cells and maintaining tissue homeostasis. In response to harmful stimuli, mitochondria release molecules that initiate the cascade of events leading to the controlled self-destruction of the cell.

d) cellular signaling: mitochondria communicate with other cellular organelles and the nucleus, influencing gene expression and the cellular response to external stresses. This intricate signaling network is crucial for cellular adaptation and survival.

Mitochondrial dysfunction, caused by genetic mutations, environmental factors or aging, is implicated in a wide spectrum of diseases, including neurodegenerative, cardiovascular, metabolic, and neoplastic disorder and understanding the molecular mechanisms underlying mitochondrial dysfunction is essential for developing novel therapeutic strategies for these pathologies (Murphy et al, 2018; Chen W. et al, 2023).

3.2.1a Mitochondria: a closer look at membranes and energy production

The double membrane of mitochondria shares some similarities with the eukaryotic plasma membrane in terms of protein and phospholipid composition. The outer mitochondrial membrane (OMM) acts as a communication hub, connecting mitochondria with components in the cytosol through various protein complexes. These include different forms of the translocase of the outer membrane (TOM) and the mitochondrial import complex (MIM) (Wiedemann et al., 2017; Guo et al., 2018). In contrast, the inner mitochondrial membrane (IMM) boasts a much larger surface area than the OMM. This extensive surface area is created by invaginations of the IMM, forming the characteristic cristae. The intricate morphology of the cristae results from a dynamic balance between mitochondrial membrane fusion and fission events. This plasticity allows the mitochondria to adapt their structure and function based on their energy demands (Guo et al., 2018). Embedded within the IMM are the respiratory chain complexes, the powerhouses of oxidative phosphorylation (OXPHOS). During OXPHOS, electron carriers like NAD+ and FAD are reduced to NADH and FADH2, respectively, fueling the process of ATP production. Electrons from NADH and FADH2 are then shuttled through the four complexes (complexes I to IV) of the electron transport chain within the IMM. The final acceptor of these electrons is oxygen (O2), leading to the formation of water (figure 7). Importantly, the energy released by the oxidation of NADH and FADH2 is not directly used to generate ATP. Instead, this energy is harnessed by the ETC to pump protons from the mitochondrial matrix across the IMM into the intermembrane space. This movement of protons creates an electrochemical gradient across the inner membrane, a store of potential energy. This energy is then utilized by ATP synthase (complex V) to phosphorylate ADP, producing ATP (Sinenko et al., 2021; Vercellino and Sazanov, 2022; Cooper et al., 2015; Nath et al., 2015).

Maintaining the structure and function of the cristae is crucial. Specific proteins, tightly regulated by the Mitochondrial Contact Site and Cristae Organizing System (MICOS), stabilize the junctions between cristae. MICOS plays a critical role in shaping the cristae, thereby influencing the assembly and efficiency of respiratory chain complexes.

Consequently, defects in cristae organization are directly linked to mitochondrial dysfunction (Li et al., 2020; Xue et al., 2019; Glancy et al., 2020).

3.2.1b Mitochondria and their role in amino acids metabolism

While renowned for their role in energy production, mitochondria extend their influence far beyond, acting as central hubs for cellular metabolism. In particular, amino acids metabolism is intricately linked to these organelles (Guda et al., 2007; Li et al., 2023).

The fate of amino acids within the cell hinges on a delicate balance: they can serve as the building blocks for protein synthesis, be oxidized for energy generation, or act as precursors for essential metabolites involved in gene expression, protein modifications, and cell fate decisions (Martínez-Reyes and Chandel, 2020). Crucially, the enzymes governing amino acid metabolism largely reside within the mitochondria (Guda et al., 2007). For instance, the degradation of Branched-Chain Amino Acids (BCAAs) – namely valine, leucine, and isoleucine – primarily occurs within the mitochondrial matrix. The lone exception is the initial transamination step, which takes place in the cytoplasm (Neinast et al., 2019). Disruptions in the function of these mitochondrial enzymes are often linked to various human mitochondrial diseases and disorders like illustrated by Burrage et al. (2014).

Interestingly, the interplay between mitochondria and amino acid metabolism extends beyond catabolism for energy production. Similar to the TCA cycle, the OXPHOS machinery plays a critical role in anabolism: specifically, the synthesis of certain amino acids hinges on a functional OXPHOS system, which is essential for cell proliferation. For example, studies have shown that inhibiting respiratory chain activity leads to auxotrophy for electron acceptors, hindering aspartate synthesis and limiting cell proliferation. However, the addition of exogenous electron acceptors, such as pyruvate or alpha-ketobutyrate, can rescue cell proliferation in cells with respiratory deficiencies. Furthermore, supplementing cells lacking an electron acceptor with aspartate can restore their proliferative capacity. These findings strongly suggest that a functional respiratory

chain is indispensable for cells to generate aspartate (Birsoy et al., 2015; Cardaci et al., 2015; Sullivan et al., 2015). Therefore, mitochondria are versatile organelles that are not only essential for the breakdown of amino acids for energy but also play a surprisingly vital role in their synthesis, thereby underscoring their multifaceted contribution to cellular function and health.

3.2.1c Mitochondria – nucleus interplay

The intricate interplay between the nucleus and mitochondria, often termed bidirectional micronucleus communication, plays a pivotal role in maintaining cellular homeostasis and influencing disease development (Quirós et al., 2016; Mottis et al., 2019). This communication extends beyond mere metabolic exchanges and encompasses a profound epigenetic dialogue, where the nuclear epigenome shapes mitochondrial function and, conversely, mitochondrial signaling molecules influence nuclear epigenetic modifications (Wiese and Bannister, 2020). Epigenetic regulation, responding to environmental stimulation to regulate gene expression without changing the genome, encompasses a diverse array of mechanisms (Golbabapour et al., 2011):

a) DNA methylation: this process involves adding a methyl group to the 5th position of cytosine residues, forming 5-methylcytosine (5mC). This modification typically occurs at CpG dinucleotides. Three DNA methyltransferases (DNMTs) – DNMT1, DNMT3A, and DNMT3B – are key players in this process. DNMT1 maintains methylation patterns after DNA replication, while DNMT3A and DNMT3B are responsible for de novo methylation (Pradhan et al., 1999; Ramsahoye et al., 2000).

b) Histone post-translational modifications: these modifications, such as acetylation and methylation, can alter chromatin structure and accessibility, affecting gene expression.

c) Chromatin open state: the physical compaction of chromatin can influence gene accessibility.

d) Non-coding RNA regulation: non-coding RNAs, such as microRNAs, play a role in regulating gene expression.

Mitochondrial metabolites serve as substrates and cofactors for enzymes involved in nuclear epigenetic modifications (figure 8) (Xu S. et al., 2021):

1) derived from fatty acid synthesis and glycolysis, acetyl-CoA serves as a source of acetyl groups for histone acetylation and can be transported between the nucleus and cytoplasm through nuclear pores;

2) NAD^+ acts as a cofactor for sirtuin (SIRT1 and 2) deacetylases. In the TCA cycle, NAD^+ is converted to NADH, and then back to NAD+ by complex I and III of the electron transport chain. NAD+ and NADH can be exchanged between the cytoplasm and mitochondria via shuttles;

3) S-adenosyl methionine (SAM) is a methionine metabolite that is a vital source of methyl groups for both DNA and histone methylation in the nucleus. SAM is synthesized through the coupled folate and methionine cycles in the cytoplasm, which are dependent on one-carbon (1C) metabolism in mitochondria. Therefore, mitochondrial 1C metabolism and ATP production contribute to maintaining cytoplasmic SAM levels and thus influence the nuclear epigenome. Changes in cellular metabolism can directly affect DNA methylation through fluctuations in SAM and SAH (S-adenosyl homocysteine) levels, which in turn regulate methyltransferase activity (Chiang et al., 1996; Medina et al., 2001; Agrimi et al., 2004; Tibbetts and Appling, 2010; Ouyang et al.,2020, Ormazabal et al., 2015; Xu S. et al., 2021; Sanderson et al., 2019).

4) α-ketoglutarate, a key intermediate in the TCA cycle, acts as a cofactor for Jumonji C domain demethylases and Ten Eleven Translocation (TET) DNA demethylases (Rasmussen et al, 2016; Xu et al., 2011). These intermediates may be directly or indirectly provided by mitochondria and affect the epigenetic regulation of the nuclear genome.

Additionally, although the mitochondrial genome lacks histones, mtDNA can be modified by methyltransferase to participate in epigenetic regulation. In recent years, there has been

an increasing interest in mtDNA methylation in neurodegenerative diseases (Coppedè F. et al., 2019; Xu S. et al., 2021).

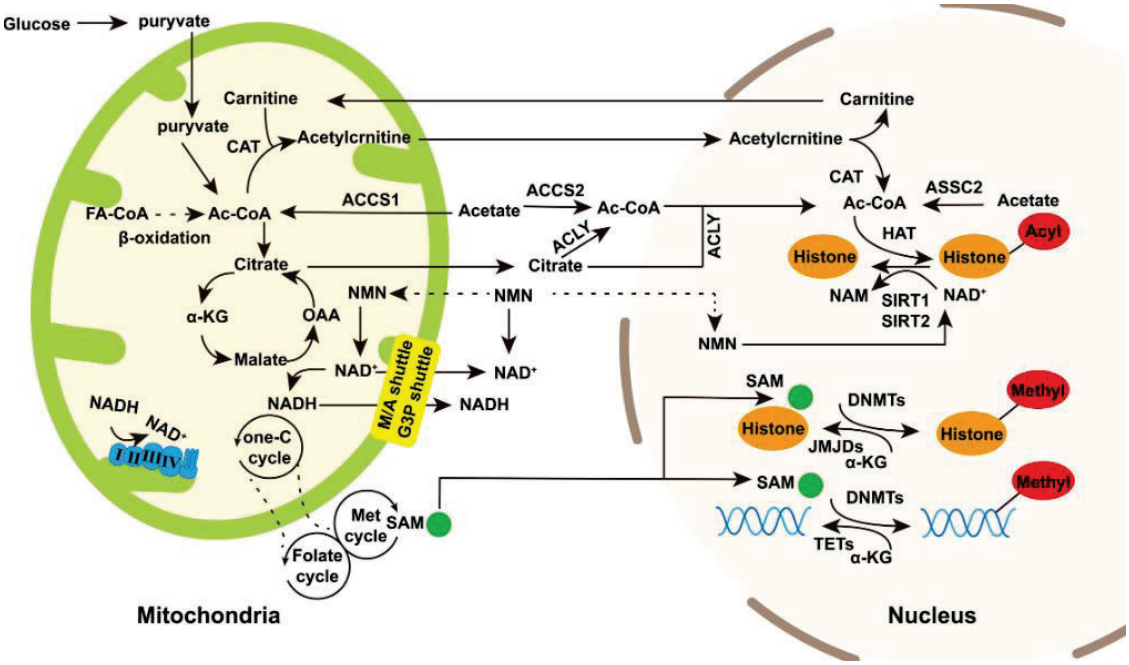

Figure 8. **The regulation of mitochondrial intermediate metabolites to nuclear epigenetics**. From Xu S. et al, 2021. Abbreviations: FA-CoA, fatty acyl CoA; ac-CoA, acetyl-CoA; CAT, carnitine acetyltransferase; OAA, oxaloacetic acid; ACLY, ATP-citrate lyase; NMN, nicotinamide mononucleotide; M/A shuttle, malate/aspartate shuttle; and G3P shuttle, glyceraldehyde 3-phosphate shuttle.

3.2.1d Mitochondria and their role in inflammation

Mitochondria, remnants of ancient α-proteobacteria, first appeared within eukaryotic cells approximately two billion years ago through a presumed endosymbiotic event (Roger et al., 2017; Hampl et al., 2019). Despite this seemingly symbiotic relationship, mitochondria retain their own genome, a potential source of conflict within the host cell. Mitochondrial DNA (mtDNA) is a compact, circular molecule of double-stranded DNA (~16.6 kb) encoding 37 genes. These genes include 13 mRNAs for key components of the oxidative phosphorylation system (including 7 of the 46 subunits of complex I, cytochrome b of complex III, 3 of the 13 subunits of complex IV, and 2 of the 16 subunits

of complex V), along with 2 ribosomal RNA (rRNA) components (12S and 16S) and 22 transfer RNAs (tRNAs) (West et al., 2015; Roger et al., 2017; Hampl et al., 2019; Mercer et al., 2011; Rackham et al., 2011). The mitochondrial transcription machinery is distinct from the nuclear system and relies on an RNA polymerase (POLRMT), two transcription factors (TFAM and TFB1M/TFB2M), and a family of termination factors (mTERFs) (Larsson et al., 1998; Bonawitz et al., 2006). Replication involves the heterotrimeric mtDNA polymerase gamma (POLG), the hexameric DNA helicase TWINKLE, and the tetrameric mitochondrial single-stranded DNA-binding protein (mtSSB) (Lee et al., 2009; Milenkovic et al., 2013; Korhonen et al., 2004). Notably, with an estimated 1,000 proteins residing in the mitochondria, all but those encoded by mtDNA are translated in the cytosol and subsequently imported (Fox, 2012).

Compared to nuclear DNA, mtDNA lacks the protective histones and is more susceptible to nuclease degradation (Gambardella et al., 2019). Consequently, mtDNA mutations accumulate at a rate 10–200 times higher than nuclear DNA, with a propensity for deletions and point mutations (Annesley and Fisher, 2019). This heightened vulnerability stems from its close proximity to the electron transport chain, a major source of reactive oxygen species. mtDNA oxidation contributes to the pathogenesis of various diseases, including cancer (Chatterjee et al., 2006), diabetes (Jiang et al., 2018), and aging (Larsson, 2010; Wang et al., 2019). A landmark study by Collins et al. (2004) demonstrated that injecting mtDNA into mice joints triggered localized inflammation and arthritis. Notably, inflammation was dependent on the presence of oxidatively damaged mtDNA bases: an injection of an oligodeoxynucleotide with the same sequence but without the oxidised residue had no effect, highlighting the role of damage-associated molecular patterns (DAMPs) in this process. This discovery unveiled mtDNA's capacity to stimulate pattern recognition receptors (PRRs), a diverse family of immune sensors that recognize pathogen-associated molecular patterns (PAMPs) and DAMPs (Brubaker et al., 2015; Gong et al., 2019). The four main classes of PRRs include NOD-like receptors (NLRs), Toll-like receptors (TLRs), RIG-I-like receptors (RLRs), and C-type lectin receptors (CLRs). Upon recognition of PAMPs or DAMPs, PRRs activate various

signaling pathways, ultimately leading to the upregulation of type I interferons, pro-inflammatory chemokines, and cytokines (Li D. et al, 2021).

Cellular stress, mitochondrial dysfunction, and cell death can lead to the release of mtDNA into the cytoplasm and even the extracellular space. This phenomenon, documented in various processes like infection, neurodegeneration, and neuroinflammation (Lin et al., 2022), positions mtDNA as a critical DAMP. As a DAMP, released mtDNA acts as a potent trigger for a diverse array of PRRs, initiating robust innate immune responses and several well-characterized pathways that mediate the proinflammatory effects of mtDNA release (figure 9). These include (Zhang X et al, 2019; Zhong F. et al.,2019, Riley et al., 2020):

a) cGAS-STING pathway: cytosolic mtDNA activates the cGAS-STING pathway, leading to the production of cyclic GMP-AMP (cGAMP), a molecule that stimulates STING and promotes inflammation (Bai et al., 2017);

b) TLR9 signaling: mtDNA contains unmethylated CpG motifs, which serve as ligands for TLR9. Upon binding to TLR9, primarily located on endosomal membranes, mtDNA triggers an inflammatory response through the NF-κB pathway via MyD88 and MAPK activation;

c) NLRP3 inflammasome activation: mtDNA can also activate the NLRP3 inflammasome, leading to the production of pro-inflammatory cytokines IL-1β and IL-8.

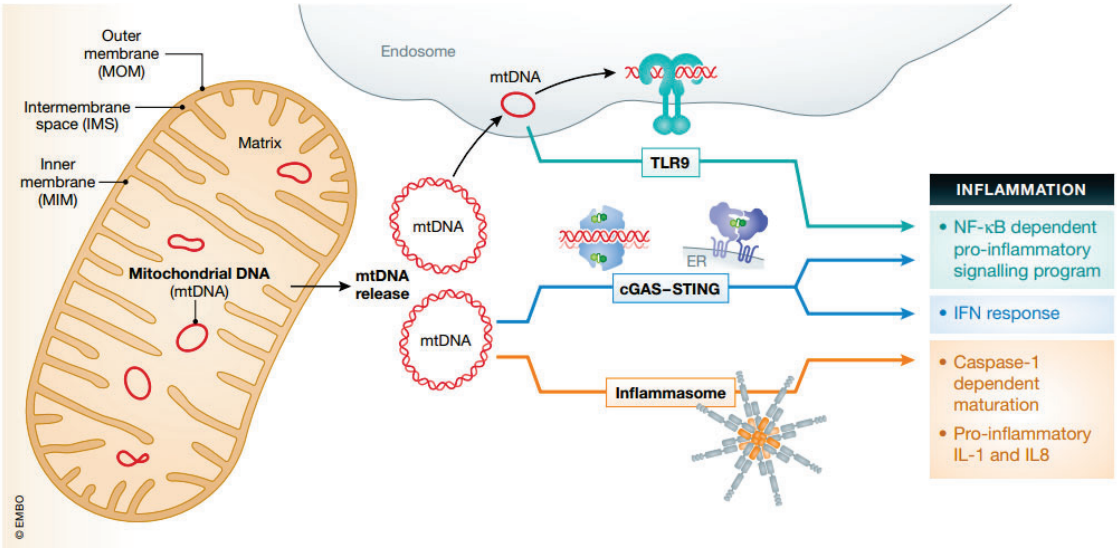

Figure 9. Overview of pro-inflammatory signalling pathways triggered by mitochondrial DNA. Top: TLR9 binds mtDNA in the endosome and triggers an NF-kB-dependent pro-inflammatory signalling programme. Middle: cGAS recognises mtDNA in the cytosol and activates endoplasmic reticulum (ER)-localised STING, triggering an interferon response. Bottom: mtDNA-dependent inflammasome activity leads to caspase-1-dependent maturation or pro-inflammatory IL-1 and IL-8 (from Riley et al., 2020).

3.2.1e Mitochondria dynamics

Mitochondria are not static structures: they undergo a continuous, coordinated cycle of fission and fusion events. This dynamic process ensures proper mitochondrial morphology, function, and quality control. Additionally, a cellular process called mitophagy selectively removes damaged or superfluous mitochondria from the network via autophagy, a form of cellular housekeeping. Maintaining a delicate balance between these various aspects of mitochondrial dynamics is crucial for optimal mitochondrial health and cellular well-being (Nisoli et al., 2004; Stetler et al., 2013).

Several GTPase proteins orchestrate the fusion and fission events that maintain normal mitochondrial shape and size. Key players in this process include (figure 10):

a) Dynamin-related protein 1 (DRP1): this cytosolic protein gets recruited to the outer mitochondrial membrane (OMM) to initiate fission events.

b) Mitochondrial fusion protein 1 (MFN1) and Mitochondrial fusion protein 2 (MFN2): these transmembrane proteins located on the outer mitochondrial membrane promote fusion events between mitochondria.

c) Optic atrophy protein 1 (OPA1): Residing in the inner mitochondrial membrane (IMM), OPA1 helps maintain a balance between fission and fusion processes (Friedman and Nunnari, 2014).

When mitochondria become dysfunctional or damaged, mitophagy comes into play. This selective degradation process involves engulfing targeted mitochondria by double-membrane autophagosomes, followed by their fusion with lysosomes for degradation. Two key proteins are essential for this mitochondrial quality control machinery:

1) Mitochondrial PTEN-induced putative kinase 1 (PINK1): located on the outer mitochondrial membrane, PINK1 plays a critical role in targeting damaged mitochondria for mitophagy.

2) Cytosolic ubiquitin E3 ligase Parkin: this cytosolic protein gets recruited to damaged mitochondria by PINK1 and facilitates their elimination through mitophagy. Interestingly, mutations in both PINK1 and Parkin are linked to familial forms of Parkinson's disease (Valente et al., 2004; Kitada et al., 1998; Pickrell and Youle, 2015).

Several abnormalities in mitochondrial dynamics and function can have detrimental consequences for cellular health (Li P. et al., 2015, Bustamante-Barrientos et al., 2023), including: disruptions in the electron transport chain and ATP synthase machinery can compromise a cell's ability to generate ATP; mitochondrial structural abnormalities due to impaired dynamics can lead to an upsurge in ROS production, further damaging cellular components; damaged mitochondria may release factors that trigger programmed cell death; increased ROS can damage mtDNA, which can contribute to aging and various chronic diseases, including neurodegenerative pathologies.

Therefore, maintaining a healthy balance between mitochondrial fission, fusion, and mitophagy is essential for proper mitochondrial function and cellular health: disruptions

in these processes can lead to a cascade of events, including decreased ATP production, increased ROS generation, and ultimately, cell death.

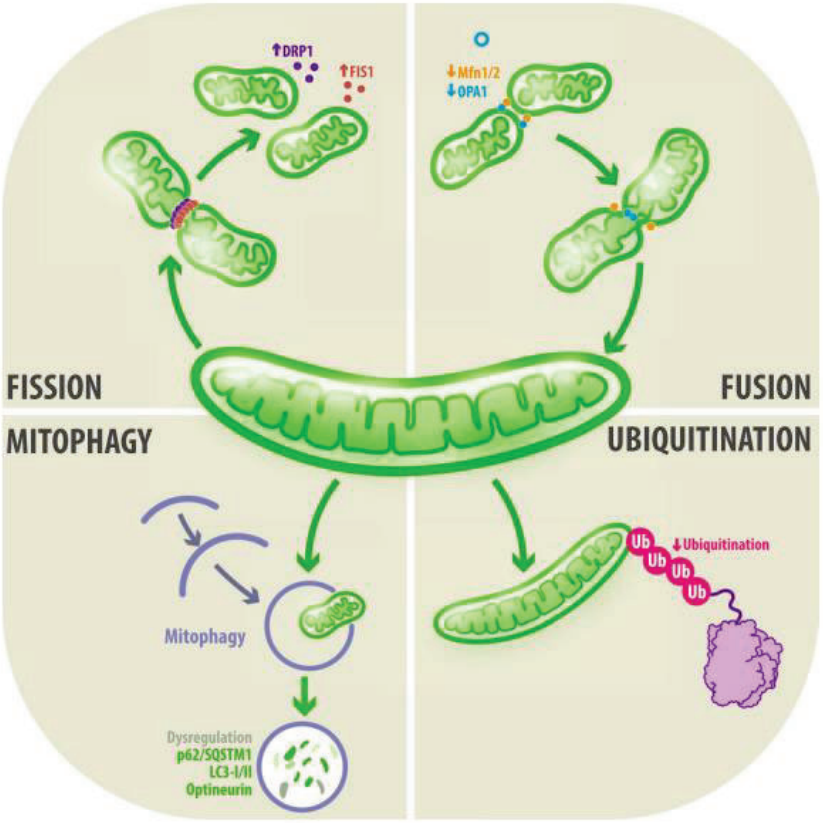

Figure 10. The accurate interaction between mitochondria dynamics and mitophagy. From Bustamante-Barrientos, 2023.

3.2.1f Mitochondria and the central nervous system

The brain, despite accounting for only 2% of total body mass, is an energy-intensive organ, consuming a remarkable 20% of the body's oxygen and 25% of its glucose (Cobley et al., 2018). This energy demand is primarily driven by neurotransmission (Bélanger et al., 2011), however, the significance of mitochondria extends beyond neurons, as proper

mitochondrial function is essential for other cells within the central nervous system as well (Angelova et al., 2016, 2018): in oligodendrocytes, the cells responsible for insulating neuronal processes with a myelin sheath, mitochondrial activity is crucial for generating the necessary lipids for this vital process (Schoenfeld et al., 2010; Silva et al., 2009; Viader et al., 2013; Ziabreva et al., 2010); similarly, astrocytes, which play a supportive role in neurotransmission by clearing glutamate from the synaptic cleft and supplying neurons with energy substrates, rely heavily on well-functioning mitochondria (Cambron et al., 2012). Thus, mitochondrial function is essential both in neurons and in glial cells, playing a central role in building and maintaining brain networks. When mitochondrial homeostasis is disrupted, it leads to progressive oxidative damage and an overall decline in cellular energy production (Gibson et al., 2010) and the delicate balance between fusion, fission, and mitophagy, the three key processes governing mitochondrial dynamics, is vital for synaptic transmission and neuronal survival.

The unique composition of the brain, characterized by high lipid content and limited antioxidant capacity, makes it highly susceptible to oxidative stress (Papadopulos et al., 2012; Cobley et al., 2018; Lee et al., 2020; Salim, 2017). This susceptibility is particularly pronounced in neurons due to several factors (Galea et al., 2012; Lee et al., 2012), like: 1) high metabolic activity: neurons have a high rate of oxidative metabolism, generating a significant amount of free radicals as a byproduct; 2) limited antioxidant defenses: compared to other cells, neurons express relatively low levels of antioxidant enzymes; 3) abundance of polyunsaturated fatty acids (PUFAs): neuronal membranes are rich in PUFAs, which are highly susceptible to oxidative damage; 4) high surface area-to-cytoplasm ratio: this large surface area makes neurons more prone to free radical attack; 5) non-replicating nature: unlike other cell types, neurons cannot readily divide to replace damaged cells.

Mounting evidence suggests a strong link between mitochondrial dysfunction and the development of neurodegenerative diseases such as Alzheimer's disease (AD), Parkinson's disease (PD), amyotrophic lateral sclerosis (ALS), and Huntington's disease (HD) (Lin and Beal, 2006; Yao et al., 2009; Chaturvedi and Flint Beal, 2013). In these diseases, mitochondria exhibit several abnormalities, including decreased activity of

respiratory chain enzymes, abnormal morphology, and a higher frequency of mutations in mtDNA (Chaturvedi and Flint Beal, 2013). Impairment of mitochondria results in defects in bioenergetics (Trigo et al., 2022), enhanced formation of free radicals/reactive oxygen species and consequent oxidative stress, ER stress, neuroinflammation, defective Ca^{2+} homeostasis (Halliwell et al., 2006; Calì et al., 2013; Abeti et al. 2015; Baev et al. 2022; Lin et al., 2006; Frank-Cannon et al., 2009), excitotoxicity, and disruption of axonal transport (Berth et al., 2023). A growing body of research suggests that dysfunctional mitochondria may not just be a consequence of neurodegenerative diseases, but potentially a primary cause (Tapias, 2019): this new perspective opens exciting avenues for therapeutic strategies focused on regulating mitochondrial function or modifying mitochondrial metabolites to combat neurodegenerative diseases (Zhang et al., 2023).

3.2.2 Mitochondrial dysfunction in X-ALD

While X-ALD is traditionally classified as a peroxisomal disease due to the underlying genetic defect, recent evidence suggests a more intricate interplay with mitochondria, positioning them as a central hub in the pathophysiology of the disease.

One study using isolated mitochondria from X-ALD mouse muscle did not detect any impairment in respiratory function (Oezen et al., 2005). However, this finding appears to contradict other observations. Morphological abnormalities in mitochondria have been reported in AMN patients (Powers et al., 2001; Schroder et al., 1996), as well as in other peroxisomal disorders like Zellweger syndrome (Goldfischer et al., 1973) and *Pex5*$^{-/-}$ mice (Baumgart et al., 2001; Peeters et al., 2015). Moreover, our group has recently revealed mitochondrial fragmentation in corticospinal axons in *Abcd1*- mice (Launay et al., 2024). These findings suggest a potential link between mitochondrial dysfunction and the broader spectrum of peroxisomal diseases.

Strengthening this connection, a functional analysis of gene expression data from X-ALD mice and patients revealed a common metabolic abnormality signature. This signature

included, among other pathways, significant mitochondrial dysregulation (Schluter et al., 2012).

Our research group has further elucidated the mechanisms by which VLCFAs contribute to mitochondrial dysfunction in X-ALD. We have demonstrated that:

a) VLCFA-derived ROS primarily originate in the mitochondria (Fourcade et al., 2008; Lopez-Erauskin et al., 2013b).

b) oxidative stress disrupts mitochondrial function: oxidative stress induced by ROS can lead to mitochondrial membrane depolarization (Fourcade et al., 2008; Lopez-Erauskin et al., 2013b); it can also trigger the opening of the mitochondrial permeability transition pore (mPTP) through the oxidation of Cyclophilin D (Lopez-Erauskin et al., 2012, 2013a), compromising mitochondrial function.

c) VLCFAs impair the Electron Transport Chain: in human skin fibroblasts, excess VLCFAs induce ROS formation specifically from complexes I and II of the ETC, while also hindering complex V function. This effect correlates with the oxidation of several subunits within complexes III and V observed in *Abcd1*- mouse spinal cord homogenates. Furthermore, both in vitro studies using fibroblasts and *ex vivo* studies using spinal cord slices have shown evidence of defective mitochondrial respiration (Lopez-Erauskin et al., 2013b).

d) In patient fibroblasts, an excess of VLCFAs triggers mitochondrial fragmentation through the redox-dependent phosphorylation of DRP1 (DRP1S616) (Launay et al., 2024).

Similar observations have been made in various cell lines and primary astrocytes: SK-NB-E neuroblastoma cell line (Zarrouk et al., 2012); B12 oligodendrocytes and U87 astrocytes (Baarine et al., 2015); primary astrocytes from wild-type and *Abcd1*-deficient mice (Kruska et al., 2015). In the latter study, Kruska et al. (2015) also reported a VLCFA-dependent reduction in calcium (Ca^{2+}) retention capacity within brain mitochondria isolated from 6 month old *Abcd1*$^{-}$ mice.

The critical role of oxidative stress and global mitochondrial dysfunction in driving axonal degeneration in X-ALD is further substantiated by studies demonstrating the ability to halt this damage through therapeutic interventions: a) the administration of antioxidant cocktails has been shown to effectively prevent axonal damage in X-ALD models (Galino et al., 2011; Lopez-Erauskin et al., 2011); this finding highlights the importance of oxidative stress in the disease process and the potential therapeutic benefit of strategies that target and neutralize free radicals; b) pioglitazone, a medication known to enhance mitochondrial function, has also demonstrated efficacy in preventing axonal degeneration in X-ALD models (Morato et al., 2013); this finding underscores the critical role of mitochondrial dysfunction in X-ALD pathogenesis and suggests that therapies aimed at improving mitochondrial health may hold promise for the treatment of this devastating disease.

4. Role of the immune system in X-ALD pathophysiology

Microglia and monocytes/macrophages are key components of the innate immune system (Li et al., 2017; Hirayama et al., 2017). In X-ALD, their dysfunction is increasingly recognized as a potential driver of pathology. Monocytes, the precursors of tissue macrophages, isolated from AMN patients, even in the absence of signs of an overt cerebral inflammation (Weinhofer et al., 2018), exhibit a proinflammatory phenotype and resist a shift towards an anti-inflammatory state. This finding aligns with the observation that, compared to multiple sclerosis (MS), another inflammatory demyelinating disease, ccALD lesions harbor minimal anti-inflammatory macrophages but retain a proinflammatory population (Weinhofer et al., 2018). This impaired phenotypic plasticity may underlie the rapid demyelination in ccALD, contrasting with the relapsing-remitting course of MS (Weinhofer et al., 2018).

Microglia, the resident immune sentinels of the CNS, collaborate with astrocytes and oligodendrocytes to maintain a balanced inflammatory environment crucial for neuronal health (Norris et al., 2019). Their activation, typically triggered by pathogen-associated molecular patterns or damage-associated molecular patterns binding to cell surface

receptors (PRRs) (Heneka et al., 2018), leads to inflammasome assembly, production of inflammatory cytokines, reactive oxygen species, and nitric oxide. Uncontrolled inflammation can culminate in neuronal death through pyroptosis. Therefore, a tightly regulated equilibrium between pro- and anti-inflammatory microglial activities is essential for CNS homeostasis. Even if the precise contribution of microglia to X-ALD pathogenesis remains elusive, intriguingly, microglia undergo programmed cell death and disappear from the perilesional white matter, where myelin and oligodendrocytes remain relatively intact (Bergner et al., 2019). The few remaining microglia lack typical markers like Tmem119 (Ruan et al., 2022) and P2ry12 (Gómez Morillas et al., 2021), suggesting an early depletion process preceding myelin breakdown and oligodendrocyte loss. Remarkably, microglia-like cells of unknown origin reappear in the advanced gliotic scar region (Bergner et al., 2019). Studies in the mouse model of X-ALD and AMN patients reveal a unique microglial response (Gong et al., 2017): despite evident morphological activation in *Abcd1*$^{-}$ mice, proinflammatory markers remain unchanged. However, in vitro challenge with lipopolysaccharide (LPS) elicits a more pronounced response, suggesting a primed state (Gong et al., 2017). Interestingly, these microglia exhibit early upregulation of phagocytic signaling molecules (MFGE8, Trem2) in the spinal cord and in vitro cultures, even preceding synaptic loss and axonal degeneration (Gong et al., 2017). A similar pattern of enhanced activation and phagocytosis markers, devoid of proinflammatory signatures, is observed in microglia isolated from the postmortem spinal cord of X-ALD patients (Gong et al., 2017).

The efficacy of hematopoietic stem cell transplantation or ex vivo gene-corrected autologous HSC transplantation in halting demyelination underscores the importance of the involvement of immune cells in the pathophysiology of the disease (Zhu J. et al., 2020). In particular, these transplanted stem cells are believed to differentiate into microglia-like cells within the brain (Zhu J. et al., 2020). Notably, this treatment fails to prevent the development of myeloneuropathy, suggesting distinct roles for different immune cell populations (van Geel et al., 2015).

5. X-ALD: working model of the disease

Based on the previous findings, our research group has proposed a model for how the excess of C26:0 VLCFA could trigger mitochondrial oxidative stress in X-ALD (Lopez-Erauskin et al., 2013) (figure 11). This model incorporates evidence suggesting that C26:0 fatty acids can replace the lateral chain of phospholipids of the MIM, increasing membrane microviscosity (Whitcomb et al., 1988), together with interfering with OXPHOS system and inducing ROS production (Lopez-Erauskin et al., 2013b).

Due to ABCD1 transporter deficiency, hexacosanoic acid (C26:0) accumulates intracellularly as it cannot be degraded within peroxisomes (point 1, figure 11). This buildup of C26:0 is hypothesized to alter the permeability of the inner mitochondrial membrane (IMM) through yet-to-be-identified mechanisms. Consequently, this altered permeability may lead to a decrease in the mitochondrial membrane potential ($\Delta\Psi m$) (point 2, figure 11). Furthermore, a degree of electron leakage from the electron transport chain could be induced, promoting the formation of reactive oxygen species (point 3, figure 11). These free radicals can then oxidize mitochondrial proteins crucial for the tricarboxylic acid cycle and OXPHOS, ultimately leading to impaired bioenergetics, compromised cellular respiration, and mtDNA oxidation. This cascade of events contributes to a vicious cycle that exacerbates mitochondrial dysfunction and ultimately culminates in cell death.

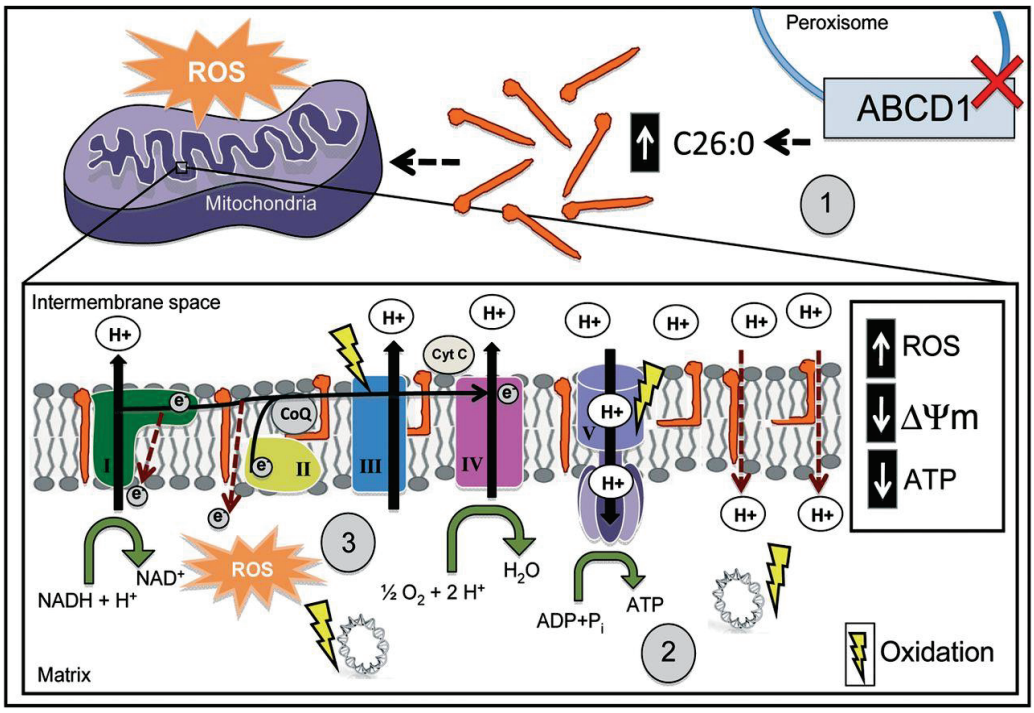

Figure 11. Working model of mitochondrial impairment mediated by excess of C26:0. Please see the text above for the detailed mechanism explanation. From Lopez-Erauskin et al., 2013.

The current model proposes that VLCFA accumulation initiates a cascade of detrimental events, including oxidative stress, inflammation, and peroxisomal dysfunction, all contributing to disease onset and progression. This concept is often referred to as the "three-hit hypothesis" (Singh and Pujol, 2010):

1) metabolic derangements**:** the first hit involves metabolic abnormalities characterized by excess VLCFAs and oxidative stress;

2) inflammatory response: this initial metabolic disruption triggers the second hit, leading to inflammatory pathology;

3) generalized peroxisome loss: subsequently, inflammatory mediators (cytokines and chemokines) further induce a generalized loss of peroxisomes, constituting the third hit.

This creates a vicious cycle culminating in cell death and progressive inflammatory demyelinating disease.

While adrenomyeloneuropathy was traditionally considered non-inflammatory, we have shown accumulating evidence suggesting the presence of significant, albeit tightly regulated, pro-inflammatory pathways (Yu J. et al., 2022). This pro-inflammatory state may represent the "default form" of the disease. Additional genetic or environmental factors could act as further "hits" on this pro-inflammatory background, potentially triggering the rapid progression and lethality observed in cerebral ALD forms.

Importantly, our research group has reported the normalization of several inflammatory markers and oxidative damage markers following antioxidant treatment. This finding highlights the intricate link between redox homeostasis and inflammatory processes in X-ALD (Casasnovas C. et al., 2019).

INTRODUCTION – PART 2

1 Bacteria structure and classification

The human body harbors a diverse community of single-celled microorganisms collectively termed the microbiota. These bacteria, lacking a nuclear membrane and replicating via binary fission, play a crucial role in health and disease (Baron, 1996). Despite their apparent simplicity, bacteria exhibit remarkable metabolic versatility, utilizing a vast array of substrates (Baron, 1996); ubiquitous and adept at adapting to changing environments, bacteria are key players across various medical fields (Baron, 1996). Co-evolution has fostered an intricate relationship between humans and their microbiota, with the latter significantly impacting the development and function of other bodily systems, including the nervous system (D'Argenio and Salvatore, 2015). This intricate link is further highlighted by the fascinating evolutionary origin of mitochondria, organelles hypothesized to have stemmed from free-living bacteria engulfed by ancestral eukaryotic cells billions of years ago (endosymbiotic theory) (Sagan, 1967). Over time, these engulfed bacteria transformed into mitochondria, establishing a symbiotic partnership with their host cells. While the endosymbiotic theory proposes a bacterial ancestry for mitochondria, the precise bacterial lineage remains under debate. Although Alphaproteobacteria are considered a potential source based on available evidence (Fan L. et al., 2020), the exact phylogenetic link to extant members within this phylum remains unclear. Alternatively, studies suggest a Rickettsiales origin for mitochondria (Andersson SG et al., 1998; Wang Z and Wu M., 2015). This shared bacterial heritage is reflected in the presence of their own circular DNA, distinct from the host nuclear genome, and their reliance on similar mechanisms for protein synthesis and energy production (Kurland CG. et al, 2000). Furthermore, the susceptibility of mitochondria to specific antibiotics targeting bacteria, such as quinolones and aminoglycosides, reinforces these structural and functional similarities (Kalghatgi S. et al., 2013).

Building upon the pioneering work of Antony van Leeuwenhoek, who observed microorganisms for the first time in 1676, Robert Koch established the field of medical microbiology two century later (Baron, 1996). Koch's contributions include the germ

theory of disease, the isolation of bacteria in pure culture, and the development of postulates to link specific bacteria to diseases (Yi-Wei et al., 2024). Initial studies of bacteria relied on light microscopy with various stains and dyes. These techniques revealed a diversity of sizes, shapes, and the presence of capsules in some bacteria. Notably, the Gram stain, developed by Hans Christian Gram in 1884, revolutionized bacterial classification by differentiating them into two major groups: gram-positive and gram-negative (Gram, 1884). This distinction hinges on the structure of the bacterial cell wall, specifically the peptidoglycan layer. Gram-positive bacteria retain the blue crystal violet stain during Gram staining due to their thicker peptidoglycan layer, while gram-negative bacteria lose this stain and require a counterstain for visualization (Gram, 1884). This method remains a cornerstone of bacterial identification today. Early microscopy also allowed visualization of inclusion bodies based on their dye reactions and the identification of a central area within the bacteria thought to be a nucleus. However, the limitations of light microscopy hindered the detailed study of bacterial ultrastructure. The invention of phase-contrast microscopy by Frits Zernike in 1930 enabled the examination of live, unstained bacteria (Zernike, 1942). Nevertheless, a complete understanding of bacterial fine structure remained elusive. The emergence of electron microscopy revolutionized our understanding of bacterial morphology. It revealed a vast array of shapes and surface appendages, including diverse injection systems employed by pathogenic bacteria (Yi-Wei et al., 2024). This leap in technology paved the way for a more precise and accurate classification system, which is fundamental for scientific exploration.

Organisms need a universally recognized name for collective study and practical applications. This is crucial, whether dealing with environmental plant pathogens, bioremediation tools, human pathogens, or symbiotic bacteria. Scientific organism classification utilizes a hierarchical ranking system with "Bacteria" occupying the highest rank or domain.

The taxonomic ranks for Escherichia coli illustrate this system (Yi-Wei et al., 2024):

1. Domain: Bacteria
2. Phylum: Proteobacteria
3. Class: Gammaproteobacteria
4. Order: Enterobacterales
5. Family: Enterobacteriaceae
6. Genus: *Escherichia*
7. Species: *Escherichia coli*

All bacteria are unicellular organisms that reproduce asexually through binary fission. Most bacteria are free-living and capable of independent growth. However, some species, like Chlamydia and Rickettsia, are obligate intracellular parasites, relying on host cells for survival (Salton and Kim, 1996). Due to their small size, bacteria are conveniently measured in microns (μm). Their size varies considerably, ranging from the large rod-shaped Bacillus anthracis (1.0-1.3 μm x 3-10 μm) to the minute coccus-shaped *Mycoplasma* (0.1-0.2 μm in diameter). This small size translates to a very high surface area-to-volume ratio, around 100,000, which significantly impacts their interactions with the environment (Salton and Kim, 1996). Bacterial cells exhibit distinct morphologies. Common shapes include cocci (spherical or oval, like *Staphylococcus aureus* and *Streptococcus*, respectively), rods (*Bacillus* and *Clostridium*), long branching filaments (*Actinomyces*), and curved or spiral forms (*Vibrio cholerae* and *Treponema pallidum*). The arrangement of these cells can also be characteristic of specific species or groups. Some bacteria form chains (*Streptococci*), grape-like clusters (*Staphylococcus aureus*), or cubic packets (certain cocci), while others grow as single cells. This morphological diversity plays a crucial role in bacterial identification and diagnosis (Salton and Kim, 1996). Electron microscopy offers superior resolution, allowing us to visualize not only the typical shapes of bacteria but also their internal organization. Unlike eukaryotes with a membrane-bound nucleus and various organelles, bacteria possess a simpler structure. Their genetic material is concentrated in a region called the nucleoid, lacking a nuclear

envelope. The plasma membrane, the outermost bacterial boundary, performs many of the functions typically carried out by organelles in eukaryotic cells (Salton and Kim, 1996).

Several surface structures can be present on bacterial cells, each contributing to various functions (figure 12):

a) flagella: these slender, hair-like protein appendages propel motile bacteria. Unlike eukaryotic flagella, bacterial flagella are anchored in the cell wall and rotate to generate movement. The number and arrangement of flagella can be diagnostically useful for specific bacterial species (Salton and Kim, 1996);

b) pili: these are thin, proteinaceous structures found on many bacteria, particularly Gram-negative ones. Pili play a crucial role in adhesion to host surfaces, enabling bacteria to attach to tissues and establish infections (Salton and Kim, 1996);

c) capsules: Some bacteria secrete a thick, viscous polysaccharide layer called a capsule around their cell wall. Others produce a more loosely organized slime layer. These structures can protect bacteria from phagocytosis by immune cells (Salton and Kim, 1996);

d) cell wall: the bacterial cell wall, a marvel of intricate engineering, stands as a defining characteristic of these microscopic organisms. Unlike their eukaryotic counterparts, bacteria rely on this complex, mesh-like structure for their very survival. The cell wall plays a multifaceted role, ensuring the maintenance of a distinct cell shape, providing structural integrity, and acting as a crucial barrier against the harsh external environment (Schneider and Sahl, 2010; Lovering et al. 2010; Clifton et al. 2013). This unique structure has garnered immense scientific interest for several reasons. Firstly, its essential nature for most bacteria, coupled with its absence in eukaryotes, makes it a prime target for antibiotic development. By disrupting the cell wall, antibiotics can effectively cripple bacterial growth and function (Schneider and Sahl, 2010). Secondly, fragments of the bacterial cell wall can trigger the immune system, sometimes with detrimental effects. These fragments can possess immunostimulatory and cytotoxic properties, contributing

to the development of various diseases (Goldman et al., 1982; Fleming et al., 1986; Royet et al., 2011; Sorbara and Philpott, 2011; Jutras et al., 2019). A key component of the bacterial cell wall is peptidoglycan (PG), a mesh-like structure shared by both Gram-positive and Gram-negative bacteria. This unique molecule, absent in eukaryotes, forms the very foundation of the bacterial cell wall and is responsible for its characteristic shape and mechanical strength. PG consists of a backbone made of sugar chains, specifically alternating units of N-acetylglucosamine (GlcNAc) and N-acetylmuramic acid (MurNAc) (Vollmer et al., 2008a). These sugar chains are further reinforced by short peptide bridges attached to the MurNAc residues. Interestingly, the degree of crosslinking between these peptides varies significantly between Gram-positive and Gram-negative bacteria. Gram-positive bacteria boast a highly crosslinked peptidoglycan network, contributing to their thicker cell walls. Conversely, Gram-negative bacteria possess a more loosely crosslinked peptidoglycan layer (Salton and Kim, 1996). This difference in crosslinking patterns is not only a defining characteristic used in bacterial classification but also plays a role in the effectiveness of certain antibiotics. Beta-lactam antibiotics, for example, target the enzymes responsible for crosslinking peptidoglycan, effectively inhibiting cell wall synthesis and compromising the integrity of the bacterial cell (Salton and Kim, 1996). The synthesis of peptidoglycan is a highly orchestrated process that unfolds outside the cytoplasm, on the cell's exterior. This intricate assembly line involves several key steps. First, precursor molecules, consisting of a disaccharide linked to a pentapeptide (five amino acids), are generated within the cytoplasm. These precursors are then shuttled across the cytoplasmic membrane by specialized transporter proteins called flippases (MurJ and/or Amj) (Ruiz, 2008). Finally, on the outside of the cell, a team of specialized enzymes takes over. Penicillin-binding proteins (PBPs) and Shape, Elongation, Division, and Sporulation (SEDS) proteins work in concert to assemble the peptidoglycan meshwork. PBPs are responsible for linking the sugar chains and crosslinking the peptide bridges, while SEDS proteins play a crucial role in shaping the cell wall during growth and division (Ruiz, 2008; Typas et al., 2011; Meeske et al., 2015, 2016; Cho et al., 2016; Taguchi et al., 2019). This elaborate assembly process is not static: the bacterial cell wall is a dynamic structure that constantly undergoes remodeling to accommodate growth and adapt to environmental changes. This vital process involves a diverse group of enzymes

known as autolysins, which can break down and modify various components of the peptidoglycan (Park and Uehara, 2008). This controlled breakdown allows for the insertion of new cell wall material during growth and facilitates cell division.

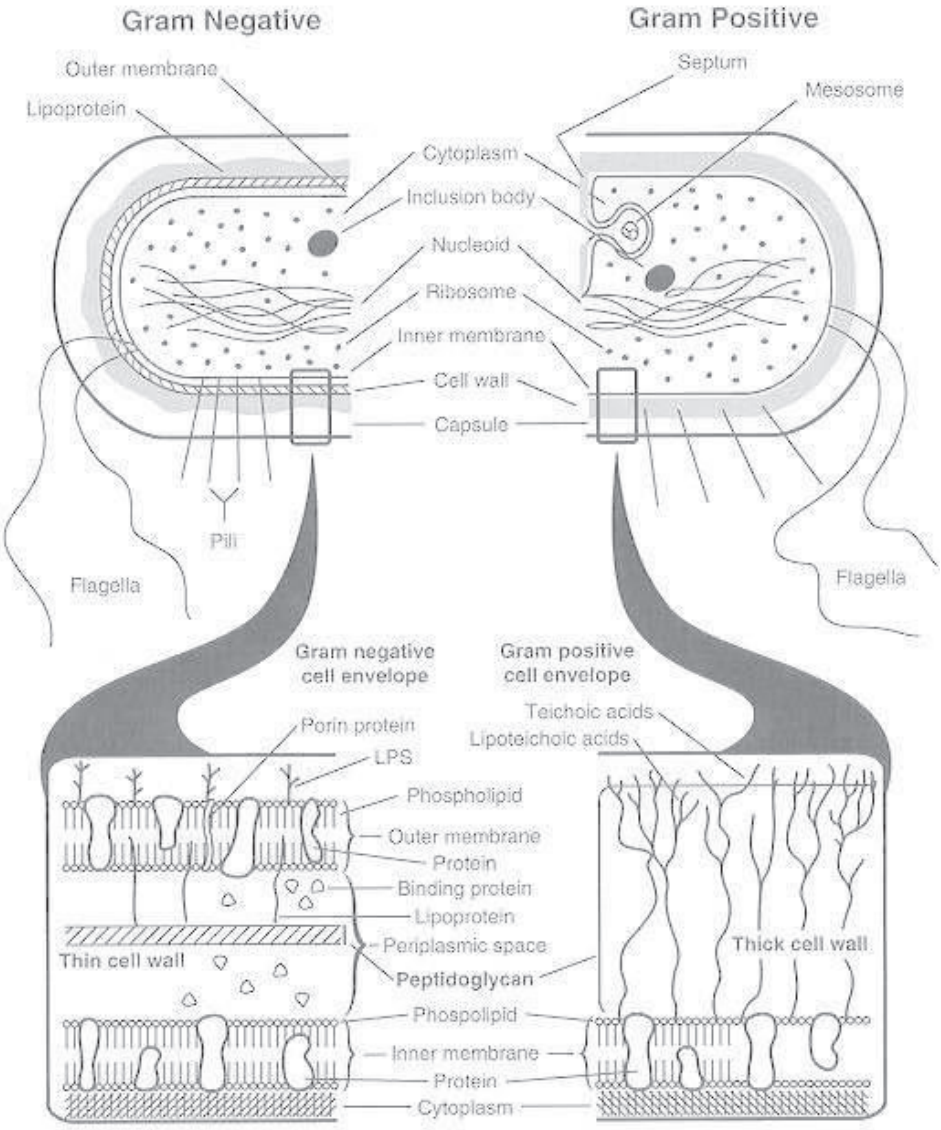

Figure 12. **Comparison of the thick cell wall of Gram-positive bacteria with the comparatively thin cell wall of Gram-negative bacteria.** Note the complexity of the Gram-negative cell envelope (outer membrane, its hydrophobic lipoprotein anchor; periplasmic space). From Salton and Kim, 1996. Hallmarks of gram-negative bacteria are the presence of an outer membrane, a well-defined periplasmic space, and the cytoplasmic membrane. In contrast, gram-positive bacteria exhibit a very thick cell wall built out of peptidoglycan (murein) and the underlying cytoplasmic membrane (Yi-Wei et al., 2024).

The intricate assembly of peptidoglycan involves a complex interplay between different enzymes. Class A PBPs and SEDS proteins work together like a well-oiled machine. Class A PBPs act as glycosyltransferases, linking the GlcNAc-MurNAc-pentapeptide units into long-chains (Zhao et al., 2017). SEDS proteins then play a crucial role in shaping the nascent peptidoglycan meshwork. Following this initial assembly, a complex dance unfolds to create the characteristic tight mesh of peptidoglycan. Class A and B PBPs, along with L, D-transpeptidases, collaborate to crosslink the peptide side chains extending from the MurNAc residues. While the specifics of this crosslinking process are still being unraveled, it is this intricate weaving of peptide bridges that creates the rigid and resilient meshwork that defines the bacterial cell wall (Zhao et al., 2017). The peptidoglycan meshwork serves as the foundation, but the bacterial cell wall can be further adorned with additional layers, adding complexity and diversity. Some Gram-positive bacteria, for instance, decorate their peptidoglycan with wall teichoic acids. These polyol phosphate polymers, bearing a strong negative charge, contribute to the overall architecture of the cell wall and can also play a role in immune recognition (Salton and Kim, 1996; Rajagopal and Walker, 2017). Lipoteichoic acids anchor themselves in the cytoplasmic membrane and extend outwards, contributing to the overall structure of the outer membrane. Interestingly, lipoteichoic acids can also play a role in pathogenesis, acting as antigens, cytotoxic agents, and even adhesins that allow bacteria to adhere to host cells (Salton and Kim, 1996). Mycobacteria, renowned for their resilience and resistance to antibiotics, take cell wall complexity to a whole new level. They add layers of polysaccharides and long-chain lipids on top of their peptidoglycan core, creating an even more formidable barrier against environmental threats (Jankute et al., 2015).

The bacterial cell wall faces a constant challenge – it needs to be rigid enough to withstand the internal pressure of the cytoplasm and the external assaults of the environment. Yet, it also needs to be flexible enough to allow for growth and division. This seemingly contradictory requirement is met through a remarkable process of dynamic remodeling. Autolysins, a diverse group of enzymes, play a critical role in this process. These enzymes can cleave and modify various components of the peptidoglycan meshwork, including the sugar backbone, peptide side chains, and crosslinks (Scheurwater et al., 2008; Vollmer et

al., 2008b). This controlled breakdown allows for the insertion of new cell wall material during growth and facilitates cell division by creating localized areas of weakness in the peptidoglycan. The remodeling process doesn't simply involve breaking down peptidoglycan components. Several enzymes, like PG-acetyltransferases, can modify the MurNAc residues, enhancing their resistance to lysozyme, an enzyme that can degrade peptidoglycan (Moynihan and Clarke, 2011). Additionally, L, D-transpeptidases can replace terminal D-alanine residues in the peptide side chains with alternative amino acids. This not only contributes to the overall diversity of the peptidoglycan structure but can also be exploited for labeling purposes with fluorescent compounds (Cava et al., 2011; Kuru et al., 2012). The importance of this dynamic remodeling process extends far beyond simple maintenance. It plays a crucial role in various cellular functions, including daughter cell separation after division, expansion of the cell wall during growth, and the insertion of essential protein complexes into the cell envelope (Scheurwater and Burrows, 2011; Vollmer, 2012; Johnson et al., 2013). While peptidoglycan is a defining characteristic of most bacteria, there are a few exceptions. Mycoplasma species, for instance, have dispensed with a cell wall altogether, relying solely on a strengthened cytoplasmic membrane for protection (Salton and Kim, 1996).

Unlike the typical phospholipid bilayer found in most bacterial membranes, Gram-negative bacteria possess a highly asymmetric outer membrane (OM) composed of an inner leaflet of phospholipids and an outer leaflet enriched with lipopolysaccharides (LPS) (Bertani and Ruiz, 2018). LPS are amphipathic molecules, meaning they possess both hydrophobic and hydrophilic regions. They typically consist of three distinct domains (figure 13):

1. Lipid A: the hydrophobic endotoxin moiety that anchors the LPS molecule to the outer membrane. This conserved region, typically an acylated β-1’-6-linked glucosamine disaccharide, plays a critical role in LPS virulence (Bertani and Ruiz, 2018; Steimle et al., 2016). The specific structure of Lipid A can vary between bacterial strains and species, influencing the degree of immune activation (Steimle et al., 2016).

2. Core Oligosaccharide: this hydrophilic region connects Lipid A to the O-antigen and is essential for maintaining membrane integrity (Bertani and Ruiz, 2018). Unlike Lipid A, the core oligosaccharide structure exhibits less variation among Gram-negative bacteria.

3. O-Antigen: the outermost and most variable domain of LPS, consisting of a repeating oligosaccharide unit. This highly diverse region is responsible for the antigenic specificity of LPS, allowing the immune system to distinguish between different bacterial strains (Bertani and Ruiz, 2018). In non-capsulated strains like *E. coli* and *Pseudomonas*, the O-antigen is directly exposed on the cell surface. Conversely, encapsulated bacteria like *Klebsiella pneumoniae* and *Haemophilus influenzae* have a capsular layer that partially obscures the LPS (Sperandeo et al., 2019).

LPS molecules play a crucial role in the structural integrity and function of the outer membrane. Lipid A serves as an effective permeability barrier, restricting the passage of small hydrophobic molecules that could freely traverse a phospholipid bilayer. This intrinsic resistance contributes to the inherent antibiotic tolerance of Gram-negative bacteria (Bertani and Ruiz, 2018).

Furthermore, LPS is a potent activator of the innate immune system. The highly conserved Lipid A moiety interacts with Toll-like receptors (TLRs) on immune cells, triggering an inflammatory response. This property allows LPS to be used as a marker for early infection detection (Sperandeo et al., 2019).

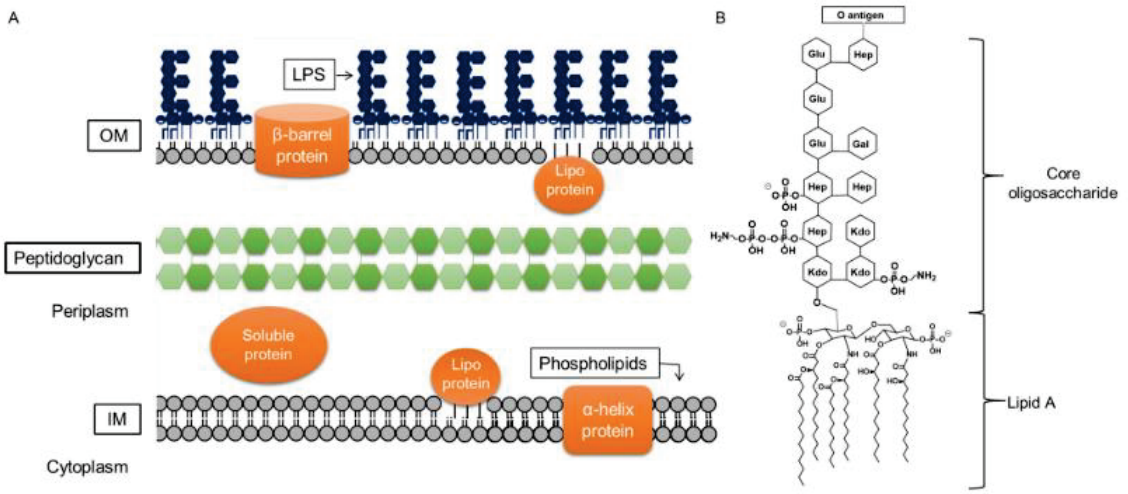

Figure 13. Architecture of the Gram-negative cell envelope. A) Depiction of the Gram-negative cell envelope and its components. The inner membrane (IM) contains phospholipids, while the outer membrane (OM) contains phospholipids in the inner leaflet and lipopolysaccharide (LPS) in the outer leaflet. B) Structure of prototypical LPS produced by *E. coli* (shown is the core structure associated with core type K-12). From Bertani and Ruiz, 2018.

2 Gut microbiota and its role in human pathophysiology

The human gut microbiota transcends the simple notion of a collection of microbes. It is a complex and ever-changing ecosystem, functioning more like a virtual organ with a metabolic prowess rivaling other vital organs (Evans et al., 2013). The sheer number of microscopic residents within our gut is staggering. The ratio of microbial cells to human cells is estimated to be close to 1:1, though this can vary depending on factors like body size and the amount of fecal matter present (Walker et al., 2023). Using advanced techniques like direct cell counts and DNA analysis (qPCR), scientists estimate that a single gram of human feces can harbor between 10 billion and 100 billion microbial cells. Despite their vast numbers, the total weight of the human gut microbiota is likely less than 500 grams (Walker et al., 2023).

The true power of the gut microbiota lies not in its mass but in its collective potential. The genes encoded within the gut microbiome surpass the human genome by a factor of over 100 (Bäckhed et al., 2005). This genetic diversity far exceeds the variations within the human genome itself, where individuals share over 99.5% genetic similarity. Remarkably, the microbial makeup of the gut can be entirely unique between people, with no overlap in resident species (Gilbert et al., 2018). This level of personalization is so profound that it holds potential applications in forensic science.

Given this vast genetic repertoire, it is not surprising that the gut microbiota has a profound influence on our health. It plays a crucial role in various physiological processes, including metabolism and immune system function (Cénit et al., 2014; Fan et al., 2021). We are now realizing the intricate connections between these systems, with the gut microbiota emerging as a central player linking our genes, the environment we live in, and our immune response (de Vos et al., 2022). In stark contrast to our relatively static inherited genes, the gut microbiome exhibits remarkable diversity and dynamism (Cryan et al., 2019). This dynamic nature, coupled with its responsiveness to external stimuli, makes the gut microbiome a highly promising target for therapeutic interventions aimed at improving human health (Walsh et al., 2014).

The profound influence of the gut microbiota becomes even more evident when we examine animals devoid of these microbial communities. These animals, termed germ-free (GF), exhibit stark developmental and physiological differences compared to their counterparts harboring a healthy gut microbiome. Studies have shown that GF animals experience stunted growth, highlighting the crucial role gut microbes play in nutrient absorption and utilization (Savage et al., 1981; Aluwihare, 1971). Additionally, their intestinal function is altered, potentially affecting digestion and waste elimination. Furthermore, research suggests variations in the levels of amino acids within the gut lumen of GF animals, indicating a potential role of the microbiota in amino acid metabolism (Yamamoto et al., 2018). The impact of the gut microbiome extends far beyond the gut itself. Germ-free animals often exhibit compromised immune systems, highlighting the intricate link between the gut microbiota and our body's defense mechanisms. Additionally, research suggests dysregulated hormone signaling, altered

metabolism, and even disrupted neurotransmission in GF animals compared to their conventional counterparts (Cryan et al., 2019). It is important to note that the specific effects of lacking a gut microbiome can vary depending on several factors. Species, sex, the research group conducting the study, and even the specific strain of animal can influence the observed effects. This highlights the complex interplay between the gut microbiota and the host's own genetic makeup (Cryan et al., 2019).

2.1 Gut microbiota composition

The initial stages of gut microbiome colonization occur primarily during the early years of life, a critical window for shaping this vital ecosystem. Newborns are exposed to a multitude of microbes from their mothers, both during birth and through breastfeeding, as well as from the surrounding environment (Gilbert et al., 2018). This initial microbial influx sets the stage for the establishment of a complex gut microbiome.

Within the first year of life, a staggering number of microbes, estimated to be between 10^{13} and 10^{14} microbes per milliliter, colonize the infant gut, encompassing a diverse range of 500 to 1000 species (Gilbert et al., 2018). This rapid expansion in diversity primarily occurs after birth, with the most dramatic increase observed following weaning (Walker et al., 2023). Longitudinal studies have revealed an interesting pattern. The gut microbiome undergoes a dramatic transformation during the first three years of life, while the adult microbiome exhibits relative stability and a unique composition for each individual (Gilbert et al., 2018) (figure 14). Remarkably, even identical twins raised in the same household can end up with distinct gut microbiota configurations (Walker et al., 2023).

The composition of the gut microbiome can be broadly categorized into two components: the "core microbiota" and the "flexible pool." The core microbiota, as the name suggests, comprises a set of bacterial phyla that are relatively consistent across individuals. These core members likely play a crucial role in establishing a stable and functional gut ecosystem. The flexible pool, on the other hand, is a more dynamic group of microbes heavily influenced by dietary habits, environmental exposures, and even interactions with

the core microbiota (Adak and Khan, 2019). Bacteria within the flexible pool are essentially acquired from various sources, including ingested food, water, and environmental components. Interestingly, there can be an exchange of genetic material between the core and flexible pools. This exchange can enhance the host's ability to adapt to specific dietary habits or environmental conditions (Adak and Khan, 2019). In essence, the core microbiota provides a foundation for stability, while the flexible pool allows for dynamic adaptation to external factors, ensuring the gut microbiome remains resilient and responsive to the ever-changing needs of the host.

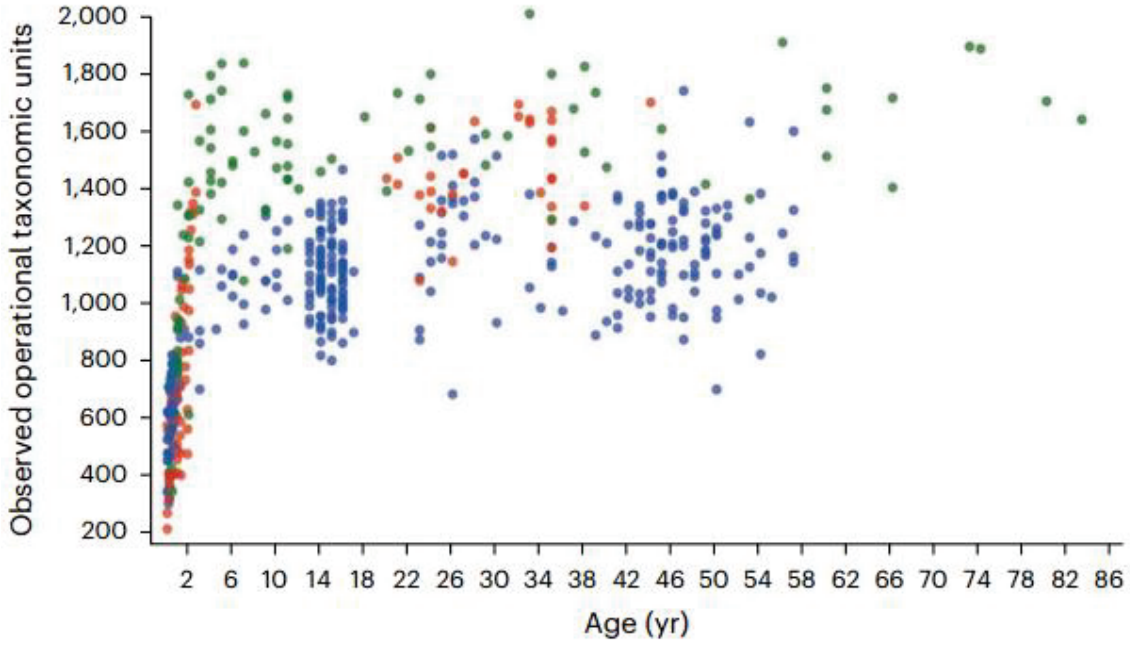

Figure 14. **Diversity of the human gut microbiota dramatically increases in the years after birth.** Diversity (as assessed using number of observed operational taxonomic units) dramatically increases during the first few years of life, particularly after weaning, before beginning to plateau in childhood. This pattern is observed across individuals living in different geographical locations: Malawi (red), Venezuela (green) and the United States (blue). From Walker et al., 2023.

The human gastrointestinal (GI) tract, encompassing a surface area of approximately 200-300 square meters, serves as a haven for a diverse and dynamic community of microorganisms collectively known as the gut microbiota (Adak and Khan, 2019). This

intricate ecosystem comprises an estimated 500-1,000 bacterial species and an astounding 7,000 strains, classified into five main phyla: Firmicutes, Bacteroidetes, Actinobacteria, Proteobacteria, and Verrucomicrobia (The Human Microbiome Project Consortium, 2012; Belizário and Napolitano, 2015; Rinninella et al., 2019). Notably, Firmicutes and Bacteroidetes phyla account for approximately 90% of the total gut microbiota, with the majority of anaerobic bacteria residing within the colon (The Human Microbiome Project Consortium, 2012).

The GI tract exhibits distinct functional and anatomical divisions, including the stomach, small intestine, and large intestine. Each compartment presents a unique microenvironment characterized by specific physiochemical properties that influence the composition and abundance of the resident microbiota (figure 15). Previously considered a sterile environment due to the presence of potent bactericidal barriers, including gastric acid, bile acids, and a thick mucus layer, the stomach has emerged as an unexpected harbor for a diverse microbial population (Adak and Khan, 2019). Research has unveiled a remarkable array of acid-resistant bacterial strains, such as *Streptococcus*, *Neisseria*, and *Lactobacillus*, capable of thriving within this challenging environment (Kazor et al., 2003). Perhaps the most well-known example is *Helicobacter pylori*, a bacterium implicated in the development of peptic ulcers (Warren and Marshall, 1984). While a significant portion of the stomach microbiota originates from the mouth, a core group of bacteria, predominantly belonging to the phyla Firmicutes, Bacteroidetes, Actinobacteria, Fusobacteria, and Proteobacteria, has been identified (Nardone and Compare, 2015). The small intestine plays a pivotal role in nutrient digestion and absorption. Further divided into the duodenum, jejunum, and ileum, the small intestine presents a dynamic landscape for microbial colonization. The duodenum, characterized by the presence of bile acids, pancreatic secretions, and antimicrobial agents, exhibits a relatively low bacterial density and diversity due to rapid food transit and oxygen availability (El Aidy et al., 2015). Firmicutes and Actinobacteria are the predominant phyla in this region. As we move along the small intestine to the jejunum, bacterial diversity and density increase, with a predominance of gram-positive aerobes and facultative anaerobes, including Lactobacilli, Enterococci, and Streptococci (El Aidy et al., 2015). The ileum, the final segment of the

small intestine, witnesses a further increase in bacterial density, with a shift towards aerobic species. Interestingly, the distal ileum, closer to the ileocecal valve, harbors a more anaerobic and gram-negative microbial population, resembling that of the colon (Adak and Khan, 2019).

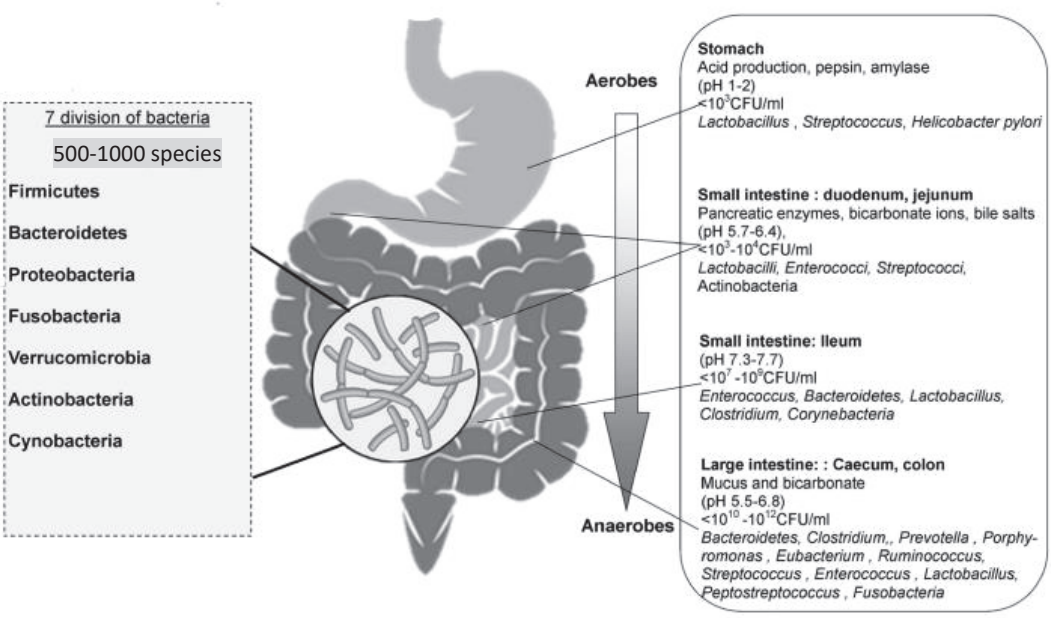

Figure 15. **Distribution of normal gut microbiota in different parts of intestine**. From Adak and Khan, 2019.

The large intestine, encompassing the ascending, transverse, descending colon, and cecum, serves as the primary site for water absorption and the fermentation of undigested food. The slower passage of food materials and the anaerobic environment create ideal conditions for the proliferation of anaerobic bacteria. In the large intestine, the number of anaerobic microbes outnumbers aerobes by a factor of 100 to 1000, with bacterial density reaching an astounding 10^{12} CFU/ml (Eckburg et al., 2005). Firmicutes and Bacteroidetes phyla reign supreme in this region, with their ratio often considered a marker of gut health (Mariat et al., 2009). The large intestine harbors a diverse array of bacterial genera, with some like Bacteroides, Bifidobacterium, Streptococcus, and Enterobacteriaceae residing within the lumen, while others like Lactobacillus, Enterococcus, and Akkermansia are more closely associated with the mucosal lining (Hollister et al., 2014). While the vast

majority of these gut microbes are beneficial or commensal, a small number of pathogens like *Campylobacter jejuni*, *Salmonella enterica*, and *Escherichia coli* can also be present in the large intestine, albeit at lower abundances (0.1%) (Hollister et al., 2014).

2.2 Gut microbiota in digestion and adsorption

The human gut microbiota, far from being a passive collection of microorganisms, actively engages in a symbiotic partnership with the digestive system, influencing a wide range of physiological processes that extend beyond the capabilities encoded by the human genome itself (Rowland et al., 2017). This intricate collaboration between the host and its microbial residents manifests in several key aspects (figure 16), like: a) nutrient acquisition and fermentation: the gut microbiota serves as an auxiliary team for gut cells, facilitating the absorption of essential nutrients from dietary sources. Additionally, it possesses the enzymatic machinery to ferment indigestible food components, unlocking their nutritional value and contributing to overall energy homeostasis (Jandhyala et al., 2015); b) pathogen defense and barrier function: certain bacterial members of the gut microbiota act as sentinels, contributing to a robust barrier function that safeguards the host against pathogenic encroachment. They achieve this by producing antimicrobial compounds that inhibit the growth of harmful microbes, maintaining a balanced intestinal ecosystem (Caballero et al., 2015); c) gut integrity and mucosal function: the gut microbiota plays a pivotal role in the formation and maintenance of the gastrointestinal mucus layer, a physical barrier that protects against pathogen invasion and facilitates nutrient absorption. Moreover, the microbiota promotes the enzymatic activity of the gut mucosa, enhancing digestive efficiency and overall gut health (Tomas et al., 2013); d) vitamin synthesis: the gut microbiota serves as a remarkable vitamin synthesis powerhouse, particularly for essential B vitamins. Studies like that of Magnusdottir et al. (2015) have demonstrated that the gut microbiota can contribute up to 86% of the recommended daily allowance (RDA) for vitamin B6, highlighting its significant role in maintaining vitamin status.

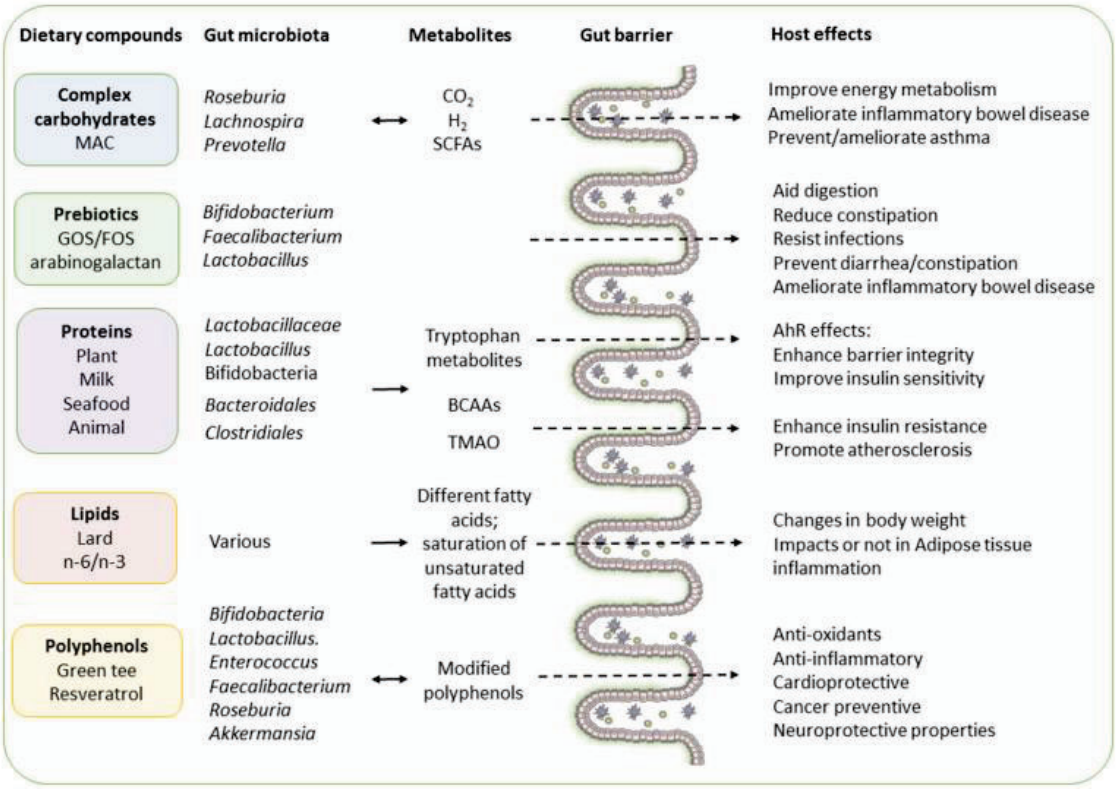

Figure 16. Overview of the interplay between food components, gut microbiota, metabolites, and host health. Dietary compounds may elicit changes in the composition and the activity of the gut microbiota resulting in the generation of secondary metabolites that modulate host responses. Arrows indicate interaction between gut microbiota and metabolites. Ahr: Aryl: aryl hydrocarbon receptor; BCAAs: branched-chain amino acids; MAC: microbiota accessible carbohydrates; SCFAs: short-chain fatty acids; TMAO: trimethylamine oxide. From Danneskiold-Samsøe et al., 2019.

2.2.1 Carbohydrates

Bacteria residing within the large intestine rely heavily on dietary substrates that escape digestion in the upper gastrointestinal tract. These undigested components serve as their primary fuel source. The fermentation process undertaken by these saccharolytic (sugar-utilizing) bacteria generally produces beneficial metabolites for the host. However, when dietary carbohydrates are limited, the gut microbiota can shift its metabolic strategy towards alternative energy sources, resulting in the production of metabolites that may be detrimental to human health (Rowland et al., 2017). Short-chain fatty acids (SCFAs) and

gases are the key products generated during the fermentation of dietary carbohydrates by the gut microbiota. Among the various SCFAs, acetate, propionate, and butyrate are the most abundant, typically present in a molar ratio ranging from 3:1:1 to 10:2:1 (Rowland et al., 2017). Simple carbohydrates are usually completely absorbed in the small intestine. However, a significant portion of complex carbohydrates from our diet, particularly non-starch polysaccharides and resistant starches, remain undigested in the upper GI tract due to their resistance to human digestive enzymes. Consequently, these complex dietary polysaccharides pass through the small intestine and reach the colon, where they become readily available substrates for the colonic microbiota (Chassard and Lacroix, 2013; Danneskiold-Samsøe et al., 2019). The breakdown of these complex carbohydrates by various gut bacterial species leads to the generation of a range of metabolites, including SCFAs, carbon dioxide (CO2), and hydrogen gas (H2). These metabolites play a crucial role in shaping the intestinal environment (Chassard and Lacroix, 2013; Danneskiold-Samsøe et al., 2019).

Since most gut bacteria exhibit a preference for metabolizing simpler carbohydrates like mono- and oligosaccharides, and their capabilities for processing complex carbohydrates vary, a phenomenon known as "cross-feeding" becomes essential for optimal digestion of these complex dietary fibers (Cockburn and Koropatkin, 2016). In essence, cross-feeding allows different bacterial species to exchange fermentation products, enabling more efficient utilization of complex carbohydrates. Ultimately, these cross-feeding interactions lead to the development of unique gut microbiota community structures that are shaped by the types of dietary fibers consumed. Therefore, changes in fiber intake can trigger complex shifts in the overall structure and function of the gut microbiota.

Among the various SCFAs produced by the gut microbiota, butyrate arguably holds the most significance for human health. It serves as a primary energy source for the colonocytes and exhibits promising anti-cancer potential through its ability to induce apoptosis in colon cancer cells. Furthermore, butyrate possesses the ability to regulate gene expression by inhibiting histone deacetylases (Steliou et al., 2012). Intriguingly, research suggests that butyrate can activate intestinal gluconeogenesis (IGN) through a mechanism dependent on cyclic AMP (cAMP). This activation of IGN may contribute to

beneficial effects on glucose and energy homeostasis (De Vadder et al., 2014). Propionate also serves as an energy source for gut epithelial cells. However, its influence extends beyond the colon, as it is transported to the liver where it plays a role in gluconeogenesis. Additionally, propionate is increasingly recognized as a significant molecule in satiety signaling. This function is mediated by its interaction with specific receptors (G protein-coupled receptors, GPR) known as GPR41 and GPR43, also referred to as FFAR2 and FFAR3 (fatty acid receptors). The activation of these receptors by propionate may, in turn, stimulate IGN (De Vadder et al., 2014; Brown et al., 2003; Tazoe et al., 2008). The conversion of propionate to glucose via intestinal gluconeogenesis directly contributes to energy homeostasis by reducing the need for the liver to produce glucose, ultimately leading to decreased adiposity (De Vadder et al., 2014). Acetate, the most abundant SCFA, plays a critical supporting role for other bacteria within the gut. It serves as an essential co-factor or metabolite for their growth. Within the human body, acetate is transported to peripheral tissues and utilized in cholesterol metabolism and lipogenesis. Research in mice suggests that acetate may also play a significant role in regulating appetite at the central nervous system level (Frost et al., 2014).

Gas production is an inevitable consequence of microbial fermentation within anaerobic environments, including the human gastrointestinal tract. Hydrogen gas (H_2) serves as a crucial intermediate metabolite in these processes. Interspecies hydrogen transfer, a phenomenon where electron flow shifts towards proton reduction, can occur. This can result in the generation of additional gases like hydrogen sulfide (H_2S) or methane (CH_4) as a means to dispose of excess reducing equivalents produced during the oxidation of organic material (Levitt, 1970). Interestingly, gas formation is not a universal feature of all anaerobic bacteria. The metabolic pathways of some species, particularly common probiotic bacteria like lactobacilli and bifidobacteria, do not involve gas generation at all (Levitt, 1970). This observation provides a theoretical basis for the use of probiotics or prebiotics to potentially reduce gas production and alleviate associated odoriferous problems in the gut. The gases generated by anaerobic bacterial fermentation within the gut are partially expelled via the lungs or as flatus (intestinal gas). Studies suggest that a healthy human can expel several liters of flatus per day (Cummings and Macfarlane,

1991). The majority of these intestinal gases are odorless, consisting primarily of hydrogen, carbon dioxide (CO_2), and methane (CH_4). In general, oxygen (O_2) and nitrogen (N_2) together account for only about 26% of flatus, with oxygen constituting less than 1% (Suarez et al., 1997). Odorous gases comprise a minor fraction (less than 1%) of total flatus and their components include ammonia (NH_3), hydrogen sulfide (H_2S), indole, skatole, and volatile amines. Among these, the sulfides (H_2S and related compounds) are particularly noteworthy due to their noxious odor and potential toxicity. Sulfides also act as precursors for other sulfur-based odoriferous components like mercaptans (Rowland et al., 2017).

2.2.2 Proteins

Pioneering work by Macfarlane and Cummings (1986) shed light on the remarkable proteolytic prowess of the colonic microbiota. This gut microbial community possesses the ability to break down dietary protein and endogenous protein sources, such as host enzymes, mucin, and shed intestinal cells, into a variety of products (Macfarlane and Cummings, 1986). These products include shorter peptides, amino acids and their derivatives, short-chain and branched-chain fatty acids, and gases like ammonia, hydrogen (H_2), carbon dioxide (CO_2), and hydrogen sulfide (H_2S). While limited by culture-based techniques at the time, this early research identified Bacteroides and Propionibacterium species as the primary proteolytic culprits within fecal samples. Additionally, proteolytic activity was observed among *Clostridia*, *Streptococci*, *Staphylococci*, and *Bacillus* species (Macfarlane and Cummings, 1986). Building upon this foundation, Gibson et al. (1989) further explored the differences between fecal and ileal microbiota in terms of proteolytic activity. They found that not only did the quantity of protein degradation differ between these compartments, but the quality of protein breakdown products also varied (Smith and Macfarlane, 1996). Their work also investigated the influence of factors like pH, carbohydrate availability, and gut model retention time on proteolytic activity. The study revealed a preference for amino acid fermentation at higher colonic pH levels. Interestingly, the presence of fermentable carbohydrates led to a 60% reduction in amino acid fermentation and the production of end products like phenols and indoles (Smith and Macfarlane, 1996). The spatial

distribution of these microbial activities within the colon further highlights the complexity of the gut ecosystem. The proximal colon exhibits a predominantly saccharolytic (sugar-fermenting) nature, while protein fermentation becomes more prominent distally, coinciding with an increase in pH as we move towards the transverse and distal colon (Macfarlane et al., 1992). This increased protein fermentation is associated with higher concentrations of branched-chain fatty acids, phenols, indole derivatives (products of amino acid fermentation), and ammonia (Macfarlane et al., 1992). Recent research has revealed a fascinating additional facet of gut microbial metabolism. Aromatic amino acids (phenylalanine, tyrosine, and tryptophan) can be fermented by the gut microbiota into phenylpropanoid metabolites, phenylacetic acid, and 4-hydroxyphenylacetic acid, which are found in abundance within feces (Russell et al., 2013).

Maintaining a healthy balance of amino acids (AA) is crucial for human health and disease prevention (Broer et al., 2017; Aliu et al., 2018; Hu, 2021). Disruptions in this balance, known as amino acid homeostasis, have been linked to the progression of various diseases, including type 2 diabetes and inflammatory bowel disease (IBD) (Adolph and Zhang, 2022; Kheriji et al., 2022; Guo et al., 2020; Sugihara et al., 2018). Furthermore, amino acid homeostasis often plays a determining role in treatment outcomes. Previous metabolomics studies have compared germ-free (GF) and specific-pathogen free (SPF) mice. These studies consistently demonstrate that gut bacteria colonization significantly affects the levels of free amino acids within the gastrointestinal (GI) tract (Zeng et al., 2022; Quinn et al., 2020; Hans et al., 2021; Mardinoglu et al., 2015; Whitt and Demoss, 1975). This suggests that the gut microbiota plays a pivotal role in regulating the bioavailability of amino acids for the host (Neis et al., 2015). There are several mechanisms by which gut microbiota may modulate host amino acid availability. Firstly, gut bacteria can influence the activity of protein digestion enzymes like trypsin in the intestine (Li et al., 2022). Secondly, they can modify intestinal permeability, impacting the transport and absorption of free amino acids across the gut barrier (Crommen and Simon, 2017; Chakaroun et al., 2020). Beyond these indirect mechanisms, gut microbes may also directly influence amino acid availability through their own metabolic activities.

They can utilize or metabolize amino acids in the intestine (Neis et al., 2015) or, conversely, synthesize and supply them to the host (Portune et al., 2016). Studies have shown that changes in the gut microbiome composition can indeed alter the profile of intestinal amino acids (Mardinoglu et al., 2015; Whitt and Demoss, 1975; Li et al., 2024). The complexities of amino acid utilization by gut bacteria and their subsequent availability to the host are becoming increasingly evident. Further in-depth research with specifically designed mechanistic studies is warranted to fully understand these intricate processes (Davila et al., 2013). Recent work by Dai et al. (2013) highlights the importance of investigating these mechanisms. Their research suggests that bacterial conversion of free amino acids into polypeptides plays a significant role in amino acid metabolism and bioavailability within the mammalian gut. Furthermore, they found that the relative concentrations of different amino acids available to intestinal bacteria can significantly impact overall amino acid utilization by the gut microbial community (Dai et al., 2013). For example, L-glutamine was found to regulate the small intestinal bacterial metabolism of specific amino acids, influencing the utilization of both essential and non-essential amino acids. These findings are particularly relevant given the dramatic impact of modern food processing on the relative concentrations of amino acids in commonly consumed foods. Additionally, recent research has revealed important physiological roles for both essential (e.g., tryptophan) and non-essential amino acids in mammalian nutrition (Hermanussen et al., 2010; Wu et al., 2013; Karau and Grayson, 2014).

2.2.3 Vitamin synthesis

For over four decades, research has revealed the remarkable vitamin-synthesizing capabilities of the gut microbiota. Studies conducted in germ-free rodents, conventional animals, and even human volunteers have demonstrated the production of essential vitamins by these microbial communities (Hill, 1997). These vitamins, including vitamin K and various B vitamins (biotin, cobalamin, folates, nicotinic acid, pantothenic acid, pyridoxine, riboflavin, and thiamine), are not only crucial for bacterial metabolism but also hold significant benefits for mammalian hosts. The importance of gut-derived vitamin K is evident in germ-free rats. These animals, deprived of a dietary vitamin K supplement, exhibit low prothrombin levels and develop hemorrhages. In contrast, their

conventional counterparts with a normal gut microbiota maintain healthy prothrombin levels and normal blood clotting activity (Gustafsson et al., 1962). Similar findings emerged from human studies. Individuals on low vitamin K diets for several weeks did not develop vitamin deficiency symptoms. However, when these subjects received broad-spectrum antibiotics to suppress their gut microbiota, they experienced a significant decrease in plasma prothrombin levels (Frick et al., 1967). These results highlight the crucial contribution of the gut microbiota to vitamin K production and its impact on blood clotting in humans. A recent study by Magnusdottir et al. (2015) delved deeper into this phenomenon by systematically analyzing the genomes of 256 common gut bacteria. Their research focused on identifying the presence of biosynthetic pathways for eight essential B vitamins. This analysis allowed them to predict the proportion of bacteria within each major gut phylum (e.g., Bacteroidetes, Firmicutes) that possess the potential to produce each vitamin. Interestingly, some bacterial genomes harbored the ability to synthesize all eight vitamins, while others lacked the necessary pathways entirely. The study revealed that riboflavin and niacin were the most commonly produced B vitamins, with a high number of potential producers identified within the Bacteroidetes, Fusobacteria, and Proteobacteria phyla. Firmicutes and Actinobacteria exhibited a lower prevalence of vitamin B biosynthesis potential. For vitamin B12, Fusobacteria stood out, with nearly all members predicted to be producers, compared to a 10-50% range within the other four phyla. Overall, Bacteroidetes emerged as the phylum with the highest predicted capacity for B vitamin production, with over 90% of its members potentially contributing to this vital function (excluding vitamin B12). Another intriguing finding from this research was the identification of complementary vitamin synthesis pathways among certain gut microbial pairs. This suggests a fascinating phenomenon of cross-feeding within the gut ecosystem, where microbes exchange essential vitamins to support their mutual growth (Magnúsdóttir et al., 2015).

2.2.4 Bile acids

Bile acids exemplify trans-genomic metabolites arising from the intricate interplay between the host genome and the gut microbiome. The liver synthesizes bile acids from cholesterol, primarily cholic acid (CA) and chenodeoxycholic acid (CDCA). Before

biliary secretion, N-acyl amidation conjugates the bile acid carboxyl group to taurine or glycine, enhancing their amphipathic nature and detergent properties at physiological pH. Upon food intake, bile stored in the gallbladder is released into the small intestine to aid lipid digestion and absorption (Rowland et al., 2017). Most bile acids undergo active reabsorption in the distal ileum and return to the liver via the enterohepatic circulation. However, a small portion (1–5%, or 200–800 mg daily in humans) escapes this cycle and enters the colon (Perino et al., 2021). Here, a bidirectional relationship exists between the gut microbiota and bile acids. The colonic microbiota can modify bile acid structure and properties, while bile acids exert selective pressure on the microbiota due to their antimicrobial properties. These properties include detergent effects on bacterial membranes and the ability to induce DNA damage and protein disruption (Kandell and Bernstein, 1991; Bernstein et al., 1999; Begley et al., 2005). Notably, the microbially derived secondary bile acid, deoxycholic acid (DCA), exhibits tenfold greater potency than its precursor, CA, due to enhanced detergent properties (Kurdi et al., 2006). Thus, increased microbial interaction with the enterohepatic circulation strengthens its antimicrobial activity, potentially regulating bacterial populations. The steroid nucleus of bile acids undergoes various microbially mediated modifications, resulting in secondary bile acids. Following deconjugation, the C7 hydroxyl group becomes susceptible to microbial dehydroxylation. Genera like Clostridium and Eubacterium convert CDCA and CA to the secondary bile acids, lithocholic acid (LCA) and DCA, respectively (Gustafsson et al., 1977). This 7α-dehydroxylation activity likely provides these bacteria with an additional electron acceptor (Ridlon et al., 2006; Mallonee et al., 1996). These secondary bile acids can be cytotoxic for the host and have been linked to colon cancer and cholesterol gallstone formation (Hussaini et al., 1995; Ridlon et al., 2016). Another bacterial modification is the epimerization of hydroxyl groups from α to β orientation. Ursodeoxycholic acid (UDCA) is the most prevalent secondary bile acid produced via this process, following the epimerization of the 7α-hydroxyl group on CDCA (Woollett et al., 2003). This modification reduces bile acid toxicity, creating a more favorable environment for the bacteria. Deconjugation by bacteria lessens the efficiency of bile acids in dietary lipid emulsification and micelle formation, potentially impacting host digestive function as bile acids are crucial for lipid, nutrient, and fat-soluble vitamin

absorption. Bile acids also act as important signaling molecules, binding to the nuclear farnesoid X receptor (FXR) and the G protein-coupled membrane receptor TGR5 (Houten et al., 2006; Eloranta et al., 2008). Through this binding, bile acids regulate genes critical for their synthesis, conjugation, transport, and detoxification (Goodwin et al., 2000; Pircher et al., 2003; Song et al., 2001), as well as lipid metabolism (Hirokane et al., 2004; Watanabe et al., 2004), glucose metabolism (Katsuma et al., 2004; Stayrook et al., 2005), and energy homeostasis (Watanabe et al., 2006).

2.2.5 Phytochemicals/polyphenols

Phenolic compounds, a class of secondary metabolites found in fruits and vegetables, are characterized by the presence of hydroxyl groups in aromatic rings and are divided into flavonoids and non-flavonoids (Santhakumar et al., 2018). These compounds have attracted significant interest due to their potential health benefits, including antioxidant, anti-inflammatory, cardioprotective, cancer preventive, and neuroprotective properties (Selma et al., 2009). The intestinal microbiota plays a crucial role in metabolizing phenolic compounds. This microbial transformation can enhance their biological activity and facilitate absorption by the body (Selma et al., 2009). Due to their structural diversity, polyphenols exhibit varying degrees of bioavailability, metabolism, and bioactivity (Manach et al., 2004). The major groups of polyphenols include phenolic acids, flavonoids (further classified as flavonols, flavones, isoflavones, etc.), stilbenes, lignans, and secoiridoids (Marín et al., 2015). Most dietary polyphenols exist as glycosides (especially flavonoids), conjugated to sugars like glucose, galactose, or rutinose. Similarly, hydroxycinnamic acids can be esterified with sugars or organic acids. Other complex polyphenols like proanthocyanidins and ellagitannins appear as high molecular weight oligomers and polymers. These conjugated and polymeric forms generally have poor bioavailability and require conversion to simpler aglycones for absorption. While some glucosides can be hydrolyzed by intestinal enzymes, the majority of conjugates and esters reach the colon, where the resident microbiota takes over (Marín et al., 2015). Bacterial species like *Bacteroides distasonis*, *Bacteroides uniformis*, and *Lachnospiraceae* species are known to be involved in this hydrolysis process (Marín et al., 2015; Braune et al., 2015). Following the breakdown of conjugates and polymers, the

microbiota further metabolizes the aglycones through processes like dehydroxylation, decarboxylation, and ring breakage, ultimately generating simpler phenolic structures. Growing evidence suggests that this microbial transformation of polyphenols can significantly influence their bioactivity. Consequently, variations in individual gut microbiota composition could impact the health benefits derived from these dietary phytochemicals (Rowland et al., 2017).

2.3 The microbiota-gut-brain axis

The gut microbiota significantly influences neurological functions through the well-established microbiota-gut-brain axis (MGBA). This complex communication network involves the vagus nerve, the immune system, the endocrine system, and crucially, the influence of bacterial metabolites produced by the gut microbiota (figure 17) (Ullah et al., 2023; Sasso et al., 2023; Zhu et al., 2022; Cryan et al., 2012, 2019; Badawy, 2017; McCarville et al., 2020). Supporting the concept of MGBA, a preclinical study by Allen et al. (2016) investigated the effects of psychobiotics on neurophysiological responses in healthy volunteers. Their findings suggest that consuming *Bifidobacterium longum* 1714 may reduce stress and improve memory.

2.3.1 Gut microbiota in brain homeostasis and disease

The constant communication between the gut and the brain, evident from an evolutionary perspective, underscores the importance of understanding the gut microbiota's role in brain health. Mammals have always harbored a gut microbiome (except in controlled laboratory settings), highlighting the brain's dependence on signals from the gut (Cryan et al., 2019). Brain development, a complex process beginning in the third gestational week and continuing through late adolescence (Sharon et al., 2016), can be influenced by various factors, including the gut microbiota. The first years of life are crucial for establishing brain synaptogenesis, the formation of neuronal connections. Studies using germ-free (GF) mice models reveal reduced levels of synaptogenesis markers, including synaptophysin and PSD95, which are essential for synaptic maturation (Tarsa and Goda,

2002; Kwon and Chapman, 2011; El-Husseini et al., 2000; Béïque and Andrade, 2003). These findings highlight the importance of commensal bacteria in brain development, suggesting a central role for the gut microbiota in shaping neural networks. Microglia, the brain's resident innate immune cells, are significantly affected by the gut microbiome and its metabolites, from pre-birth to adulthood (Wang et al., 2018; Mu et al., 2016). Microglia, derived from embryonic progenitors, are capable of self-renewal and play a multifaceted role in the central nervous system (CNS) beyond immune functions like phagocytosis and antigen presentation. They are crucial for neuronal development, adult brain function, and synaptic remodeling (Matcovitch-Natan et al., 2016; Li Q. and Barres, 2018). Notably, microglia are responsible for sculpting neuronal networks through synaptic pruning during brain development (Abdel-Haq et al., 2019). Disruptions in gut microbiota composition are linked to various microglia-associated neurological disorders in humans (Erny et al., 2015). Interestingly, treatment with short-chain fatty acids, a key microbial metabolite, restores impaired innate immune responses in GF mice. This suggests that signals from the gut microbiota play a pivotal role in maintaining microglial function (Erny et al., 2015). Conversely, the absence of a complex gut microbiota, as seen in GF animals or those treated with antibiotics, leads to an increase in microglial populations with defects in maturation, activation, and differentiation (Erny et al., 2015). These alterations are accompanied by morphological changes and compromised immune responses. Importantly, recolonization with gut microbiota in GF mice reverses these detrimental effects (Erny et al., 2015). These findings solidify the concept that a diverse and healthy gut microbiota is essential for maintaining healthy microglia and optimal brain function throughout life (Sampson and Mazmanian, 2015; Abdel-Haq et al., 2018).

Unsurprisingly then, the intricate relationship between microbiota, the gut, and the brain has become a focal point in neuroscience research. Disruption of this delicate balance within the gut microbiota can trigger a cascade of detrimental effects. Increased blood-brain barrier (BBB) permeability, neuroinflammation, and various pathological processes can all potentially result from such imbalances (Rutsch et al., 2020). A growing body of evidence suggests a significant role for the gut microbiota in the development of neurodegenerative diseases (Zhang H. et al., 2022; Sasso et al., 2023). This influence is

mediated by diverse microbial metabolites that travel through the gut-brain axis to reach the brain. Changes in the levels of these metabolites have been linked to various neurological conditions, including Parkinson's disease, anorexia nervosa, Alzheimer's disease, autism spectrum disorders, chronic stress, and depression (Zhang et al., 2022). Studies using mouse models highlight the necessity of gut microbiota for motor deficits, microglia activation, and α-synuclein pathology in Parkinson's disease (Sampson et al., 2016). These researchers transplanted gut microbiota from Parkinson's patients into mice and observed enhanced physical impairments compared to mice receiving microbiota from healthy donors. This suggests a potential role for gut microbes in neurodegenerative diseases and opens doors for their exploration as therapeutic targets. Intriguingly, clinical studies reveal a high co-occurrence of intestinal inflammation in patients diagnosed with neurodegenerative diseases like Alzheimer's disease (AD) (Haran et al., 2019; Sochocka et al., 2019), Parkinson's disease (PD) (Brudek, 2019), and Huntington's disease (HD) (Wasser et al., 2020). Further supporting the importance of the MGBA is the established clinical practice of manipulating gut microbiota with antibiotics to treat hepatic encephalopathy (Rocco et al., 2021). These observations underscores the potential for a bidirectional gut-brain influence in neurological health.

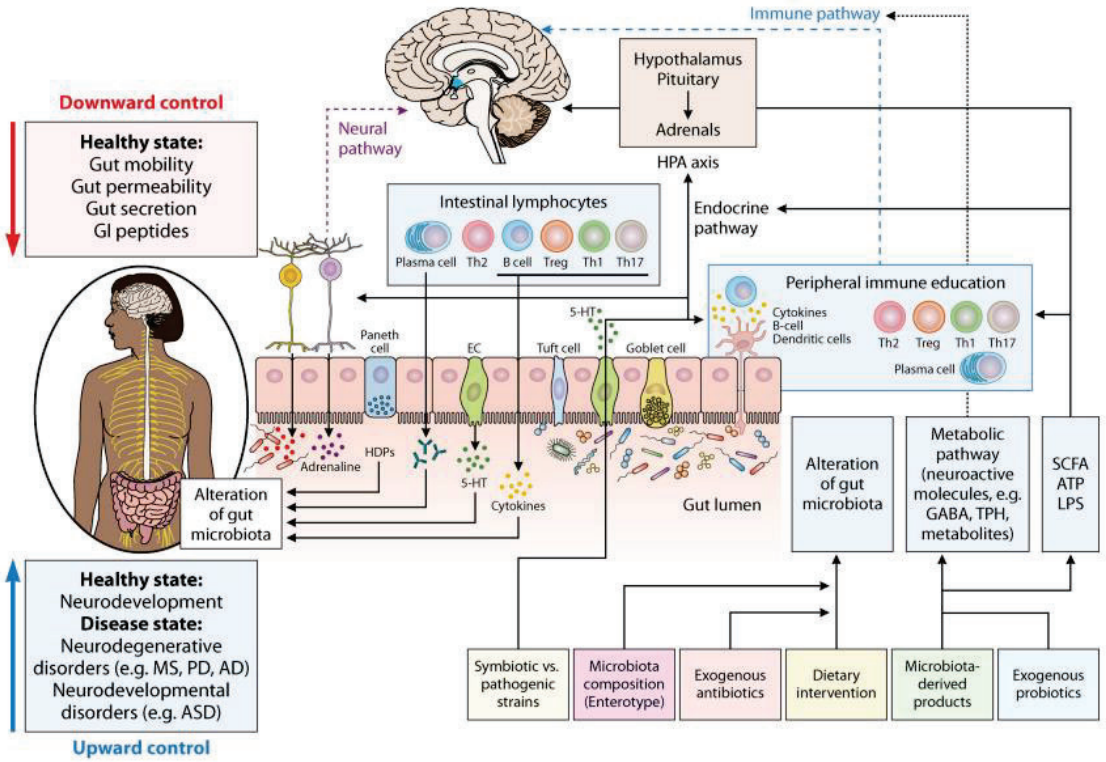

Figure 17. Molecular communication pathways among the microbiota and the brain via the gut-brain axis (GBA). Several direct including, vagus nerve, and indirect pathways, such as cytokines, SCFA, and essential dietary amino acids (e.g., tyrosine, histidine, and tryptophan), have roles in modulation of the gut-brain axis by gut microbiota. The gut-brain axis is comprised of the immune pathway (including cytokines); microbial metabolites; the neuroactive pathway, such as neuroactive metabolites and neurotransmitters; and the neural pathway (spinal nerves, enteric nervous system, and vagus nerve); the endocrine pathway; and the hypothalamic-pituitary-adrenal axis. Microbes residing in gastrointestinal tract are capable of neurotransmitters synthesis, including GABA, serotonin, dopamine, and noradrenaline, locally playing an essential part of the cross talk between the host and the microbiome. Bacterial neuroactive metabolites and dietary molecules can alter the brain and behavior in several ways that are still being discovered, such as influencing epithelial cells to affect the function of the epithelial barrier, hormone release from enteroendocrine cells, and modulation of microglial and immune cells functions through dendritic cells. Abbreviations: AD, Alzheimer's disease; ASD, autism spectrum disorder; MS, multiple sclerosis; PD, Parkinson's disease; HDP, host defense proteins; EC, enterochromaffin cells; 5-HT, 5-hydroxytryptamine (serotonin); SCFAs, short-chain fatty acids; GABA, gamma-aminobutyric acid; LPS, lipopolysaccharide; TPH, tryptophan hydroxylase. From Sorboni et al., 2022.

2.3.2 Neuronal Pathways for Gut-Brain Axis Interactions

The 1980s marked a turning point in our understanding of the gut-brain axis, thanks to advancements in brain imaging (Cryan et al., 2019). Research confirmed this axis as a two-way communication channel crucial for maintaining homeostasis. Gut distension, for instance, can activate brain pathways, while these same pathways can be involved in gut disorders like irritable bowel syndrome (IBS) (Farmer and Aziz, 2014). Signals travel along the gut-brain axis through interactions between the autonomic nervous system (ANS), the enteric nervous system (ENS), and the central nervous system. The brain and gut communicate directly via the vagus nerve (VN) and the ANS in the spinal cord (Sorboni et al., 2022). The ANS, a complex network controlling gut functions like movement and mucus production, integrates communication between the gut and the brain. Since the CNS processes visceral information, it can also induce CNS effects within the gut (Wang H-X. and Wang Y-P., 2016). The ANS directly triggers neurological responses in the gut, leading to physiological changes. Additionally, the ANS mediates interactions between the gut microbiota and the ENS. When stimulated by the ANS, the ENS facilitates the absorption and delivery of prebiotics and probiotics in the gastrointestinal tract, including starches and other microbial nutrients (Maier et al., 2017). Notably, bacteria establish a direct neural connection with the brain through the vagus nerve and stimulation of ENS afferent neurons (Fülling et al., 2019). Vagus nerve activation is associated with anti-inflammatory effects and numerous positive impacts on the gut microbiota and probiotic strains (Wang H-X. and Wang Y-P., 2016).

2.3.3 Chemical Signaling between the Gut and the Brain

Gut microbiota communicates with the host through various mechanisms, including hormones (like corticotrophin-releasing hormone in the HPA axis) and a diverse array of metabolites produced in the gut lumen (Strandwitz, 2018; Cryan et al., 2019; Lyte, 2013; Dinan and Cryan, 2017; Holzer and Farzi, 2014; Rogers et al., 2016). These metabolites include tryptophan, the neurotransmitters GABA, serotonin (5-HT), dopamine, and noradrenaline, as well as vitamins and short-chain fatty acids. While the blood-brain barrier (BBB) and feedback loops limit direct access to the brain, some of these molecules

can reach the brain and influence neuronal circuits (McCarville et al., 2020; Kennedy et al., 2017; Fülling et al., 2019; Roager and Licht, 2018). The BBB, with its selective permeability, allows essential molecules to pass while restricting potentially harmful substances. However, specific circumventricular organs like the median eminence have fenestrated capillaries, enabling a more direct route for certain molecules (Daneman and Prat, 2015; Kiecker, 2018). Microbial metabolites can exert influence on the brain either directly after crossing the BBB or indirectly through neuroendocrine, immune, or vagal pathways (McCarville et al., 2020; Kennedy et al., 2017; Fülling et al., 2019; Roager and Licht, 2018). Animal studies provide evidence for this gut-brain communication. For instance, research using mice models suggests that the gut microbial metabolite 4-ethylphenylsulfate can induce anxiety-like behavior (Wall et al., 2014). Another study in rats demonstrated the influence of the microbial tryptophan metabolite indole on vagus nerve activity. Interestingly, this study found that acute, high indole production led to decreased motor activity, while chronic, moderate indole increase resulted in heightened anxiety-like behavior (Jaglin et al., 2018). These findings highlight the complex interplay between gut microbiota, their metabolites, and brain function.

The gut microbiota is a major producer of serotonin (5-HT) in humans and communicates with the enteric nervous system (ENS) through 5-HT receptors. De Vadder et al. (2018) demonstrated this interaction by using pharmacological modulation of 5-HT receptors and depletion of endogenous 5-HT. Their findings showed that the presence of 5-HT receptor antagonists negatively affects ENS activity. Additionally, *Bifidobacterium infantis* has been shown to influence central serotonin transmission by increasing plasma tryptophan, a precursor to serotonin (Desbonnet et al., 2010). Several other neurotransmitters, including acetylcholine, dopamine, and noradrenaline, are also synthesized by different bacterial species (Lyte, 2014).

The gut microbiota also interacts with the hypothalamic-pituitary-adrenal (HPA) axis, a major neuroendocrine system that regulates the stress response (Mayer, 2008). Signaling molecules produced by the HPA axis influence the gut microbiota throughout the body. Studies using germ-free (GF) mice illustrate this connection. GF mice exhibit elevated plasma corticosterone, indicating a hyperactive HPA axis and the regulatory role of gut

microbiota (Sudo et al., 2004). In humans, patients with irritable bowel syndrome (IBS), often accompanied by gut microbiota changes, tend to have an exaggerated adrenocorticotrophic hormone (ACTH) response to corticotrophin-releasing hormone (CRH) infusion (Dinan et al., 2006; Hou et al., 2022).

Among microbial metabolites, SCFAs play a critical role in regulating various body functions, including neuroimmunoendocrine, metabolic, infectious, and inflammatory processes (Silva et al., 2020; Ríos-Covián et al., 2016). Produced by colonic bacteria during dietary fiber fermentation, SCFAs have been shown to enhance the function and number of regulatory T lymphocytes in the enteric system. They also promote anti-inflammatory effects and strengthen the gut barrier through their inhibitory effects on the transcription factor NF-kB and HDAC activity (Smith et al., 2013; Thorburn et al., 2014; Maslowski et al., 2011; Furusawa et al., 2013). Beyond their role in the gut, SCFAs serve as energy source for neurons and glial cells in the central nervous system, contributing to brain development. Moreover, studies show that butyrate and propionate can have systemic effects, influencing gene expression and the host's epigenome by acting as histone deacetylase (HDAC) inhibitors and ligands for G protein-coupled receptors (Bourassa et al., 2016). Another group of gut-derived metabolites influencing the gut-brain axis are tryptophan derivatives produced by gut microbiota. These molecules bind to the aryl hydrocarbon receptor (AhR), affecting the function of the intestinal immune system. For instance, indole-3-aldehyde and tryptophan catabolism by *Lactobacillus reuteri* can trigger the IL-22 pathway through AhR activation (Schiering et al., 2017; Hubbard et al., 2015).

3 Microbiota and (auto)immunity

The human immune system and the microbiota share a complex, symbiotic relationship, forged through co-evolution between vertebrates and microbes (Maynard et al., 2012). The development of a healthy immune system depends on the presence of commensal microorganisms (Owaga et al., 2015) and this bidirectional relationship is intricate and dynamic (figure 18). While genetics plays a major role in immune response variability,

recent human studies suggest that the gut microbiome contributes to at least 10% of the variation in how individuals respond to immune stimulation (Gilbert et al., 2018).

The human immune system interacts extensively with the microbiota through both innate and adaptive immune responses. The innate immune system plays a critical role in maintaining a balanced gut environment by eliminating harmful bacteria while regulating the adaptive immune response to the microbiota (Salzman et al., 2010; Thomson and Knolle, 2010). Molecules produced by gut microbes, known as microbial-associated molecular patterns (MAMPs), include double-stranded RNA, lipopolysaccharides, and lipoproteins. These MAMPs are recognized by various host receptors, particularly Toll-like receptors (TLRs) (Dias et al., 2021; Vaishnava et al., 2008; Duerkop et al., 2009). Beyond their benefit to the bacteria, MAMPs like peptidoglycans, polysaccharides, and other bacterial antigens serve another crucial function: they train the immune system to identify the diverse bacterial populations within the gut and detect disruptions in gut homeostasis. Epithelial pattern recognition receptors (PRRs), especially the TLR family, recognize these unique bacterial signatures (pathogen-associated molecular patterns, PAMPs) (Duerkop et al., 2009). Upon activation, PRRs trigger the recruitment of inflammatory mediators, cytokine production, and immune cell infiltration through chemokine signaling, leading to an acute inflammatory response if necessary (Takeda and Akira, 2004).

The adaptive immune response also plays a vital role in maintaining a healthy microbiota and immune balance (Alexander et al., 2014). The activation of the innate immune system by the microbiota acts as a primer for the adaptive response. For instance, gut microbiota can influence the immune system by mediating neutrophil migration, which impacts the maturation of B cells and the differentiation of T cells into various subtypes, including helper T cells (Th1, Th2, Th17) and regulatory T cells (Owaga et al., 2015; Zhao and Elson, 2018).

The gut microbiota contributes to the development of the immune system via the gut-associated lymphoid tissues (GALT), which include Peyer's patches (PPs), plasma cells, and lymphocytes. Studies have shown that gut bacteria interact with mucosal antibodies

taken up by CD11+ dendritic cells in the PPs. Secretory IgA (slgA) produced by plasma cells can bind to and form complexes with commensal bacteria, selectively presenting bacterial components to tolerogenic dendritic cells. A key example of this interplay is flagellin, the principal component of the bacterial flagellum. Flagellin is recognized by TLR5, which is actively expressed in B cells and CD4+ T cells. Differentiated B cells produce IgA, which neutralizes pathogens and prevents subsequent infection (Cullender et al., 2013). As an anti-inflammatory molecule, slgA can reduce the inflammatory response triggered by the immense bacterial load in the gut. Conversely, dysbiosis of microbiota can alter the sIgA response and lead to unregulated bacterial growth. Studies by Hapfelmeier et al. (2010) using a reversible microbial colonization system in germ-free (GF) mice demonstrated a microbiota-specific sIgA response. The gradual increase in sIgA production observed suggests a continuous dialogue between the microbiota and the immune system. Furthermore, research has shown that luminal microbiota bound to sIgA increases their presence within PPs (Macpherson and Uhr, 2004). Microbiota plays a major role also in the T cell mediated response: studies have shown that GF mice exhibit reduced intestinal CD8+ T cells, primarly located in the gut's intraepithelial compartment, highlighting the microbiota's influence (Helgeland et al., 2004).

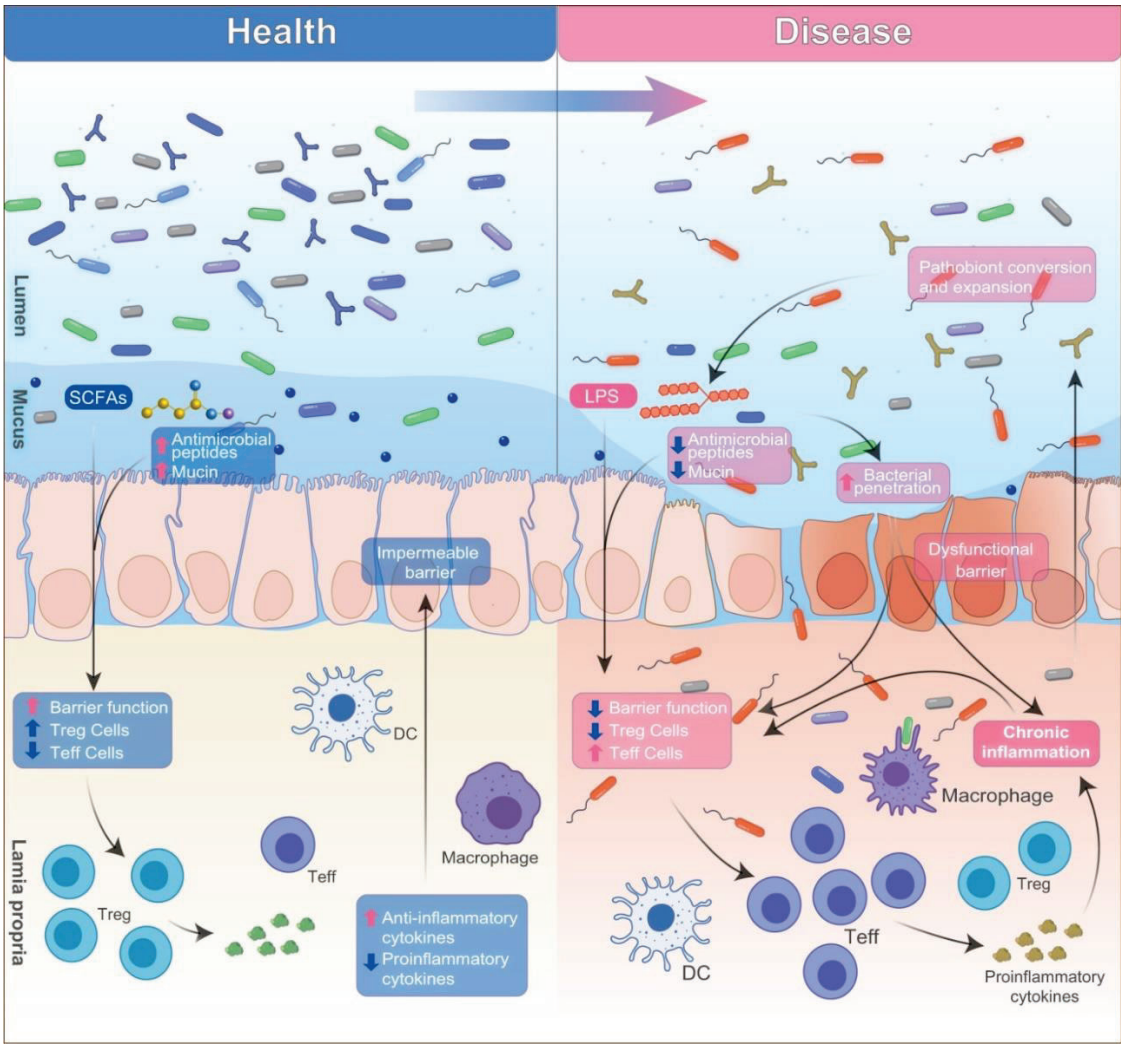

Figure 18 Factors affecting microbiota-associated chronic inflammation in healthy and disease state. The adaptive and innate immune system and the gut microbiota engage in a complex interplay, with each influencing the other's development and function. This intricate communication is vital for maintaining a healthy gut environment and overall immune balance. From Hou K. et al., 2022.

The close relationship between the host and its gut microbiota can be a double-edged sword. Disruptions in microbiota development during immune system maturation can lead to impaired immunological tolerance and potentially trigger autoimmune diseases (Sekirov et al., 2010).

The initial introduction of microbiota to a child typically occurs vertically, from the mother during birth. Infants delivered by cesarean section are primarily colonized with bacteria from the skin, which has been linked to a higher risk of allergies and asthma compared to infants exposed to the mother's vaginal flora (Bager et al., 2008). These differences in immune system and microbiota composition gradually diminish during childhood. A comparative study of children in Finland, Russia, and Estonia, with varying rates of early-onset autoimmune diseases, revealed a potential link between specific gut bacteria and immune development. *Bacteroides* sp. were prevalent in the gut microbiota of Finnish and Estonian children, where autoimmune disease rates were lower. This specific bacterial group was hypothesized to provide essential lipopolysaccharide (LPS) exposure, potentially shaping immune tolerance (Vatanen et al., 2016). Similar research explored the link between childhood asthma and household dust. Dust extracts from Amish and Hutterite homes, known to have distinct microbiota profiles, were tested in a mouse model of asthma. The study found that exposure to dust from Amish homes, but not Hutterite homes, offered protection against asthma development. This suggests a potential role for dust microbiota in influencing asthma risk (Stein et al., 2016). These findings highlight the potential impact of early-life microbiota exposure on immune development and disease susceptibility. These strategies are broadly applicable to many other situations in which differential exposure to environmental bacteria may play a role in disease etiology (Gilbert et al., 2018).

Moreover, under certain conditions, shared epitopes between gut microbes and human tissues can contribute to autoimmune diseases (Wu HJ and Wu E, 2012; Xu H. et al., 2019). A prime example of molecular mimicry involves the Bifidobacterium regulare (Bfr) genome. The *Bfr ubb* gene encodes BfUbb, a protein with 63% sequence identity to the human ubiquitin protein, Ubc52 (Patrick and Blakely, 2012). This remarkable similarity raises the concern that BfUbb could mimic human ubiquitin, triggering the production of antibodies that mistakenly target the body's own ubiquitin. Ubiquitin plays a critical role in regulating the immune response and preventing autoimmunity by facilitating the removal of cellular debris. The production of cross-reactive anti-ubiquitin

antibodies due to BfUbb mimicry could disrupt this process and contribute to autoimmune conditions (Stewart et al., 2018).

Recent research challenges the traditional view of the brain as an immune-privileged organ. The discovery of meningeal lymphatic vessels suggests a potential direct connection between the central nervous system and the peripheral immune system (Louveau et al., 2018). This newfound connection is particularly relevant to brain autoimmune diseases like multiple sclerosis (MS) and experimental autoimmune encephalomyelitis (EAE). Studies investigating the gut microbiome in these diseases have yielded intriguing results. When germ-free mice received microbiome transplants from individuals with MS, they exhibited a higher risk of EAE compared to mice receiving transplants from healthy donors (Emani et al., 2015; Berer et al., 2017). These findings suggest that the gut microbiota can influence the development of autoimmune responses in the brain. Furthermore, the gut microbiota and its metabolites, such as short-chain fatty acids, can modulate T lymphocytes, leading to reduced EAE-associated axon damage (Berer et al., 2017; Kadowaki et al., 2016; Haghikia et al., 2015). Other microbial metabolites, like tryptophan, have been shown to regulate CNS inflammation in EAE models and may contribute to increased astrocyte activation (Cekanaviciute et al., 2017).

4 The Infection Hypothesis of Neurodegenerative Disease

Gut microbiome-derived products, including lipopolysaccharides (LPS) and amyloids, may contribute to neurodegenerative inflammation through specific signaling pathways and proinflammatory cytokines. In Alzheimer's disease (AD), for example, gut dysbiosis and "leaky gut syndrome" are hypothesized to play a central role. A leaky gut barrier could allow the transport of these neurotoxic products across the blood-brain barrier (BBB), potentially accelerating AD progression (Zhao Y et al., 2017). However, some evidence suggests that microbes themselves might directly access the brain and trigger inflammation leading to neurodegeneration (Fulop et al., 2018). This hypothesis is based on the presence of viruses, bacteria, and even protozoa in the brains of individuals with neurodegenerative diseases (Patrick et al., 2019). Additionally, researchers have observed

similar biomarker patterns of infection in both dementia and some infectious diseases (Shinomoto et al., 2021). Building on the concept of infection as a driver of neurodegeneration, the "Antimicrobial Protection Hypothesis" (Moir et al., 2018) proposes a novel perspective. This hypothesis suggests that the deposition of protein aggregates, such as amyloid-beta (Aβ), might represent an innate immune response to microbial invasion rather than a solely pathological process. While no specific pathogen has been definitively linked to neurodegenerative disease development, this hypothesis opens new avenues for research, suggesting that general inflammatory responses to infections could contribute to neurodegenerative pathology.

Periodontitis, a chronic inflammatory condition of the gums, is associated with specific oral bacteria, such as *Porphyromonas gingivalis*. Studies suggest a possible link between these bacteria and an increased risk of Alzheimer's Disease (AD) (Chen et al., 2017). This association highlights the oral cavity microbiota as a potential area of interest in understanding neurodegenerative disease. Beyond the oral cavity, the respiratory pathogen *Chlamydia pneumoniae* has also been linked to neurodegeneration. Post-mortem studies have shown a significantly higher prevalence of *C. pneumoniae* in the brains of individuals with late-onset AD compared to healthy controls (Balin et al., 1998; Hervé et al., 2006). Furthermore, cell staining has identified *C. pneumoniae* near neurofibrillary tangles and amyloid plaques in the brains of AD patients. *Toxoplasma gondii,* a common parasite that can establish lifelong brain residency in humans, has also been associated with neurodegeneration in both animal models and human populations (Torres et al., 2018; Nayeri et al., 2019) (figure 19).

Interestingly, the concept of amyloids as an innate immune response is further complicated by the fact that microbes themselves produce amyloid-like fibers during biofilm formation. This raises the possibility that amyloid plaques in the brain could be microbial biofilms created to evade the immune system (Miklossy, 2016). Several common gut bacteria, including *Streptococcus*, *Staphylococcus*, *Klebsiella*, and *Escherichia coli*, are capable of forming amyloids (Friedland and Chapman, 2017). In animal models, exposure to amyloid-producing *E. coli* increased alpha-synuclein production in the gut and its accumulation in the brain. Furthermore, animals over-

expressing alpha-synuclein were unable to form Lewy bodies, a hallmark of Parkinson's disease, without the presence of microbes, suggesting a crucial role for bacteria in this disease (Sampson et al., 2016). These findings suggest that bacterial amyloids might act similarly to prions, cross-seeding and promoting enhanced amyloid production from various bacterial species (Zhou et al., 2012). Additionally, these bacterial fibers may trigger an immune response by activating inducible nitric oxide synthase (iNOS) and nuclear-factor kappa-B (NF-κB) (Tükel et al., 2009, 2010).

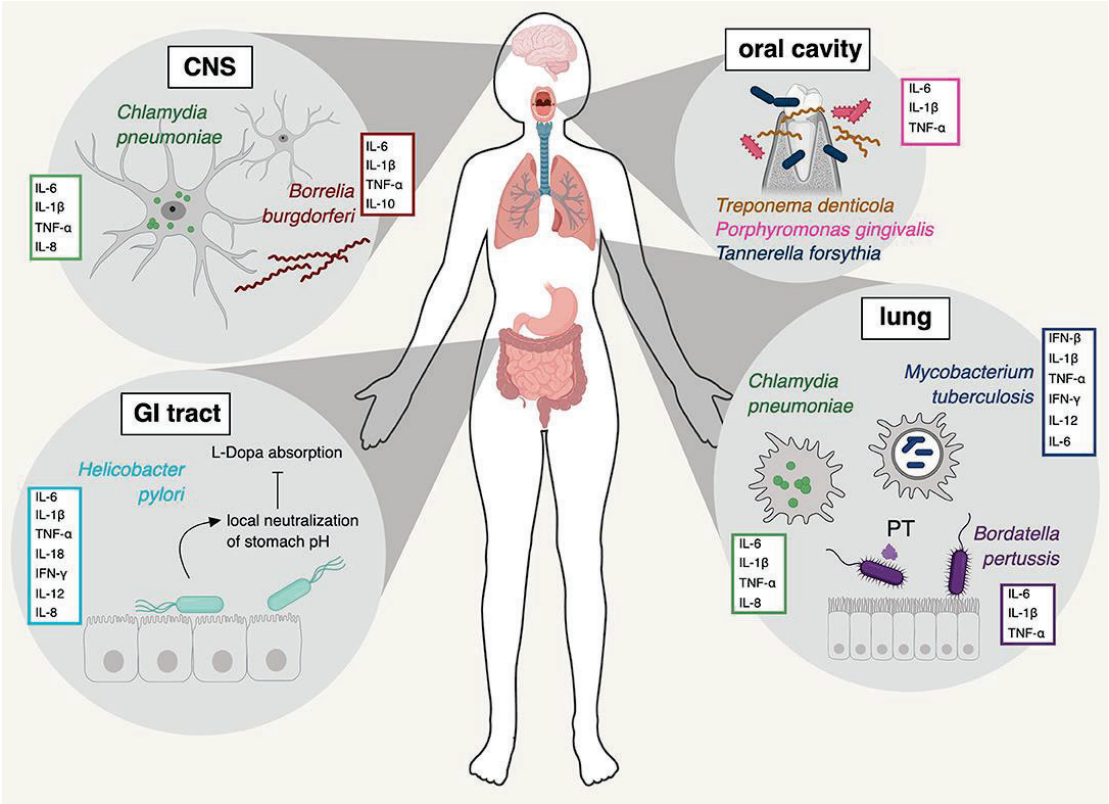

Figure 19. The Infection Hypothesis of Neurodegenerative Disease: schematic representation of some of the pathogens discussed in the previous text, the major organ system(s) they infect, and the primary innate immune cytokines they induce. *Chlamydia pneumoniae* is shown in its primary location (lung) but also in the CNS, where the bacterium has been repeatedly detected in association with AD. The major resident oral pathogens, *Treponema denitcola*, *Porphyromonas gingivalis*, and *Tannerella forsythia* are shown in the mouth and gums. *Borrelia burgdorferi* is a systemic infection, shown here in the CNS, where it too has been detected. *Helicobacter pylori* causes infection of the stomach and duodenum. *Mycobacterium tuberculosis* and *Bordetella pertussis* are mainly pathogens of the lung. PT: pertussis toxin. From Patrick et al., 2019.

5 Microbiota: how can we study it?

5.1 Culture dependent methods

In 1881, Robert Koch introduced the plating technique, a cornerstone of microbiology, for culturing and identifying microorganisms based on their biochemical and physiological properties. However, this traditional approach has limitations. Culture-based methods can only detect 30-50% of the bacteria residing in the human gut (Browne et al., 2016) as artificial culturing environments often fail to provide optimal conditions for growth of many uncultivable bacteria. Conventionally, microbiologists rely on various selective and nutrient agar media to isolate and culture gut bacteria. Efforts to improve these techniques have included enrichment cultures, pre-incubation of fecal samples in blood culture bottles, rumen fluid, and sterile stool extract (Lagier et al., 2015, 2016; Lau et al., 2016). These modifications mimic the natural gut environment and facilitate the isolation of previously uncultivable bacteria. However, even with these improvements, the overgrowth of dominant bacterial populations in fecal samples can hinder the detection of less abundant species. Researchers have addressed this challenge by incorporating additional modifications, such as antibiotics, bacteriophages, and filtration. For instance, the predominant presence of *Escherichia coli* can mask the identification of novel species. The addition of specific bacteriophages that lyse *E. coli* in culture plates allows for the growth and identification of previously undetectable bacterial species, like *Enterobacter massiliensis* (Lagier et al., 2016). Extensive research on the culturomics approach has highlighted the significant gap between culture-dependent and culture-independent methods used to study the microbiome. One study estimated the vast number of uncultivated microbes potentially present based on data from various microbiome projects (Lagier et al., 2016). This study also introduced three key modifications to isolate previously uncultivable bacteria: (1) pre-incubation in blood culture bottles, (2) supplementation with rumen fluid, and (3) addition of sheep blood. These modifications increased bacterial isolation success rates by 56%, 40%, and 25%, respectively.

The culturomics approach often combines culture-based methods with advanced identification techniques such as matrix-assisted laser desorption/ionization time-of-flight mass spectrometry (MALDI-TOF MS) for rapid discrimination of a large number

of colonies, followed by 16S rRNA gene sequencing for definitive bacterial identification (Greub et al., 2012). Using this approach, researchers have identified a staggering 1057 prokaryotic species, including: 531 novel additions to the human gut microbiota, of which 146 species were previously unreported; 187 bacterial species and 1 archaeal species (Haloferax alexandrinus) not previously isolated from humans; 197 potential entirely new species. The field of host-pathogen interactions has traditionally relied on culturing pathogenic strains, often isolated from clinical cases, and introducing them to isolated cells, tissues, or whole animals for intervention studies. However, many members of the human gut microbiome have been inaccessible to such techniques because they are uncultivable. Although recent advances in culturing techniques are expanding the repertoire of isolates from the gut (Browne et al., 2016), this barrier may not be entirely eliminated. Despite its limitations, the culturable portion of the microbiome remains a valuable tool for understanding host-microbe interactions. A recent study exemplifies this point. Researchers isolated 53 bacterial strains from the human gut and used them to monocolonize germ-free mice. This study revealed significant differences in the immunomodulatory properties of these bacteria, even among closely related strains. The bacteria differentially affected the production of cytokines like IL-10, IL-17a, IL-22, and interferon-gamma, with some strains promoting their production and others inhibiting it (Geva-Zatorsky et al., 2017). These findings highlight the importance of characterizing microbial activity at the strain level, moving beyond the broader taxonomic classifications typically provided by amplicon sequencing. Such detailed analysis, especially when applied to more complex microbial communities, will likely reveal crucial links between the microbiome and various diseases (Gilbert et al., 2018; Adak and Khan, 2019).

5.2 Culture independent methods

The advent of Sanger sequencing in 1970 opened doors for studying bacterial taxa and phylogeny. Carl Woese and colleagues pioneered the use of 16S rRNA gene sequencing for this purpose, focusing on conserved sequences within hypervariable regions (V1-V9) (Sanger et al., 1977). Early microbiome studies were limited by sequencing costs and time. Since Sanger sequencing priced each sequence individually, the number of sequences analyzed per sample remained relatively small. These studies typically

involved amplifying the 16S rRNA gene through PCR, followed by multiple sequence alignment and phylogenetic reconstruction (Knight et al., 2017). A crucial aspect of this analysis was comparing individual sequences to a reference database, such as the Ribosomal Database Project, or integrating them into existing phylogenetic trees within GenBank (Olsen et al., 1992). Tools like ARB facilitated sequence alignment, phylogenetic placement, and tree visualization, becoming commonplace in these workflows (Ludwig et al., 2004). However, cost limitations restricted the number of sequences analyzed per sample, making it difficult to accurately estimate the abundance of organisms represented by the sequences. Additionally, fingerprinting methods were sometimes used to select only unique and diverse sequences for sequencing, further impacting abundance estimates (Knight et al., 2017). The high diversity of the microbiome, often containing unknown sequences and sequencing errors, also posed challenges for existing phylogenetic reconstruction software and computational limitations at the time. Further complicating the issue was the ongoing debate about optimal phylogenetic methods, with more powerful options like maximum likelihood being restricted to smaller datasets (Adak and Khan, 2019). To address these limitations, researchers began clustering sequences into Operational Taxonomic Units (OTUs). Often, a 97% sequence identity threshold was used as a proxy for species, with the number of sequences within an OTU serving as a proxy for abundance and allowing for ecological diversity estimates (McCaig et al., 1999). Initial clustering approaches relied on Basic Local Alignment Search Tool (BLAST), but these were slow, especially for large datasets (Altschul et al., 1990). Optimized methods like DOTUR, which leveraged the Phylogeny Inference Package (PHYLIP) for distance calculations, significantly improved OTU table generation and selection of representative sequences for phylogenetic reconstruction (Schloss et al., 2005). DOTUR further refined the OTU concept by introducing different clustering methods beyond a simple identity threshold. The adoption of OTUs facilitated the involvement of ecologists in microbiome research. Their expertise in ecological theory and methods for studying macroscopic environments brought valuable insights to microbiome analysis (Knight et al., 2017). This included approaches like ordination techniques well-suited for assessing relationships between environmental factors and microbial communities (Bray and Curtis, 1957). Another powerful concept introduced

was beta diversity, which represents the dissimilarity between microbial communities in different samples. Beta diversity allows for the creation of distance matrices that describe the similarity between all pairs of samples within a dataset. While OTU-level analysis remains prevalent in amplicon-based microbiome studies, recent advancements are driving a shift towards sub-OTU analysis.

For decades, DNA sequencing remained a cost-prohibitive bottleneck for large-scale studies of microbial communities. This barrier fell with the advent of next-generation sequencing (NGS) technologies, making metagenomic analyses significantly more cost-effective (ENCODE Project Consortium, 2007). Metagenomics refers to the application of sequencing and bioinformatics tools to directly analyze the genetic makeup of environmental samples, including microbial communities. These studies aim to characterize the taxonomic diversity of the microbiota and, through functional metagenomics, elucidate the biological roles of its constituent members (Quince et al., 2017; Valencia et al., 2024). Prior to NGS, Sanger sequencing was the primary method for DNA sequencing. However, Sanger sequencing suffered from limitations in terms of ease, cost, and throughput. In 2005, NGS emerged as a revolutionary advancement, overcoming these limitations (Metzker, 2005). In NGS, adapter-tagged DNA molecules are clonally amplified on a flow cell. During amplification, fluorescently labeled nucleotides are incorporated and identified during each sequencing cycle, allowing for massive parallel sequencing. A typical workflow for a culture-independent analysis of the microbiota is depicted in figure 20. The power of NGS is evident in the exponential increase in the number of microbial genes identified from fecal samples. In 2010, NGS enabled the cataloging of 3.3 million non-redundant genes, a 200-fold increase compared to previous studies (Qin et al., 2010). Building on this foundation, subsequent studies using NGS data from over 1200 individuals identified a staggering 9.8 million non-redundant microbial genes (Li et al., 2014). This vast dataset included samples from the MetaHIT (European), Human Microbiome Project (American), and a large Chinese diabetes study. Interestingly, analyses revealed that approximately 300,000 genes, representing 40% of the total, were common to over half of the individuals studied. Furthermore, a Danish study of 540 adults highlighted a potential link between gut

microbiome gene counts and obesity (Le Chatelier et al., 2013). These findings suggest that the functional potential of the gut microbiome, as revealed by metagenomic analysis, may play a role in human health and disease. Recent advancements in NGS technology allow for whole-genome sequencing. In this approach, DNA is fragmented before sequencing, and then assembled computationally to reconstruct the original, contiguous sequence (Liu L. et al., 2012). These ongoing advancements continue to revolutionize our understanding of the microbiome and its functional potential.

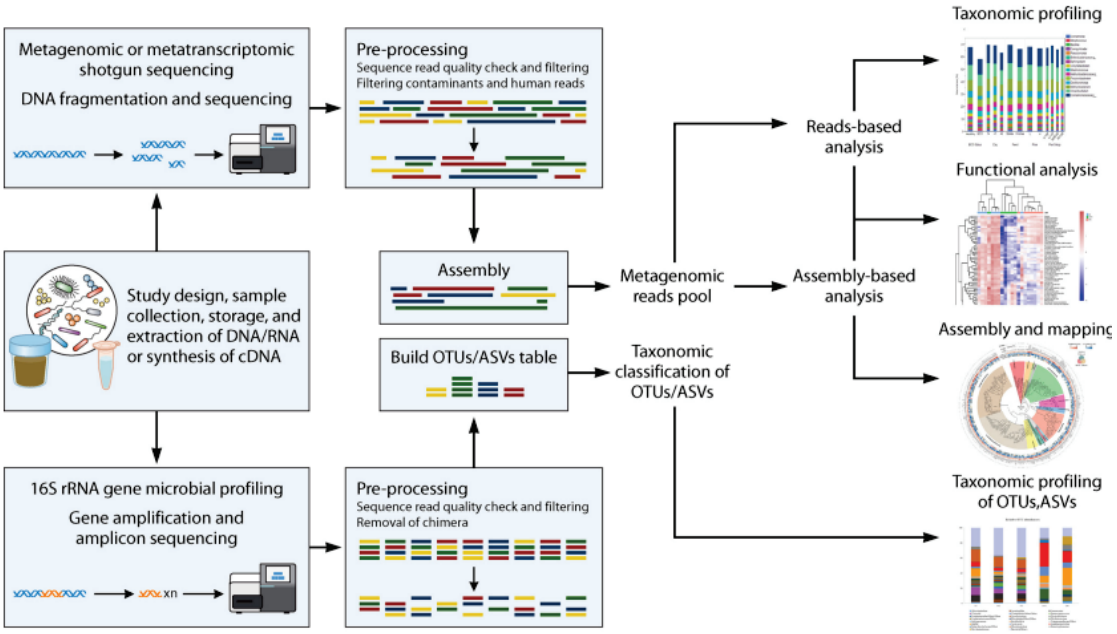

Figure 20. Organizational structure of the main steps implicated in the bioinformatic analysis of the gastrointestinal microbiome. The general overview of the bioinformatic analysis pipelines is divided into two branches based on the type of sequencing, including 16S rRNA gene microbial profiling and shotgun metagenomics. After microbial DNA extraction and sequencing, the pipeline determines the taxonomic profiling of the gut microbiota and the genomes' reconstruction, in addition to a functional analysis of the genes. This schematic presentation depicts the major steps and may be modified according to the analysis' ultimate objective. ASV, amplicon sequence variant; OTU, operational taxonomic unit. From Sorboni et al., 2022.

5.3 Animal models

Mechanistic studies of the microbiome are typically difficult to perform in humans, in part because of tremendous genetic and lifestyle heterogeneity, and there are ethical issues associated with colonizing human subjects with microbes that are hypothesized to cause disease. Therefore, most of what we know currently stems from experiments in animal models. However, recent studies that complement observations in humans with interventions in animal models have produced striking new insight into the microbial origins of disease that cannot be acquired from human studies alone (Gilbert et al., 2018). Two main methods have emerged to explore the effects of the microbiota on physiology and disease in mice: germ-free models and antibiotics treatment regimens. Both germ-free mice and antibiotic treatment offer advantages and disadvantages for studying the gut microbiome. Understanding these limitations is crucial for researchers to design appropriate studies and accurately interpret their findings (Kennedy et al., 2018).

5.3.1 Germ-free mice

Germ-free (GF) mice offer a unique research tool for studying the gut microbiome. They are bred and maintained in isolators to completely prevent exposure to microorganisms, including bacteria, viruses, and eukaryotes. This concept, originally envisioned by Louis Pasteur in 1885, led to the establishment of the first GF rodent colonies in the 1940s (Yi et al., 2012; Al-Asmakh et al., 2015). GF mice serve two key purposes in microbiome research. First, they allow scientists to study the effects of a complete absence of microbes on the host. Second, they can be used to generate gnotobiotic animals colonized by specific, pre-defined microbial communities. This feature is particularly valuable because it enables researchers to establish a cause-and-effect relationship between specific microbes and their influence on the host (Lundberg et al., 2016). However, generating and maintaining GF mice requires specialized facilities, expertise, and ongoing monitoring to ensure they remain germ-free. These factors contribute to the high cost associated with using GF models, potentially limiting their accessibility to some researchers (Fontaine et al., 2015; Nicklas et al., 2015). Monitoring involves a combination of techniques such as culturing, microscopy, serology, visual inspection, and

sequencing to detect potential contamination by bacteria, viruses, or parasites (Charles River Germ-Free Mouse Report). Another limitation is that any unique mouse strain intended for GF studies needs to be rederived within these specialized facilities. This restricts the genetic diversity of mice that can be studied using this model. Additionally, certain research areas, such as behavioral testing or pathogen infection studies, may be impractical or challenging to conduct with mice housed in isolators. Despite their advantages, limitations inherent to GF mice must be considered when designing microbiome research studies (Kennedy et al., 2018). A major constraint on the translatability of findings to humans is the incomplete understanding of the human gut microbiota and the lack of standardized protocols for creating humanized gnotobiotic mouse models (Park and Im, 2020). Species-specific microbes may also pose challenges in generating models that accurately reflect the human gut environment. Although human and murine gut microbiotas share similarities at the phylum and genus level (90% and 89% respectively) (Guinane et al., 2013; Alkadhi et al., 2014), closer examination reveals significant discrepancies in composition and abundance. One key difference is the ratio of the two dominant bacterial phyla, Bacteroidetes and Firmicutes. Humans have a higher Firmicutes to Bacteroidetes (F/B) ratio compared to mice (Ley et al., 2005). Furthermore, the specific member families within each phylum differ between the two species (Nagpal et al., 2018). For example, in mice, the Bacteroidetes phylum is dominated by the S24-7 family, while Firmicutes are mainly composed of Clostridiales. In contrast, human Bacteroidetes are primarily Bacteroidaceae and Prevotellaceae, and Firmicutes are dominated by the Ruminococcaceae family (Nagpal et al., 2018). These variations extend beyond just the phylum level. The top 15 bacterial genera present in mice and humans differ by five genera, and their relative abundances diverge significantly. Mice exhibit a much higher abundance of S24-7, Clostridiales, and Oscillospira compared to humans, while humans have a greater abundance of Bacteroides and Ruminococcaceae (Nagpal et al., 2018). Additionally, both mice and humans harbor unique genera not found in the other species (Krych et al., 2013).

5.3.2 Antibiotics treatment models

Germ-free mice offer a valuable tool for studying the microbiome, but limitations exist. Antibiotic treatment presents an alternative approach that avoids some of these complications. Broad-spectrum antibiotics are commonly used to deplete the gut microbiota in mice and can be readily applied to any mouse genotype or condition. Unlike germ-free mice, which are maintained in a sterile environment throughout their lives, antibiotics can deplete bacterial populations in conventionally colonized mice (Park and Im, 2020; Kennedy et al., 2018). A key advantage of antibiotic treatment is that it allows researchers to specifically study the role of bacteria in adult mice. Germ-free mice, due to their complete lack of microbial exposure, exhibit various developmental and immune system impairments. In contrast, antibiotic treatment in adult mice enables the isolation of bacterial effects on cell function and signaling pathways after development has occurred. For studies requiring microbiota depletion early in development, some researchers administer antibiotics to pregnant dams in their drinking water. This limits the transfer of microbes to offspring, and the antibiotic regimen can be continued after weaning to maintain the depleted state (Lamousé-Smith et al., 2011; Deshmukh et al., 2014; Gonzalez-Perez et al., 2016; Li et al., 2017). Antibiotics can have selective effects on the microbiota due to their varying mechanisms of action. For instance, metronidazole and clindamycin target anaerobic bacteria, vancomycin is specific to gram-positive bacteria, and polymyxin B targets gram-negative bacteria (Atarashi et al., 2011; Schubert et al., 2015). Researchers can leverage these selective effects to manipulate the gut microbiota composition and identify bacterial classes relevant to specific phenotypes (Schubert et al., 2015; Zackular et al., 2016). Alternatively, a cocktail of antibiotics from different classes can be used for broader depletion of the gut microbiota. These regimens vary in antibiotic combinations, doses, and treatment duration, but all target gram-positive, gram-negative, and anaerobic bacteria. While antibiotic-treated mice aim to mimic germ-free conditions, achieving complete microbial elimination is neither guaranteed nor without unintended consequences (Lundberg et al., 2016). This is exemplified by a study by Yongwon Choi's group, where antibiotic treatment in one mouse strain resulted in gut inflammation observed to be dependent on the microbiota (Han et al., 2013). However, when the same model was placed under germ-free

conditions, the opposite effect was observed, suggesting the initial findings were due to off-target effects of the antibiotics, not the gut microbiota itself (Han et al., 2015).

6 Microbiota as a therapeutic target in mental and neurological diseases

A plethora of consumer products, including foods and supplements, have already entered the market, promising to improve gut health, mood, sleep, or cognitive function. However, the scientific evidence supporting the claims of many of these products remains weak or nonexistent. Rigorous clinical trials are necessary to establish the efficacy and safety of these interventions (Chakrabarti et al., 2022; Draper et al., 2017, Cheng L-H et al, 2019). Despite the current limitations, further exploration of the MGBA could lead to the development of more targeted and effective treatments. For example, manipulating the gut microbiota composition might offer benefits for neurodegenerative diseases like Parkinson's and Alzheimer's by positively impacting mitochondrial function and overall brain health (Zhu Y et al., 2022). Understanding the molecular mechanisms underlying this communication between the gut and the brain could pave the way for new medications to treat these currently incurable conditions.

Several promising avenues exist for manipulating the gut microbiota (figure 21). Fecal microbiota transplantation (FMT), where stool from a healthy donor is introduced into the gut of a recipient, has shown efficacy in treating antibiotic-resistant Clostridium difficile infections (Ericsson and Franklin, 2015). Additionally, various "biotics" - probiotics (live microorganisms), prebiotics (fibers that nourish gut microbes), postbiotics (metabolites produced by gut microbes), and synbiotics (combinations of prebiotics and probiotics) - are being explored for their potential to modulate the gut microbiome and improve both mental and digestive health (Brugman et al., 2018). Dietary and lifestyle interventions, such as managing stress and consuming a balanced diet rich in fiber, may also play a role in promoting a healthy gut microbiome.

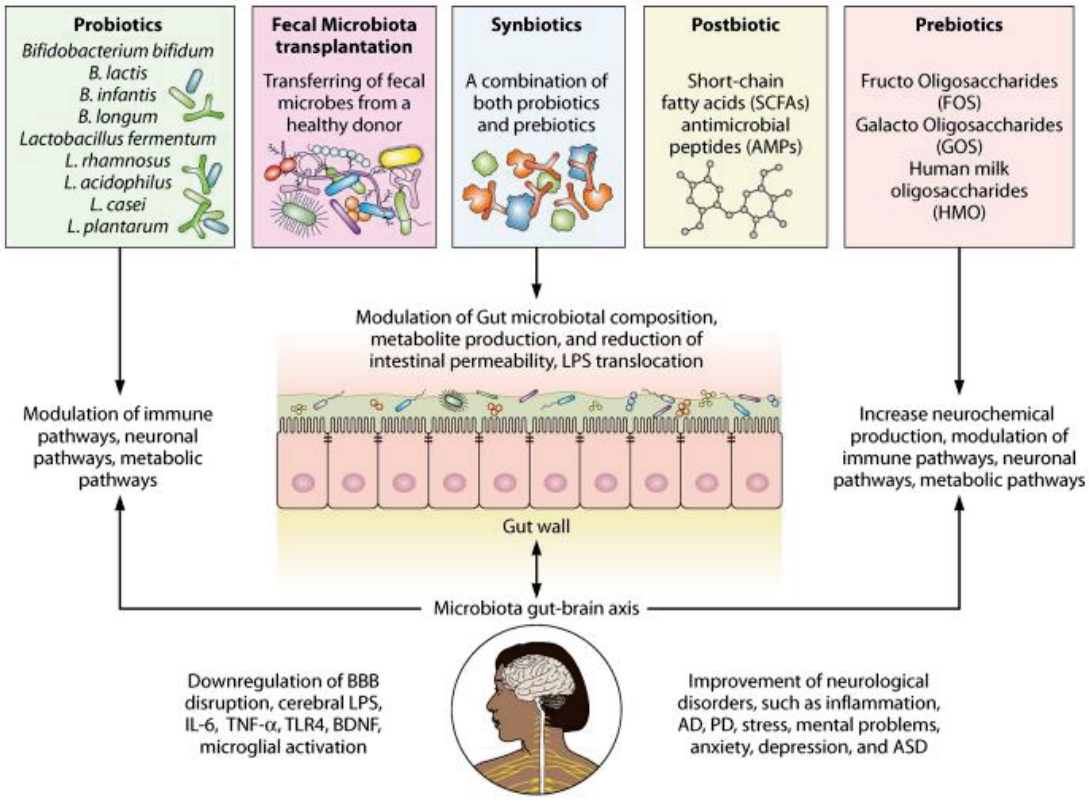

Figure 21. Modulation of gut microbiota by therapeutic microbial interventions. Microbial interventions, including probiotics, prebiotics postbiotics, synbiotics, and fecal microbiota transplant (FMT), improve the microbiota-gut-brain axis through modification of the microbial communities. Modulation of the microbial composition, regulation of their essential metabolites, or both can improve neurological complications by increasing neurochemicals and SCFAs and reducing intestinal permeability, regulation of neural, metabolic, and immune pathways. Each approach can be improved by personalized medicine for more effective management of a patient's pathophysiology. From Sorboni et al., 2022.

A growing body of research is investigating the therapeutic potential of prebiotics and probiotics in managing symptoms and conditions associated with neurodegenerative diseases and altered mental health (Barbosa and Vieira-Coelho, 2020; Ansari et al., 2020). The International Scientific Association for Probiotics and Prebiotics (ISAPP) defines probiotics as live microorganisms that confer a health benefit on the host when administered in adequate amounts (Hill et al., 2014). Preclinical studies utilizing animal models offer intriguing insights into this potential. For instance, administration of

Lactobacillus rhamnosus (JB-1) in BALB/c mice resulted in decreased anxiety and corticosterone levels, accompanied by upregulation of GABA receptors in the brain (Sorboni et al., 2022). Furthermore, the absence of these effects in vagotomized animals highlights the potential involvement of the vagus nerve in the microbiota-gut-brain axis (MGBA), which can be modulated by certain probiotics (Sorboni et al., 2022). These findings are further supported by human studies demonstrating personalized approaches. An investigation revealed that probiotic treatment could alleviate anxiety symptoms in healthy adults with a specific genetic variant associated with increased IL-1β production, suggesting potential for personalized psychobiotic therapy for anxiety disorders (Sorboni et al., 2022). Beyond individual strains, research has shown efficacy with specific probiotic combinations. Formulas containing Lactobacillus and Bifidobacteria strains have been demonstrated to significantly reduce psychological distress (Messaoudi et al., 2010), enhance cognition and communication in Alzheimer's disease patients (Akbari et al., 2016), and improve symptoms in Parkinson's disease (Tamtaji et al., 2018). In addition, a study investigating children with autism spectrum disorder (ASD) and gastrointestinal (GI) symptoms found that a specific probiotic formulation containing Lactobacillus strains was safe and improved both ASD and GI symptoms in patients who retained the probiotic bacteria (Arnold et al., 2019). Similarly, preclinical models of Alzheimer's disease suggest that *Lactobacillus plantarum* can enhance cognitive function and modulate neurotransmitter levels (Nimgampalle and Kuna, 2017). These findings are echoed in studies investigating the effects of other probiotic combinations on rodent models of AD (Athari et al., 2018; AsL et al., 2019; Rezaeiasl et al., 2019). Furthermore, a clinical trial suggests that *Lactobacillus rhamnosus* GG supplementation may reduce Attention Deficit Hyperactivity Disorder (ADHD) risk in infants with a family history of ASD (Pärtty et al., 2015). Emerging evidence also suggests potential benefits in Parkinson's disease, with long-term probiotic administration showing promise in alleviating motor impairments and protecting dopaminergic neurons in a genetic mouse model (Hsieh et al., 2020).

ISAPP defines prebiotics as "selectively utilized substrates that confer a health benefit on the host by promoting the growth of advantageous microorganisms" (Gibson et al., 2017).

This definition encompasses a broader range of compounds beyond traditional polysaccharide carbohydrates, including non-digestible oligosaccharides (NDOs), human milk oligosaccharides (HMOs), and soluble, fermentable fibers (Hill et al., 2014). These prebiotics promote gut health by selectively nourishing beneficial bacteria like Bifidobacteria and Lactobacilli (figure 21). The impact of prebiotics on the gut microbiota holds great potential, and although studies in this area remain limited, some encouraging results have already emerged. For example, galacto- and fructo-oligosaccharides or their combinations in male mice displayed antidepressant and anxiolytic effects, reversing the effects of chronic stress (Burokas et al., 2017). Similarly, prebiotic lactulose has been shown to improve cognitive deficits in AD mouse models by promoting autophagy and anti-inflammatory pathways (Lee Y.S. et al., 2021). These findings suggest that prebiotics, alongside probiotics, could be viable therapeutic options for neurological disorders. However, further research is needed to elucidate the underlying mechanisms, as correlation does not necessarily imply causation.

Synbiotics combine prebiotics and probiotics, with the prebiotics promoting the growth and metabolism of the probiotic microorganisms, enhancing their viability and benefits for the host (Lorente-Picón and Laguna, 2021). This synergistic approach aims to increase the abundance of beneficial microbes in the gastrointestinal tract (GIT). Careful selection of prebiotic and probiotic strains is crucial to ensure the survival and efficacy of the probiotic within the GIT. Studies suggest that synbiotics may be more effective than individual prebiotics or probiotics (Barathikannan et al., 2019; Krumbeck et al., 2018). For instance, a synbiotic combination of GOS and a multistrain probiotic containing *Lactobacillus helveticus* and *Bifidobacterium longum* demonstrated a reduction in depression symptoms and improved tryptophan signaling in patients with major depressive disorder (MDD) (Kazemi et al., 2019). Furthermore, a randomized controlled trial using a synbiotic containing multistrain probiotics and a prebiotic showed improvement in functional GI symptoms in a Parkinson's disease (PD) cohort (Barichella et al., 2016). However, further investigation is needed to fully understand the influence of synbiotics on the microbiota-gut-brain axis (MGBA) (Gocan et al., 2012).

Fecal microbiota transplantation (FMT) has emerged as a revolutionary therapeutic approach for restoring a healthy gut microbiota composition, offering potential for the management of various diseases (Hamamah et al., 2022). This technique involves the transfer of a healthy donor's fecal microbiota, encompassing both microbes and metabolites, to a recipient (Cheng Y.W. et al., 2023). The transplanted microbiota establishes itself within the recipient's gut, replicating and producing bioactive metabolites that contribute to a restored microbial ecosystem. FMT can be administered through colonoscopies, enemas, or oral ingestion of freeze-dried material. This groundbreaking approach has led to the development of the first approved FMT-based therapies. Australia's Therapeutic Goods Administration paved the way, granting approval to BiomeBank's microbiome-based therapy product, "Biomictra," specifically designed for treating *Clostridioides difficile* infections (Sasso et al., 2023). Similarly, the US Food and Drug Administration (FDA) approved Rebyota, Ferring Pharmaceuticals' first fecal microbiota product, for preventing recurrent C. Diff. infections in adults (Sasso et al., 2023).

Beyond *Clostridioides difficile* treatment, FMT holds promise for neurological disorders such as Parkinson's disease (PD), autism spectrum disorders (ASD), and multiple sclerosis (MS) (Cattaneo et al., 2017; Kim et al., 2020; Hegelmaier et al., 2020; Yang et al., 2019). FMT offers a potentially safe therapeutic option, with minimal reported side effects, even in high-risk patients (Haikal et al., 2019; Wimo et al., 2017). A study by Zhao et al. (2019) investigating FMT in ASD patients reported significant improvements in ASD-related symptoms and a shift towards a healthier gut microbiota composition following colonoscopic FMT. However, further research is needed to definitively establish the long-term efficacy and underlying mechanisms of FMT in ASD. Preclinical studies using mouse models of AD suggest a link between cognitive dysfunction and gut microbiota composition. FMT in these models effectively alleviated cognitive decline, highlighting the potential of FMT for treating neurological disorders (Reitz, 2012).

While extensive research has explored the gut microbiome and its response to dietary patterns (Wu et al., 2011; David et al., 2013), investigations into the influence of diet on microbiomes at other body sites remain relatively nascent. Dietary modulation presents a

compelling avenue for therapeutic intervention due to its low-risk profile, cultural acceptability, and potential for personalization. This approach is contingent upon establishing a causal link between gut microbiota composition and specific diseases. Current evidence demonstrates that long-term dietary patterns significantly impact gut microbiota composition (Wu et al., 2011). Remarkably, even short-term dietary shifts can induce rapid convergence in gut microbial profiles between individuals (David et al., 2013). Intriguingly, the gut microbiome can mediate individual variability in blood glucose responses to dietary components (Zeevi et al., 2015). Furthermore, the microbiome's influence extends to leptin regulation and, consequently, appetite control in humans. A captivating, yet unanswered question, is whether the microbiome can influence dietary preferences, potentially leading to positive feedback loops where dietary choices further shape the gut microbiota (Gilbert et al., 2018). Elucidating this intricate interplay between diet and the microbiome across various body sites holds immense potential for the development of personalized, dietary-based interventions for disease management.

AIM AND OBJECTIVES

The aims of this study are:

a) to highlight a possible trigger or modulator role of the gut microbiota in the natural history of X-ALD patients and its possible discriminatory value between different phenotypes;

b) to identify new diagnostic and prognostic biomarkers for X-ALD, based both on the existing knowledge of the features of X-ALD, which are also shared with other neurodegenerative diseases, and on possible new microbiota-derived metabolites, which will contribute to the understanding of the pathophysiology of this disease and could be implemented in clinical trials and, in the future, in routine diagnostics.

To accomplish these objectives:

- we performed an untargeted metabolomic analysis of the NAWM of ccALD and cAMN patients, searching for metabolites of possible bacterial origin on the one hand, and metabolites attributable to altered mitochondrial function and/or the presence of an inflammatory state on the other;

- we characterised the composition and functional potential of the gut microbiota of X-ALD patients by performing a shotgun metagenomic study of their stools.

- on the basis of the results obtained with the previous methods, we analysed in the peripheral blood and/or CSF of the patients markers of: neuronal, glial and mitochondrial impairment (NfL, GFAP, UCHL-1, tau and GDF15 respectively) and altered bacterial metabolism (amino acids profile).

MATERIAL AND METHODS

1 Brain white matter collection

Frozen blocks of normal-appearing brain white matter (NAWM) were obtained from male X-ALD patients (9 ccALD, mean age 9.7 years; 12 cAMN, mean age 37 years) and age-matched male controls (12 children, mean age 12.1 years; 12 adults, mean age 34.2 years) from the National Institutes of Health (NIH) NeuroBioBank. The frontal or parietal lobes were used for dissection. White matter sections from both ALD patients and controls were stained with Luxol fast blue (LFB) to identify demyelination, the demyelination edge, and normal-looking areas. Brain tissue sections were processed only when two to three adjacent sections showed no signs of demyelination with LFB staining and no perivascular cuffs of lymphocytes using hematoxylin and eosin staining.

2 Stool samples collection

Stool samples were self-collected from 32 male adult X-ALD patients (30 AMN and 2 cAMN, mean age 44.6 years), 6 male ccALD patients (mean age 9 years), and 48 male controls (19 children, mean age 8.7 years; 29 adults, mean age 43 years) using the OMNIgene-GUT™ kit (DNA Genotek). The samples were then aliquoted in our laboratory and stored at -80ºC until analysis.

3 Blood and CSF samples collection

A total of 178 peripheral venous blood samples were collected in EDTA-containing tubes. 4ml of blood was gently added to 4ml of Histopaque (Sigma-Aldrich) and centrifuged at 400xg for 30 min at room temperature without brake. Plasma, the uppermost layer, was immediately collected and transferred with a sterile Pasteur pipette into a cryovial and directly frozen at -80ºC. The PBMCs, localised at the interface between the Histopaque layer and the plasma, were transferred to a special cryotube, resuspended in DMSO, rapidly frozen at -80°C and then transferred to liquid nitrogen vials for long-term storage.

A total of 59 CSF samples were obtained by lumbar puncture and centrifuged (2000g, 4°C, 10 min) to collect the clear supernatant, which was aliquoted and immediately stored at -80°C.

The use of human samples was approved by the Clinical Research Ethics Committee of the Bellvitge University Hospital (AC130/10, PR170/18, PR328/20 and PR261/22).

4 Untargeted metabolomics on NAWM

Following methanol/water extraction, each NAWM sample was directly analyzed on two orthogonal chromatographic systems (Zic-pHilic and PFPP columns) to increase metabolome coverage. High-performance liquid chromatography (HPLC) systems were coupled to a high-resolution mass spectrometer (HMRS, Q-Exactive™ Hybrid Quadrupole-Orbitrap™) operating in negative ion mode for the Zic-pHilic column and positive ion mode for the PFPP column with a mass resolution of 140k at m/z 200. The XCMS/CentWave algorithm was used to detect, integrate, and align signals via the Workflow4Metabolomics Galaxy platform. Metabolite annotation and identification were achieved using an in-house database containing information (retention time, m/z, and MS/MS spectra) about 1000 standards belonging to central metabolism analyzed under the same conditions as the studied samples.

5 Shotgun metagenomic analysis on stool

DNA was obtained from stool samples using the Qiagen MagAttract PowerSoil DNA KF kit (Formerly MOBio PowerSoil DNA Kit) according to the manufacturer's instructions and protocols. DNA quality was evaluated visually via gel electrophoresis and quantified using a Qubit 3.0 fluorometer (Thermo-Fischer, Waltham, MA, USA). Libraries were prepared using an Illumina Nextera library preparation kit with an in-house protocol (Illumina, San Diego, CA, USA). Paired-end sequencing (150 bp x 2) was done on a NextSeq 500 in medium-output mode. Shotgun metagenomic sequence reads were processed with the Sunbeam pipeline (Clarke et al., 2019). Initial quality evaluation was done using FastQC v0.11.5 (Babraham Institute. Software available at: http://www.bioinformatics.babraham.ac.uk/projects/fastqc). Processing took part in four

steps: adapter removal, read trimming, low-complexity-reads removal, and host-sequence removals. Adapter removal was done using cutadapt v2.6 (Martin M., 2015). Trimming was done with Trimmomatic v0.36 (Bolger and Lohse, 2014) using custom parameters (LEADING:3 TRAILING:3 SLIDINGWINDOW:4:15 MINLEN:36). Low-complexity sequences were detected with Komplexity v0.3.6 (Clarke et al., 2019). High-quality reads were mapped to the human genome (Genome Reference Consortium Human Reference 37) and those that mapped to it were with at least 50% similarity across 60% of the read length were removed.

6 SCFA analysis on stool

The SCFA extraction procedure is similar to the one described by Zhao et al (2006). Briefly, faecal material were resuspended in MilliQ-grade H2O, and homogenized using MP Bio FastPrep, for 1 minute at 4.0 m/s. 5M HCl was added to acidify faecal suspensions to a final pH of 2.0. Acidified faecal suspensions were incubated and centrifuged at 10,000 RPM to separate the supernatant. Faecal supernatants were spiked with 2-Ethylbutyric acid for a final concentration of 1 mM. Extracted SCFA supernatants were stored in 2-ml GC vials, with glass inserts. SCFA were detected using gas chromatography (Thermo Trace 1310), coupled to a flame ionization detector (Thermo). The SCFA column used was the 'Thermo TG-WAXMS A GC Column, 30 m, 0.32 mm, 0.25 um'.

7 NfL, GFAP, UCHL-1 and TAU determination on plasma and CSF

Analysis of plasma and CSF samples from X-ALD patients was conducted at the Vall d'Hebron Institut de recerca (VHIR) using the Single Molecule Array (SiMoA™) HD-1 Analyzer (Quanterix Corporation), which runs ultrasensitive paramagnetic bead-based enzyme-linked immunosorbent assays (Korley et al., 2018). The assays were performed according to the manufacturer's instructions. Briefly, plasma samples were diluted 1:4 with assay buffer and incubated with the appropriate capture beads for 60 minutes at room temperature on a plate shaker at 750 rpm. The beads were then washed three times with wash buffer using a magnetic plate washer. After the final wash, the beads were incubated with the detection antibodies for 30 minutes at room temperature on a plate shaker at 750

rpm. The beads were washed again three times with wash buffer and resuspended in reading buffer before being analyzed on the SIMOA HD-1 Analyzer. The SIMOA HD-1 Analyzer uses a two-step process to detect the beads. First, the beads are passed through a laser beam that excites the fluorescent dyes on the beads. Second, the beads are passed through a detector that measures the emitted fluorescence. The amount of fluorescence is proportional to the number of beads present, which is in turn proportional to the amount of analyte in the sample. A standard curve was generated for each analyte using a serial dilution of a certified reference material. The results of the assay were analyzed using the SIMOA HD-1 Analyzer software. The software calculates the concentration of each analyte in the sample based on the standard curve. The determination of plasma and CSF concentrations of NfL, GFAP, UCHL1, and total-TAU was performed with the commercially available "Neurology 4-plex Advantage" kit; the lower limits of detection (LOD) of the assay are 0.104 pg/mL, 0.221 pg/mL, 1.74 pg/mL and 0.024 pg/mL for NfL, GFAP, UCHL1, and total TAU, respectively.

8 Targeted amino acids analysis on plasma

The amino acid standard solutions contained 2500 µmol/L of each amino acid, except for cystine (1250 µmol/L), and were diluted in 0.1 mol/L HCl. These solutions were further diluted in water resulting in a final concentration of 250 µmol/L for each amino acid, except for cystine (125 µmol/L). The mixture of isotope-labeled amino acids was diluted in water to reach a final concentration of 250 µmol/L for each amino acid, except for cystine (13C6, 15N2) (125 µmol/L). Standard and plasma samples aliquots of 25 µL were vortexed with 25 µL of the internal standard solution and 150 µL of methanol/0.1% formic acid to precipitate the proteins. Then, the samples were centrifuged at 6000×g for 10 min. For the derivatization reaction, 5 µL of the supernatant was mixed with 35 µL of borate buffer (pH 8.8) and 10 µL of the AQC solution (3 mg/mL in acetonitrile; AccQ·Tag Ultra Derivatization Kit). Amino acids were extracted from 1 punch of 6 mm in diameter with 130 µL of 3% trichloroacetic acid and 10 µL of the internal standard solution. The mixture was extracted for 1 h at room temperature and centrifuged at 2200×g for 10 min. Ten microliters of the supernatant was mixed with 60 µL of borate buffer and 10 µL of AQC solution. The reaction mixtures were heated at 55 °C for 10

min. After that, the samples were ready to be analyzed. The amino acid standard solutions and plasma samples from X-ALD patients and controls were analyzed to determine amino acid levels using a Waters ACQUITY UPLC H-class instrument equipped with a reversed-phase C-18 column. Chromatographic separation was performed at 55 °C with a CORTECS C18 2.1×150, 1.6 µm column (Waters). A gradient of water (mobile phase A) and acetonitrile (mobile phase B), both containing 0.1% formic acid, was used at a flow rate of 0.5 mL/min. The gradient program used was as follows: initial 99% A, hold for 1 min; gradient to 87% A in 1 min; gradient to 85% A in 3.5 min; gradient to 5% A in 1 min, hold for 1 min; return to initial conditions in 0.1 min and equilibrate for 1.4 min. The run time was 9 min, and the injection volume was 2 µL. Detection was performed with a Waters Xevo TQD triple-quadrupole mass spectrometer using positive electrospray ionization in the multiple reaction monitoring (MRM).

9 ccfmtDNA determination on CSF

The CSF circulating cell-free mtDNA (ccfmtDNA) copy number was calculated by droplet digital (dd)PCR according to the method described by Trifunov et al. The 20 µl reactions consisted of 5 µl of CSF samples, 1 × ddPCR supermix for probes (no dUTP), 250 nmol/l ND1 probe, 500 nmol/l ND1 primers, 125 nmol/l ND4 (or B2M or BAX) probe, 250 nmol/l ND4 (or B2M or BAX) primers and nuclease-free water. Reactions were transferred to ddPCR 96-well plates. Droplet generation was carried out manually using a QXDx droplet generator. For this purpose, 70 µl of droplet generation oil was added to each sample, and DG8 cartridges and DG8 gaskets were used for the QX200/QX100 droplet generator. Droplets were transferred to 96-well plates and then sealed for amplification. PCRs were carried out in a C1000 touch thermal cycler using standard cycling conditions: 95°C for 10 min, 40 cycles of 94°C for 30 and 60°C for 1 min and then 98°C for 10 min. Following PCR amplification, droplets were read on a QX200 droplet reader, and ddPCR data were analysed using QuantaSoft software.

10 GDF15 determination on plasma

GDF15 levels were measured using a specific human GDF15 solid phase sandwich ELISA kit (Quantikine, R&D Systems, Minneapolis), according to the manufacturer's instructions.

11 Bulk RNAseq of PBMCs

After isolation on a Histopaque layer, samples were homogenized and total RNA was isolated by Trizol® reagent. To determine the total RNA quality and quantity, the Qubit® RNA HS Assay (Life Technologies) and the RNA 6000 Nano Assay on a Bioanalyzer 2100 (Agilent) were used. The mRNASeq libraries were prepared following the TruSeq Stranded mRNA LT Sample Prep Kit protocol (Illumina). Briefly, total RNA (500 ng) was enriched for the polyA mRNA fraction and fragmented. The blunt-ended double-stranded cDNA was 3′-adenylated, and Illumina platform-compatible adaptors with unique dual indexes and unique molecular identifiers (Integrated DNA Technologies, IDT) were ligated. The mRNASeq libraries were sequenced on a NovaSeq 6000 (Illumina) with a read length of 2x101 bp following the manufacturer's protocol for dual indexing. Image analysis, base calling, and quality scoring of the run were processed using the manufacturer's software Real Time Analysis (RTA v3.4.4), followed by the generation of FASTQ sequence files. RNA-seq reads were mapped against the Homo sapiens reference genome (GRCh38) with STAR/2.7.8a using ENCODE parameters. Genes were quantified with RSEM/1.3.0 using the gencode38 human annotation. Lowly expressed genes were removed (genes with at least one sample with >1 count per million were kept) and differential expression of genes was performed with limma using the TMM method for normalization and the voom transformation of the counts (the counts are converted to log counts per million – logCPM- values, adding 0.5 to all the counts to avoid taking the logarithm of zero).

12 Statistical analysis

For data processing, including filtering and normalization, of untargeted metabolomics on NAWM samples, we used the MetaboAnalystR package (Chong et al., 2018). Then, differentially intensities between groups were detected using the Limma package (Ritchie et al., 2015). A major benefit of the Limma procedure is that it allows for factorial analysis in the specification of the linear model. As such, we were able to adjust for age between phenotypes by including two-levels, children and adult in the specification of the Age factor. Therefore, for ccALD and cAMN differences, the design analysis specified only one contrast [(ALD.child-CTL.child) – (ALD.adult-CTL.adult)], characterizing the genotype-by-age interaction between X-ALD and controls in children and adults. In addition, a two-factor analysis of variance (ANOVA) was performed to account for the potential effect of age on metabolite levels between X-ALD phenotypes (ccALD and cAMN). This analysis included "age" as a factor with two levels (children and adults) in the model specification. The threshold for statistical significance (p-value) was set at 0.05. For multivariate analysis representation Partial Least-Squares Discriminant Analysis (PLS-DA) was performed using the MetaboAnalystR package (Chong et al., 2018).

For the shotgun metagenomic analysis, after quality control and removal of human-derived reads, taxonomic classification of the remaining sequences was performed using Kraken2 with the PlusPF database (version dated 27 January, 2021) (Wood et al., 2019). For functional profiling, high-quality filtered reads were aligned against the SEED database using a translated homology search. Subsequently, these reads were annotated to functional levels 1-3 (Subsystems) using Super-Focus (Silva et al., 2015). The vegan package (Jari et al., 2019) was employed for ordination analysis (beta diversity) of taxonomic profiles, comparing species-level taxonomic profiles using Bray-Curtis dissimilarities. Non-metric multidimensional scaling (NMDS) was used to visualize sample distribution based on these dissimilarities. Alpha diversity was estimated calculating the Shannon’s index. Differential abundance analysis was performed using the DESeq2 R package (Love et al., 2014): we employed a negative binomial model to test for significant differences in abundance of taxonomic features and functional categories. The analysis aimed to identify differences between groups and disease status

while controlling for age differences (sequential model). p-values were calculated using the likelihood ratio test (LRT) with an adjusted threshold of 0.05. All statistical analyses were conducted using R software (R Core Team, 2022). Box plots illustrating significant differences in bacterial taxa or functions identified by shotgun metagenomic analysis and dot plots showing SCFA levels were created using GraphPad Prism version 9.4.1 (GraphPad Software, San Diego, California, USA).

For comparisons of NfL, GFAP, UCHL1 and TAU levels in plasma and CSF or ccfmtDNA in CSF between the control, asymptomatic X-ALD (when available), AMN and cerebral X-ALD groups, analysis was performed on natural log-transformed data. We applied a linear model analysis to compare log-transformed data between groups, for the association analysis between NfL and GFAP markers with Loes score and the association analysis between the NfL values in plasma and CSF. We included the patient age as a covariate. Then, we applied t-test pairwise comparisons between group levels with Benjamini-Hochberg (BH) corrections for multiple testing. A linear mixed model was performed instead of a basic linear model when the AMN group was present by using the nlme R package (Pinheiro et al., 2021). We added the patient age as a fixed factor and the patient ID as a random factor to take replications within patients into account. For association evaluation between the NfL values in plasma and CSF, we added the age and the days between the CSF and plasma sample extraction as dependent variables in the model. Then, we applied estimated marginal means (EMMs) adjusted by Bonferroni's method to obtain pairwise comparisons between groups by using emmeans R package (Lenth, 2021).

The distribution of amino acids and GDF15 levels in plasma from controls, AMN, ccALD, and cAMN groups was assessed using the Shapiro-Wilk test. Outliers were identified using the Rout test and excluded from subsequent analyses. Unpaired t-tests were used to compare plasma amino acid levels between the child control group and the ccALD group, provided the data distribution was normal. Otherwise, the non-parametric Mann-Whitney test was employed. For the adult groups (controls, AMN, and cAMN), one-way ANOVA was used for normally distributed data, while the Kruskal-Wallis test was applied for non-normal data. The threshold for statistical significance (p-value) was

set at 0.05. Spearman's rank correlation coefficient was calculated to assess the correlation between amino acid levels or GDF15 and NfL or GFAP levels. The p-value threshold for correlation analysis was set at 0.05.

We calculated the area under the curve (AUC) of the receiver operating characteristic (ROC) curve of NfL, GFAP, UCHL1, TAU, GDF15 and the amino acids that were significantly different between X-ALD patients and controls, to evaluate their diagnostic accuracy. The confidence interval was set at 95% and the p-value threshold was set at 0.05. Statistical analyses and graphs for comparison of amino acids and GDF15 levels between groups, their ROC curves and their correlation with NfL and GFAP levels were performed using GraphPad Prism version 9.4.1 (GraphPad Software, San Diego, California, USA).

RNAseq counts from PBMC samples were analysed using a two-factor analysis with age (child and adult) and genotype (CTL and X-ALD) as the defining factors. A volcano plot was generated using the EnhancedVolcano package R software (R Core Team, 2022) showing differentially expressed genes between ccALD and AMN phenotypes adjusted for age (@ symbol), commonly upregulated genes in both ccALD and AMN (up triangle), commonly downregulated genes in both ccALD and AMN (down triangle), up- or down-regulated genes in only one ccALD or AMN group compared to age-matched controls (cross). Genes with a log2 fold change greater than 0.2 and a probability value less than 0.05 were highlighted.

RESULTS– PART I

1.1 The NAWM of patients with X-ALD has a specific metabolic signature

Untargeted metabolomic analysis of non-affected brain white matter (NAWM) samples from X-ALD patients revealed distinct metabolite profiles compared to controls. For NAWM samples a total of 7589 peaks was detected. The peak annotation led to the identification of a total of 132 metabolites with the Zic-pHilic system and 73 metabolites with the PFPP system. Utilizing the Zic-pHilic chromatography system and PFPP system, Least-Squares Discriminant Analysis (PLS-DA) demonstrated a separation of X-ALD and control samples. Only the Zic-pHilic chromatography system Hilic provides a separation between ccALD and cAMN patients (figures 22 A, B).

1.2 Mitochondrial impairment, redox imbalance and bacteria derived metabolites contributes to the X-ALD signature in the NAWM

A total of 64 of identified metabolites (excluding duplicates, i.e. annotated with both systems) were found to be significantly altered in X-ALD NAWM compared to controls (figures 23 A, B): 30 metabolites were elevated, while 34 were reduced. Notably, decreased levels of N-acetylaspartic acid (NAA) and L-aspartate are compatible with mitochondrial dysfunction (Jeffrey, 2021; Birsoy et al., 2015) while reduced carnosine (Car) and taurine (Tau) levels support the presence of a redox imbalance (Caruso et al., 2019; Lambert et al., 2014). Moreover, we detected low levels of β-alanine and L-histidine (His), precursors of Car, in the NAWM of X-ALD patients (figures 23 A, B). Additionally, X-ALD patients displayed decreased levels of other amino acids like serine (Ser) and lysine (Lys) (figures 23 A, B). Interestingly, X-ALD brain samples exhibited elevated levels of phenylacetyl-L-glutamine, hydroxyphenyllactic acid, and phenyllactic acid, all metabolites associated with microbial aromatic amino acid metabolism (Kathryn et al., 2021; Achilles et al., 2022; Dodd et al., 2017) (figure 23 A).

Moreover, twelve of the identified metabolites were found to be significantly different in the NAWM samples of ccALD patients compared to cAMN patients. Interestingly, the two amino acids serine and histidine were less represented in the NAWM of ccALD patients compared to cAMN (figures 24 A, B). Remarkably Hippurate, a mammalian-microbial co-metabolite, is increased in ccALD patients respect to cAMN. Hippurate is synthesized from benzoate in the mitochondrial matrix while benzoate could be produced from the microbial degradation of dietary aromatic compounds in the intestine (Williams et al., 2010).

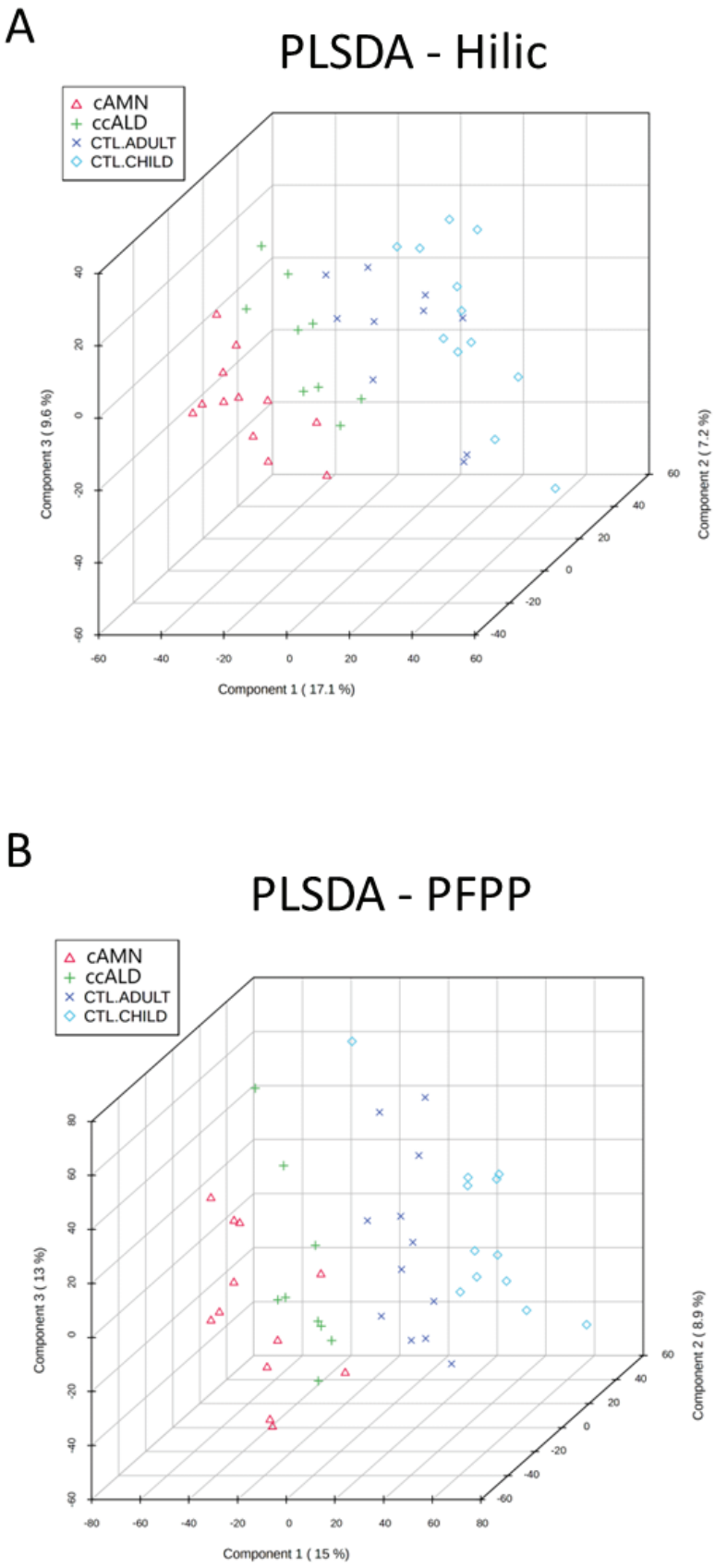

Figure 22. X-ALD metabolic profile in normal-appearing white matter.

(A) Tridimensional PLS-DA plot showing the sample distribution for controls and X-ALD subjects (cAMN and ccALD) in the untargeted metabolomic study with the Zic-pHilic system.

(B) Tridimensional PLS-DA plot of showing the sample distribution for controls and X-ALD subjects (cAMN and ccALD) in the untargeted metabolomic study with the PFPP system.

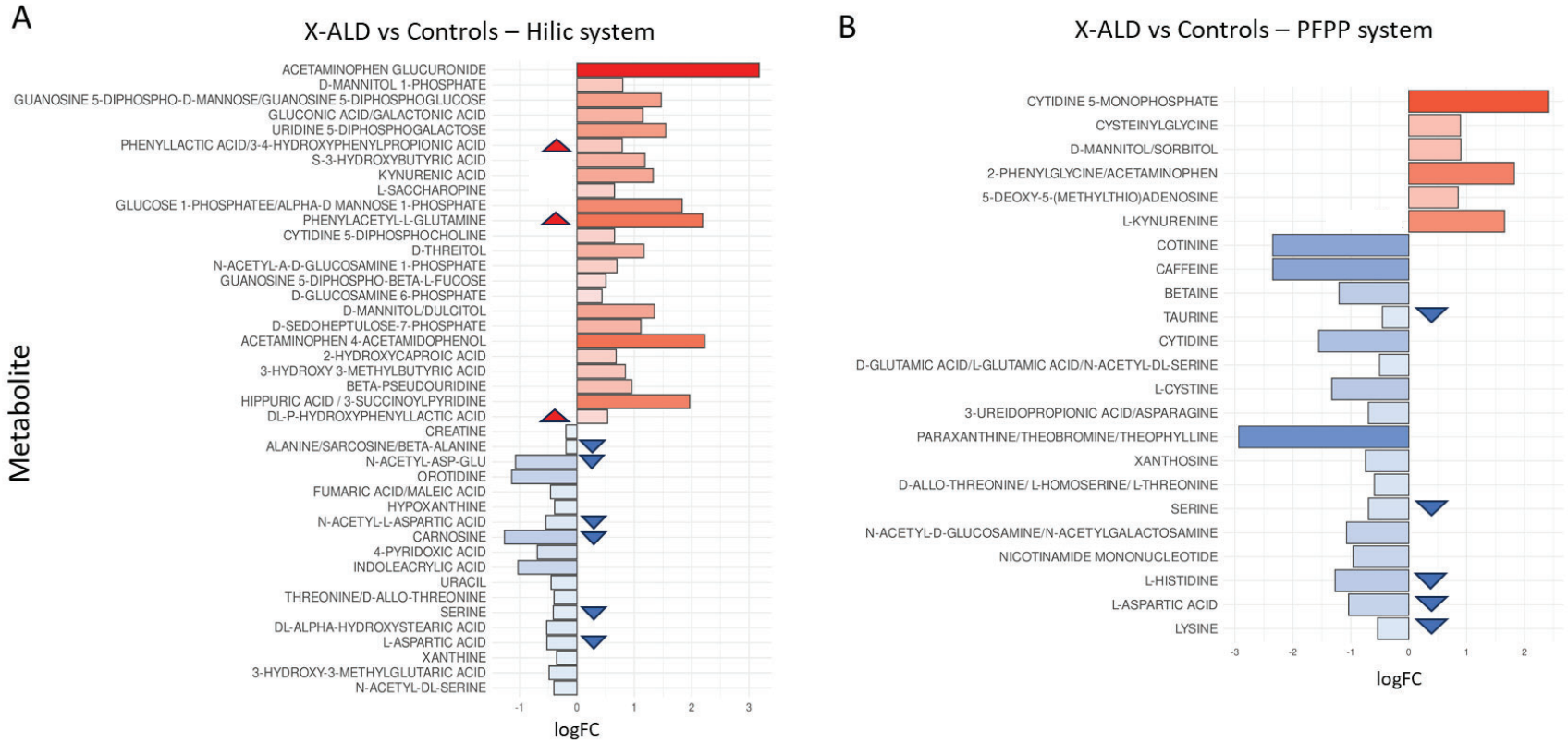

Figure 23. Metabolites significantly different between X-ALD patients and controls NAWM.

Bar plot representation of peak intensities and log2 changes of the differential annotated metabolites obtained in X-ALD patients respect to controls with HILIC (A) and PFPP (B) system (adjusted p value<0.05). Each bar represents a significant annotated metabolite species colored according to its abundance intensity normalized to the median across the samples. The scale from blue to red represents this normalised abundance in arbitrary units. The triangle symbol indicates some of the most interesting metabolites.

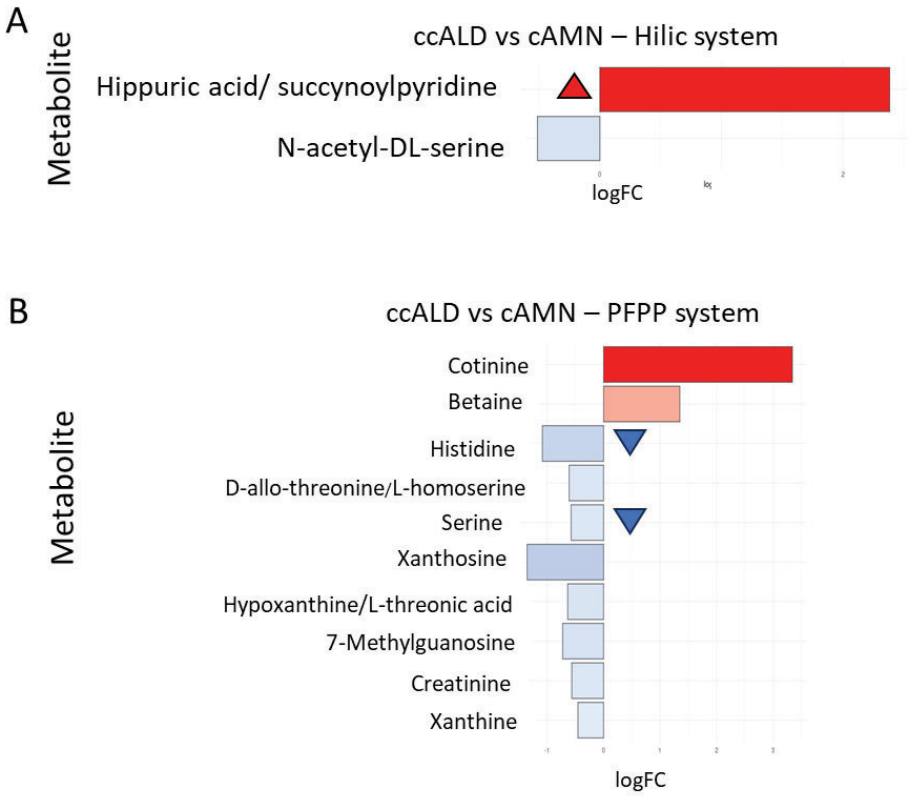

Figure 24. Metabolites significantly different between ccALD and cAMN patients NAWM. Bar plot representation of peak intensities and log2 changes of the differential annotated metabolites obtained in ccALD respect to cAMN patients with HILIC (A) and PFPP (B) system. Each bar represents a significant annotated metabolite species (adjusted p value < 0.05) colored according to its abundance intensity normalized to the median across the samples. The scale from blue to red represents this normalised abundance in arbitrary units. The triangle symbol indicates some of the most interesting metabolites.

1.3 Gut microbiota taxonomic profile in X-ALD patients

The gut microbiota play a crucial role in regulating the amino acid pool and profile during intestinal digestion and absorption, with significant implications for host health and disease (Beaumont et al., 2022). Therefore, we hypothesized that the observed alterations of amino acids or their derivatives in the NAWM of X-ALD patients could be related to a gut microbiota dysbiosis in X-ALD patients, with a potential impact on disease pathogenesis. Hence, we conducted an analysis of the gut microbiota composition and

function using shotgun metagenomics. At the phylum level, the fecal bacterial profiles of both X-ALD patients and controls were dominated by Bacteroidetes and Firmicutes (figure 25 A). At the genus level, Bacteroides, Faecalibacterium, and Phocaeicola were most abundant (figure 25 B).

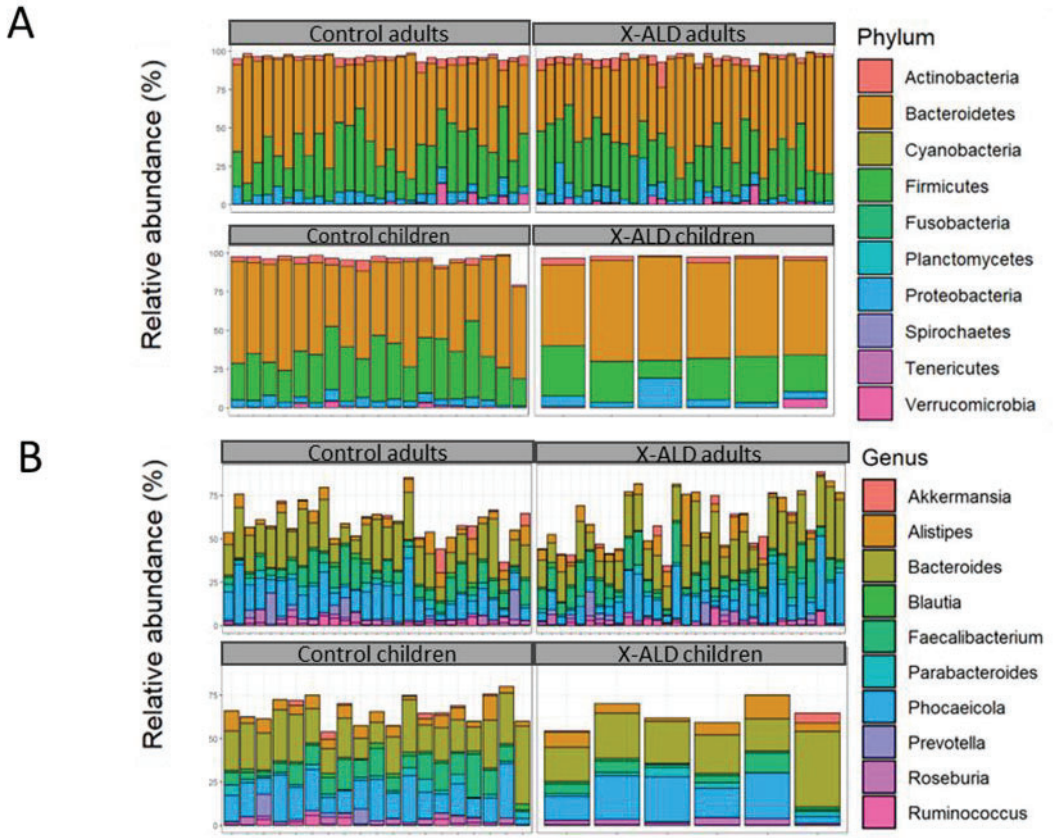

Figure 25. X-ALD gut microbiota taxonomic profile. (A, B) Bar charts showing the relative abundances (%) of the ten most abundant bacteria phila (A) and genera (B) in 32 male adult X-ALD patients (30 AMN and 2 cAMN patients, mean age 44.6 years), 6 male ccALD patients (mean age 9 years), and 48 male controls (19 children, mean age 8.7 years; 29 adults, mean age 43 years)

Analysis of species diversity (beta-diversity) using Bray-Curtis dissimilarities did not show a clear separation between the ccALD, cAMN, AMN and controls groups (figure 26 A). Alpha diversity was calculated from taxonomic profiles using Shannon's diversity index (figure 26 B). Alpha diversity was not significantly different across the groups,

although the sequential model indicated an age effect between groups (Scheirer-Ray-Hare-test). However, the comparison of Shannon's index between patients with the cerebral form and AMN showed no significant difference.

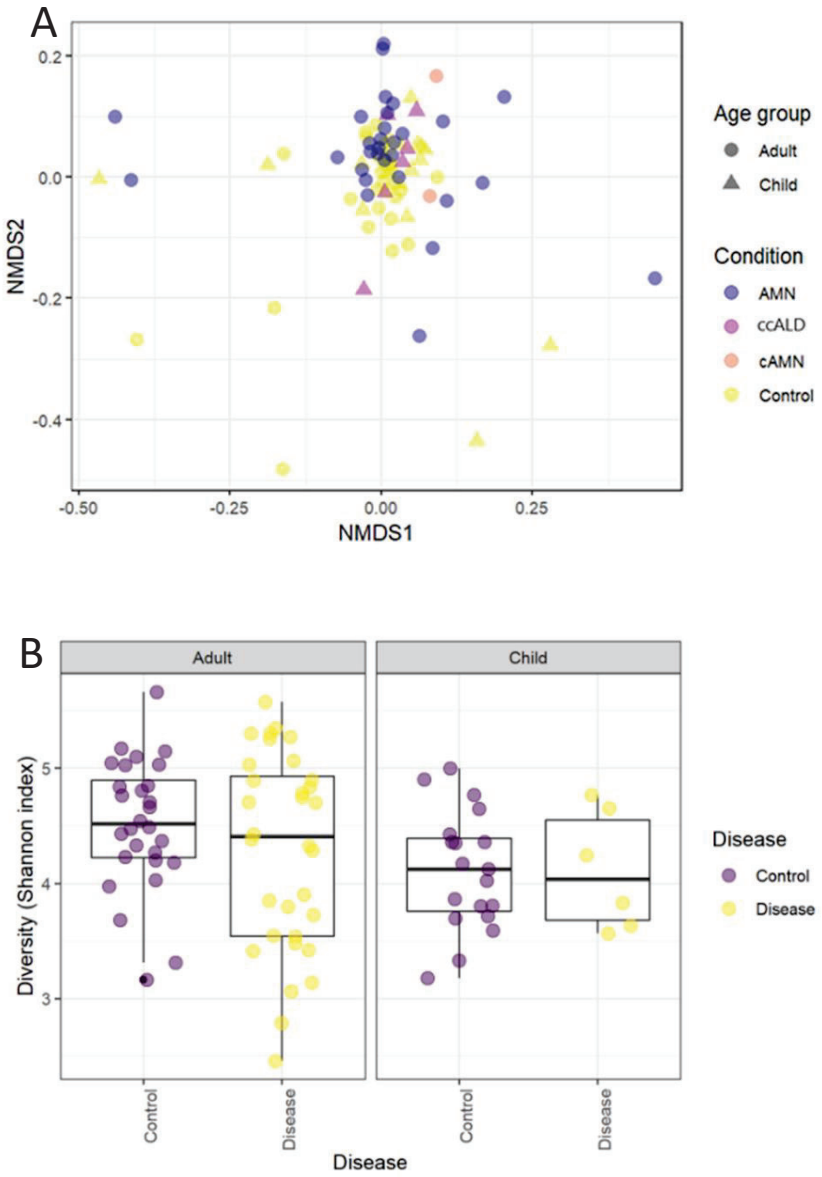

Figure 26. Variability in community composition among X-ALD and controls samples. (A) Bidimensional PCA corresponding to the Bray–Curtis dissimilarity index (beta diversity) in X-ALD and controls samples (AMN, n = 30; ccALD, n = 6; cAMN, n=2), child control (n=19), and adult control (n=29). Samples were visualized using non-metric multidimensional scaling (NMDS). (B) Box plots showing the Shannon index distribution (alpha diversity) in adults and child X-ALD patients and Controls.

1.4 Gut microbiota in X-ALD patients presents specific taxa and function alterations

The differential abundance analysis between CALD patients (cAMN+ccALD) and AMN patients showed only one bacterium (Anaerotignum propionicum, adjusted p-value of 0.016) with increased abundance in CALD patients compared to AMN at the taxa level and no differential functions between the two groups. In view of this and the previous beta and alpha diversity results, we therefore continue the analysis comparing the X-ALD group (cAMN+ccALD+AMN) with the control group (adult + child), looking for differences in disease or healthy status after controlling for differences in age. The differential abundance analysis revealed 226 and 144 significant distinct taxa and functions, respectively, in X-ALD patients compared to controls (see Appendix 1 and 2). Among X-ALD patients, the most consistent taxonomic alterations were noted for *Streptococcus* spp., which exhibited increased abundance (figure 27 A), and for *Flavobacterium* spp. and *Chryseobacterium* spp., which displayed decreased abundance (figure 27 B). Functionally, the most recurrent alterations were observed in pathways related to: a) modulation of amino acid bioavailability, with a reduction in bacterial functions involved in the biosynthesis of several amino acids such as branched-chain amino acids (BCAAs, i.e. isoleucine, leucine and valine), glutamine, glutamate, aspartate, asparagine, serine, alanine, methionine and proline. This reduction was accompanied by an increased abundance of the lysine degradation function (figure 28); b) bacterial adaptation to environmental stress, characterized by an increased abundance of pathways associated with oxidative stress regulation, glyoxylate response bypass, universal stress protein family, lipid A modification and biofilm adhesin biosynthesis (figure 29). Interestingly, we found that the functional potential of vitamin B6 and folate production is also reduced in X-ALD patients compared to controls (figure 30).

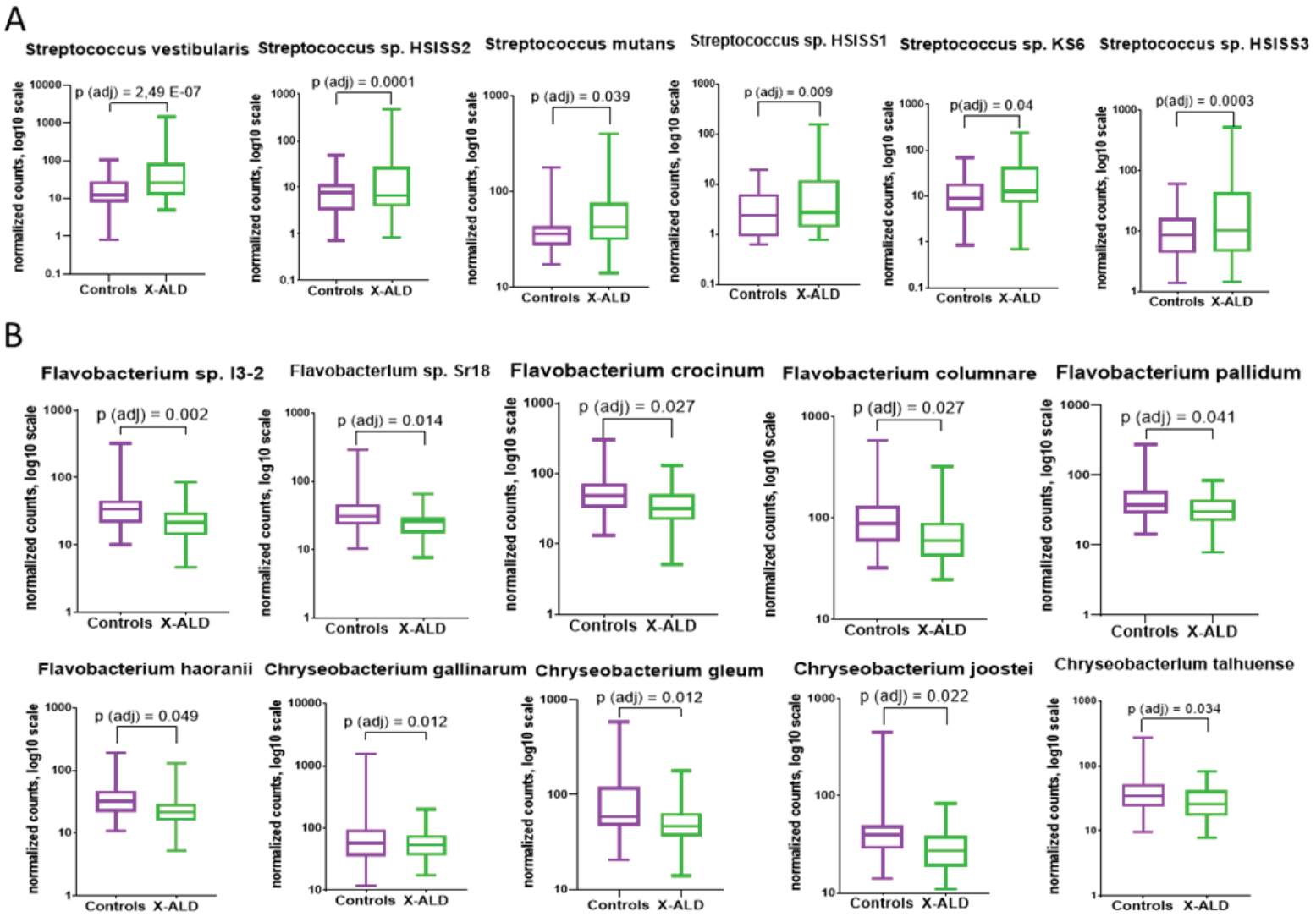

Figure 27. The most consistent alterations at species level in X-ALD microbiota (figure legend in the next page).

Figure 27. The most consistent alterations at species level in X-ALD microbiota. Box plots showing the differential abundances (normalised read counts on log10 scale) of several species of (A) *Streptococcus* spp, (B) *Flavobacterium* spp and *Chryseobacterium* spp in X-ALD patients respect to controls. Negative binomial models were used for differential abundance testing of taxonomic features. We looked for differences between among groups, and also for difference in disease status after controlling for age differences. p-values were calculated with LRT test with an adjusted p-value cut off = 0.05. Whiskers from minimum to maximum, median abundances and interquartile ranges have been indicated in the plots.

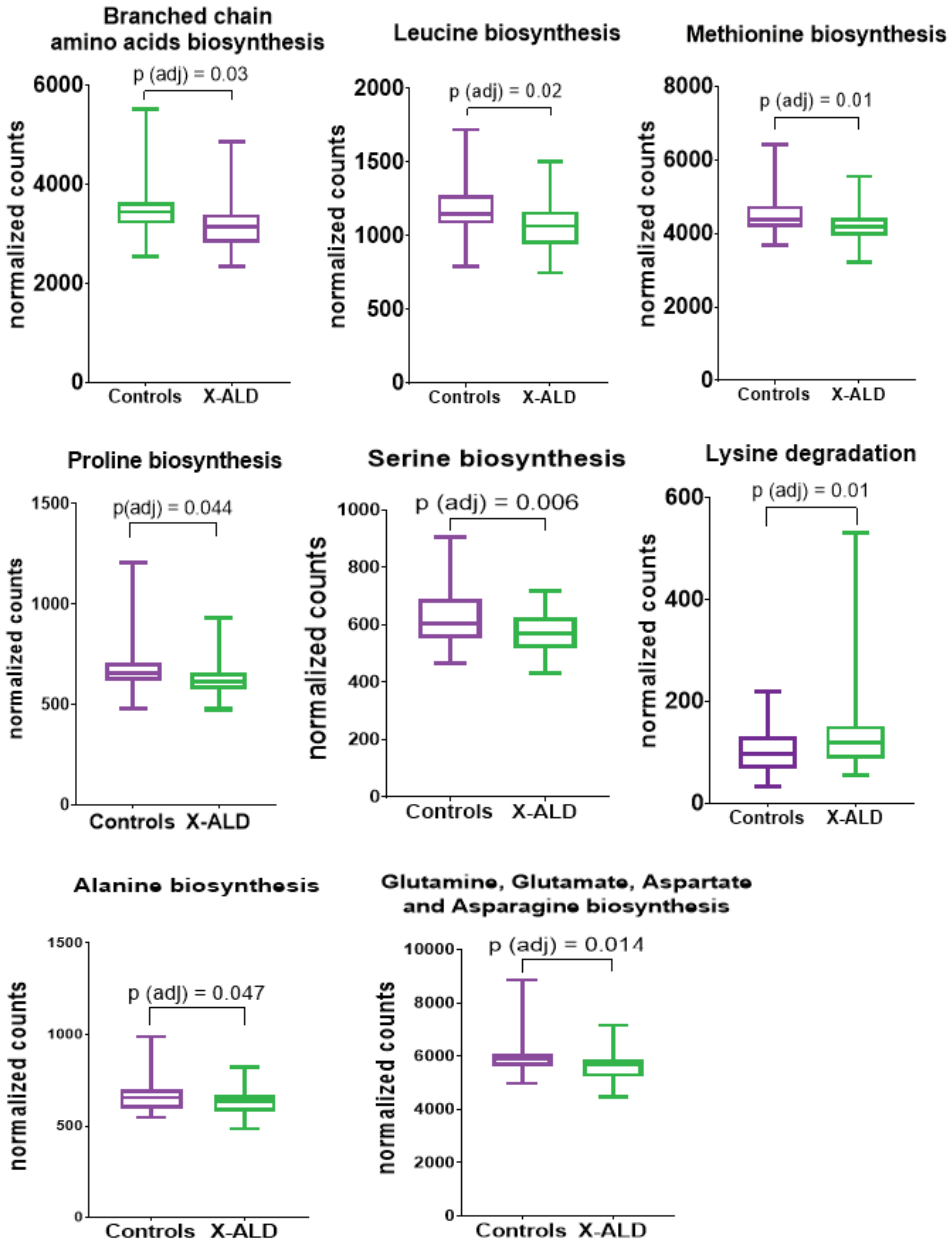

Figure 28. Microbiota functional features of amino acids metabolism in X-ALD patients (figure legend in the next page)**.**

Figure 28. Microbiota functional features of amino acids metabolism in X-ALD patients. Box plots showing the differential abundances (normalized read counts) of functions implicated in amino acid metabolism in the gut microbiota of X-ALD patients compared to controls. Negative binomial models were used for differential abundance testing of subsystem level 3 (function) features. p-values were calculated with LRT test with an adjusted p-value cut off = 0.05. Whiskers from minimum to maximum, median abundances and interquartile ranges have been indicated in the plots.

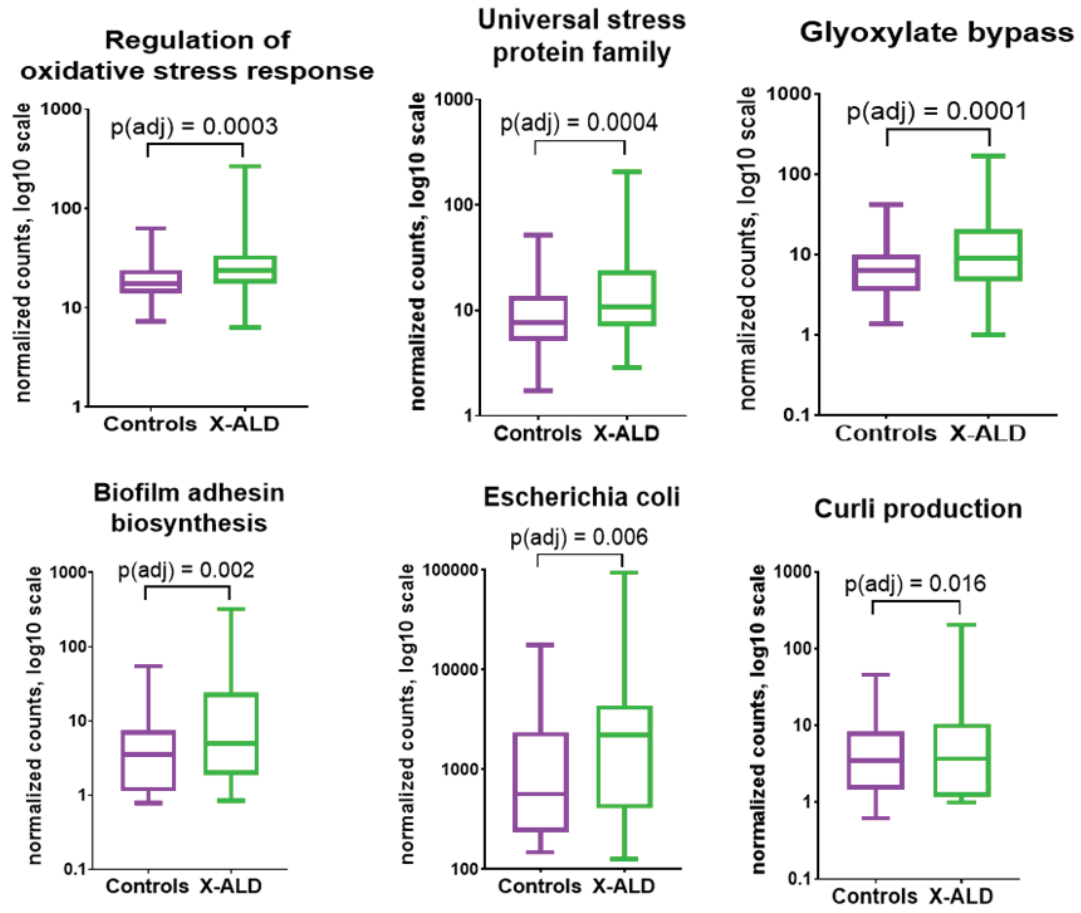

Figure 29. Microbiota features of environment adaptation in X-ALD patients. Box plots showing the differential abundances (normalized read counts on log10 scale) of functions and/or species implicated in gut environmental response in X-ALD patients respect to controls. Negative binomial models were used for differential abundance testing of subsystem level 3 (function) and taxonomic features. p-values were calculated with LRT test with an adjusted p-value cut off = 0.05. Whiskers from minimum to maximum, median abundances and interquartile ranges have been indicated in the plots.

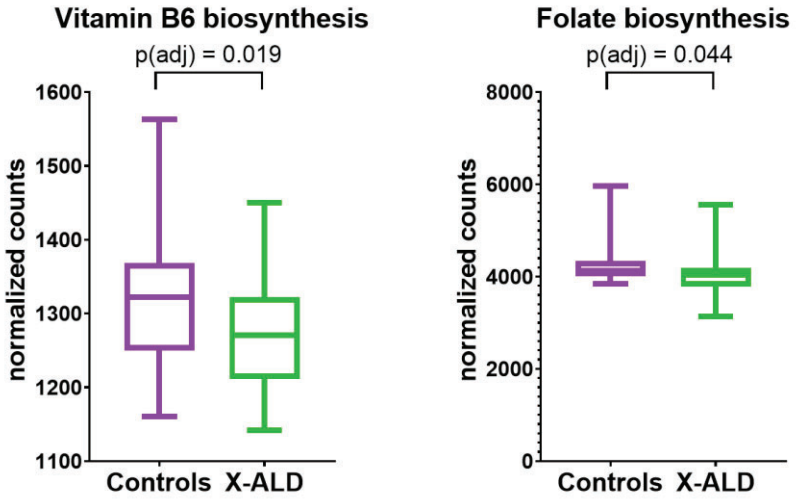

Figure 30. Microbiota functional features of reduced vitamins biosynthesis in X-ALD patients. Box plots showing the differential abundances (normalized read counts) of functions implicated in vitamin B6 and folate biosynthesis in the gut microbiota of X-ALD patients compared to controls. Negative binomial models were used for differential abundance testing of subsystem level 3 (function) features. p-values were calculated with LRT test with an adjusted p-value cut off = 0.05. Whiskers from minimum to maximum, median abundances and interquartile ranges have been indicated in the plots.

RESULTS – PART II

2.1.1 NfL, GFAP, UCHL1, and TAU plasma levels in X-ALD patients

AMN patients and the inflammatory cerebral form of X-ALD (ccALD + cAMN group) showed significantly increased plasma levels of NfL respected to the control group (figure 31 A). In addition, NfL levels are higher in patients with cerebral X-ALD compared to AMN patients (figure 31 A). Plasma GFAP concentrations were higher in AMN and cerebral X-ALD compared to healthy individuals. Moreover, a significant difference was observed in cerebral X-ALD patients' samples compared to AMN patients (figure 31 B). The plasma UCHL1 concentrations differ significantly between the cerebral X-ALD patients and both AMN and healthy individuals while no increase was observed in AMN patients (figure 31 C). No significant difference for plasma TAU is observed between AMN, cerebral X-ALD patients, and healthy control (figure 31 D).

ROC analysis demonstrated that NfL and GFAP were effective in differentiating ccALD, cAMN and AMN patients from their respective controls. In contrast, UCHL1 and Tau values were not capable of distinguishing cAMN, AMN or ccALD patients from their controls (figure 32). The highest accuracy was achieved for NfL in discriminating cAMN patients from controls, whereas the lowest accuracy was observed for GFAP in separating AMN patients from controls. Taken together, these results suggest that among the 4 possible biomarkers analysed only NfL and GFAP retain useful diagnostic potential in X-ALD patients.

2.1.2 Positive association between plasma NfL and GFAP and the Loes score in cerebral X-ALD patients.

A statistically significant positive association is observed between NfL or GFAP plasma levels and Loes score in cerebral X-ALD patients (ccALD and cAMN) (figure 33 A-D). However, this association between NfL or GFAP and Loes does not exist in the group of AMN patients.

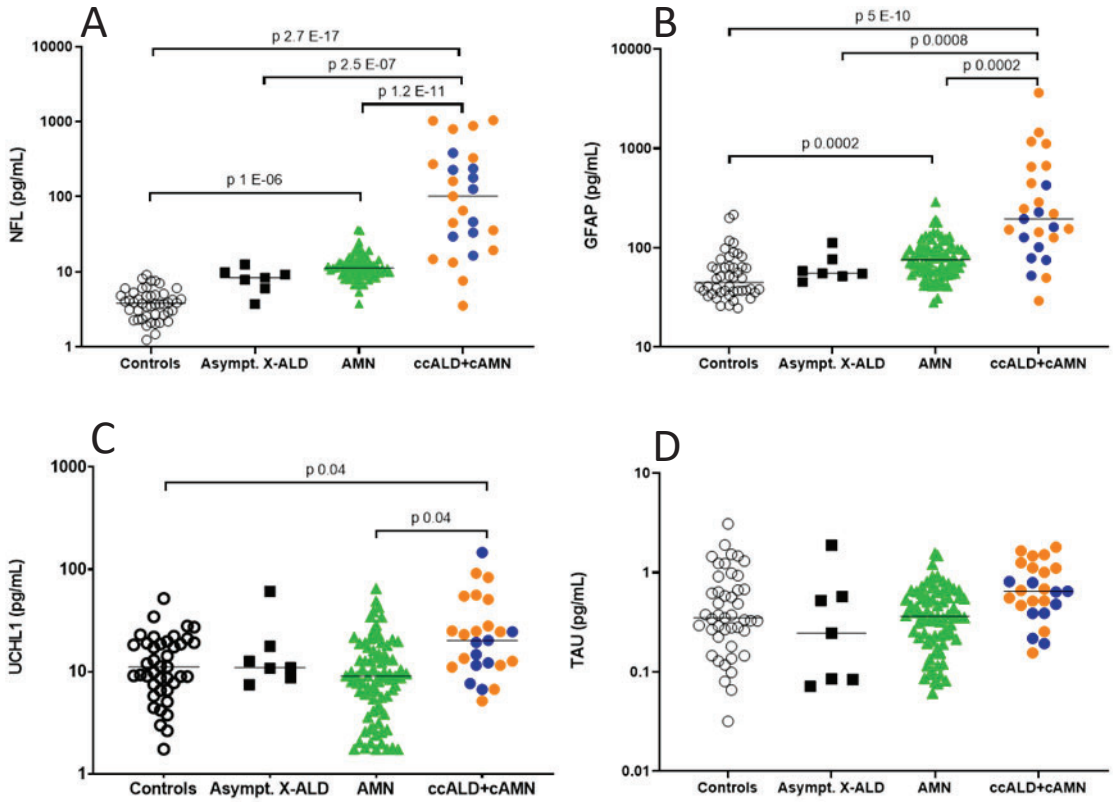

Figure 31. NfL (A), GFAP (B), UCHL1 (C) and TAU (D) levels in plasma from X-ALD patients and controls. These biomarkers were measured in samples of healthy controls (n = 46, mean age = 24.2 years), neurologically asymptomatic (Addison only) X-ALD patients (n = 6, mean age = 27.1 years, total sample number = 7), AMN patients (n = 47, mean age = 43.2 years, total sample number = 80), cerebral X-ALD patients (n = 24, 16 ccALD and 8 cAMN, mean age = 18.8 years, total sample number = 25). The median of NfL, GFAP, UCHL1 and TAU levels are indicated by a horizontal line. Blue dots indicate cAMN patients while orange dots indicate ccALD patients. Statistical analysis: a linear mixed model was used with age as a covariate and a random patient ID factor to account for patient replications. For pairwise comparisons estimated marginal means (EMMs) were performed adjusted with Bonferroni's method.

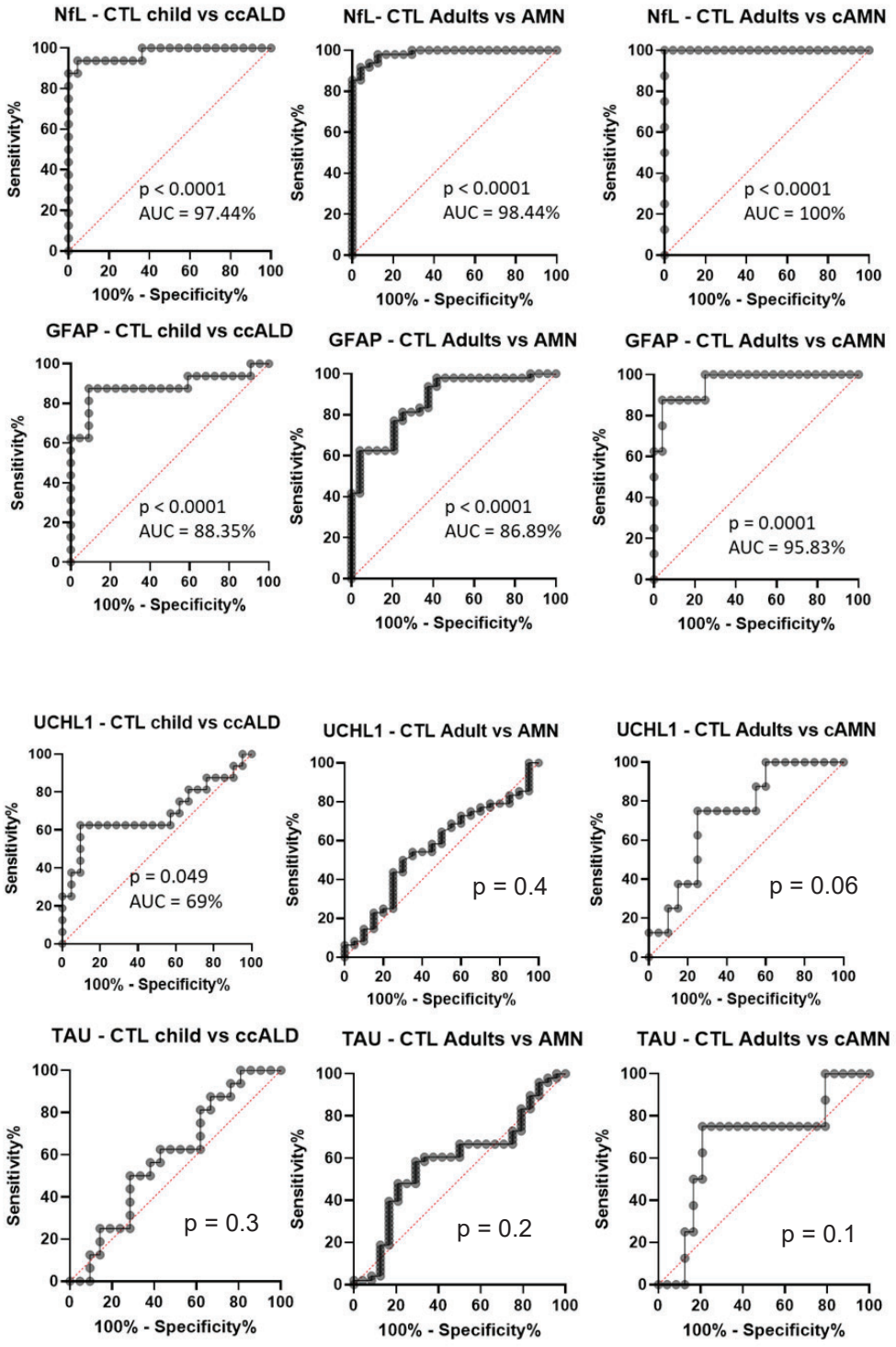

Figure 32. ROC curves with the AUC (in %) comparing each X-ALD phenotype with its age-matched controls for testing the diagnostic accuracy for the plasma levels of NfL, GFAP, UCHL1 and TAU. The confidence interval was set at 95% and the p-value threshold was set at 0.05

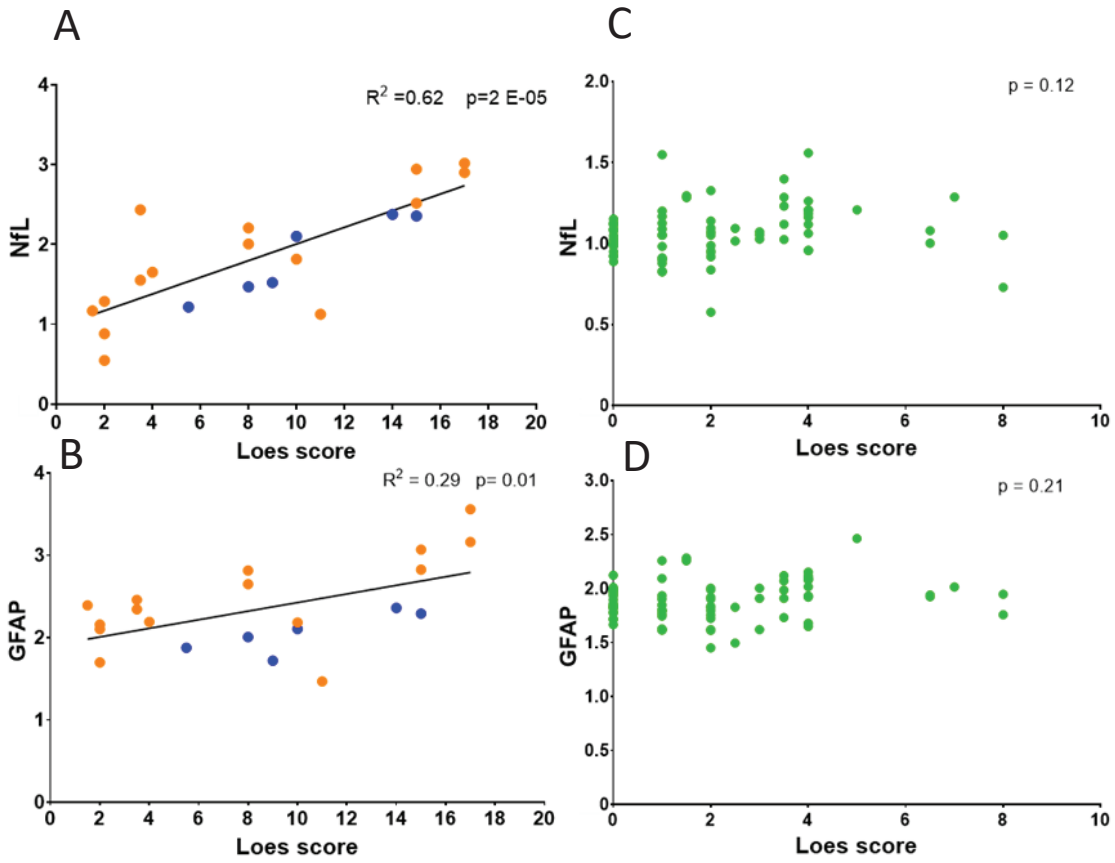

Figure 33. Association between NfL or GFAP levels and Loes score in X-ALD patients. Association between plasma NfL and GFAP levels and Loes score in cerebral X-ALD patients (n = 21, 15 ccALD and 6 cAMN) (A, B) and plasma NfL and GFAP levels and Loes score in AMN patients (n = 42, total sample number = 73) (C, D). ccALD are represented with orange dots, cAMN patients with blue dots, and AMN with green dots. In the graphs, the Log transformed values of NfL and GFAP are showed. The line represents the simple linear regression line. The association between Loes score and NfL and GFAP levels in plasma for cerebral X-ALD patients and AMN patients was determined with a linear model and a linear mixed model, respectively.

2.2.1 NfL, GFAP, UCHL1, and TAU CSF levels in X-ALD patients

AMN patients and the inflammatory cerebral form of X-ALD (ccALD + cAMN group) showed significantly increased levels of NfL respect to the control group in CSF. In addition, NfL levels are higher in patients with the cerebral X-ALD phenotype compared to AMN patients (figure 34 A). GFAP levels in CSF are elevated in cerebral X-ALD

respect to controls but not in AMN compared to controls. In addition, GFAP levels are higher in patients with the cerebral X-ALD phenotype compared to AMN patients (figure 34 B).

In CSF, UCHL1 concentrations differ significantly between the cerebral X-ALD patients and both AMN and healthy individuals while no increase was observed in AMN patients (figure 34 C). TAU level in CSF is increased in cerebral X-ALD patients compared to both AMN and controls while TAU is reduced in AMN patients (figure 34 D).

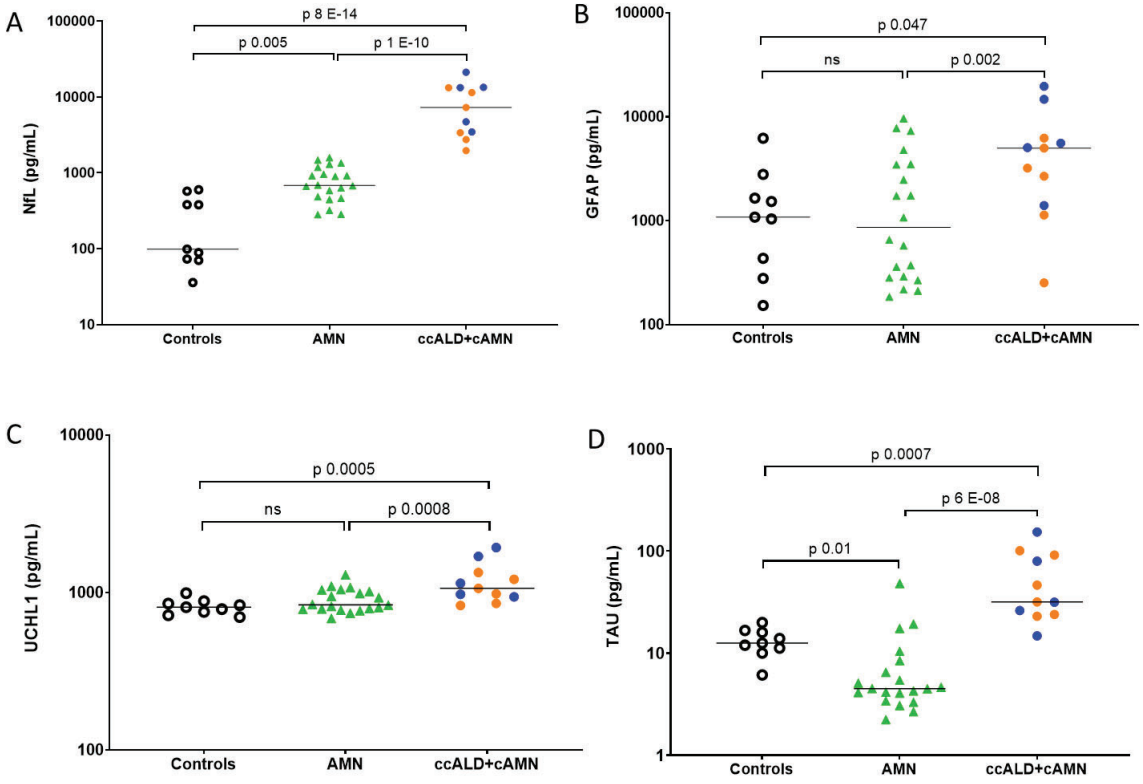

Figure 34. NfL (A), GFAP (B), UCHL1 (C) and TAU (D) levels in CSF from X-ALD patients and controls. These biomarkers were measured in samples of healthy controls (n = 9, mean age = 26.2 years), AMN patients (n = 15, mean age = 44.1 years, total sample number = 20) and cerebral X-ALD patients (n = 11, 6 ccALD and 5 cAMN, mean age = 23.5 years). The median of the NfL, GFAP, UCHL1 and TAU levels are indicated by a horizontal line. Blue dots indicate cAMN patients while orange dots indicate ccALD patients. Statistical analysis: a linear mixed model was used with age as a covariate and a random patient ID factor to account for patient replications. For pairwise comparisons estimated marginal means (EMMs) were performed adjusted with Bonferroni's method.

2.2.2 Positive association between CSF NfL levels and the Loes score in cerebral X-ALD patients.

A statistically significant positive association is observed between CSF NfL levels and Loes score in patients with cerebral X-ALD (ccALD and cAMN) (figure 35 A). However, this association between NfL and Loes score does not exist in the group of AMN patients in this fluid (figure 35 C). No significant association is observed between CSF GFAP levels and Loes score in patients with the cerebral form, nor in AMN (figures 35 B, D).

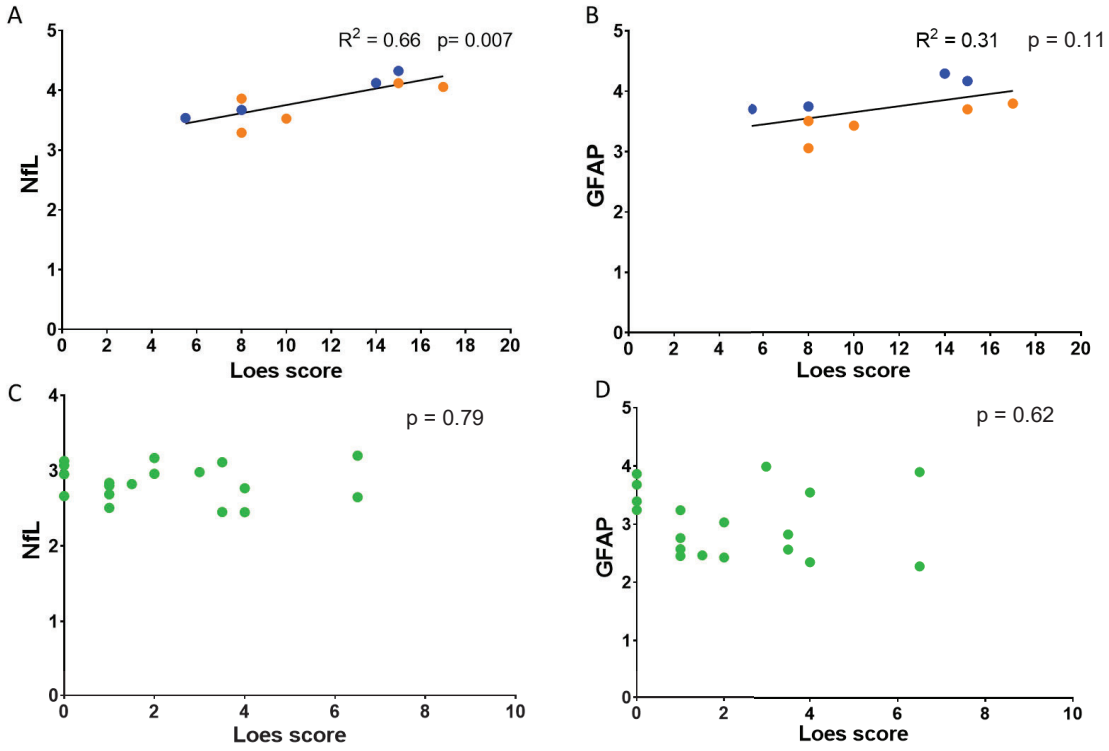

Figure 35. Association between NfL or GFAP levels and Loes score in cerebral and AMN X-ALD patients. Association between CSF NfL and GFAP levels and Loes score in cerebral X-ALD patients (5 ccALD and 4 cAMN) (A, B) and AMN patients (n =18) (C, D). ccALD are represented with orange dots, cAMN patients with blue dots, and AMN with green dots. In the graphs, the Log transformed values of NfL and GFAP are showed. The line represents the simple linear regression line. The association between Loes score and NfL and GFAP levels in CSF for cerebral X-ALD patients and AMN patients was determined with a linear model and a linear mixed model, respectively.

2.2.3 Positive association between NfL levels in plasma and CSF in cerebral X-ALD patients.

A statistically significant positive association is observed between NfL in plasma and CSF in cerebral X-ALD patients (ccALD and cAMN) (figure 36 A) while no association is observed in AMN patients probably due to a lower order of magnitude and a low deviation of NfL levels (figure 36 B). This suggests that there is no added value to measure NfL in both plasma and CSF of cerebral X-ALD patients in future studies.

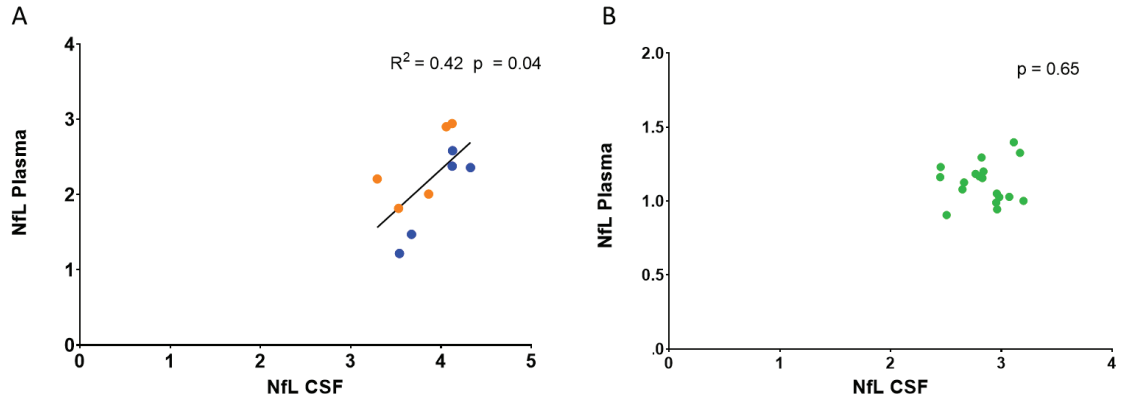

Figure 36. Scatter plots showing NfL levels association between plasma and CSF in (A) cerebral X-ALD patients (n=10, 5 ccALD and 5 cAMN) and (B) AMN patients (n = 13, total sample number = 18). Blue dots indicate cAMN patients while orange dots indicate ccALD patients. The straight black line represents the line of best fit between the values. Statistical analysis: a linear model (A) or linear mixed model (B) was used on log transformed data, with age as a covariate. In (B) we added a random patient ID factor to account for patient replications.

2.3 NfL but not GFAP is a good plasma biomarker to follow AMN that will convert to cAMN

We have longitudinally analyzed the plasma of 2 patients (P48 and P49) before and after converting to cerebral X-ALD. We followed the patient P48 every 6 months for the last 2 years before its conversion to the cerebral form (5.5 to 7.5 years). In these six first months, NfL level is maintained while it started to raise after 1 year with a maintained Loes score (3.5) but no gadolinium enhancement. Six months later, NfL continued to rise and drastically increased after 2 years when the patient was diagnosed as cAMN (figure

37 A). The increase of NfL levels after 1 year in absence of gadolinium enhancement suggests that NfL could be considered as a predictive marker for the conversion of AMN patients to cAMN. Indeed, NfL was already elevated before the appearance of signs of demyelination in an MRI. GFAP levels, on the other hand, although already high compared to control values in the patient's AMN phase, did not increase as much after conversion to the brain form, fluctuating over time at high but more or less constant values; that is evidencing that GFAP it is not a good marker to predict whether an AMN patient will be converted to cAMN (figure 37 B).We also analysed longitudinally the plasma of patient P49, who underwent a bone marrow transplant during the natural history of the disease, and obtained a halt to the progression of the cerebral disease. Remarkably, NFL but not GFAP levels are normalized to the level before the apparition of the disease (P49) (figure 37 C, D). This suggests that NfL is a good marker to follow the clinical progression of the cerebral form of the disease.

Moreover, we follow 3 AMN patients (P32, P35, and P38) with stable brain pathology but no cerebral inflammation with a constant Loes score between 2 and 4. GFAP values showed a similar pattern of values as NfL for patients P35 and P38, while more fluctuating for patient P32 (figure 38).

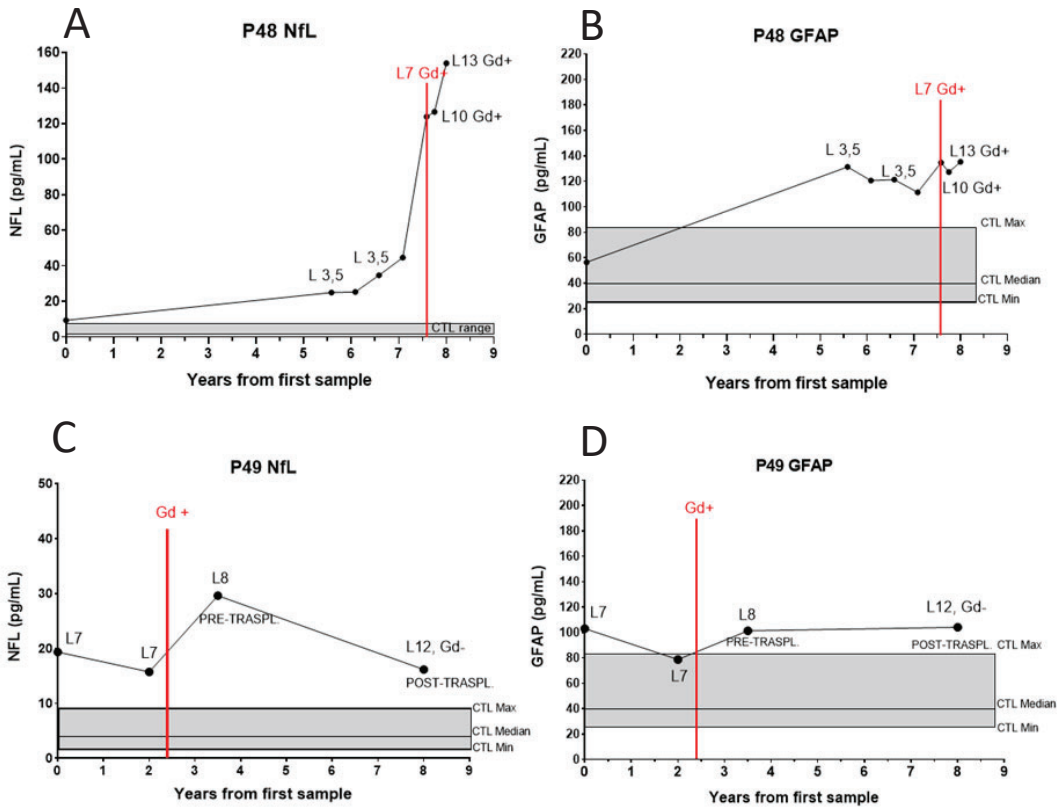

Figure 37. Follow up of NfL and GFAP plasma levels of two AMN patients converted to the cerebral form. Plasma (A) NFL and (B) GFAP levels in patient P48. Plasma (C) NFL and (D) GFAP levels in patient P49. Loes score (L) value is written above each dot. The vertical line corresponds to the conversion to the cerebral form of the disease. The grey area corresponds to the minimum, maximum, and median of control values.

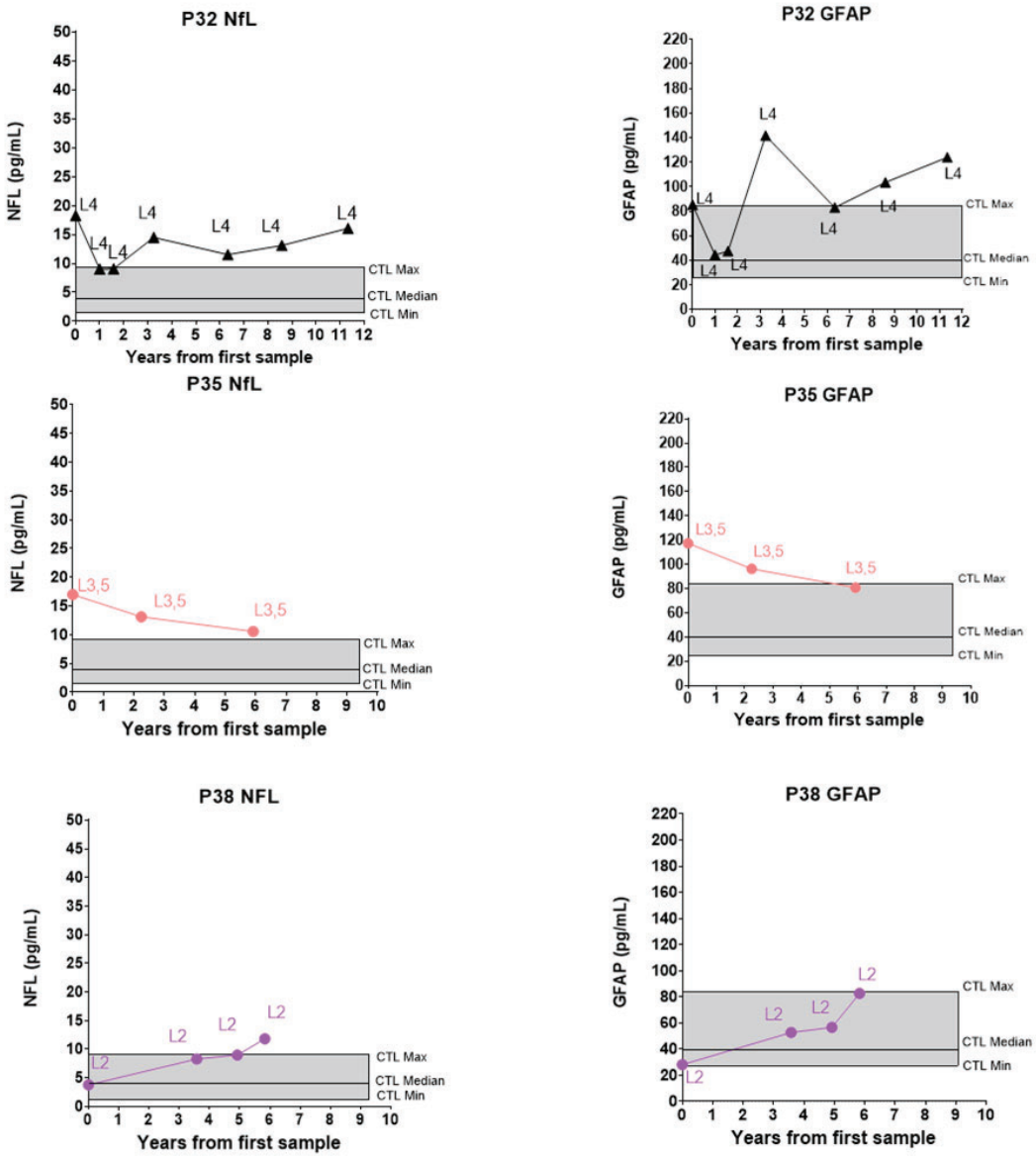

Figure 38. Follow up of NfL and GFAP plasma levels of three stable AMN patients. Plasma NFL (on the left) and GFAP levels (on the right) in patient P32, P35 and P38. Loes score (L) value is written above each dot. The grey area corresponds to the minimum, maximum, and median of control values.

2.4 Methionine and BCAA: new biomarkers for X-ALD patients?

Our finding of an altered amino acid profile in the NAWM of X-ALD patients and the identification of an X-ALD gut microbial signature of altered amino acid metabolism strengthened our hypothesis of a pathophysiological involvement of the gut microbiota in the disease. We therefore decided to evaluate the patients' plasma amino acid profile to further support these observations. Targeted analysis of plasma amino acids revealed decreased levels of essential amino acids, particularly BCAAs isoleucine (Ile), leucine (Leu), and valine (Val), in X-ALD patients (figure 39 A1, B1, C1). All three BCAAs were significantly lower in cAMN and/or AMN patients compared to adult controls. Additionally, Ile and Leu were significantly reduced in ccALD patients compared to their controls. Remarkably, these data are consistent with the functional alteration in BCAA biosynthesis of the microbiota in X-ALD patients observed by shotgun metagenomic analysis (figure 28). Interestingly, we noted a significant inverse correlation between plasma levels of Leu and Ile and those of NfL and GFAP in both cerebral and AMN forms of the disease. However, for valine, this inverse correlation was only observed in AMN patients (figure 39 A2, A3, B2, B3, C2, C3). ROC analysis demonstrated that Ile and Leu were effective in differentiating ccALD, cAMN and AMN patients from their respective controls. In contrast, Val values were capable of distinguishing cAMN and AMN patients, but not ccALD patients, from their controls. The highest accuracy was achieved for Ile in discriminating cAMN patients from controls (AUC of 79.74%), whereas the lowest accuracy was observed for Val in separating AMN patients from controls (AUC of 65.84%) (figure 40). Taken together, this evidences that BCAAs could serve as promising new biomarkers for X-ALD patients, representing a distinctive disease signature.

Methionine (Met) levels were reduced in both cerebral form of the disease (ccALD and cAMN patients) relative to controls (figure 41 A1). Notably, a significant inverse correlation was found between Met and NfL plasma levels in the cerebral form of the disease, but not in AMN patients (figure 41 A2, A3). This suggests that methionine could potentially serve as a new biomarker for the cerebral X-ALD phenotype and be more specific for the neuronal population respect to the astrocytic population. ROC analysis demonstrated that Met was capable of distinguishing cAMN and ccALD patients from

their respective controls, yet unable to differentiate AMN patients from their controls. For the patient groups affected by the cerebral forms, Met shows the best accuracy in discriminating cAMN patients from controls (AUC of 75.45%) (figure 42).

Levels of cysteine (Cys), a product generated from methionine and serine, were found to be elevated in plasma of ccALD and AMN patients compared to controls (figure 43 A1). However, no correlations with NfL or GFAP were observed in any of the X-ALD groups (figure 43 A2, A3). Interestingly, we observed a positive association between methionine and cysteine levels only in AMN patients (figure 44). This could indicate a defect in the conversion of methionine to cysteine in patients affected by the cerebral form but not in AMN patients. The remaining plasma amino acids profile in X-ALD patients is depicted in figure 45.

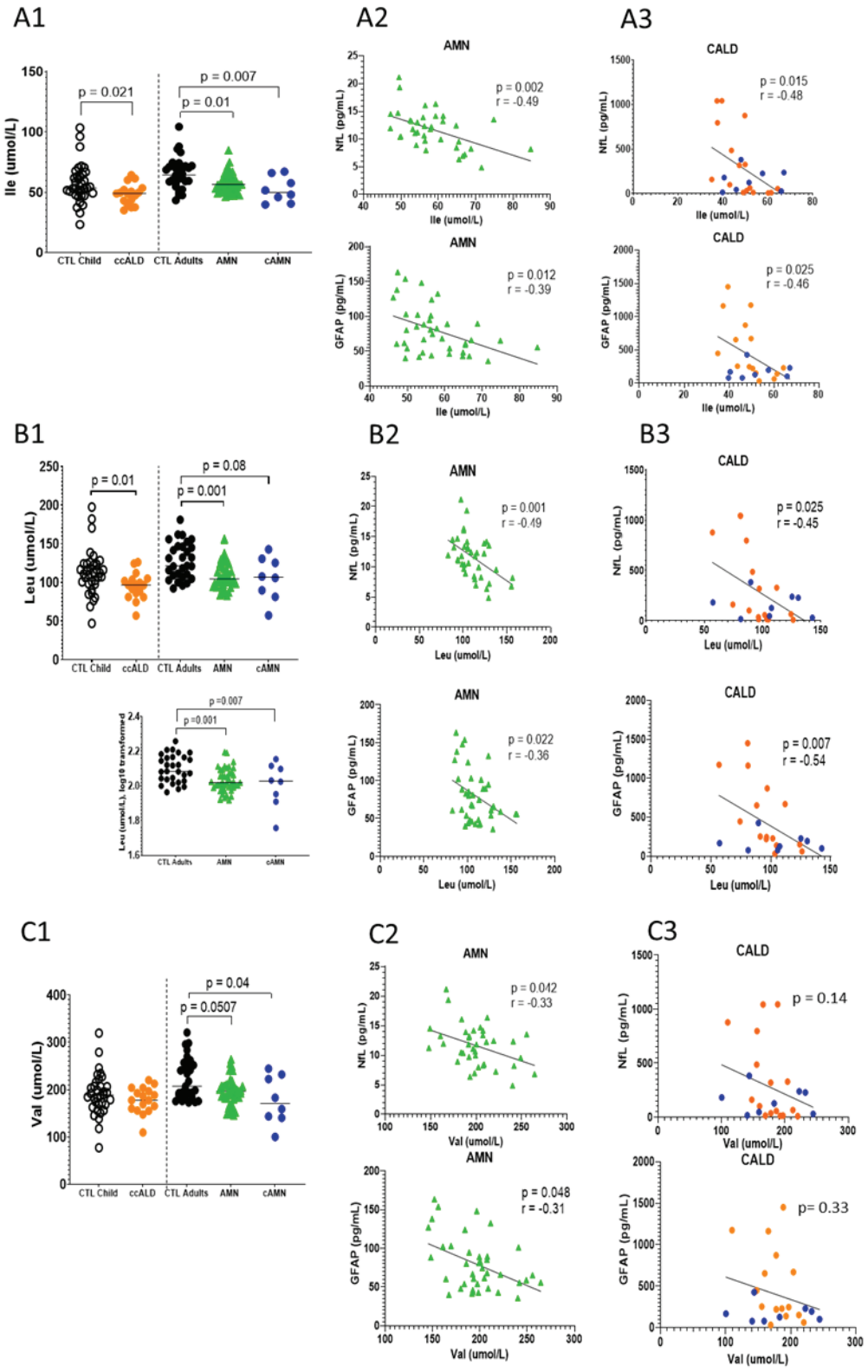

Figure 39. X-ALD BCAA signature in plasma (figure legend in the next page).

Figure 39. X-ALD BCAA signature in plasma. Dot plots showing the different concentrations (umol/L) of the amino acids isoleucine (Ile) (A1), leucine (Leu) (B1) and valine (Val) (C1) (i.e. branched-chain amino acids, BCAA) in X-ALD patients (ccALD n = 17, mean age 9 years ; AMN, n = 43, mean age 45.6 years and cAMN, n = 8, mean age 38.8 years) respect to controls (control child n = 35, mean age 10.6 years; control adult n = 29, mean age 37.9 years). The median of the amino acid levels in each group is indicated by a horizontal line. Outliers were removed with Rout test. An unpaired t-test was used to compare Val in ccALD patients with respect to their controls, while the analogous non-parametric Mann-Whitney test was used to compare Ile and Leu levels in ccALD patients with respect to their controls. The non-parametric Kruskal-Wallis test was used to compare Ile and Val levels in cAMN and AMN patients with respect to their controls, while one-way ANOVA was performed on Leu log transformed levels. p value threshold was set at 0.05. The scatter plots are showing the correlation between the plasma concentrations of isoleucine (Ile) (A2, A3), leucine (Leu) (B2, B3) and valine (Val) (C2, C3), (umol/L, X axis) and the variables NfL or GFAP (pg/ml, Y axis) in X-ALD patients. CALD patients (cAMN and ccALD) are represented on the graphs on the right whereas AMN on the left. Orange dots represents ccALD patients whereas blue dots represent cAMN patients. The straight black line represents the line of best fit between the values.

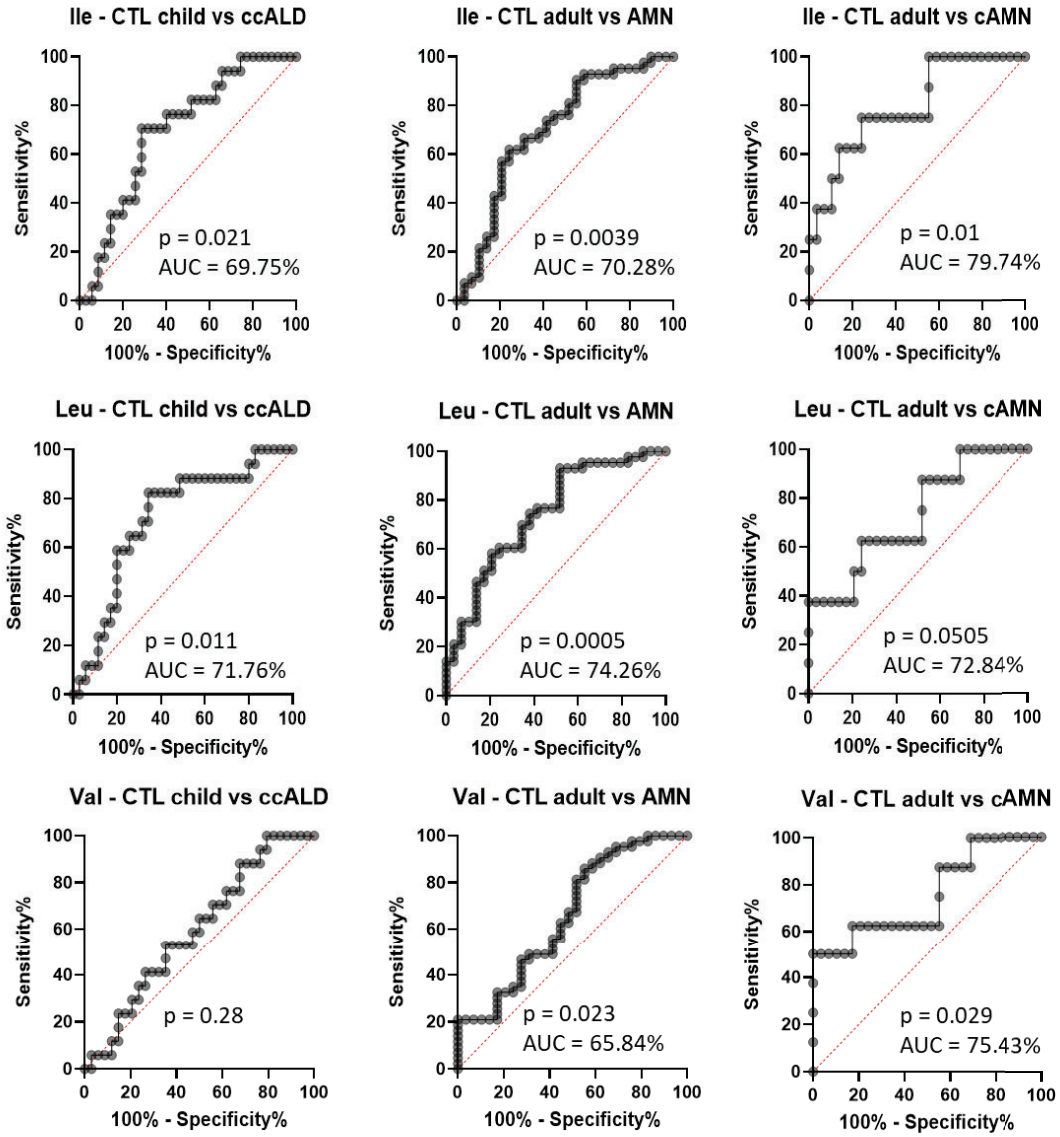

Figure 40. ROC curves with the AUC (in %) comparing each X-ALD phenotype with its age-matched controls for testing the diagnostic accuracy for the plasma levels of the amino acids isoleucine (Ile), leucine (Leu) and valine (Val). The confidence interval was set at 95% and the p-value threshold was set at 0.05.

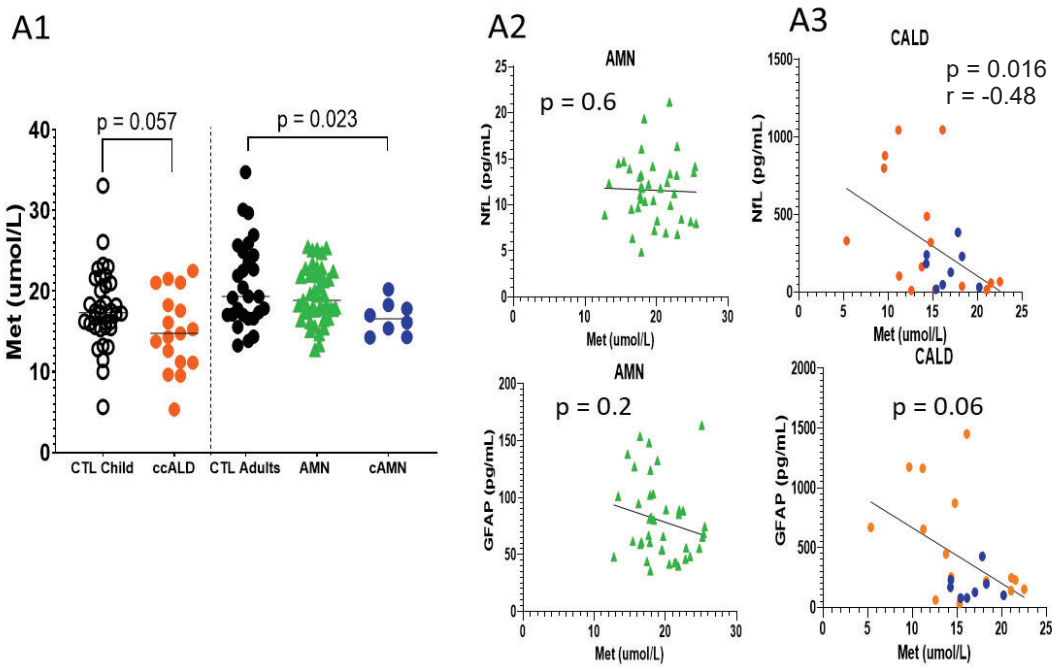

Figure 41. X-ALD methionine signature in plasma. Dot plots showing the different concentrations (umol/L) of the amino acid methionine (Met) in X-ALD patients (ccALD n = 17, mean age 9 years ; AMN, n = 43, mean age 45.6 years and cAMN, n = 8, mean age 38.8 years) respect to controls (control child n = 35, mean age 10.6 years; control adult n = 29, mean age 37.9 years). (A1). The median of the amino acid levels in each group is indicated by a horizontal line. Outliers were removed with Rout test. An unpaired t-test was used to compare Met levels in ccALD patients with respect to their controls. One-way ANOVA was used to compare Met levels in cAMN and AMN patients with respect to their controls. p value threshold was set at 0.05. The scatter plots are showing the correlation between the plasma concentrations of methionine (Met) (umol/L, X axis) and the variables NfL or GFAP (pg/ml, Y axis) in X-ALD patients (A2, A3). CALD patients (cAMN and ccALD) are represented on the graphs on the right whereas AMN on the left. Orange dots represents ccALD patients whereas blue dots represent cAMN patients. The straight black line represents the line of best fit between the values.

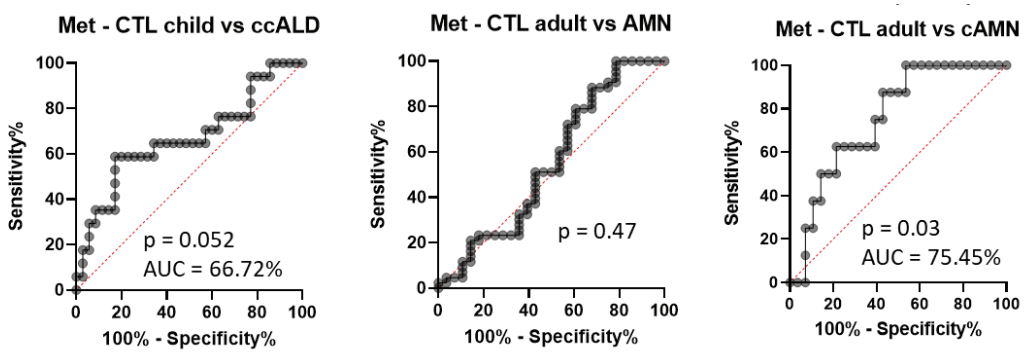

Figure 42. ROC curves with the AUC (in %) comparing each X-ALD phenotype with its age-matched controls for testing the diagnostic accuracy for the plasma levels of the amino acid methionine (Met). The confidence interval was set at 95% and the p-value threshold was set at 0.05.

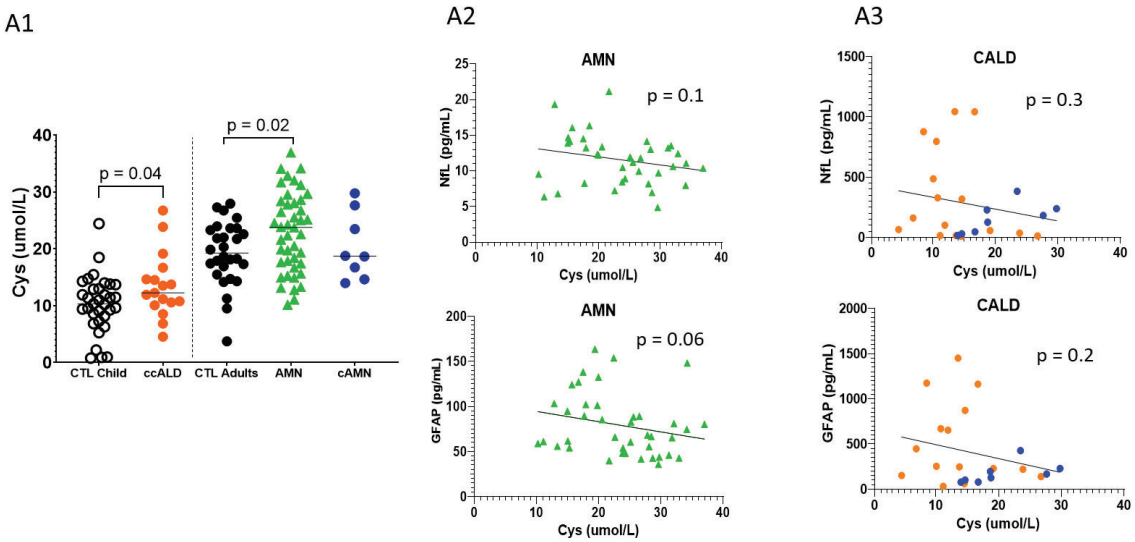

Figure 43. X-ALD cysteine signature in plasma. Dot plots showing the different concentrations (umol/L) of the amino acid Cysteine (Cys) in X-ALD patients (ccALD n = 17, mean age 9 years; AMN, n = 43, mean age 45.6 years and cAMN, n = 8, mean age 38.8 years) respect to controls (control child n = 35, mean age 10.6 years; control adult n = 29, mean age 37.9 years). (A1). The median of the amino acid levels in each group is indicated by a horizontal line. Outliers were removed with Rout test. An unpaired t-test was used to compare Cys levels in ccALD patients with respect to their controls. For Cys levels in the adult groups, the one-way ANOVA test yielded a borderline significant p-value (p = 0.059); therefore, the p-value shown in the graph reflects the result of an unpaired t-test between the adult control and AMN groups. p value threshold was set at 0.05. The scatter plots are showing the correlation between the plasma concentrations of Cys (umol/L, X axis) and the variables NfL or GFAP (pg/ml, Y axis) in X-ALD patients (A2, A3). CALD patients (cAMN and ccALD) are represented on the graphs on the right whereas AMN on the left. Orange dots represents ccALD patients whereas blue dots represent cAMN patients. The straight black line represents the line of best fit between the values.

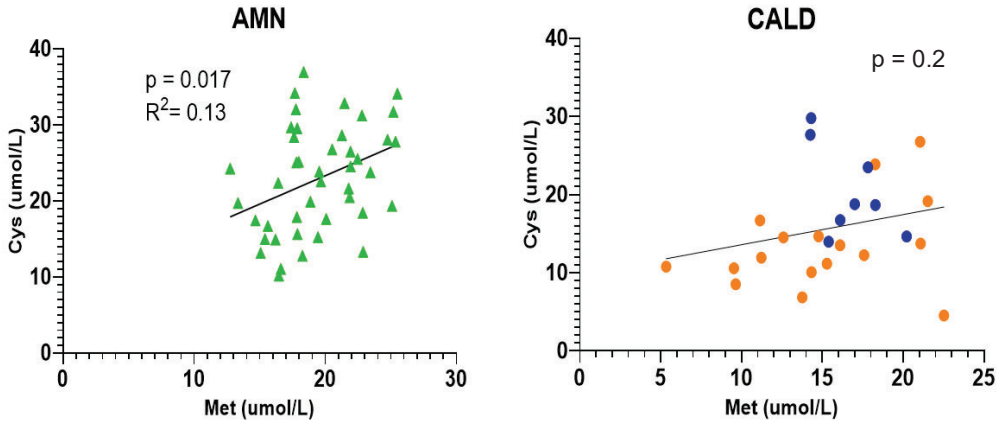

Figure 44. Scatter plots showing the association between the plasma concentrations (umol/L) of methionine (Met, X axis) and cysteine (Cys, Y axis) in X-ALD patients. CALD patients (cAMN and ccALD) are represented on the graphs on the right whereas AMN on the left. Orange dots represents ccALD patients whereas blue dots represent cAMN patients. The straight black line represents the line of best fit between the values.

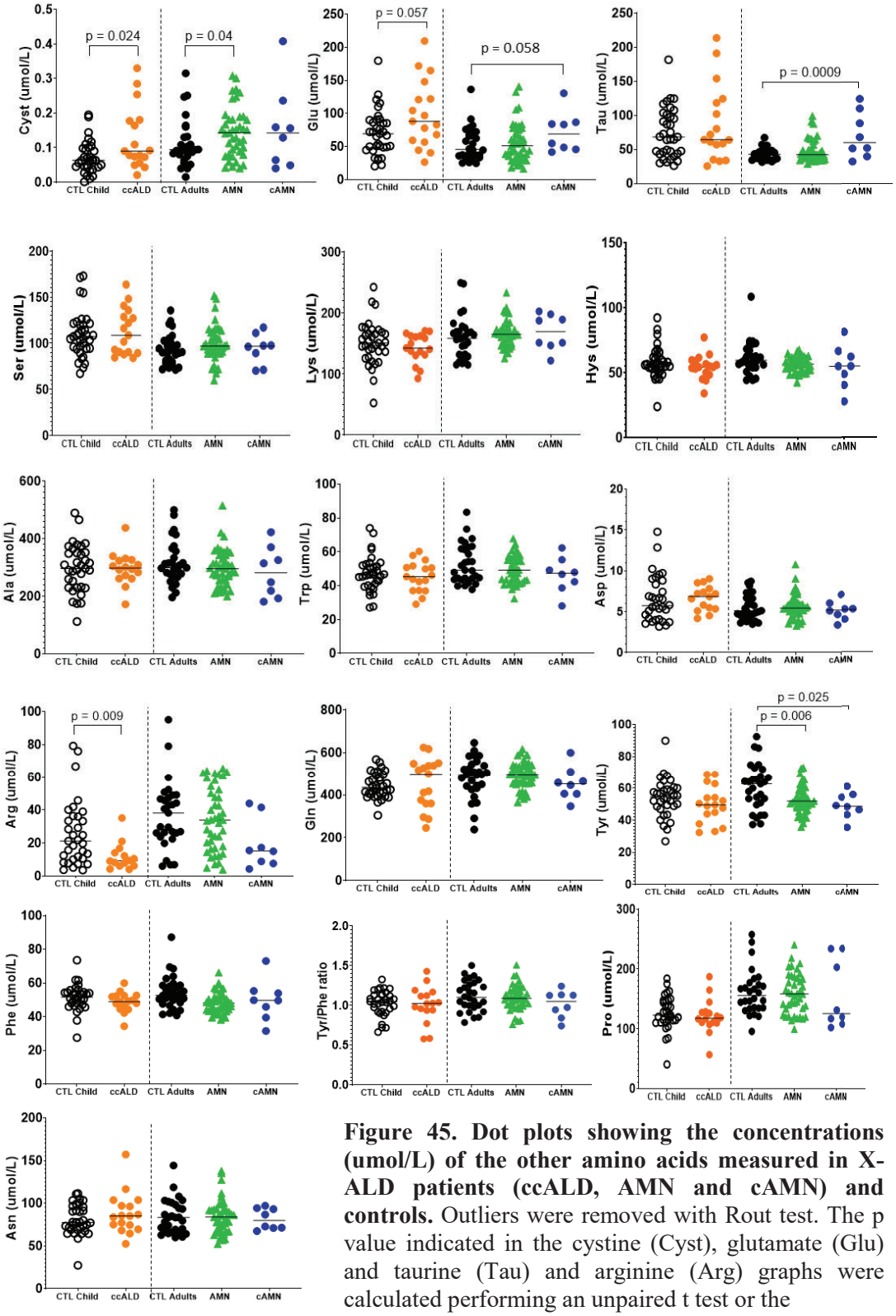

Figure 45. Dot plots showing the concentrations (umol/L) of the other amino acids measured in X-ALD patients (ccALD, AMN and cAMN) and controls. Outliers were removed with Rout test. The p value indicated in the cystine (Cyst), glutamate (Glu) and taurine (Tau) and arginine (Arg) graphs were calculated performing an unpaired t test or the corresponding non-parametric Mann-Whitney test, depending on the distribution of the values. The one-way ANOVA test was used to compare Tyr levels in cAMN and AMN patients with respect to their controls. p value threshold was set at 0.05. The median of the amino acid levels in each group is indicated by a horizontal line.

2.5 BCAAs and one carbon metabolism pathways gene expression pattern in X-ALD PBMCs

Interesting observations emerged from the PBMC bulk RNAseq study concerning BCAA (figures 46, 47), methionine and folates (figures 48, 49) metabolism and on mitochondrial function.

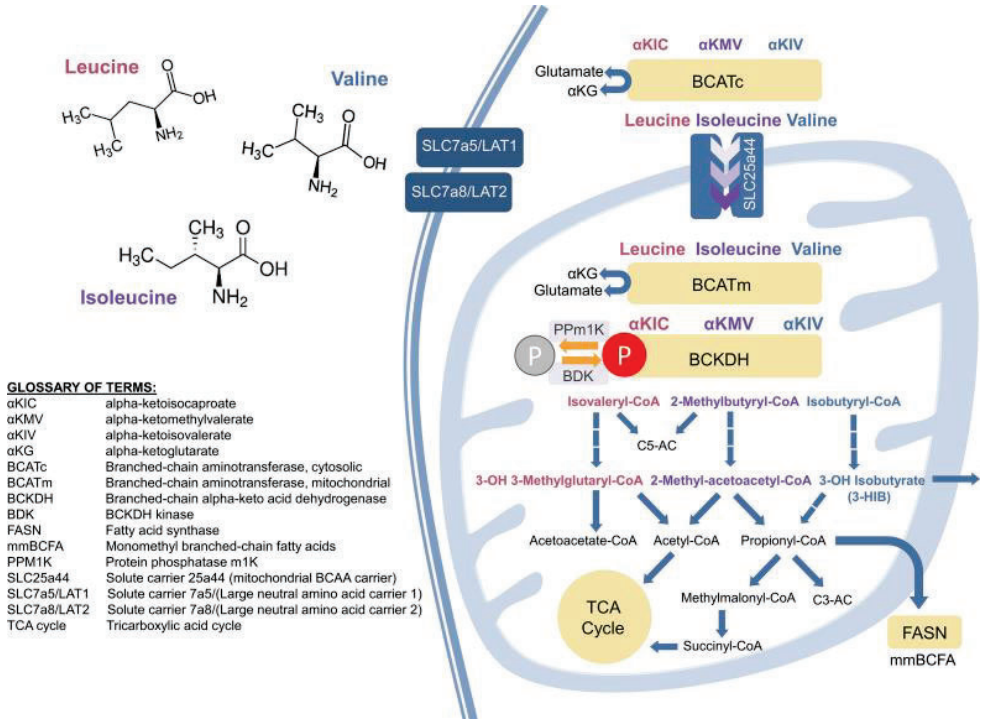

Figure 46: Overview of the pathways of branched-chain amino acid (BCAA) catabolism. From White et al., 2021 (figure legend in the next page).

Figure 46. Overview of the pathways of branched-chain amino acid (BCAA) catabolism. In mammals, all three branched-chain amino acids (BCAAs) are initially transaminated by branched-chain amino transferases (BCATs) to form branched-chain α-ketoacids (BCKAs). Two distinct genes are responsible for encoding the enzymes known as branched-chain amino transferases (BCATs). *BCAT1* (or *cBCAT*) encodes a cytoplasmic protein and is predominantly expressed in the brain, whereas *BCAT2* (or *mBCAT*) encodes a mitochondrial protein and is expressed in a ubiquitous manner. The irreversible initiation of BCKA oxidation occurs in the branched-chain amino acid dehydrogenase (BCKDH) complex. The branched-chain alpha-keto acid dehydrogenase (BCKDH) complex is located on the inner mitochondrial membrane. It catalyzes the oxidative decarboxylation of branched-chain keto acids, releasing CO_2 and covalently adding a coenzyme A (CoA) group to the oxidized branched-chain keto acid (BCKA) product. The BCKDH complex comprises three components: a thiamine (vitamin B1)-dependent decarboxylase, which exists as an alpha2/beta2 heterotetramer and is encoded by the *BCKDHA* and *BCKDHB* genes, respectively; a lipoate-dependent dihydrolipoyl transacylase, which transfers the acyl groups to CoA and is encoded by the *DBT* gene; and a FAD-dependent dihydrolipoyl dehydrogenase, which transfers the released electrons to NAD+ and is encoded by the *DLD* gene. BCKDH kinase (BCKDK) adds a phosphate group to three residues of BCKDHA, thereby suppressing BCKDH activity. The complementary activating dephosphorylation is carried out by the recently identified phosphatase, PPm1K (PP2Cm). Subsequent to the decarboxylation of BCKDH, the catabolism of BCAAs exhibits similarities to that of fatty acids. Indeed, these two processes share a number of enzymatic subunits. Each set of reactions is specific to each BCAA and occurs within the mitochondrial matrix. In conclusion, the carbons of BCAAs are either lost as CO_2 or enter the tricarboxylic acid (TCA) cycle. From Neinast et al, 2019; Dimou et al., 2022; Mann et al, 2021; White et al., 2021.

SLC7A5 functions as a sodium-independent high-affinity transporter that mediates the uptake of large neutral amino acids such as methionine, valine, leucine and isoleucine into the cytoplasm (Scalise et al., 2018), while SLC25A26 is involved in the transport of S-adenosylmethionine produced by methionine adenosyltransferase (MAT) from methionine into mitochondria (Schober et al., 2022). Both genes were less expressed in ccALD patients than in controls and AMN patients (figures 47, 48): this argues against the consumption of BCAAs and methionine by the circulating immune system and confirms the importance of methionine metabolism in patients with the cerebral form of the disease. The increased expression of BCKDH kinase (BDK or BCKDK) and the decreased expression of phosphatase PPm1K (PP2Cm) further argue against increased catabolism of BCAAs at the PBMCs level (figure 47).

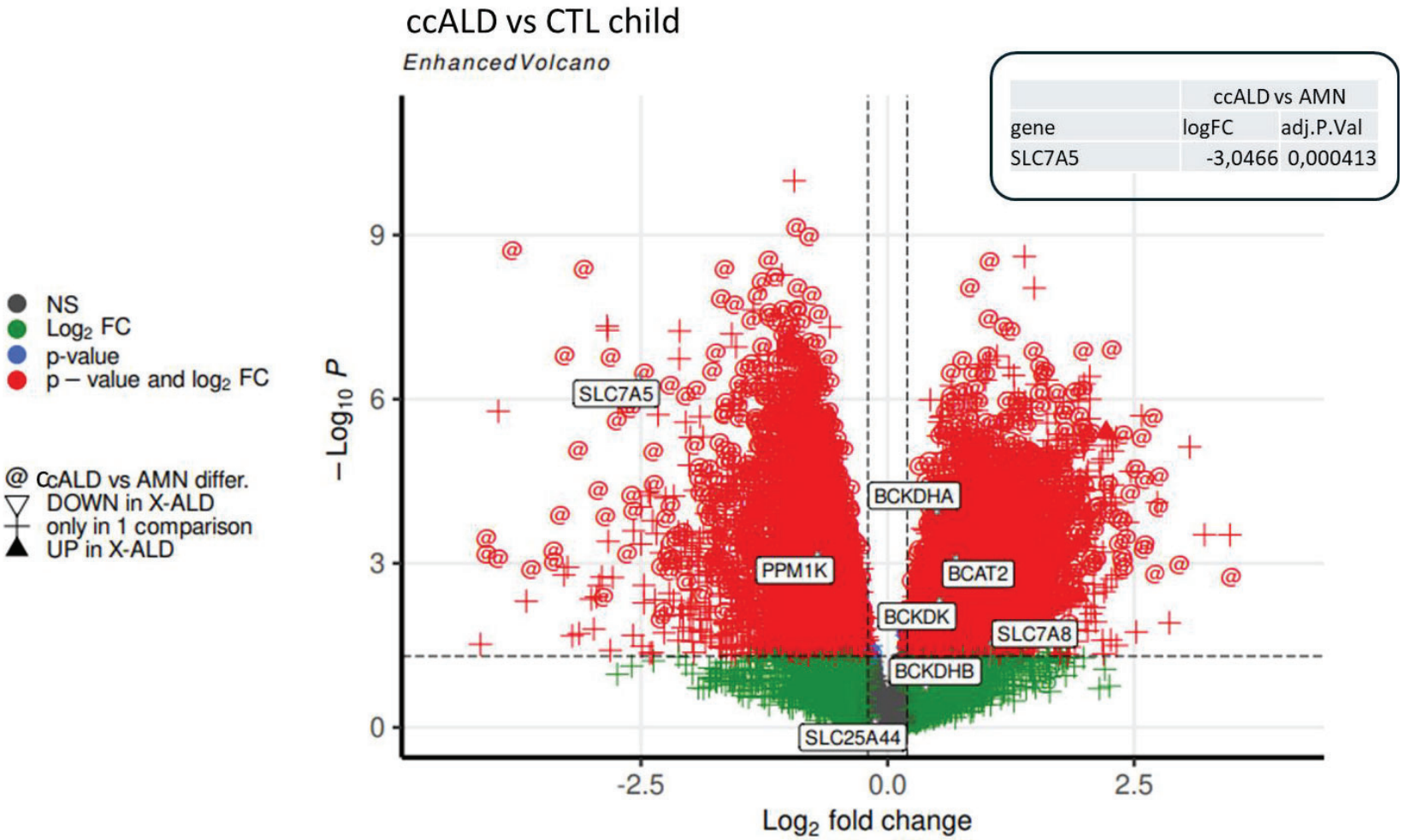

Fig. 47. Volcano plot showing significant differential expression of genes in ccALD patients compared to child controls in PBMC -Focus on BCAAs transport and metabolism.

Figure 47. Volcano plot showing significant differential expression of genes in ccALD patients compared to child controls in PBMCs. The graph is showing differentially expressed genes between ccALD and AMN phenotypes adjusted for age (@ symbol), commonly upregulated genes in both ccALD and AMN (up triangle), commonly downregulated genes in both ccALD and AMN (down triangle), up- or down-regulated genes in only one ccALD or AMN group compared to age-matched controls (cross). PBMCs were analysed from 11 ccALD patients (mean age 8,4 years), 15 AMN patients (mean age 46 years) and their respective controls (15 children, mean age 9,5 years; 18 adults, mean age 31 years). Genes related to branched-chain amino acids and membrane transporters differentially expressed in ccALD compared to child controls are highlighted. The table above the volcano plot graph is specifying the fold and p value for the selected genes related to the branched-chain amino acids and membrane transporters that are also differentially expressed in the comparison between ccALD and AMN patients. Abbreviations: BCAT2 = Branched Chain Amino Acid Transaminase 2; BCKDHA = Branched Chain Keto Acid Dehydrogenase E1 Subunit Alpha; BCKDK = Branched Chain Keto Acid Dehydrogenase Kinase; SLC7A5 = Solute Carrier Family 7 Member 5; SLC7A8 = Solute Carrier Family 7 Member 8; SLC25A44 = Solute Carrier Family 25 Member 44.

On the other hand, the increased expression of the membrane folate transporters SLC19A1 and SLC46A1, together with the enzymes DHFR, SHMT2 and MTHFD1 (figure 48), which are involved in the intracellular metabolism of folates (figure 49), indicate a possible increased peripheral consumption of these vitamins by blood mononuclear cells, which could modulate the pool of systemic bioavailability of these molecules. Furthermore, the reduced expression of the transporter SLC25A32 in ccALD patients (figure 48), which facilitates the translocation of flavin adenine dinucleotide (FAD) across the inner mitochondrial membrane (Kim J. et al., 2018), suggests the presence of a possible mitochondrial dysfunction also at the level of peripheral mononuclear immune cells.

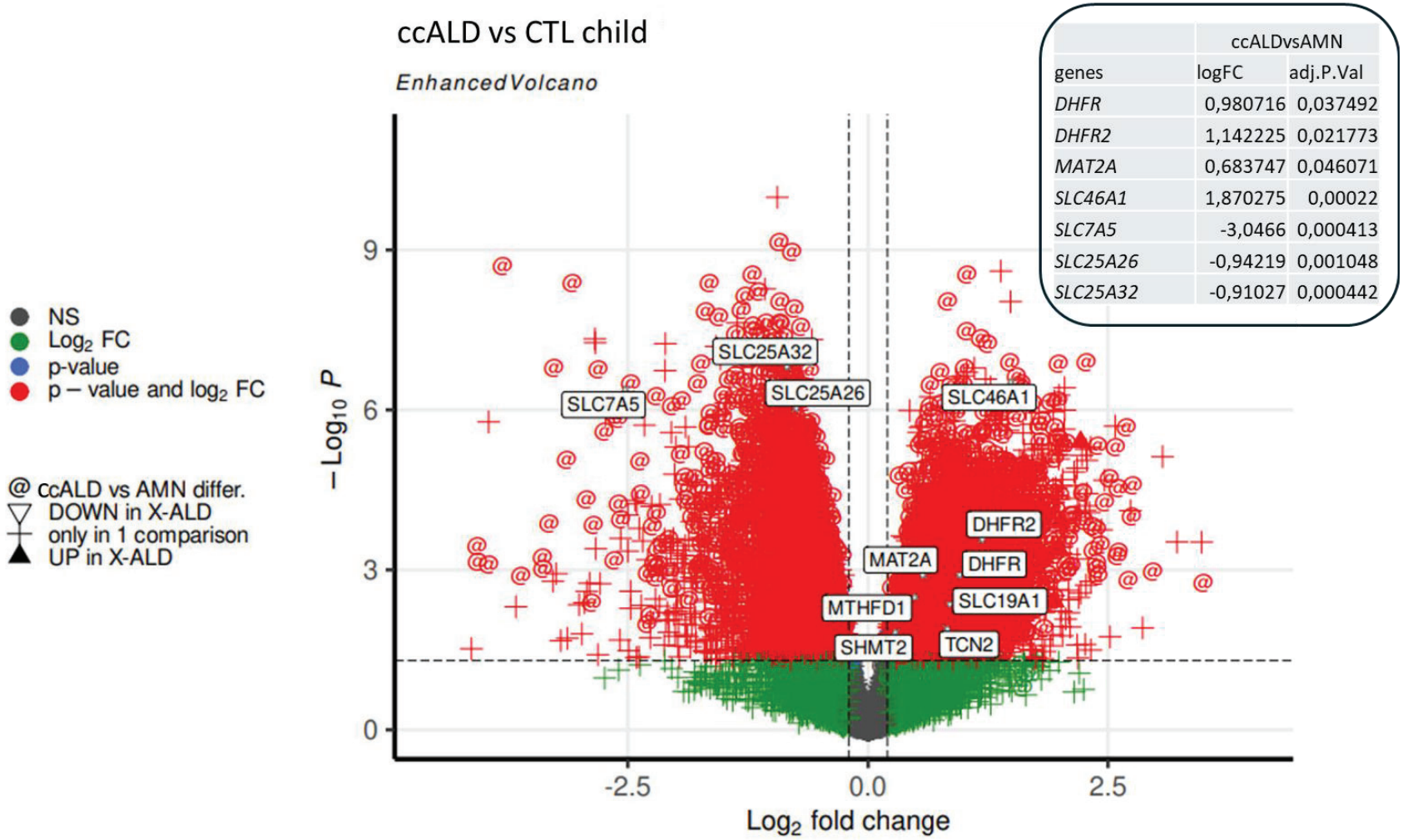

	ccALDvsAMN	
genes	logFC	adj.P.Val
DHFR	0,980716	0,037492
DHFR2	1,142225	0,021773
MAT2A	0,683747	0,046071
SLC46A1	1,870275	0,00022
SLC7A5	-3,0466	0,000413
SLC25A26	-0,94219	0,001048
SLC25A32	-0,91027	0,000442

Fig. 48. Volcano plot showing significant differential expression of genes in ccALD patients compared to child controls in PBMCs -Focus on methionine and folates transport and metabolism.

Figure 48. Volcano plot showing significant differential expression of genes in ccALD patients compared to child controls in PBMCs. The graph is showing differentially expressed genes between ccALD and AMN phenotypes adjusted for age (@ symbol), commonly upregulated genes in both ccALD and AMN (up triangle), commonly downregulated genes in both ccALD and AMN (down triangle), up- or down-regulated genes in only one ccALD or AMN group compared to age-matched controls (cross). PBMCs were analysed from 11 ccALD patients (mean age 8,4 years), 15 AMN patients (mean age 46 years) and their respective controls (15 children, mean age 9,5 years; 18 adults, mean age 31 years). Genes related to folates and methionine metabolism and membrane transporters differentially expressed in ccALD compared to child controls are highlighted. The table above the volcano plot graph is specifying the fold and p value for the selected genes related to folates and methionine metabolism and membrane transporters that are also differentially expressed in the comparison between ccALD and AMN patients. Abbreviations: DHFR = Dihydrofolate reductase; SHMT2 = Serine Hydroxymethyltransferase 2; MTHFD1 = Methylenetetrahydrofolate Dehydrogenase; MAT2A = Methionine Adenosyltransferase 2A; TCN2 = Transcobalamin 2; SLC7A5 = Solute Carrier Family 7 Member 5; SLC25A32 = Solute Carrier Family 25 Member 32; SLC25A26 = Solute Carrier Family 25 Member 26; SLC19A1 = Solute Carrier Family 19 Member 1; SLC46A1 = Solute Carrier Family 46 Member 1.

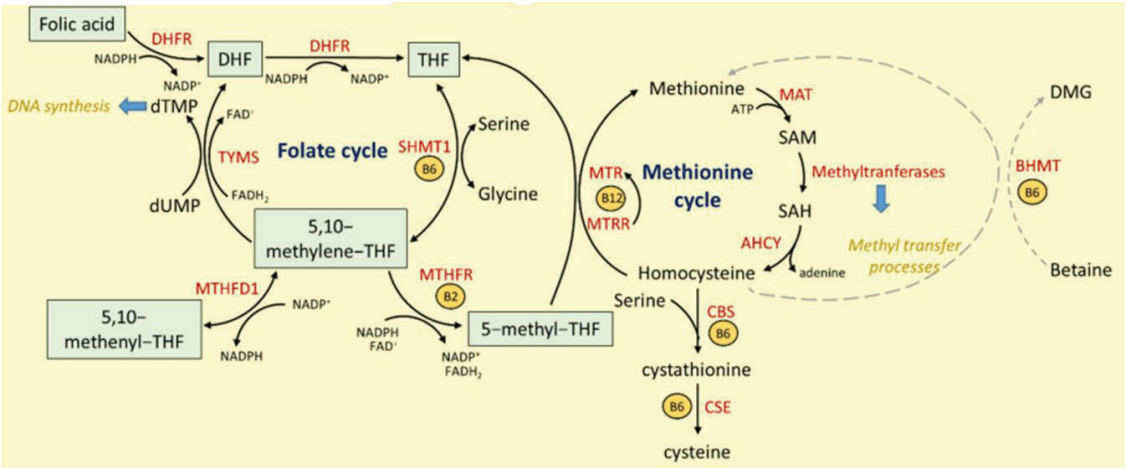

Figure 49. **Folates and methionine intracellular metabolism.** Intersections of folates and methionine metabolic pathways in the intracellular compartment. The involved folate forms are depicted in green boxes, while the respective enzymes are written in red. Abbreviations: DHFR = Dihydrofolate reductase; SHMT = Serine Hydroxymethyltransferase; TYMS = Thymidylate synthase MTHFD1 = Methylenetetrahydrofolate Dehydrogenase; MTHFR = methylene-THF-reductase; MTR = Methionine synthase; MTRR= Methionine Synthase Reductase; MAT = Methionine Adenosyltransferase; AHCY = S-adenosyl-L-homocysteine hydrolase; CBS = Cystathionine beta synthase; CSE = cystathionine γ-lyase; BHMT = betaine-homocysteine S-methyltransferase. From Lionaki et al., 2022.

2.6 mtDNA and the mitokine GDF15 are increased in X-ALD patients

Mitochondrial dysfunction is part of the hallmarks of X-ALD (Fourcade et al., 2015; Lopez-Erauskin et al., 2013; Schlüter et al, 2012). A possible consequence of this pathogenic process is the release into the body fluids like plasma and/or CSF of mitochondrial DNA, which, while it may further feed the inflammatory processes in a vicious circle (as described in the introduction), may represent a possible biomarker of clinical utility. We therefore proceeded to compare the copy number of circulating cell-free mitochondrial DNA (ccf mtDNA) in the CSF of controls, symptomatic patients with adrenomyeloneuropathy (AMN) and patients with the cerebral form of the disease (ccALD and cAMN). ccf mtDNA was found to be increased in AMN patients compared to controls, confirming the presence of mitochondrial damage in these patients, but not in patients with the cerebral form of the disease (figure 50). No correlation was observed between CSF levels of NfL or GFAP and ccf mtDNA copy number in either group of patients (figure 51). Considering the puncture site (lumbar) for obtaining CSF, we can hypothesize the presence of a rostral caudal gradient for ccf mtDNA: this biomarker might exhibit insufficient sensitivity for more rostral pathologic processes, as in the case of brain lesions, but sufficient for pathologic processes closer to the puncture site, as in the case of spinal cord involvement in AMN patients. Different persistence kinetics of ccf mtDNA, NfL and GFAP in body fluids could also underlie the lack of correlation observed between these molecules.

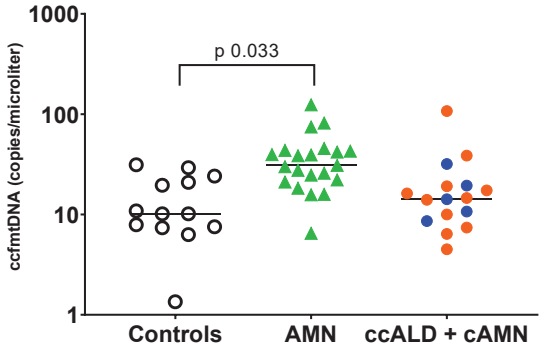

Figure 50. ccf mtDNA (copies/microliter) in CSF from X-ALD patients and controls. ccf mtDNA was measured in CSF samples of healthy controls (n = 13, mean age = 6.3 years), AMN patients (n = 15, mean age = 43.6 years, total sample number = 21) and cerebral X-ALD patients (n = 16, 11 ccALD and 5 cAMN, mean age = 19.5 years). The median of the ccf mtDNA levels are indicated by a horizontal line. Blue dots indicate cAMN patients while orange dots indicate ccALD patients. Statistical analysis: a linear mixed model was used with age as a covariate and a random patient ID factor to account for patient replications. For pairwise comparisons estimated marginal means (EMMs) were performed adjusted with Bonferroni's method.

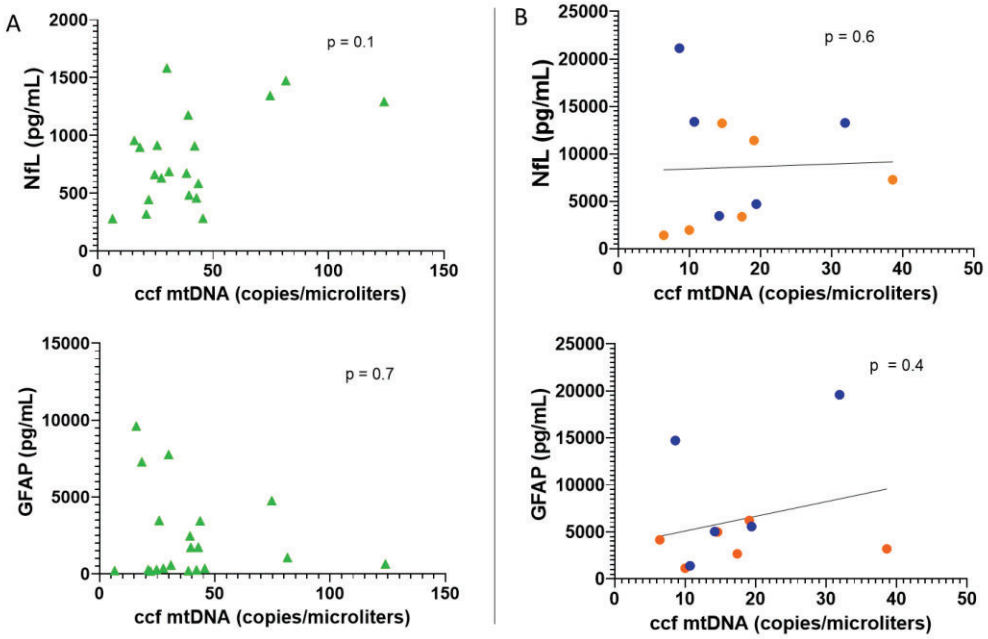

Figure 51. Scatter plots showing NfL and GFAP levels association with ccf mtDNA levels in AMN patients (n = 20, on the left) and cerebral X-ALD patients (on the right; n=11, 6 ccALD and 5 cAMN). Blue dots indicate cAMN patients while orange dots indicate ccALD patients. The straight black line represents the line of best fit between the values. Statistical analysis: a linear mixed model (A) or a linear model (B) was used. In (A) we added a random patient ID factor to account for patient replications.

The emerging role of growth differentiation factor 15 (GDF15) as a mitokine bridges mitochondrial dysfunction and inflammatory responses. Mitochondrial dysfunction, cellular stress, inflammation, and activation of the mitochondrial unfolded protein response (UPRmt) pathway all potently induce GDF15 expression (Durieux et al., 2011; Conte et al., 2022); given the importance of these processes in the pathogenesis of X-ALD, we evaluated the plasma concentrations of this molecule in ccALD, AMN, cAMN patients and their controls. GDF15 levels were higher in both cerebral form of the disease (ccALD and cAMN patients) and in AMN patients relative to controls (figure 52 A). ROC analysis demonstrated that GDF15 was capable of distinguishing ccALD, AMN and cAMN patients from their respective controls, with the best accuracy in discriminating cAMN patients from controls (AUC of 82.83%) (figure 52 B). No significant correlation was found between GDF15 and NfL or GFAP plasma levels in any of the X-ALD patient groups (figure 53).

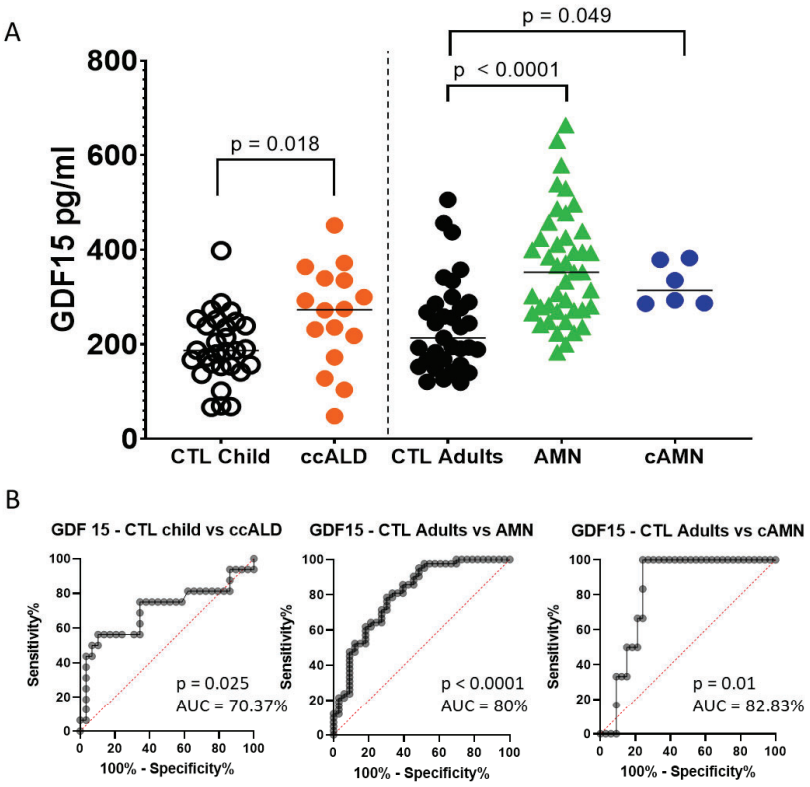

Figure 52. See the figure legend in the next page.

Figure 52. Dot plots showing the concentration (pg/ml) of GDF15 in plasma of X-ALD patients (ccALD n = 17, mean age 9 years; AMN, n = 42, mean age 45.8 years and cAMN, n = 8, mean age 38.8 years) respect to controls (control child n = 30, mean age 10.2 years; control adult n = 33, mean age 37.6 years). Outliers were removed with Rout test. The p value indicated in the comparison between CTL child and ccALD patients were calculated performing the Mann-Whitney test, while the Kruskal-Wallis test was used to compare control adult, AMN and cAMN groups. p value threshold was set at 0.05. The median of the amino acid levels in each group is indicated by a horizontal line. (B) ROC curves with the AUC (in %) comparing each X-ALD phenotype with its age-matched controls for testing the diagnostic accuracy for the plasma levels of GDF15. The confidence interval was set at 95% and the p-value threshold was set at 0.05.

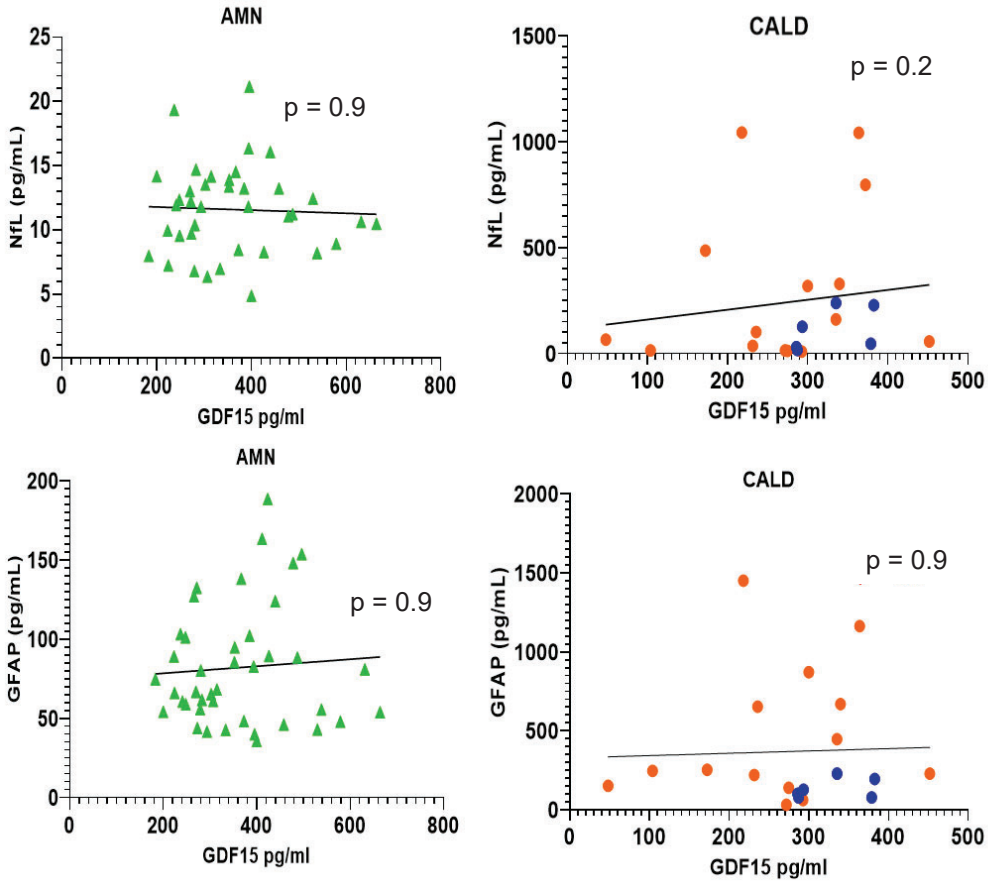

Figure 53. Scatter plots showing the association between the plasma concentrations (pg/ml) of GDF15 (X axis) and NfL or GFAP (Y axis) in X-ALD patients. CALD patients (cAMN and ccALD) are represented on the graphs on the right whereas AMN on the left. Orange dots represents ccALD patients whereas blue dots represent cAMN patients. The straight black line represents the line of best fit between the values.

2.7 SCFA levels are not altered in the stool of X-ALD patients

Given the importance of SCFAs in the gut-brain axis and locally for proper intestinal epithelial trophism, we proceeded to evaluate the levels in the stool of X-ALD patients and controls. No statistically significant difference was found for butyric acid, isobutyric acid, valeric acid, isovaleric acid, or acetate levels among the various groups analyzed (AMN, ccALD, and respective controls) (figure 54). Propionic acid was found to be determinable in only 25% of the total samples, equally distributed among the various groups analyzed.

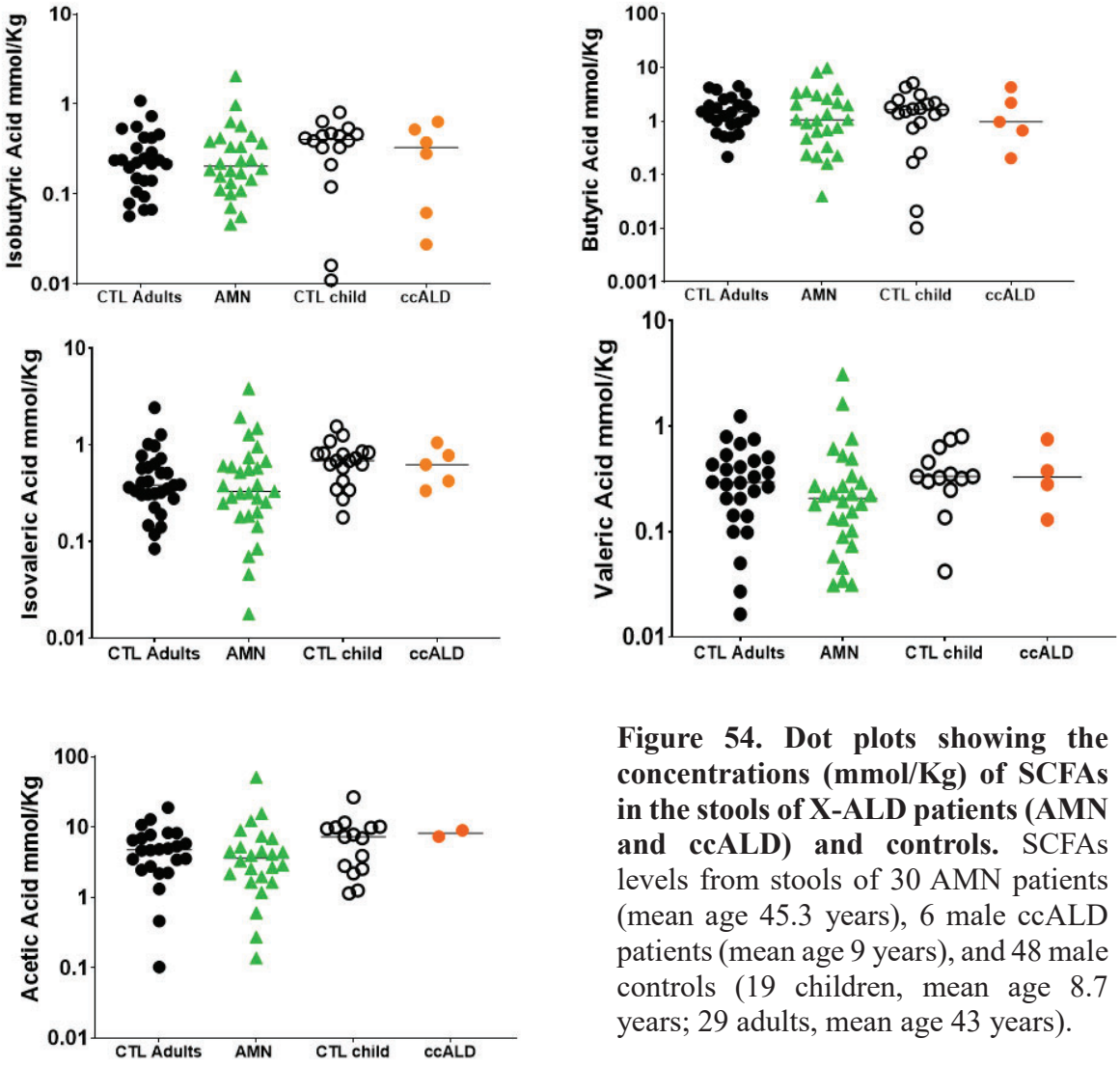

Figure 54. Dot plots showing the concentrations (mmol/Kg) of SCFAs in the stools of X-ALD patients (AMN and ccALD) and controls. SCFAs levels from stools of 30 AMN patients (mean age 45.3 years), 6 male ccALD patients (mean age 9 years), and 48 male controls (19 children, mean age 8.7 years; 29 adults, mean age 43 years).

DISCUSSION

1 X-ALD: confirmations and new clues from NAWM on disease pathogenesis

Our untargeted metabolomics analysis revealed an alteration in metabolites associated with mitochondrial function and cellular redox homeostasis within the non-affected white matter (NAWM) of X-ALD patients. This finding aligns with and strengthens previous observations from our group (Lopez-Erauskin et al., 2013; Schlüter et al, 2012). Notably, we observed a significant decrease in N-acetylaspartic acid (NAA) levels (figure 23 A), a well-established biomarker of mitochondrial and neuronal dysfunction, being synthesized by neurons within the mitochondria from acetyl-CoA and L-aspartate (Jeffrey et al., 2021). Consistent with our hypothesis of mitochondrial impairment, we also detected reduced aspartate levels in the NAWM of X-ALD patients (figures 23 A, B), potentially reflecting diminished activity of the mitochondrial TCA cycle and ETC, both crucial for aspartate production (Birsoy et al., 2015; Hart et al., 2023).

Furthermore, we propose that the observed reduction in NAA and N-acetylaspartylglutamate (NAAG) levels (figure 23 A) in the NAWM of X-ALD patients could contribute to two key pathological processes: impaired myelinogenesis and heightened susceptibility to excitotoxicity. This hypothesis is supported by the following observations: a) high levels of NAA are found in oligodendrocytes, and it is thought to be a vital source of acetate, a precursor molecule necessary for the synthesis of myelin lipids (Nordengen et al., 2015; Moffet et al., 2007); b) NAA serves as the precursor for NAAG, a neuronal dipeptide that acts as a negative regulator at glutamatergic synapses via the metabotropic glutamate receptor 3 (mGluR3 or GM3), thereby preventing excitotoxic damage (Morland and Nordengen, 2022; Joseph and Tatsuo, 2019) (figure 55).

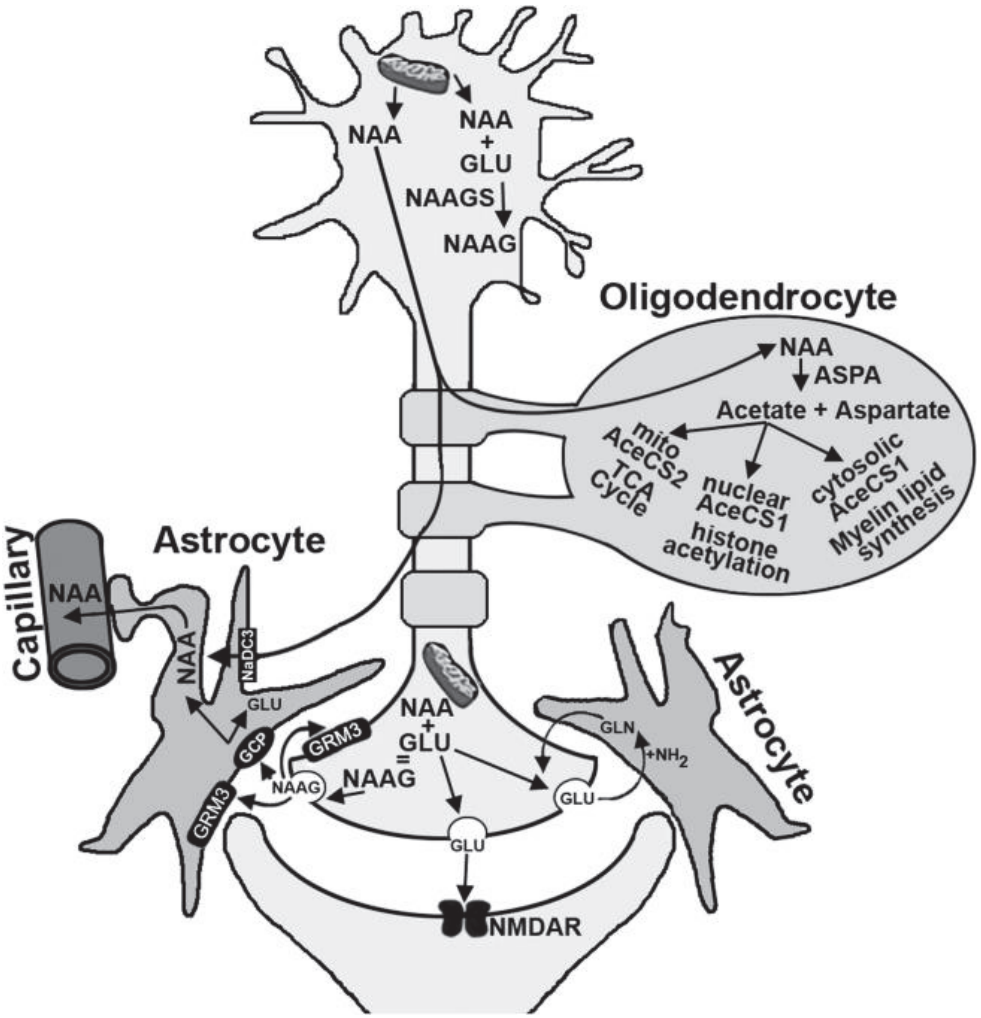

Figure 55. NAA and NAAG synthesis and catabolism. Subsequent to synthesis in neuronal mitochondria, NAA is transported to astrocytes via either the NAA dicarboxylate transporter NaDC3 for release into the circulatory system or to oligodendrocytes where it is catabolized to aspartate and acetate by ASPA. Aspartate is utilized in protein synthesis or metabolized in the tricarboxylic acid cycle (Krebs cycle), whereas the acetate must be converted to acetyl-coenzyme A by one of two AceCSs, mitochondrial AceCS2 for use in the tricarboxylic acid cycle or the cytosolic/nuclear regulated AceCS1 for use in fatty acid synthesis or histone acetylation. NAA may be converted to NAAG via NAAG synthetase (NAAGS). It has been proposed that NAAG activates GRM3 signaling in an autocrine or astrocytic paracrine manner, but some controversy exists whether activation is due to NAAG or glutamate (GLU) generated by catabolism of NAAG via GCP. Glutamate, either generated via NAAG catabolism or perisynaptic up-take, binds post-synaptic N-methyl-d-aspartate receptors (NMDAR) and is taken up by astrocytes for conversion to glutamine (GLN) then returned to neurons for conversion to glutamate. From Long et al., 2013.

We additionally observed a decrease in serine (Ser) levels within the NAWM of X-ALD patients (figures 23 A, B). The critical role of serine in neuronal function and CNS development is underscored by the severe neurological manifestations, coupled with hypomyelination and white matter atrophy, observed in patients with de novo serine synthesis enzyme deficiency (Vanderver and Wolf, 2017). Notably, serine serves as a building block for complex macromolecules like phosphatidylserine and sphingolipids, both essential constituents of lipid membranes (Hirabayashi and Furuya, 2008). Interestingly, a study suggests that serine deprivation can induce mitochondrial morphological alterations, independent of alterations in nucleotide and redox metabolism (Gao et al., 2018).

Moreover, our data revealed low levels of carnosine (Car) and taurine in the NAWM of X-ALD patients (figures 23 A, B). Car, a dipeptide with established anti-inflammatory, antioxidant, and anti-aggregatory properties (Schön et al., 2019; Solana-Manrique et al., 2022), is highly concentrated in muscle and brain tissues. Synthesized by mature oligodendrocytes, carnosine is primarily utilized by neurons and astrocytes. Deficient Car levels could potentially contribute to a disrupted redox balance and/or neuroinflammation, as observed in various neurodegenerative disorders (Schön et al., 2019; Solana-Manrique et al., 2022). Interestingly, we also detected low levels of β-alanine and L-histidine, precursors of Car, in the NAWM of X-ALD patients (figures 23 A, B). Taurine, another antioxidant, plays a role in maintaining mitochondrial health (Jong et al., 2021) and supplementation with taurine has been shown to mitigate age-related cellular decline, including telomere shortening, DNA damage, cellular senescence, and impaired mitochondrial function (Singh et al., 2023).

The endosymbiotic hypothesis proposes that mitochondria originated within eukaryotic cells from a symbiotic relationship with bacteria. This theory, along with the shared structural and functional similarities between mitochondria and bacteria, has led to the intriguing possibility that bacterial metabolites released by the gut microbiota can directly influence the central nervous system (CNS) via mitochondrial pathways (Zhu Y et al., 2022). Given the established role of mitochondrial dysfunction in X-ALD (Lopez-Erauskin et al., 2013; Schlüter et al, 2012) and the detection of metabolites potentially

derived from gut bacteria in the NAWM of X-ALD patients, we investigated the potential involvement of the gut microbiota in this disease. Our analysis of the NAWM in X-ALD patients revealed altered levels of metabolites derived from microbial metabolism of aromatic amino acids (AAAs) (figure 23A). Phenylacetylglutamine originates from oxidative bacterial metabolism of phenylalanine, while phenyllactic acid and hydroxyphenyllactic acid are products of the reductive metabolism of phenylalanine and tyrosine, respectively (Kathryn et al., 2021; Achilles et al., 2022; Dodd et al., 2017) (figure 56). Phenylacetylglutamine has been shown to reduce neuronal electrical activity independent of effects on the mitochondrial respiratory chain or oxidative stress generation (Achilles et al., 2022). This amino acid derivative has also been implicated in increased cardiovascular risk through its interaction with the platelet adrenergic receptor (Stanley and Hazen, 2020).

Conversely, phenyllactic acid and hydroxyphenyllactic acid have recently been identified as agonists for the human hydroxycarboxylic acid receptor 3 (HCA3), a receptor abundantly expressed on innate immune cells. Activation of HCA3 is thought to exert anti-inflammatory effects (Peters et al., 2019). Interestingly, the levels of phenylacetylglutamine in the NAWM of X-ALD patients appear to be higher compared to those of phenyllactic acid and hydroxyphenyllactic acid (figure 23A). This observation suggests a potential imbalance of AAAs metabolites in X-ALD patients, favoring the production of potentially neurotoxic metabolites like phenylacetylglutamine, as previously observed in a study on MS (Kathryn et al., 2021).

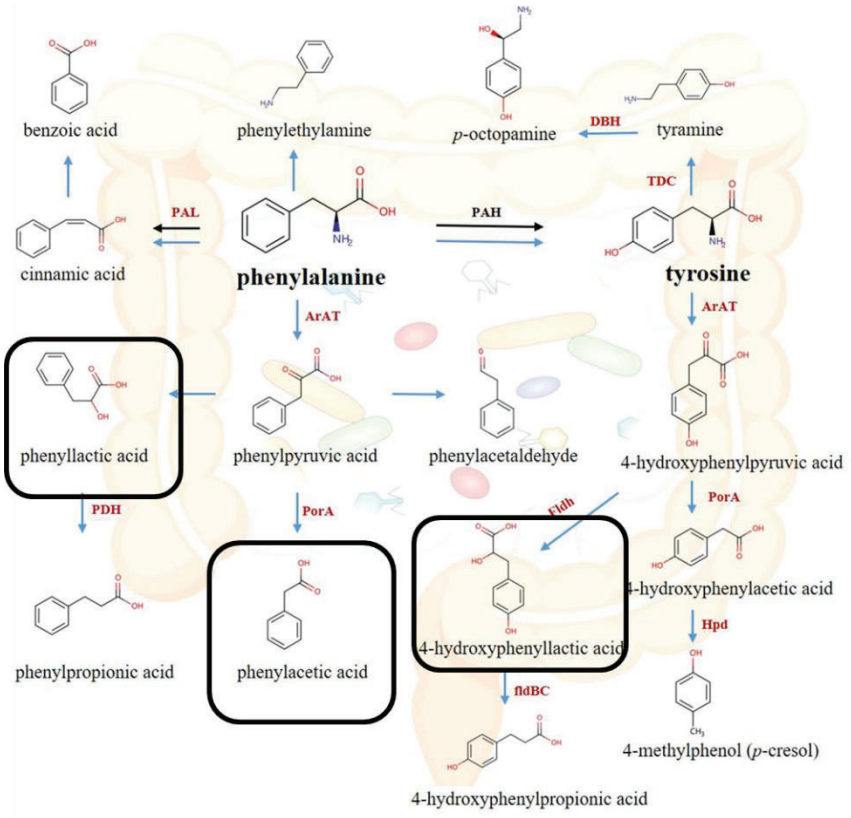

Figure 56. Host and Microbial Metabolism Pathways of Phenylalanine and Tyrosine. Host and microbial pathways are indicated by blue and black arrows, respectively. Abbreviations: ArAT, aromatic amino acid aminotransferas; FldBC, phenyllactate dehydratase; Fldh, phenyllactate dehydrogenase; Hpd, hydroxyphenylacetate decarboxylase; PAH, phenylalanine hydroxylase; PAL, phenylalanine ammonia lyase; PDH, phenylacetaldehyde dehydrogenase; PorA, phenylpyruvate oxidoreductase A; TDC, tyrosine decarboxylase. From Liu Y et al., 2020.

2 The identification of novel biomarkers in X-ALD and the modulatory potential of the gut microbiota.

The most pressing unmet needs in this disease are to identify biomarkers that will allow discriminating between the rapid cerebral form (ccALD and cAMN) and the slowly progressive form (AMN) of the disease and evaluating the efficacy of the treatment in clinical trials for AMN patients. NfL, UCHL1, and total TAU are recognized as markers for neuroaxonal damage (Kawata et al., 2016; Khalil et al., 2018) while GFAP reflects astrocyte activation or injury (Yang Z., 2015) (figure 57). These proteins are released into the extracellular space after neuronal or glial injury and subsequently detectable in the

cerebrospinal fluid (CSF) and then in blood. This study has validated the increased levels of NfL and GFAP in the plasma of both AMN patients and those with the cerebral form of the disease; furthermore, the study has demonstrated the ability of these two biomarkers to discriminate between the less severe (progressive) phenotype and the rapid cerebral course (figure 31). In addition, our findings demonstrated that NfL is also elevated in the CSF of X-ALD patients in comparison to controls, with a more pronounced increase observed in cerebral X-ALD patients compared to those with AMN (figure 34). Furthermore, the levels of UCHL1 were found to be elevated in plasma and CSF of cerebral X-ALD patients compared to controls and AMN (figures 31, 34). As plasma TAU level is not altered in AMN patients, we speculate that this marker could be useful to identify whether AMN patients could develop other neurodegenerative disorders such as AD, frontotemporal dementia (FTD), and tauopathies which are highly prevalent in the older population. Moreover, the positive correlation between NfL in plasma and CSF in cerebral X-ALD patients indicates that measurement of NfL in CSF after a lumbar puncture, which is an invasive procedure, does not bring any added value in the diagnostic procedure for these patients (figure 36). We demonstrated an association between NfL levels and the Loes score in cerebral X-ALD, both in plasma and CSF; in contrast, for GFAP this association was observed only in plasma (figures 33, 35). These findings are consistent with the initial study on NfL in X-ALD (Weinhofer et al., 2021) and represents the first report on NfL and GFAP levels in both fluids. We subsequently postulated that NfL is a superior biomarker to GFAP for the discrimination of AMN and cerebral X-ALD patients. This is supported by longitudinal data from two AMN patients who have converted to cAMN. In these two patients, NfL is increased following the conversion to the cerebral form, whereas GFAP levels, which were already elevated compared to control values during the patient's AMN phase, did not increase as much after the conversion. Instead, they fluctuated over time at high but more or less constant values (figure 37). This indicates that GFAP is an unreliable indicator for predicting whether an AMN patient will be converted to cAMN. In addition, NfL level is normalized in one patient after HSCT, as previously reported (Weinhofer et al., 2021) (figures 37 C). This suggests that astrocyte damage is not a primary event in the disease compared to axonal neurodegeneration in X-ALD. Recent studies have confirmed that NfL levels can reflect

inflammatory activity and progression in patients affected by the cerebral form of the disease (Weinhofer et al., 2021) and that NfL and GFAP levels can reflect spinal cord degeneration in AMN patients (van Ballegoij et al., 2020). We, therefore, hypothesize that NfL could be used as a predictive biomarker for personalized medicine in X-ALD patients who will convert to the typical rapidly progressive cerebral form of the disease. In the future, we propose to quantify NfL levels in plasma every 3-6 months in asymptomatic X-ALD children and adult AMN patients who will undergo an MRI with gadolinium every year. The utility of NfL monitoring every 3-6 months for individual patient management should increase the possibility of successfully treating X-ALD patients who convert to cAMN or ccALD by HSCT. Furthermore, the quantitative measurement of NfL in plasma could be employed to monitor the efficacy of a treatment in future phase II randomised, placebo-controlled trials in AMN patients. The acknowledged significance of NfL and GFAP in monitoring the natural history of the disease also presents an opportunity to corroborate a potential diagnostic/prognostic value of other metabolites/new biomarkers involved in the pathophysiology of the disease.

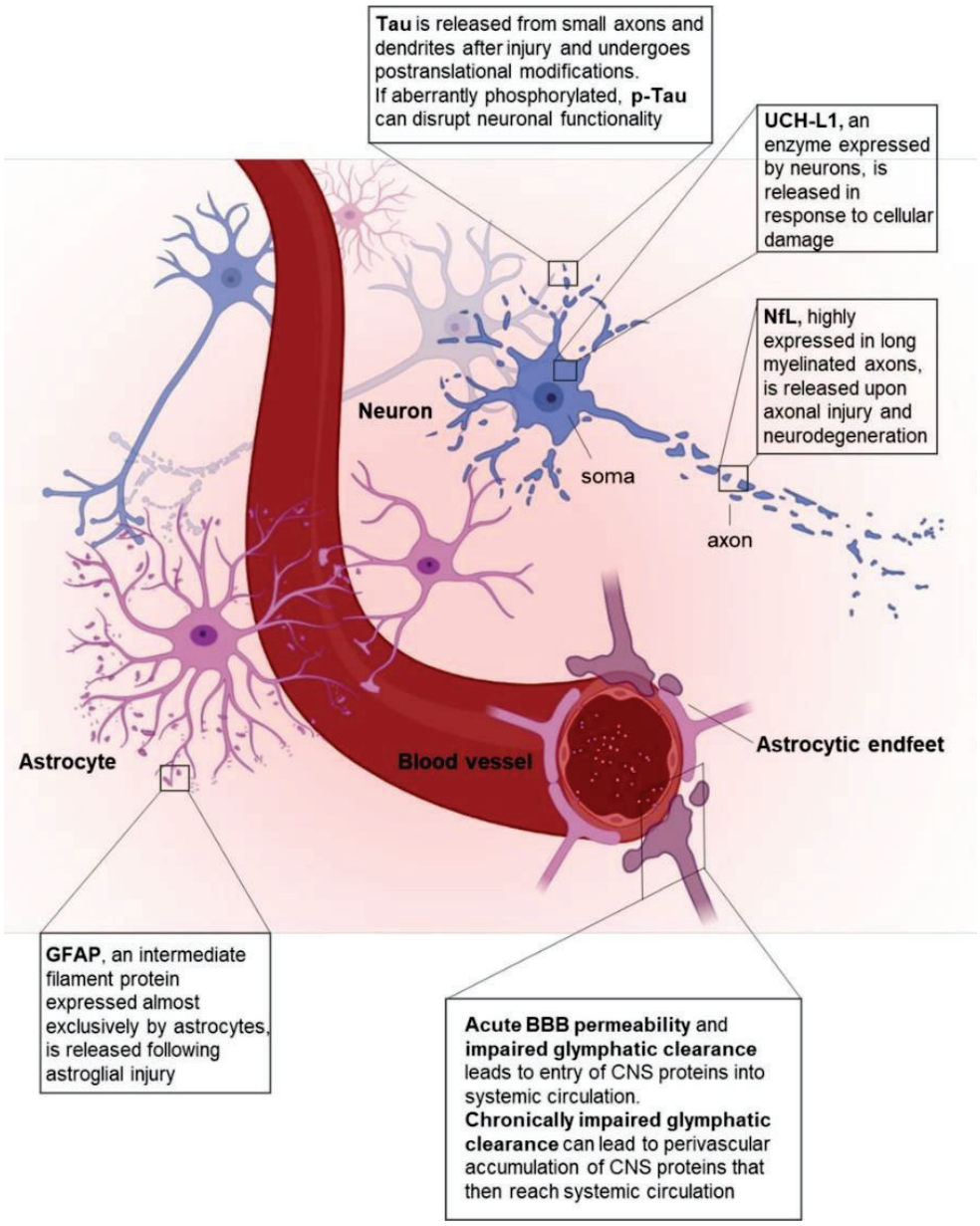

Figure 57. Key protein biomarkers for neuronal and astrocytic damage. Abbreviations: NfL: neurofilament-light; GFAP: glial fibrillary acidic protein; p-Tau: phosphorylated Tau; UCH-L1: ubiquitin C-terminal hydrolase; BBB: blood-brain barrier. From Lisi et al., 2023.

The gut microbiota plays a crucial role in regulating the amino acid pool and profile during intestinal digestion and absorption, significantly impacting host health and disease (Lin R et al., 2017; Ma N. and Ma X., 2018). Bacteria utilize dietary AAs for their own protein synthesis and are also capable of de novo synthesis of AAs, including essential

ones, establishing a reciprocal relationship with the host. In our X-ALD patient cohort, we observed a reduction in bacterial functions involved in the biosynthesis of branched-chain amino acids (BCAAs), glutamine, glutamate, asparagine, serine, alanine, and methionine, accompanied by an increased abundance of the lysine degradation function (figure 28). Notably, we also observed an increased abundance of several *Streptococcal* species (figure 27 A), bacteria known for their significant proteolytic capacity (Ma N. and Ma X., 2018; Macfarlane and Cummings, 1986).

Furthermore, we demonstrated reduced plasma levels of BCAAs in X-ALD patients (figure 39). These low BCAA levels inversely correlated with neurofilament light chain and glial fibrillary acidic protein levels (figure 39). Additionally, we observed decreased plasma methionine (Met) levels, but only in patients with cerebral forms of the disease (figure 41). In these cerebral X-ALD patients, Met levels inversely correlated with plasma NfL levels (figure 41 A3).

BCAAs constitute approximately 35% of essential amino acids in most mammals. Although mammalians lack the enzymes needed for the de novo synthesis of BCAAs, gut microbiota contain rich enzymes responsible for synthesis of BCAAs (Amorim and Blanchard, 2017). Since BCAAs can be degraded from food and synthesized by gut microbiota, both the daily supplementation of BCAAs containing food and modulating the composition of gut microbiota can affect the circulating BCAAs and further affect the health and disease associated with BCAAs (Feng W et al., 2022). Within the branched-chain amino acid dehydrogenase (BCKDH) complex located on the inner mitochondrial membrane, BCAAs undergo oxidation, contributing carbons to the TCA cycle. Valine is classified as glucogenic, leucine as ketogenic, and isoleucine exhibits mixed characteristics (Neinast et al., 2019). Additionally, BCAAs play a crucial role in inter-organ and inter-cellular nitrogen exchange. Notably, BCAA nitrogen can be transferred to the neuroprotective astrocyte/neuron glutamine/glutamate shuttle, also known as the "leucine-glutamate cycle" (figure 58) This cycle provides a mechanism for "buffering" brain glutamate when levels of this excitatory (and potentially toxic) neurotransmitter become elevated (Yudkoff, 1997). The modulation of amino acid bioavailability by the gut microbiota can also exert detrimental effects through the immune system via an

immunometabolic effect. Studies have shown that BCAA deficiency can alter the function of regulatory T (Treg) cells in vivo (Kayo et al., 2017). A reduction in the suppressive activity of these cells would then disrupt the balance of the T-cell immune response, tipping it towards a pro-inflammatory state.

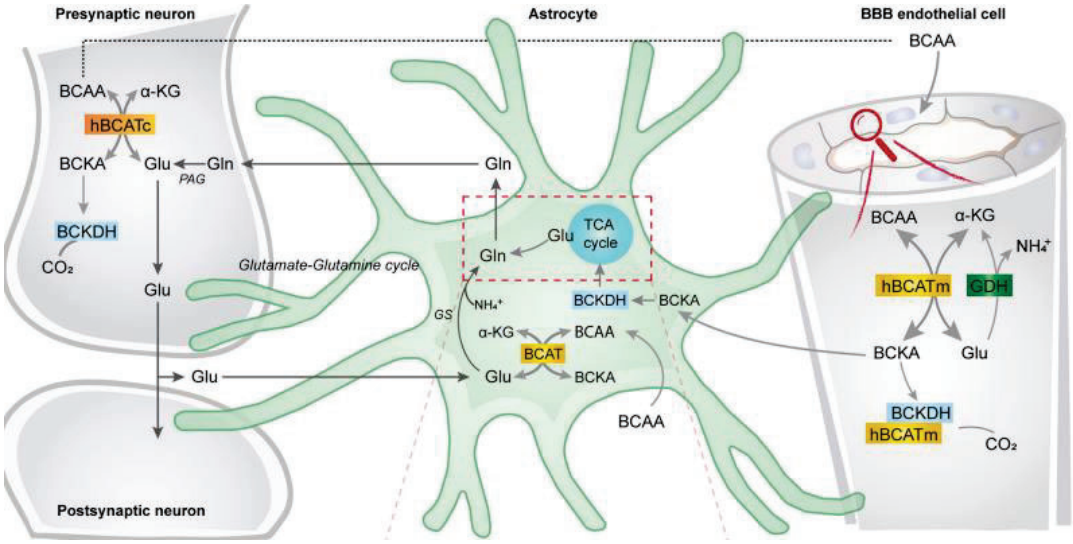

Figure 58. BCAA oxidative metabolism and nitrogen transfer in human astrocytes and potential blood brain barrier-astrocyte-neuron axis. BCAAs are taken up by the blood brain barrier (BBB) endothelial cells, and then BCAAs can undergo transamination by the action of BCATm, forming glutamate and the branched-chain α-keto acids (BCKAs), KIC, KIV, and KVM. In the reverse reaction when α-ketoglutarate is formed from glutamate, the BCAT/GDH metabolon in the endothelial cells may release ammonia, and BCAAs can be released and taken up by neurons or astrocytes. Alternatively, BCKAs from endothelial cells can be released or metabolized by the BCKDH/BCATm metabolon. Likewise, in neurons, BCAAs can also be transaminated, producing BCKAs and glutamate. BCKAs can be further metabolized by BCKDH, and glutamate can be used for neurotransmission. Glutamate from neurons in the synaptic cleft can be taken up by astrocytes. Astrocytes synthesize glutamine from glutamate and ammonia which is catalyzed by glutamine synthetase (GS) and is released for neuronal uptake to replenish the glutamate pool, in the so-called glutamate-glutamine cycle. BBB, blood brain barrier; BCATm, mitochondrial branched-chain aminotransferase; Glu, glutamate; α-KG, α-ketoglutarate; GDH, glutamate dehydrogenase; BCKA, branched-chain α-keto acids; KIC, α-ketoisocaproate; KIV, α-ketoisovaleric; KMV, α-keto-β-methylvalerate; BCAT, branched-chain aminotransferase; BCKDH, branched-chain α-keto acid dehydrogenase; Gln, glutamine; GS, glutamine synthetase; BCATc, cytosolic branched-chain aminotransferase; PAG, phosphate-activated glutaminase. From Salcedo et al., 2021.

For humans, methionine (Met) is an essential sulfur-containing amino acid obtainable from the diet or synthesized by gastrointestinal microbes. Met plays a well-established role as an initiator of protein synthesis in both prokaryotes and eukaryotes. Additionally, it functions as an endogenous antioxidant on the surface of proteins. S-adenosylmethionine (SAM) represents the final product of methionine metabolism through the transmethylation pathway (Parkhitko et al., 2019; Surtees et al., 1991; Martínez et al., 2017; Dash et al., 2016). Importantly, SAM donates methyl groups for the synthesis of phosphatidylcholine, a major phospholipid component of cell membranes. In some inborn errors of the methyl transfer pathway, demyelination has been associated with S-adenosylmethionine deficiency in cerebrospinal fluid (Surtees et al., 1991). Furthermore, methionine serves as the precursor for cysteine (Cys) through the transsulfuration pathway. Cys plays a role in protein translation and the synthesis of glutathione, a low-molecular-weight antioxidant. It has also been shown to chelate and remove lead from tissues, thereby contributing to reduced oxidative stress (Parkhitko et al., 2019; Surtees et al., 1991; Martínez et al., 2017; Dash et al., 2016). In our study, we observed increased levels of cysteine in the plasma of both ccALD and AMN patients (figure 43). However, a positive correlation between methionine and cysteine levels was only found in AMN patients (figure 44). These observations suggest a potential alteration in the transsulfuration pathway in X-ALD patients suffering from cerebral complications. Based on our findings, we hypothesise that reduced de novo amino acid biosynthesis by gut bacteria in X-ALD patients may contribute to the reduced circulating pool of BCAA and Met found in these patients, which may have detrimental effects on the nervous system and contribute to the pathophysiology of the disease through a metabolic/immunometabolic pathway.

While our study did not identify any metagenomic alterations in functions related to the bacterial metabolism of aromatic amino acids (AAAs) in this X-ALD patient cohort, we cannot definitively rule out the possibility of identifying novel enzymes or taxa involved in AAA metabolism in the future, particularly with the expansion of study subjects. As acknowledged in the literature, the study of bacterial metabolism remains an ongoing area of research that requires further investigation and characterisation due to the redundancy and complexity of certain biosynthetic machineries (Dodd et al., 2017; Visconti et al.,

2019) and functional comparisons are typically made after discarding the large proportion of metagenomic data that does not map to reference databases. Much of what does map to these databases is likely to be derived from common housekeeping and/or well-characterised genes that are found in many different bacteria and are also relatively well represented in reference databases. These comparative analyses therefore fail to accurately capture specialised or less well-characterised functions (Walker et al., 2023).

One-carbon (1C) metabolism encompasses the folate cycle, methionine remethylation, and transsulfuration pathways (figure 49). This complex network of biochemical reactions is compartmentalised between the cytoplasm, nucleus, and mitochondria, facilitating the transfer of 1C moieties in the form of methenyl, formyl, and methyl groups, which are required for a range of cellular processes. Such processes include molecular biosynthesis (e.g. proteins, polyamines, creatine, phospholipids), genomic maintenance via regulation of nucleotide pools, epigenetic control of gene expression by methylation of DNA, RNA, and histones, and redox defence. Dietary constituents that mediate one-carbon (1C) metabolism include folate (B9), other B vitamins (B2, B6, and B12), methionine, and choline (betaine), all of which act as essential substrates or cofactors (Clare et al., 2019). In contrast to plants, fungi, and certain prokaryotic organisms, which are capable of synthesising de novo folate, mammals depend on its dietary uptake. The biologically active form of folate is the reduced pteridine species, tetrahydrofolate (THF). The majority of naturally occurring folate species present in the diet and within the body are in the reduced form, with 5-methyl-THF being the most prevalent in humans. The most reduced form of folate, 5-methyl-THF, has a distinctive cellular fate, namely the remethylation of homocysteine to form methionine (Ducker et al., 2017). In adults, the neurological manifestations of folate deficiency are similar to those of vitamin B12 deficiency and include cognitive impairment, dementia, depression, and, less commonly, peripheral neuropathy and subacute combined degeneration of the spinal cord. The occurrence of developmental abnormalities of the neural tube in folate deficiency during pregnancy underscores the vital role of these vitamins in the physiology of the central nervous system (Reynolds, 2014; US Preventive Services Task Force, 2023). PLP is the coenzyme form of vitamin B6 that serves as a cofactor in over 160 different catalytic functions, including folate and methionine cycles (figure 49). The

majority of PLP-dependent enzymes are involved in amino acid biosynthesis and degradation. They play a pivotal role in the metabolism of neurotransmitters, including dopamine, serotonin, glycine, glutamate, and γ-aminobutyric acid (GABA), as well as organic acids, glucose, sphingolipids, and fatty acids (Ueland et al., 2015). Interestingly, we observed a dysregulation of the expression of folate and methionine cycle genes at the level of PBMCs of ccALD patients (figure 48), which could favours an increased peripheral metabolism of folate at the expense of the central nervous system metabolism. The observed reduced functional potential of the intestinal microbiota of X-ALD patients in the biosynthesis of folate and vitamin B6 (figure 30) could contribute to this pathogenic mechanism by exacerbating it. In addition, we also found increased expression of the *TCN2* gene in the PBMCs of ccALD patients (figure 48). Transcobalamin II (TCN2) belongs to the family of vitamin B12 binding proteins and in PBMCs is mainly expressed in monocytes. Its function is to facilitate the cellular uptake of vitamin B12, making it the most reliable biomarker for active and available vitamin B12 (Häberle et al, 2009), which serves as a cofactor for methionine synthase (MTR) and methionine synthase reductase (MTRR). These enzymes play a critical role in catalysing the remethylation of homocysteine to methionine in one-carbon metabolism (Rizzo and Laganà, 2020; Lyon et al., 2020). Interestingly, studies have reported increased levels of TCN2 and decreased levels of vitamin B12 in the blood of patients with the autoimmune disease systemic lupus erythematosus (SLE) (Fràter-Schröder et al., 1983; Segal et al., 2004; Tsai et al., 2021) and Liu B et al. (2024) found increased expression of *TCN2* in monocytes from SLE patients, which correlated positively with disease activity. Furthermore, TCN2 in monocytes was upregulated by SLE patient serum and lipopolysaccharide (LPS). Therefore, we cannot exclude a role of TCN2 as an immune modulator in X-ALD patients as well.

3 The gut microbiota in X-ALD: a potential mediator between a stressed gut and (auto)immunity

Metagenomic analysis of fecal samples from X-ALD patients revealed an increased abundance of pathways associated with oxidative stress regulation, glyoxylate response bypass, universal stress protein family, and biofilm adhesin biosynthesis (figure 29). These findings suggest potential mechanisms employed by gut bacteria to tolerate oxidative stress (Ahn et al., 2016; O'Connor and McClean, 2017; Yin W et al., 2019). This observation points towards the presence of a redox imbalance at the gastrointestinal level in X-ALD patients. In the intestine, peroxisomes are most abundant in epithelial cells throughout the tract, where they reside at the apical side of enterocytes (Morvay et al, 2017; Baumgart et al., 2003). With regard to the crypt-villus axis, the number of peroxisomes increases as intestinal epithelial cells differentiate (Cablé et al., 1993). Whereas catalase activity was higher in the crypt cells than in the mature enterocytes, peroxisomal oxidases, i.e., fatty acyl-CoA oxidase, D-amino acid oxidase, and polyamine oxidase, increased during differentiation (Morvay et al, 2017). Interestingly, a study utilizing the Drosophila melanogaster model demonstrated that dysfunctional peroxisomes lead to redox imbalance and lipotoxicity, ultimately causing alterations in gut microbiota composition (Di Cara et al., 2018). Additionally, research suggests that redox imbalance can disrupt the growth cycle of intestinal epithelial cells, resulting in abnormal proliferation, growth stagnation, and apoptosis-mediated damage to the intestinal barrier. Consequently, this can lead to a compromised barrier function and increased translocation of bacterial products into systemic circulation (Aw, 2005; Theiss et al., 2007). Environmental stress may therefore disrupt the equilibrium of the gut microbiota ecosystem, triggering bacterial adaptive mechanisms with potentially systemic and sometimes dualistic effects on the host. The observed increase in the abundance of the lipid A modification pathway in X-ALD patients (figure 29) could represent a bacterial compensatory response to environmental pressure, potentially influencing the dynamics of the host's immune system. Lipopolysaccharide (LPS), a component of the outer membrane of Gram-negative bacteria, possesses two key properties: (1) it protects the bacterium from external stress, and (2) it functions as a pathogen-associated molecular pattern (PAMP) capable of stimulating the innate immune

response through interaction with Toll-like receptors (TLRs) (Dias et al., 2021; Steimle et al., 2016). Lipid A, a subunit of LPS, not only confers increased bacterial resistance to environmental stresses like pH changes through modifications but also influences its immunogenicity (Steimle et al., 2016). Traditionally, LPS is thought to induce an inflammatory response ("agonistic LPS") by interacting with TLR4. However, depending on the structure of the lipid A, LPS can interact with TLR4 to either block the inflammatory response ("antagonistic LPS") or produce a weak stimulatory effect ("weak agonistic LPS"). The effect of LPS can also be mediated through its interaction with TLR2. Fundamentally, lipid A consists of a β (1→6)-linked glucosamine disaccharide backbone, typically phosphorylated at positions 1 and 4' of the saccharides and acylated at positions 2 and 3 of each monosaccharide portion (Steimle et al., 2016) Therefore, variations in the number and length of acyl chains can significantly impact the inflammatory response. Modifications of lipid A induced by environmental stress could consequently lead to a change in the immunogenic properties of LPS, potentially affecting immune priming during infancy and the development of the peripheral and/or central immune system (Dias et al., 2021; Brown et al., 2023).

The potential role of LPS in the pathophysiology of X-ALD appears even more important in light of our previous observations of increased expression of TLR2 and its coreceptor CD14 in the NAWM of cAMN patients (Schlüter et al., 2012). Our analysis revealed an increased abundance of *Escherichia coli* bacteria at the taxa level and 'Curli production' at the functional level in X-ALD patients compared to controls (figure 29). *E. coli* flourishes in pro-inflammatory environments (Winter et al., 2013), which also triggers the expression of Curli proteins by this bacterium, that are essential components of the extracellular matrix within bacterial biofilms. These proteins form amyloid complexes with a quaternary structure remarkably similar to human amyloids and are capable of activating the intracellular NLRP3 inflammasome and TLRs 1 and 2 (Miller et al., 2021). Additionally, we observed an increased abundance of *Streptococcus mutans* (figure 27 A), a bacterial species known to produce amyloid-like proteins (Besingi et al., 2017). Intriguingly, recent studies suggest a potential role for Curli proteins in the pathogenesis of some neurological diseases such as Parkinson's disease, amyotrophic lateral sclerosis

(ALS), and Alzheimer's disease (Schmit et al., 2023; Kurlawala et al., 2023; Das et al., 2022).

4 Mitochondrial dysfunction and inflammation: two sides of the same coin

With the work of this thesis, we have also confirmed the presence of two closely interwined hallmarks of X-ALD: mitochondrial damage/dysfunction and the presence of inflammation, even in AMN patients with a milder phenotype of the disease. While in fact we observed an increase in mtDNA in the CSF of AMN patients (figure 50), a sign of mitochondrial damage and which is itself capable of triggering an inflammatory response (as described in the introduction), we also observed an increase in plasma GDF15 in the cohort of our patients, reflecting both the presence of mitochondrial impairment and the presence of inflammation (figure 52). Mitochondrial dysfunction (Montero et al., 2016), cellular stress, inflammation, and activation of the mitochondrial unfolded protein response (UPRmt) pathway all potently induce GDF15 expression (Durieux et al., 2011; Conte et al., 2022). This aligns perfectly with the defining characteristics of a mitokine. GDF15 belongs to the transforming growth factor β (TGF-β) superfamily, readily identifiable by its seven conserved cysteine residues forming a signature cysteine knot. It possesses a rich nomenclature, including macrophage inhibitory cytokine-1, placental transforming growth factor-β, gene placental bone morphogenic protein, prostate-derived factor, NSAID (nonsteroidal anti-inflammatory drug)-activated gene 1, and placental transforming growth factor-β (Lindahl, 2013; Wischhusen et al., 2020). Cell types capable of expressing GDF15 encompass cardiomyocytes, adipocytes, macrophages, endothelial cells, and vascular smooth muscle cells, present in both healthy and diseased states (Wischhusen et al., 2020). The precise mechanisms governing GDF15 expression remain under investigation, although activating transcription factor 4 (ATF4), a stress-responsive gene, is hypothesized to play a key role in its upregulation during cellular insults (Yatsuga et al., 2015); interestingly, in a previous study, our group found a significant upregulation of ATF4 levels in the brain affected areas of ccALD and cAMN patients and increased ATF4 levels in the spinal cord tissue of *Abcd1*$^{-}$ mice (Launay et al., 2017). Furthermore, a multitude of inflammatory and stress-related proteins, including interleukin (IL)-1β, tumor necrosis factor (TNF)-α,

interleukin-2, and macrophage colony-stimulating factor (MCSF)-1, have been demonstrated to positively regulate GDF15 expression (Wischhusen et al., 2020). Interestingly, bacterial components like LPS also contribute to GDF15 upregulation (Patel et al., 2022). This finding aligns with clinical observations of elevated serum GDF15 in patients with sepsis of diverse etiologies (bacterial, viral, or mixed), suggesting its potential as a universal marker of infection-induced inflammation (Luan et al., 2019). Notably, GDF15 has been identified as a component of the senescence-associated secretory phenotype (SASP), a pro-inflammatory secretome encompassing various cytokines, chemokines, growth factors, and proteases released by senescent cells into the surrounding tissue microenvironment (Lindahl, 2013; Conte et al., 2022). The question of whether elevated serum GDF15 concentrations directly contribute to tissue damage or represent a compensatory response to cellular stress remains a subject of ongoing investigation: GDF15 exhibits a remarkable degree of contextual dependency, displaying a spectrum of, and even opposing, functions depending on the cellular environment. The context-dependent nature of GDF15 function extends to its potential role in various pathologies. In rheumatoid arthritis (RA), elevated GDF15 serum levels have been observed and exhibit a positive correlation with disease severity markers, including erythrocyte sedimentation rate, morning stiffness, tender joint count, and carotid intima-media thickness (Wischhusen et al., 2020). Conversely, in type 1 diabetes (T1D), GDF15 displays a seemingly protective effect. Studies report elevated GDF-15 activity within pancreatic beta cells, suggesting its potential as a biomarker for T1D (Wischhusen et al., 2020). Furthermore, functional studies in non-obese diabetic (NOD) mice demonstrated the ability of GDF15 to safeguard pancreatic beta cells under inflammatory conditions (Nakayasu et al., 2020). GDF15 can exert pro-apoptotic or anti-apoptotic effects, promote or inhibit angiogenesis, and possess both pro-proliferative and anti-inflammatory/immunosuppressive properties (Lindahl et al., 2013; Conte et al., 2022). Future research elucidating the precise molecular mechanisms governing pleiotropic effects of GDF15 will be crucial for unraveling this intriguing paradox.

5 Global discussion

This study sheds light on the potential significance of altered metabolite profiles in X-ALD pathogenesis, particularly their association with mitochondrial dysfunction, impaired myelinogenesis, and neuroinflammatory processes. Our findings emphasize the importance of plasma methionine (Met) as a readily accessible and measurable biomarker, especially in the context of cerebral inflammatory X-ALD. Furthermore, we introduce a novel hypothesis suggesting that the gut microbiota dysbiosis may contribute to some of the metabolic changes observed in X-ALD patients. As we move towards transforming microbiome research from descriptive to causal and ultimately translational science, the ability to define biomarkers that can stratify patient populations within a disease state represents 'low-hanging fruit' (Gilbert et al., 2018). The characterisation of microbial biomarkers has great potential for precision medicine and is therefore a relatively straightforward way to translate microbiome research into clinical practice. However, a major challenge in microbiota-based medicine is to define a healthy gut microbiome (Shanahan F. et al., 2021). The inter-individual variation in microbiota composition is substantial, making a 'one-size-fits-all' approach impractical (Chen L et al., 2022). However, this very personalisation presents an opportunity, as the gut microbiota holds immense potential as a target for future personalised medicine strategies (Wang S. et al., 2024). Microbiome stability (resistance to change) and resilience (return to initial state after perturbation) are essential but poorly understood ecological properties that can be quantified in longitudinal studies through serial collection of DNA sequence data from the microbiome, perhaps complemented by metabolite and gene expression profiling (Gilbert et al., 2018).

Our human studies utilizing a combined -omics approach have identified several disrupted homeostatic pathways, some of which hold promise as potential therapeutic targets (Zhou X. et al., 2018; Yang L. et al., 2023; Sato et al., 2021; Seckler and Lewis, 2020; Amorim and Blanchard, 2017). While further research is necessary to elucidate the underlying mechanisms and potential therapeutic implications of these metabolic abnormalities, this study suggests the possibility of a multi-targeted therapeutic approach for X-ALD. This approach could combine medications to normalize amino acid levels

and prevent gut microbiota alterations acting on intestinal inflammation potentially leading to synergistic and disease-modifying effects. Additionally, the assessment of plasma Met levels holds significant promise as a valuable metric for monitoring disease activity and progression in clinical trials aimed at addressing inflammatory demyelination and neurodegeneration in cerebral X-ALD patients.

CONCLUSIONS

Based on the aims established for this thesis, the conclusions of the present dissertation can be formulated as follows:

1- Untargeted metabolomic analysis of non-affected white matter (NAWM) samples from X-ALD patients revealed distinct metabolite profiles compared to controls and between cerebral phenotypes of the disease;

2- Some of the metabolic changes in NAWM can be attributed to X-ALD hallmarks such as mitochondrial dysfunction and redox imbalance; others can be attributed to bacterial metabolism of aromatic amino acids and polyphenols.

3- The gut microbiota composition is altered in X-ALD patients: at the taxa level, the most consistent alterations compared to controls are at the level of specific species of *Streptococci, Chryseobacteria* and *Flavobacteria*.

4- The functional potential of the gut microbiota is altered in X-ALD patients, with features of response to environmental stress, possibly underlying some of the hallmarks of the X-ALD disease like redox imbalance and inflammation also at the gut level.

5- Plasma and CSF levels of both NfL and GFAP are capable of discriminating between the different phenotypes of X-ALD.

6- Plasma NfL emerges as a potential predictive marker of the conversion to the cerebral form

7- Branched-chain amino acids were lower in the plasma of X-ALD patients, they inversely correlated with NfL and GFAP levels and their biosynthesis by X-ALD gut microbiota resulted impaired: they therefore may represent a disease signature and microbiota may represent a modulator for the disease severity.

8- Methionine was lower in the plasma of cerebral X-ALD patients and it inversely correlated only with NfL: it they therefore may represent a novel biomarker of the cerebral form of the disease.

9- Plasma GDF15 levels and CSF mtDNA levels were higher in X-ALD patients respect to controls, confirming the presence of mitochondrial impairment hallmark.

BIBLIOGRAPHY

Abdel-Haq R, Schlachetzki JC, Glass CK, Mazmanian SK. 2019. Microbiome-microglia connections via the gut-brain axis. J Exp Med 216: 41–59.

Achilles Ntranos, Hye-Jin Park, Maureen Wentling, Vladimir Tolstikov, Mario Amatruda, Benjamin Inbar, Seunghee Kim-Schulze, Carol Frazier, Judy Button, Michael A Kiebish, Fred Lublin, Keith Edwards, Patrizia Casaccia, Bacterial neurotoxic metabolites in multiple sclerosis cerebrospinal fluid and plasma, Brain, Volume 145, Issue 2, February 2022, Pages 569–583.

Adak A, Khan MR. An insight into gut microbiota and its functionalities. Cell Mol Life Sci. 2019 Feb;76(3):473-493. doi: 10.1007/s00018-018-2943-4. Epub 2018 Oct 13. PMID: 30317530; PMCID: PMC11105460.

Adolph, T.E., and Zhang, J. (2022). Diet fuelling inflammatory bowel diseases: preclinical and clinical concepts. Gut 71, 2574–2586. https://doi. org/10.1136/gutjnl-2021-326575. Abeti, R.; Abramov, A.Y. Mitochondrial Ca2+ in Neurodegenerative Disorders. Pharmacol. Res. 2015, 99, 377–381.

Agrimi, G., Di Noia, M. A., Marobbio, C. M. T., Fiermonte, G., Lasorsa, F. M., and Palmieri, F. (2004). Identification of the human mitochondrial S-adenosylmethionine transporter: bacterial expression, reconstitution, functional characterization and tissue distribution. Biochem. J. 379, 183–190. doi: 10.1042/BJ20031664

Ahn S, Jung J, Jang IA, Madsen EL, Park W. Role of Glyoxylate Shunt in Oxidative Stress Response. J Biol Chem. 2016 May 27;291(22):11928-38. doi: 10.1074/jbc.M115.708149. Epub 2016 Apr 1. PMID: 27036942; PMCID: PMC4882458

Akbari E, Asemi Z, Daneshvar Kakhaki R, Bahmani F, Kouchaki E, Tamtaji OR, Hamidi GA, Salami M. Effect of Probiotic Supplementation on Cognitive Function and Metabolic Status in Alzheimer's Disease: A Randomized, Double-Blind and Controlled Trial. Front Aging Neurosci. 2016 Nov 10;8:256. doi: 10.3389/fnagi.2016.00256. PMID: 27891089; PMCID: PMC5105117.

Al-Asmakh, M., and Zadjali, F. (2015). Use of germ-free animal models in microbiota-related research. J. Microbiol. Biotechnol. 25, 1583–1588. doi: 10.4014/jmb.1501.01039

Alexander, K. L., Targan, S. R. & Elson, C. O. 3rd Microbiota activation and regulation of innate and adaptive immunity. Immunol. Rev. 260, 206–220 (2014).

Aliu, E., Kanungo, S., and Arnold, G.L. (2018). Amino acid disorders. Ann. Transl. Med. 6, 471. https://doi.org/10.21037/atm.2018.12.12.

Alkadhi, S., Kunde, D., Cheluvappa, R., Randall-Demllo, S. & Eri, R. The murine appendiceal microbiome is altered in spontaneous colitis and its pathological progression. Gut. Pathog. 6, 2510 (2014).

Allen AP, Hutch W, Borre YE, Kennedy PJ, Temko A, Boylan G, Murphy E, Cryan JF, Dinan TG, Clarke G. Bifidobacterium longum 1714 as a translational psychobiotic: modulation of stress, electrophysiology and neurocognition in healthy volunteers. Transl Psychiatry. 2016 Nov 1;6(11):e939. doi: 10.1038/tp.2016.191. PMID: 27801892; PMCID: PMC5314114.

Altschul SF, Gish W, Miller W, Myers EW, Lipman DJ. 1990. Basic local alignment search tool. J. Mol. Biol. 215:403–10

Aluwihare AP. An ultrastructural study of the effect of neomycin on the colon in the human subject and in the conventional and the germ-free mouse. Gut 12: 341–349, 1971. doi:10.1136/gut.12.5.341

Amorim Franco TM, Blanchard JS. Bacterial branched-chain amino acid biosynthesis: structures, mechanisms, and drugability. Biochemistry. (2017) 56:5849–65. doi:10.1021/acs.biochem.7b00849

An H.M, S.Y. Park, D.K. Lee, J.R. Kim, M.K. Cha, S.W. Lee, N.J. Ha Antiobesity and lipid-lowering effects of Bifidobacterium spp. in high fat diet-induced obese rats Lipids in Health and Disease, 10 (2011), p. 116

Andersson SG, Zomorodipour A, Andersson JO, Sicheritz-Pontén T, Alsmark UC, Podowski RM, Näslund AK, Eriksson AS, Winkler HH, Kurland CG. The genome sequence of Rickettsia prowazekii and the origin of mitochondria. Nature. 1998 Nov 12;396(6707):133-40. doi: 10.1038/24094. PMID: 9823893.

Angelova PR, Abramov AY. Functional role of mitochondrial reactive oxygen species in physiology. Free Radic Biol Med. (2016) 100:81–5. doi: 10.1016/j. freeradbiomed.2016.06.005

Angelova PR, Abramov AY. Role of mitochondrial ros in the brain: from physiology to neurodegeneration. FEBS Lett. (2018) 592:692–702. doi: 10. 1002/1873-3468.12964

Anne Stetler, R., Leak, R.K., Gao, Y., and Chen, J. (2013). The dynamics of the mitochondrial organelle as a potential therapeutic target. Journal of cerebral blood flow and metabolism : official journal of the International Society of Cerebral Blood Flow and Metabolism 33, 22-32.

Annesley SJ, Fisher PR. Mitochondria in health and disease. Cells. 2019;8:680.

Ansari F, Pourjafar H, Tabrizi A, Homayouni A. The Effects of Probiotics and Prebiotics on Mental Disorders: A Review on Depression, Anxiety, Alzheimer, and Autism Spectrum Disorders. Curr Pharm Biotechnol. 2020;21(7):555-565.

Arnold LE, Luna RA, Williams K, Chan J, Parker RA, Wu Q, Hollway JA, Jeffs A, Lu F, Coury DL, Hayes C, Savidge T. 2019. Probiotics for gastrointestinal symptoms and quality of life in autism: a placebo-controlled pilot trial. J Child Adolesc Psychopharmacol 29:659–669. https://doi.org/10.1089/cap.2018.0156.

Asl ZR, Sepehri G, Salami M. 2019. Probiotic treatment improves the impaired spatial cognitive performance and restores synaptic plasticity in an animal model of Alzheimer's disease. Behav Brain Res 376:112183. https://doi.org/10.1016/j.bbr.2019.112183.

Atarashi, K., Tanoue, T., Shima, T., Imaoka, A., Kuwahara, T., Momose, Y., et al. (2011). Induction of colonic regulatory T cells. Science 331, 337–342. doi: 10.1126/science.1198469

Athari Nik Azm S, Djazayeri A, Safa M, Azami K, Ahmadvand B, Sabbaghziarani F, Sharifzadeh M, Vafa M. 2018. Lactobacilli and bifidobacteria ameliorate memory and learning deficits and oxidative stress in b-amyloid (1–42) injected rats. Appl Physiol Nutr Metab 43:718–726.

Aw TY. Intestinal glutathione: determinant of mucosal peroxide transport, metabolism, and oxidative susceptibility. Toxicol Appl Pharmacol. 2005 May 1;204(3):320-8. doi: 10.1016/j.taap.2004.11.016. PMID: 15845421.

Baarine, M., Andreoletti, P., Athias, A., Nury, T., Zarrouk, A., Ragot, K., Vejux, A., Riedinger, J.M., Kattan, Z., Bessede, G., et al. (2012). Evidence of oxidative stress in very long chain fatty acid - Treated oligodendrocytes and potentialization of ROS production using RNA interference-directed knockdown of ABCD1 and ACOX1 peroxisomal proteins. Neuroscience 213, 1-18.

Baarine, M., Beeson, C., Singh, A., and Singh, I. (2015). ABCD1 deletion-induced mitochondrial dysfunction is corrected by SAHA: implication for adrenoleukodystrophy. J. Neurochem. 133, 380-396.

Baarine M., Khan M., Singh A., Singh I. Functional Characterization of IPSC-Derived Brain Cells as a Model for X-Linked Adrenoleukodystrophy. PLoS ONE. 2015;10:e0143238. doi: 10.1371/journal.pone.0143238.

Bäckhed F, Ley RE, Sonnenburg JL, Peterson DA, Gordon JI. Host-bacterial mutualism in the human intestine. Science. 2005 Mar 25;307(5717):1915-20. doi: 10.1126/science.1104816. PMID: 15790844.

Baev, A.Y.; Vinokurov, A.Y.; Novikova, I.N.; Dremin, V.V.; Potapova, E.V.; Abramov, A.Y. Interaction of Mitochondrial Calcium and ROS in Neurodegeneration. Cells 2022, 11, 706.

Bager, P., Wohlfahrt, J. & Westergaard, T. Caesarean delivery and risk of atopy and allergic disease: meta-analyses. Clin. Exp. Allergy. J. Br. Soc. Allergy. Clin. Immunol. 38, 634–642 (2008)

Bai J, Cervantes C, Liu J, He S, Zhou H, Zhang B, et al. DsbA-L prevents obesityinduced inflammation and insulin resistance by suppressing the mtDNA release activated cGAS-cGAMP-STING pathway. Proc Natl Acad Sci USA. 2017;114:12196–201

Baker A, Carrier DJ, Schaedler T, Waterham HR, van Roermund CW, Theodoulou FL. Peroxisomal ABC transporters: functions and mechanism. Biochem Soc Trans. 2015 Oct;43(5):959-65. doi: 10.1042/BST20150127. Epub 2015 Oct 9. PMID: 26517910; PMCID: PMC4652930.

Balin BJ, Gérard HC, Arking EJ, Appelt DM, Branigan PJ, Abrams JT, Whittum-Hudson JA, Hudson AP. Identification and localization of Chlamydia pneumoniae in the Alzheimer's brain. Med Microbiol Immunol. 1998 Jun;187(1):23-42. doi: 10.1007/s004300050071. PMID: 9749980.

Barathikannan K, Chelliah R, Rubab M, Daliri EB-M, Elahi F, Kim D-H, Agastian P, Oh S-Y, Oh DH. 2019. Gut microbiome modulation based on probiotic application for anti-obesity: a review on efficacy and validation. Microorganisms 7:456.

Barbosa RSD, Vieira-Coelho MA. Probiotics and prebiotics: focus on psychiatric disorders - a systematic review. Nutr Rev. 2020 Jun 1;78(6):437-450. doi: 10.1093/nutrit/nuz080. PMID: 31769847.

Barichella M, Pacchetti C, Bolliri C, Cassani E, Iorio L, Pusani C, Pinelli G, Privitera G, Cesari I, Faierman SA, Caccialanza R, Pezzoli G, Cereda E. 2016. Probiotics and prebiotic fiber for constipation associated with Parkinson disease: an RCT. Neurology 87:1274–1280. https://doi.org/10 .1212/WNL.0000000000003127

Baron S, editor. Medical Microbiology. 4th edition. Galveston (TX): University of Texas Medical Branch at Galveston; 1996. Introduction to Bacteriology. Available from: https://www.ncbi.nlm.nih.gov/books/NBK8120/

Baum BR. 1989. PHYLIP: Phylogeny Inference Package. Version 3.2. Q. Rev. Biol. 64:539–41

Baumgart, E., Vanhorebeek, I., Grabenbauer, M., Borgers, M., Declercq, P.E., Fahimi, H.D., and Baes, M. (2001). Mitochondrial alterations caused by defective peroxisomal biogenesis in a mouse model for Zellweger syndrome (PEX5 knockout mouse). Am. J. Pathol. 159, 1477-1494.

Baumgart E, Fahimi HD, Steininger H, Grabenbauer M. A review of morphological techniques for detection of peroxisomal (and mitochondrial) proteins and their corresponding mRNAs during ontogenesis in mice: application to the PEX5-knockout mouse with Zellweger syndrome. Microsc Res Tech 61: 121–138, 2003. doi:10.1002/jemt.10322.

Beaumont M, Roura E, Lambert W, Turni C, Michiels J, Chalvon-Demersay T. Selective nourishing of gut microbiota with amino acids: A novel prebiotic approach? Front Nutr. 2022 Dec 19;9:1066898. doi: 10.3389/fnut.2022.1066898. PMID: 36601082; PMCID: PMC9806265.

Bedard, K., and Krause, K. H. (2007). The NOX family of ROS-generating NADPH oxidases: physiology and pathophysiology. Physiol. Rev. 87, 245–313. doi: 10. 1152/physrev.00044.2005

Begley M, Gahan CGM, Hill C (2005) The interaction between bacteria and bile. FEMS Microbiol Rev 29:625–651

Behnam JT, Williams EL, Brink S, Rumsby G, Danpure CJ. Reconstruction of human hepatocyte glyoxylate metabolic pathways in stably transformed Chinese-hamster ovary cells. Biochem J. 2006 Mar 1;394(Pt 2):409-16. doi: 10.1042/BJ20051397. PMID: 16309382; PMCID: PMC1408671.

Béïque JC, Andrade R. 2003. PSD-95 regulates synaptic transmission and plasticity in rat cerebral cortex. J Physiol 546:859–867. https://doi.org/10 .1113/jphysiol.2002.031369

Bélanger, M., Allaman, I., and Magistretti, Pierre J. (2011). Brain Energy Metabolism: Focus on Astrocyte-Neuron Metabolic Cooperation. Cell Metab. 14, 724-738.

Belizário JE, Napolitano M. Human microbiomes and their roles in dysbiosis, common diseases, and novel therapeutic approaches. Front Microbiol. 2015 Oct 6;6:1050. doi: 10.3389/fmicb.2015.01050. PMID: 26500616; PMCID: PMC4594012.

Bellizzi, D., Daquila, P., Giordano, M., Montesanto, A., and Passarino, G. (2012). Global DNA methylation levels are modulated by mitochondrial DNA variants. Epigenomics 4, 17–27. doi: 10.2217/epi.11.109

Berer K, Gerdes LA, Cekanaviciute E, Jia X, Xiao L, Xia Z, Liu C, Klotz L, Stauffer U, Baranzini SE, Kümpfel T, Hohlfeld R, Krishnamoorthy G, Wekerle H. 2017. Gut microbiota from multiple sclerosis patients enables spontaneous autoimmune encephalomyelitis in mice. Proc Natl Acad Sci U S A 114:10719–10724. https://doi.org/10.1073/pnas.1711233114.

Berger J, Forss-Petter S, Eichler FS. Pathophysiology of X-linked adrenoleukodystrophy. Biochimie. 2014 Mar;98(100):135-42. doi: 10.1016/j.biochi.2013.11.023. Epub 2013 Dec 4. PMID: 24316281; PMCID: PMC3988840.

Bergner CG, van der Meer F, Winkler A, Wrzos C, Türkmen M, Valizada E, Fitzner D, Hametner S, Hartmann C, Pfeifenbring S, Stoltenburg-Didinger G, Brück W, Nessler S, Stadelmann C. Microglia damage precedes major myelin breakdown in X-linked adrenoleukodystrophy and metachromatic leukodystrophy. Glia. 2019 Jun;67(6):1196-1209. doi: 10.1002/glia.23598. Epub 2019 Feb 11. PMID: 30980503; PMCID: PMC6594046.

Bernstein H, Payne CM, Bernstein C et al (1999) Activation of the promoters of genes associated with DNA damage, oxidative stress, ER stress and protein malfolding by the bile salt, deoxycholate. Toxicol Lett 108:37–46

Bertani B, Ruiz N. Function and Biogenesis of Lipopolysaccharides. EcoSal Plus. 2018 Aug;8(1):10.1128/ecosalplus.ESP-0001-2018. doi: 10.1128/ecosalplus.ESP-0001-2018. PMID: 30066669; PMCID: PMC6091223.

Berth, S.H.; Lloyd, T.E. Disruption of Axonal Transport in Neurodegeneration. J. Clin. Investig. 2023, 133, e168554.

Besingi RN, Wenderska IB, Senadheera DB, Cvitkovitch DG, Long JR, Wen ZT, Brady LJ. Functional amyloids in Streptococcus mutans, their use as targets of biofilm inhibition and initial characterization of SMU_63c. Microbiology (Reading). 2017 Apr;163(4):488-501. doi: 10.1099/mic.0.000443. Epub 2017 Apr 26. PMID: 28141493; PMCID: PMC5775903.

Bhandari, S., Lee, J.N., Kim, Y.I., Nam, I.K., Kim, S.J., Kim, S.J., Kwak, S., Oh, G.S., Kim,H.J., Yoo, H.J., et al. (2016). The fatty acid chain elongase, Elovl1, is required for kidney and swim bladder development during zebrafish embryogenesis. Organogenesis 12, 78-93.

Birsoy, K., Wang, T., Chen, W. W., Freinkman, E., Abu-Remaileh, M., and Sabatini, D. M. (2015). An essential role of the mitochondrial electron transport chain in cell proliferation is to enable aspartate synthesis. Cell 162, 540–551. doi:10.1016/j.cell.2015. 07.016

Bizzozero, O.A., Zuniga, G., and Lees, M.B. (1991). Fatty acid composition of human myelin proteolipid protein in peroxisomal disorders. J. Neurochem. 56, 872-878.

Bleier, L., Wittig, I., Heide, H., Steger, M., Brandt, U., and Drose, S. (2015). Generator-specific targets of mitochondrial reactive oxygen species. Free Radic. Biol. Med. 78, 1–10. doi: 10.1016/j.freeradbiomed.2014.10.511

Bolger AM., Lohse M. Trimmomatic: a flexible trimmer for Illumina sequence data. Usadel B. 2014.Bioinformatics.Aug 1;30(15):2114-20. doi:10.1093/bioinformatics/btu170.

Bonawitz, N.D., Clayton, D.A., and Shadel, G.S. (2006). Initiation and beyond: multiple functions of the human mitochondrial transcription machinery. Mol. Cell 24, 813-825.

Bourassa MW, Alim I, Bultman SJ, Ratan RR. 2016. Butyrate, neuroepigenetics and the gut microbiome: can a high fiber diet improve brain health? Neuroscience Lett 625:56–63.

Boveris, A., Oshino, N., and Chance, B. (1972). The cellular production of hydrogen peroxide. Biochem. J. 128, 617-630.

Brand, M. D. (2016). Mitochondrial generation of superoxide and hydrogen peroxide as the source of mitochondrial redox signaling. Free Radic. Biol. Med. 100, 14–31. doi: 10.1016/j.freeradbiomed.2016.04.001

Braune A, Engst W, Blaut M (2015) Identification and functional expression of genes encoding flavonoid O-and C-glycosidases in intestinal bacteria. Environ Microbiol 18:2117–2129

Bray JR, Curtis JT. 1957. An ordination of the upland forest communities of southern Wisconsin. Ecol. Monogr. 27:325–49

Broer, S., and Broer, A. (2017). Amino acid homeostasis and signalling in mammalian cells and organisms at Portland Press Ltd. Biochem. J. 474, 1935–1963.

Brown AJ, Goldsworthy SM, Barnes AA, Eilert MM, Tcheang L, Daniels D, Muir AI, Wigglesworth MJ, Kinghorn I, Fraser NJ, Pike NB, Strum JC, Steplewski KM, Murdock PR, Holder JC, Marshall FH, Szekeres PG, Wilson S, Ignar DM, Foord SM, Wise A, Dowell SJ. The Orphan G protein-coupled receptors GPR41 and GPR43 are activated by propionate and other short chain carboxylic acids. J Biol Chem. 2003 Mar 28;278(13):11312-9. doi: 10.1074/jbc.M211609200. Epub 2002 Dec 19. PMID: 12496283.

Brown EM, Clardy J, Xavier RJ. Gut microbiome lipid metabolism and its impact on host physiology. Cell Host Microbe. 2023 Feb 8;31(2):173-186. doi: 10.1016/j.chom.2023.01.009. PMID: 36758518; PMCID: PMC10124142.

Browne HP, Forster SC, Anonye BO, Kumar N, Neville BA, Stares MD, Goulding D, Lawley TD. Culturing of 'unculturable' human microbiota reveals novel taxa and extensive sporulation. Nature. 2016 May 26;533(7604):543-546. doi: 10.1038/nature17645. Epub 2016 May 4. PMID: 27144353; PMCID: PMC4890681.

Brubaker SW, Bonham KS, Zanoni I, Kagan JC (2015) Innate immune pattern recognition: a cell biological perspective. Annu Rev Immunol 33: 257 – 290

Brudek T. Inflammatory Bowel Diseases and Parkinson's Disease. J Parkinsons Dis. 2019;9(s2):S331-S344. doi: 10.3233/JPD-191729. PMID: 31609699; PMCID: PMC6839501.

Brugman S, Ikeda-Ohtsubo W, Braber S, Folkerts G, Pieterse CMJ, Bakker PAHM. A Comparative Review on Microbiota Manipulation: Lessons From Fish, Plants, Livestock, and Human Research. Front Nutr. 2018 Sep 5;5:80. doi: 10.3389/fnut.2018.00080. PMID: 30234124; PMCID: PMC6134018.

Budka, H., Sluga, E., and Heiss, W.D. (1976). Spastic paraplegia associated with Addison's disease: adult variant of adreno-leukodystrophy. J. Neurol. 213, 237-250.

Burokas A, Arboleya S, Moloney RD, Peterson VL, Murphy K, Clarke G, Stanton C, Dinan TG, Cryan JF. 2017. Targeting the microbiota-gut-brain axis: prebiotics have anxiolytic and antidepressant-like effects and reverse the impact of chronic stress in mice. Biol Psychiatry 82:472–487. https://doi.org/10.1016/j.biopsych.2016.12.031.

Burrage LC, Nagamani SC, Campeau PM, Lee BH. Branched-chain amino acid metabolism: from rare Mendelian diseases to more common disorders. Hum Mol Genet. 2014 Sep.15;23(R1):R1-8. doi: 10.1093/hmg/ddu123. Epub 2014 Mar 20. PMID: 24651065; PMCID: PMC4170715.

Bustamante-Barrientos FA, Luque-Campos N, Araya MJ, Lara-Barba E, de Solminihac J, Pradenas C, Molina L, Herrera-Luna Y, Utreras-Mendoza Y, Elizondo-Vega R, Vega-Letter AM, Luz-Crawford P. Mitochondrial dysfunction in neurodegenerative disorders: Potential therapeutic application of mitochondrial transfer to central nervous system-residing cells. J Transl Med. 2023 Sep 9;21(1):613. doi: 10.1186/s12967-023-04493-w. PMID: 37689642; PMCID: PMC10493034.

Caballero S, Pamer EG. Microbiota-mediated inflammation and antimicrobial defense in the intestine. Annu Rev Immunol. 2015;33:227-56. doi: 10.1146/annurev-immunol-032713-120238. Epub 2015 Jan 2. PMID: 25581310; PMCID: PMC4540477.

Cablé S, Kedinger M, Dauça M. Peroxisomes and peroxisomal enzymes along the crypt-villus axis of the rat intestine. Differentiation. 1993 Sep;54(2):99-108. doi: 10.1111/j.1432-0436.1993.tb00712.x. PMID: 8243894.

Calì, T.; Ottolini, D.; Brini, M. Calcium and Endoplasmic Reticulum-Mitochondria Tethering in Neurodegeneration. DNA Cell Biol. 2013, 32, 140–146.

Cambron, M., D'Haeseleer, M., Laureys, G., Clinckers, R., Debruyne, J., and De Keyser, J. (2012). White-matter astrocytes, axonal energy metabolism, and axonal degeneration in multiple sclerosis. J. Cereb. Blood Flow Metab. 32, 413-424.

Cappa M, Todisco T, Bizzarri C. X-linked adrenoleukodystrophy and primary adrenal insufficiency. Front Endocrinol (Lausanne). 2023 Nov 16;14:1309053. doi: 10.3389/fendo.2023.1309053. PMID: 38034003; PMCID: PMC10687143.

Cardaci, S., Zheng, L., MacKay, G., Broek, N. J. F., MacKenzie, E. D., Nixon, C., et al. (2015). Pyruvate carboxylation enables growth of SDH-deficient cells by supporting aspartate biosynthesis. Nat. Cell Biol. 17, 1317–1326. doi:10.1038/ncb3233

Cartier, N., Hacein-Bey-Abina, S., Bartholomae, C.C., Veres, G., Schmidt, M., Kutschera, I., Vidaud, M., Abel, U., Dal-Cortivo, L., Caccavelli, L., et al. (2009). Hematopoietic stem cell gene therapy with a lentiviral vector in X-linked adrenoleukodystrophy. Science 326, 818-823.

Cartier N, Hacein-Bey-Abina S, Bartholomae CC, Bougnères P, Schmidt M, Kalle CV, Fischer A, Cavazzana-Calvo M, Aubourg P. Lentiviral hematopoietic cell gene therapy for X-linked adrenoleukodystrophy. Methods Enzymol. 2012;507:187-98. doi: 10.1016/B978-0-12-386509-0.00010-7. PMID: 22365775.

Caruso G, Caraci F, Jolivet RB. Pivotal role of carnosine in the modulation of brain cells activity: Multimodal mechanism of action and therapeutic potential in neurodegenerative disorders. Prog Neurobiol. 2019 Apr;175:35-53. doi: 10.1016/j.pneurobio.2018.12.004. Epub 2018 Dec 26. PMID: 30593839.

Casanova A, Wevers A, Navarro-Ledesma S, Pruimboom L. Mitochondria: It is all about energy. Front Physiol. 2023 Apr 25;14:1114231. doi: 10.3389/fphys.2023.1114231. PMID: 37179826; PMCID: PMC10167337.

Casasnovas C, Ruiz M, Schlüter A, Naudí A, Fourcade S, Veciana M, Castañer S, Albertí A, Bargalló N, Johnson M, Raymond GV, Fatemi A, Moser AB, Villarroya F, Portero-Otín M, Artuch R, Pamplona R, Pujol A. Biomarker Identification, Safety, and Efficacy of High-Dose Antioxidants for Adrenomyeloneuropathy: a Phase II Pilot Study. Neurotherapeutics. 2019 Oct;16(4):1167-1182. doi: 10.1007/s13311-019-00735-2. PMID: 31077039; PMCID: PMC6985062.

Cattaneo A, Cattane N, Galluzzi S, Provasi S, Lopizzo N, Festari C, Ferrari C, Guerra UP, Paghera B, Muscio C, Bianchetti A, Volta GD, Turla M, Cotelli MS, Gennuso M, Prelle A, Zanetti O, Lussignoli G, Mirabile D, Bellandi D, Gentile S, Belotti G, Villani D, Harach T, Bolmont T, Padovani A, Boccardi M, Frisoni GB. 2017. Association of brain amyloidosis with proinflammatory gut bacterial taxa and peripheral inflammation markers in cognitively impaired elderly. Neurobiol Aging 49:60–68. https://doi .org/10.1016/j.neurobiolaging.2016.08.019

Cava, F., de Pedro, M. A., Lam, H., Davis, B. M., and Waldor, M. K. (2011). Distinct pathways for modification of the bacterial cell wall by non-canonical D-amino acids. EMBO J. 30, 3442–3453. doi: 10.1038/emboj.2011.246

Cekanaviciute E, Yoo BB, Runia TF, Debelius JW, Singh S, Nelson CA, Kanner R, Bencosme Y, Lee YK, Hauser SL, Crabtree-Hartman E, Sand IK, Gacias M, Zhu Y, Casaccia P, Cree BAC, Knight R, Mazmanian SK, Baranzini SE. 2017. Gut bacteria from multiple sclerosis patients modulate human T cells and exacerbate symptoms in mouse models. Proc Natl Acad Sci U S A 114: 10713–10718.

Cénit MC, Matzaraki V, Tigchelaar EF, Zhernakova A. Rapidly expanding knowledge on the role of the gut microbiome in health and disease. Biochim Biophys Acta. 2014 Oct;1842(10):1981-1992. doi: 10.1016/j.bbadis.2014.05.023. Epub 2014 Jun 2. PMID: 24882755.

Chakaroun, R.M., Massier, L., and Kovacs, P. (2020). Gut Microbiome, Intestinal Permeability, and Tissue Bacteria in Metabolic Disease: Perpetrators or Bystanders? Nutrients 12, 1082. https://doi.org/10.3390/NU12041082.

Chakrabarti A, Geurts L, Hoyles L, Iozzo P, Kraneveld AD, La Fata G, Miani M, Patterson E, Pot B, Shortt C, Vauzour D. The microbiota-gut-brain axis: pathways to better brain health. Perspectives on what we know, what we need to investigate and how to put knowledge into practice. Cell Mol Life Sci. 2022 Jan 19;79(2):80. doi: 10.1007/s00018-021-04060-w. PMID: 35044528; PMCID: PMC8770392

Chan, D.C. Fusion and Fission: Interlinked Processes Critical for Mitochondrial Health. Annu. Rev. Genet. 2012, 46, 265–287.

Chassard, C., & Lacroix, C. (2013). Carbohydrates and the human gut microbiota. Current Opinion in Clinical Nutrition and Metabolic Care, 16(4), 453–460.

Chaturvedi, R. K., and Flint Beal, M. (2013). Mitochondrial diseases of the brain. Free Radic. Biol. Med. 63, 1–29. doi: 10.1016/j.freeradbiomed.2013.03.018

Chatterjee A, Mambo E, Sidransky D (2006) Mitochondrial DNA mutations in human cancer. Oncogene 25: 4663 – 4674

Chen CK, Wu YT, Chang YC. Association between chronic periodontitis and the risk of Alzheimer's disease: a retrospective, population-based, matched-cohort study. Alzheimers Res Ther. 2017 Aug 8;9(1):56. doi: 10.1186/s13195-017-0282-6. PMID: 28784164; PMCID: PMC5547465.

Chen L, Zhernakova DV, Kurilshikov A, Andreu-Sánchez S, Wang D, Augustijn HE, Vich Vila A; Lifelines Cohort Study; Weersma RK, Medema MH, Netea MG, Kuipers F, Wijmenga C, Zhernakova A, Fu J. Influence of the microbiome, diet and genetics on inter-individual variation in the human plasma metabolome. Nat Med. 2022 Nov;28(11):2333-2343. doi: 10.1038/s41591-022-02014-8. Epub 2022 Oct 10. PMID: 36216932; PMCID: PMC9671809.

Chen W, Zhao H, Li Y. Mitochondrial dynamics in health and disease: mechanisms and potential targets. Signal Transduct Target Ther. 2023 Sep 6;8(1):333. doi: 10.1038/s41392-023-01547-9. PMID: 37669960; PMCID: PMC10480456.

Cheng L-H, Liu Y-W, Wu C-C, Wang S, Tsai Y-C. 2019. Psychobiotics in mental health, neurodegenerative and neurodevelopmental disorders. J Food Drug Anal 27:632–648.

Cheng YW, Fischer M. Fecal Microbiota Transplantation. Clin Colon Rectal Surg. 2023 Jan 25;36(2):151-156. doi: 10.1055/s-0043-1760865. PMID: 36844708; PMCID: PMC9946715.

Chiang, P. K., Gordon, R. K., Tal, J., Zeng, G. C., Doctor, B. P., Pardhasaradhi, K., et al. (1996). S-Adenosylmethionine and methylation. FASEB J. Off. Publ. Fed. Am. Soc. Exp. Biol. 10, 471–480.

Cho, H., Wivagg, C. N., Kapoor, M., Barry, Z.P, Rohs, D. A., Suh, J. A., et al. (2016). Bacterial cell wall biogenesis is mediated by SEDS and PBP polymerase families functioning semi-autonomously. Nat. Microbiol. 1:16172. doi: 10.1038/nmicrobiol.2016.172

Chong, Jasmine, and Jianguo Xia. "MetaboAnalystR: an R package for flexible and reproducible analysis of metabolomics data." Bioinformatics 34.24 (2018): 4313-4314.

Chouchani, E. T., Pell, V. R., Gaude, E., Aksentijevic, D., Sundier, S. Y., Robb, E. L., et al. (2014). Ischaemic accumulation of succinate controls reperfusion injury through mitochondrial ROS. Nature 515, 431–435. doi: 10.1038/nature13909

Clare CE, Brassington AH, Kwong WY, Sinclair KD. One-Carbon Metabolism: Linking Nutritional Biochemistry to Epigenetic Programming of Long-Term Development. Annu Rev Anim Biosci. 2019 Feb 15;7:263-287. doi: 10.1146/annurev-animal-020518-115206. Epub 2018 Nov 9. PMID: 30412672.

Clarke, E.L., Taylor, L.J., Zhao, C. et al. Sunbeam: an extensible pipeline for analyzing metagenomic sequencing experiments. Microbiome7, 46 (2019) doi:10.1186/s40168-019-0658-x. https://github.com/eclarke/komplexity.

Clifton LA, Skoda MWA, Daulton EL, Hughes AV, le Brun AP, Lakey JH, Holt SA (2013) Asymmetric phospholipid: lipopolysaccharide bilayers; a gram-negative bacterial outer membrane mimic. J R Soc Interface 10:20130810.

Cobley JN, Fiorello ML, Bailey DM. 13 reasons why the brain is susceptible to oxidative stress. Redox Biol. (2018) 15:490–503. doi: 10.1016/j.redox.2018. 01.008

Cockburn, D. W., & Koropatkin, N. M. (2016). Polysaccharide degradation by the intestinal microbiota and its influence on human health and disease. Journal of Molecular Biology, 428(16), 3230–3252.

Coelho D., Kim J.C., Miousse I.R., Fung S., du Moulin M., Buers I., Suormala T., Burda P., Frapolli M., Stucki M., et al. Mutations in ABCD4 cause a new inborn error of vitamin B12 metabolism. Nat. Genet. 2012;44:1152–1155. doi: 10.1038/ng.2386.

Collins LV, Hajizadeh S, Holme E, Jonsson I-M, Tarkowski A (2004) Endogenously oxidized mitochondrial DNA induces in vivo and in vitro inflammatory responses. J Leukoc Biol 75: 995 – 1000

Conte M, Giuliani C, Chiariello A, Iannuzzi V, Franceschi C, Salvioli S. GDF15, an emerging key player in human aging. Ageing Res Rev. 2022 Mar;75:101569. doi: 10.1016/j.arr.2022.101569. Epub 2022 Jan 19. PMID: 35051643.

Cooper GM. The cell: a molecular approach. Sunderland: ASM Press; Sinauer Associates; 2000.

Coppa, A., Guha, S., Fourcade, S., Parameswaran, J., Ruiz, M., Moser, A.B., Schlüter, A., Murphy, M.P., Lizcano, J.M., Miranda-Vizuete, A., et al. (2020). The peroxisomal fatty acid transporter ABCD1/PMP-4 is required in the C. elegans hypodermis for axonal maintenance: A worm model for adrenoleukodystrophy. Free Radic. Biol. Med. 152, 797-809.

Coppedè F, Stoccoro A. Mitoepigenetics and Neurodegenerative Diseases. Front Endocrinol (Lausanne). 2019 Feb 19;10:86. doi: 10.3389/fendo.2019.00086. PMID: 30837953; PMCID: PMC6389613.

Crommen, S., and Simon, M.C. (2017). Microbial regulation of glucose metabolism and insulin resistance. Genes (Basel) 9, 10. https://doi.org/ 10.3390/genes9010010.

Cross, C.E., Halliwell, B., Borish, E.T., Pryor, W.A., Ames, B.N., Saul, R.L., McCord, J.M., and Harman, D. (1987). Oxygen radicals and human disease. Ann. Intern. Med. 107, 526-545.

Cryan JF, Dinan TG. 2012. Mind-altering microorganisms: the impact of the gut microbiota on brain and behaviour. Nat Rev Neurosci 13:701–712.

Cryan JF, O'Riordan KJ, Cowan CSM, Sandhu KV, Bastiaanssen TFS, Boehme M, Codagnone MG, Cussotto S, Fulling C, Golubeva AV, Guzzetta KE, Jaggar M, Long-Smith CM, Lyte JM, Martin JA, Molinero-Perez A, Moloney G, Morelli E, Morillas E, O'Connor R, Cruz-Pereira JS, Peterson VL, Rea K, Ritz NL, Sherwin E, Spichak S, Teichman EM, van de Wouw M, Ventura-Silva AP, Wallace-Fitzsimons SE, Hyland N, Clarke G, Dinan TG. The Microbiota-Gut-Brain Axis. Physiol Rev. 2019 Oct 1;99(4):1877-2013. doi: 10.1152/physrev.00018.2018. PMID: 31460832.

Cullender TC, Chassaing B, Janzon A, Kumar K, Muller CE, Werner JJ, Angenent LT, Bell ME, Hay AG, Peterson DA, Walter J, Vijay-Kumar M, Gewirtz AT, Ley RE. Innate and adaptive immunity interact to quench microbiome flagellar motility in the gut. Cell Host Microbe. 2013 Nov 13;14(5):571-81. doi: 10.1016/j.chom.2013.10.009. PMID: 24237702; PMCID: PMC3920589.

Cummings JH, Macfarlane GT (1991) The control and consequences of bacterial fermentation in the human colon. J Appl Bacteriol 70:443–459

D'Argenio V, Salvatore F. The role of the gut microbiome in the healthy adult status. Clin Chim Acta. 2015 Dec 7;451(Pt A):97-102. doi: 10.1016/j.cca.2015.01.003. Epub 2015 Jan 10. PMID: 25584460.

Dai Z-L, Zhang J, Wu G, Zhu W-Y (2010) Utilization of amino acids by bacteria from the pig small intestine. Amino Acids 39:1201–1215

Dai Z-L, Li XL, Xi PB, Zhang J, Wu G, Zhu WY. L-Glutamine regulates amino acid utilization by intestinal bacteria. Amino Acids. 2013 Sep;45(3):501-12. doi: 10.1007/s00726-012-1264-4. Epub 2012 Mar 24. PMID: 22451274.

Daneman R, Prat A. 2015. The blood-brain barrier. Cold Spring Harb Perspect Biol 7:a020412. https://doi.org/10.1101/cshperspect.a020412.

Danneskiold-Samsøe NB, Dias de Freitas Queiroz Barros H, Santos R, Bicas JL, Cazarin CBB, Madsen L, Kristiansen K, Pastore GM, Brix S, Maróstica Júnior MR. Interplay between food and gut microbiota in health and disease. Food Res Int. 2019 Jan;115:23-31. doi: 10.1016/j.foodres.2018.07.043. Epub 2018 Jul 30. PMID: 30599936.

Das TK, Blasco-Conesa MP, Korf J, Honarpisheh P, Chapman MR, Ganesh BP. Bacterial Amyloid Curli Associated Gut Epithelial Neuroendocrine Activation Predominantly Observed in Alzheimer's Disease Mice with Central Amyloid-β Pathology. J Alzheimers Dis. 2022;88(1):191-205. doi: 10.3233/JAD-220106. PMID: 35527554; PMCID: PMC9583710.

Dash PK, Hergenroeder GW, Jeter CB, Choi HA, Kobori N, Moore AN. Traumatic Brain Injury Alters Methionine Metabolism: Implications for Pathophysiology. Front Syst Neurosci. 2016 Apr 29;10:36. doi: 10.3389/fnsys.2016.00036. PMID: 27199685; PMCID: PMC4850826.

David LA, Maurice CF, Carmody RN, Gootenberg DB, Button JE, Wolfe BE, Ling AV, Devlin AS, Varma Y, Fischbach MA, Biddinger SB, Dutton RJ, Turnbaugh PJ. Diet rapidly and reproducibly alters the human gut microbiome. Nature. 2014 Jan 23;505(7484):559-63. doi: 10.1038/nature12820. Epub 2013 Dec 11. PMID: 24336217; PMCID: PMC3957428.

Davila AM, Blachier F, Gotteland M, Andriamihaja M, Benetti PH, Sanz Y, Tomé D. Intestinal luminal nitrogen metabolism: role of the gut microbiota and consequences for the host. Pharmacol Res. 2013 Feb;68(1):95-107. doi: 10.1016/j.phrs.2012.11.005. Epub 2012 Nov 24. PMID: 23183532.

De Biase I, Tortorelli S, Kratz L, J Steinberg S, Cusmano-Ozog K, Braverman N; ACMG Laboratory Quality Assurance Committee. Laboratory diagnosis of disorders of peroxisomal biogenesis and function: a technical standard of the American College of Medical Genetics and Genomics (ACMG). Genet Med. 2020 Apr;22(4):686-697. doi: 10.1038/s41436-019-0713-9. Epub 2019 Dec 11. PMID: 31822849.

De Duve C, Baudhuin P. Peroxisomes (microbodies and related particles). Physiol Rev. 1966 Apr;46(2):323-57. doi: 10.1152/physrev.1966.46.2.323. PMID: 5325972.

Deon, M., Sitta, A., Barschak, A.G., Coelho, D.M., Pigatto, M., Schmitt, G.O., Jardim, L.B., Giugliani, R., Wajner, M., and Vargas, C.R. (2007). Induction of lipid peroxidation and decrease of antioxidant defenses in symptomatic and asymptomatic patients with X-linked adrenoleukodystrophy. Int. J. Dev. Neurosci. 25, 441-444.

Deon, M., Sitta, A., Barschak, A.G., Coelho, D.M., Terroso, T., Schmitt, G.O., Wanderley, H.Y., Jardim, L.B., Giugliani, R., Wajner, M., et al. (2008). Oxidative stress is induced in female carriers of X-linked adrenoleukodystrophy. J. Neurol. Sci. 266, 79-83.

Depreter M, Espeel M, Roels F. Human peroxisomal disorders. Microsc Res Tech 61: 203–223, 2003. doi:10.1002/jemt.10330

Desbonnet L, Garrett L, Clarke G, Kiely B, Cryan JF, Dinan TG. 2010. Effects of the probiotic Bifidobacterium infantis in the maternal separation model of depression. Neuroscience 170:1179–1188. https://doi.org/10 .1016/j.neuroscience.2010.08.005.

Deshmukh, H. S., Liu, Y., Menkiti, O. R., Mei, J., Dai, N., O'Leary, C. E., et al. (2014). The microbiota regulates neutrophil homeostasis and host resistance to Escherichia coli K1 sepsis in neonatal mice. Nat. Med. 20, 524–530. doi: 10.1038/nm.3542

De Vadder F, Kovatcheva-Datchary P, Goncalves D, Vinera J, Zitoun C, Duchampt A, Bäckhed F, Mithieux G. Microbiota-generated metabolites promote metabolic benefits via gut-brain neural circuits. Cell. 2014 Jan 16;156(1-2):84-96. doi: 10.1016/j.cell.2013.12.016. Epub 2014 Jan 9. PMID: 24412651.

De Vadder F, Grasset E, Mannerås Holm L, Karsenty G, Macpherson AJ, Olofsson LE, Bäckhed F. Gut microbiota regulates maturation of the adult enteric nervous system via enteric serotonin networks. Proc Natl Acad Sci U S A. 2018 Jun 19;115(25):6458-6463. doi: 10.1073/pnas.1720017115. Epub 2018 Jun 4. PMID: 29866843; PMCID: PMC6016808.

de Vos WM, Tilg H, Van Hul M, Cani PD. Gut microbiome and health: mechanistic insights. Gut. 2022 May;71(5):1020-1032. doi: 10.1136/gutjnl-2021-326789. Epub 2022 Feb 1. PMID: 35105664; PMCID: PMC8995832.

Dias ML, O'Connor KM, Dempsey EM, O'Halloran KD, McDonald FB. Targeting the Toll-like receptor pathway as a therapeutic strategy for neonatal infection. Am J Physiol Regul Integr Comp Physiol. 2021 Dec 1;321(6):R879-R902. doi: 10.1152/ajpregu.00307.2020. Epub 2021 Oct 6. PMID: 34612068.

Di Biase, A., Salvati, S., VarÃ, R., Avellino, C., Sforza, F., Cappa, M., and Masella, R. (2000). Susceptibility to oxidation of plasma low-density lipoprotein in X-linked adrenoleukodystrophy: effects of simvastatin treatment. Mol. Genet. Metab. 71, 651-655.

Di Cara F, Bülow MH, Simmonds AJ, Rachubinski RA. Dysfunctional peroxisomes compromise gut structure and host defense by increased cell death and Tor-dependent autophagy. Mol Biol Cell. 2018 Nov 1;29(22):2766-2783. doi: 10.1091/mbc.E18-07-0434. Epub 2018 Sep 6. PMID: 30188767; PMCID: PMC6249834.

Di Cara F, Andreoletti P, Trompier D, Vejux A, Bulow MH, Sellin J,Lizard G, Cherkaoui-Malki M, Savary S. Peroxisomes in immuneresponse and inflammation.IntJMolSci20: 3877, 2019.doi:10.3390/ijms20163877.

Dimauro, I., Paronetto, M. P., and Caporossi, D. (2020). Exercise, redox homeostasis and the epigenetic landscape. Redox Biol. 35:101477. doi: 10.1016/ j.redox.2020.101477

Dimou A, Tsimihodimos V, Bairaktari E. The Critical Role of the Branched Chain Amino Acids (BCAAs) Catabolism-Regulating Enzymes, Branched-Chain Aminotransferase (BCAT) and Branched-Chain α-Keto Acid Dehydrogenase (BCKD), in Human Pathophysiology. Int J Mol Sci. 2022 Apr 5;23(7):4022. doi: 10.3390/ijms23074022. PMID: 35409380; PMCID: PMC8999875.

Dinan TG, Quigley EM, Ahmed SM, Scully P, O'Brien S, O'Mahony L, O'Mahony S, Shanahan F, Keeling PW. Hypothalamic-pituitary-gut axis dysregulation in irritable bowel syndrome: plasma cytokines as a potential biomarker? Gastroenterology. 2006 Feb;130(2):304-11. doi: 10.1053/j.gastro.2005.11.033. PMID: 16472586.

Dinan TG, Cryan JF. 2017. Brain-gut-microbiota axis and mental health. Psychosom Med 79:920–926.

Dodd, D., Spitzer, M., Van Treuren, W. et al. A gut bacterial pathway metabolizes aromatic amino acids into nine circulating metabolites. Nature 551, 648–652 (2017).

Dörr T, Moynihan PJ, Mayer C. Editorial: Bacterial Cell Wall Structure and Dynamics. Front Microbiol. 2019 Sep 4;10:2051. doi: 10.3389/fmicb.2019.02051. PMID: 31551985; PMCID: PMC6737391.

Draper K, Ley C, Parsonnet J. 2017. Probiotic guidelines and physician practice: a cross-sectional survey and overview of the literature. Benef Microbes 8:507–519. https://doi.org/10.3920/BM2016.0146

Droge, W. (2002). Free radicals in the physiological control of cell function. Physiol. Rev. 82, 47–95. doi: 10.1152/physrev.00018.2001

Duda-Chodak A, Tarko T, Satora P, Sroka P (2015) Interaction of dietary compounds, especially polyphenols, with the intestinal microbiota: a review. Eur J Nutr 54:325–341

Duerkop BA, Vaishnava S, Hooper LV. Immune responses to the microbiota at the intestinal mucosal surface. Immunity. 2009 Sep 18;31(3):368-76. doi: 10.1016/j.immuni.2009.08.009. PMID: 19766080.

Du G, Xiong L, Li X, Zhuo Z, Zhuang X, Yu Z, Wu L, Xiao D, Liu Z, Jie M, Liu X, Luo G, Guo Z, Chen H. Peroxisome Elevation Induces Stem Cell Differentiation and Intestinal Epithelial Repair. Dev Cell. 2020 Apr 20;53(2):169-184.e11. doi: 10.1016/j.devcel.2020.03.002. Epub 2020 Apr 2. PMID: 32243783.

Ducker GS, Rabinowitz JD. One-Carbon Metabolism in Health and Disease. Cell Metab. 2017 Jan 10;25(1):27-42. doi: 10.1016/j.cmet.2016.08.009. Epub 2016 Sep 15. PMID: 27641100; PMCID: PMC5353360.

Durieux J, Wolff S, Dillin A. The cell-non-autonomous nature of electron transport chain-mediated longevity. Cell. 2011 Jan 7;144(1):79-91. doi: 10.1016/j.cell.2010.12.016. PMID: 21215371; PMCID: PMC3062502.

Eckburg PB, Bik EM, Bernstein CN, Purdom E, Dethlefsen L, Sargent M et al (2005) Diversity of the human intestinal microbial flora. Science 308(5728):1635–1638. https://doi. org/10.1126/science.1110591

El Aidy S, van den Bogert B, Kleerebezem M (2015) The small intestine microbiota, nutritional modulation and relevance for health. Curr Opin Biotechnol 32:14–20. https://doi.org/10.1016/j. copbio.2014.09.005

El Bejjani, R., and Hammarlund, M. (2012). Neural regeneration in Caenorhabditis elegans. Annu. Rev. Genet. 46, 499-513.

El-Husseini AE-D, Schnell E, Chetkovich DM, Nicoll RA, Bredt DS. 2000. PSD-95 involvement in maturation of excitatory synapses. Science 290: 1364–1368. https://doi.org/10.1126/science.290.5495.1364.

Eloranta JJ, Kullak-Ublick GA (2008) The role of FXR in disorders of bile acid homeostasis. Physiology 23:286–295

Emani R, Alam C, Pekkala S, Zafar S, Emani M, Hänninen A. 2015. Peritoneal cavity is a route for gut-derived microbial signals to promote autoimmunity in non-obese diabetic mice. Scand J Immunol 81:102–109.

ENCODE Project Consortium;Identification and analysis of functional elements in 1% of the human genome by the ENCODE pilot project. Nature. 2007 Jun 14;447(7146):799-816. doi: 10.1038/nature05874. PMID: 17571346; PMCID: PMC2212820.

Engelen M, Kemp S, de Visser M, van Geel BM, Wanders RJ, Aubourg P, Poll-The BT. X-linked adrenoleukodystrophy (X-ALD): clinical presentation and guidelines for diagnosis, follow-up and management. Orphanet J Rare Dis. 2012 Aug 13;7:51. doi: 10.1186/1750-1172-7-51. PMID: 22889154; PMCID: PMC3503704

Engelen M, Kemp S, Poll-The BT. X-linked adrenoleukodystrophy: pathogenesis and treatment. Curr Neurol Neurosci Rep. 2014 Oct;14(10):486. doi: 10.1007/s11910-014-0486-0. PMID: 25115486.

Engelen M, van Ballegoij WJC, Mallack EJ, Van Haren KP, Köhler W, Salsano E, van Trotsenburg ASP, Mochel F, Sevin C, Regelmann MO, Tritos NA, Halper A, Lachmann RH, Davison J, Raymond GV, Lund TC, Orchard PJ, Kuehl JS, Lindemans CA, Caruso P, Turk BR, Moser AB, Vaz FM, Ferdinandusse S, Kemp S, Fatemi A, Eichler FS, Huffnagel IC. International Recommendations for the Diagnosis and Management of Patients With Adrenoleukodystrophy: A Consensus-Based Approach. Neurology. 2022 Nov 22;99(21):940-951. doi: 10.1212/WNL.0000000000201374. Epub 2022 Sep 29. PMID: 36175155; PMCID: PMC9687408.

Ericsson AC, Franklin CL. Manipulating the Gut Microbiota: Methods and Challenges. ILAR J. 2015;56(2):205-17. doi: 10.1093/ilar/ilv021. PMID: 26323630; PMCID: PMC4554251.

Erny D, Hrabé de Angelis AL, Jaitin D, Wieghofer P, Staszewski O, David E, Keren-Shaul H, Mahlakoiv T, Jakobshagen K, Buch T, Schwierzeck V, Utermöhlen O, Chun E, Garrett WS, McCoy KD, Diefenbach A, Staeheli P, Stecher B, Amit I, Prinz M. 2015. Host microbiota constantly control maturation and function of microglia in the CNS. Nat Neurosci 18:965–977.

Evans JM, Morris LS, Marchesi JR. The gut microbiome: the role of a virtual organ in the endocrinology of the host. J Endocrinol. 2013 Aug 28;218(3):R37-47. doi: 10.1530/JOE-13-0131. PMID: 23833275.

Everard A., C. Belzer, L. Geurts, J.P. Ouwerkerk, C. Druart, L.B. Bindels, P.D. Cani. Cross-talk between Akkermansia muciniphila and intestinal epithelium controls diet-induced obesity Proceedings of the National Academy of Sciences of the United States of America, 110 (22) (2013), pp. 9066-9071

Fan L, Wu D, Goremykin V, Xiao J, Xu Y, Garg S, Zhang C, Martin WF, Zhu R. Phylogenetic analyses with systematic taxon sampling show that mitochondria branch within Alphaproteobacteria. Nat Ecol Evol. 2020 Sep;4(9):1213-1219. doi: 10.1038/s41559-020-1239-x. Epub 2020 Jul 13. PMID: 32661403.

Fan Y, Pedersen O. Gut microbiota in human metabolic health and disease. Nat Rev Microbiol. 2021 Jan;19(1):55-71. doi: 10.1038/s41579-020-0433-9. Epub 2020 Sep 4. PMID: 32887946.

Fanconi, A., Prader, A., Isler, W., Luethy, F., and Siebenmann, R. (1963). Addison's Disease With Cerebral Sclerosis in Childhood. A Hereditary Syndrome Transmitted Through Chromosome X? Helv. Paediatr. Acta 18, 480-501.

Farhana A, Khan YS. Biochemistry, Lipopolysaccharide. [Updated 2023 Apr 17]. In: StatPearls [Internet]. Treasure Island (FL): StatPearls Publishing; 2024 Jan-. Available from: https://www.ncbi.nlm.nih.gov/books/NBK554414/

Farmer, A. D. & Aziz, Q. Mechanisms and management of functional abdominal pain. J. R. Soc. Med. 107, 347–354 (2014).

Feng W, Liu J, Cheng H, Zhang D, Tan Y, Peng C. Dietary compounds in modulation of gut microbiota-derived metabolites. Front Nutr. 2022 Jul 19;9:939571. doi: 10.3389/fnut.2022.939571. PMID: 35928846; PMCID: PMC9343712.

Ferdinandusse S., Jimenez-Sanchez G., Koster J., Denis S., Van Roermund C.W., Silva-Zolezzi I., Moser A.B., Visser W.F., Gulluoglu M., Durmaz O., et al. A novel bile acid biosynthesis defect due to a deficiency of peroxisomal ABCD3. Hum. Mol. Genet. 2015;24:361–370. doi: 10.1093/hmg/ddu448.

Ferrer, I., Kapfhammer, J.P., Hindelang, C., Kemp, S., Troffer-Charlier, N., Broccoli, V., Callyzot, N., Mooyer, P., Selhorst, J., Vreken, P., et al. (2005). Inactivation of the peroxisomal ABCD2 transporter in the mouse leads to late-onset ataxia involving mitochondria, Golgi and endoplasmic reticulum damage. Hum. Mol. Genet. 14, 3565-3577.

Ferrer I, Aubourg P, Pujol A. General aspects and neuropathology of X-linked adrenoleukodystrophy. Brain Pathol. 2010 Jul;20(4):817-30. doi: 10.1111/j.1750-3639.2010.00390.x. PMID: 20626743; PMCID: PMC8094714.

Fleming, T. J., Wallsmith, D. E., and Rosenthal, R. S. (1986). Arthropathic properties of gonococcal peptidoglycan fragments: implications for the pathogenesis of disseminated gonococcal disease. Infect. Immun. 52, 600–608.

Fontaine, C. A., Skorupski, A. M., Vowles, C. J., Anderson, N. E., Poe, S. A., and Eaton, K. A. (2015). How free of germs is germ-free? Detection of bacterial contamination in a germ free mouse unit. Gut Microbes 6, 225–233. doi: 10.1080/19490976.2015.1054596

Forss-Petter, S., Werner, H., Berger, J., Lassmann, H., Molzer, B., Schwab, M.H., Bernheimer, H., Zimmermann, F., and Nave, K.A. (1997). Targeted inactivation of the X-linked adrenoleukodystrophy gene in mice. J.Neurosci.Res. 50, 829-843.

Fouquet F, Zhou JM, Ralston E, Murray K, Troalen F, Magal E, Robain O, Dubois-Dalcq M, Aubourg P. Expression of the adrenoleukodystrophy protein in the human and mouse central nervous system. Neurobiol Dis. 1997;3(4):271-85. doi: 10.1006/nbdi.1997.0127. PMID: 9173925.

Fourcade, S., Lopez-Erauskin, J., Galino, J., Duval, C., Naudi, A., Jove, M., Kemp, S., Villarroya, F., Ferrer, I., Pamplona, R., et al. (2008). Early oxidative damage underlying neurodegeneration in X-adrenoleukodystrophy. Hum. Mol. Genet. 17, 1762-1773.

Fourcade, S., Ruiz, M., Guilera, C., Hahnen, E., Brichta, L., Naudi, A., Portero-Otin, M., Dacremont, G., Cartier, N., Wanders, R., et al. (2010). Valproic acid induces antioxidant effects in X-linked adrenoleukodystrophy. Hum. Mol. Genet. 19, 2005-2014.

Fourcade, S., Goicoechea, L., Parameswaran, J., Schlüter, A., Launay, N., Ruiz, M., Seyer, A., Colsch, B., Calingasan, N.Y., Ferrer, I., et al. (2020). High-dose biotin restores redox balance, energy and lipid homeostasis, and axonal health in a model of adrenoleukodystrophy. Brain Pathol. 30, 945-963.

Fox TD. Mitochondrial protein synthesis, import, and assembly. Genetics. 2012 Dec;192(4):1203-34. doi: 10.1534/genetics.112.141267. PMID: 23212899; PMCID: PMC3512135.

Frank-Cannon, T.C.; Alto, L.T.; McAlpine, F.E.; Tansey, M.G. Does Neuroinflammation Fan the Flame in Neurodegenerative Diseases? Mol. Neurodegener. 2009, 4, 47.

Fràter-Schröder M, Lässer U, Kierat L. Transcobalamin II dynamics in a plasma turnover study of patients with lupus erythematosus. Preliminary report. Schweiz Med Wochenschr. (1983) 113:1476–7.

Freudenberg A, K.J. Petzke, S. Klaus Comparison of high-protein diets and leucine supplementation in the prevention of metabolic syndrome and related disorders in mice Journal of Nutritional Biochemistry, 23 (11) (2012), pp. 1524-1530

Freudenberg A, K.J. Petzke, S. Klaus Dietary L-leucine and L-alanine supplementation have similar acute effects in the prevention of high-fat diet-induced obesity Amino Acids, 44 (2) (2013), pp. 519-528

Frick PG, Riedler G, Brögli H (1967) Dose response and minimal daily requirement for vitamin K in man. J Appl Physiol 23:387–389

Friedland RP, Chapman MR. The role of microbial amyloid in neurodegeneration. PLoS Pathog. 2017 Dec 21;13(12):e1006654. doi: 10.1371/journal.ppat.1006654. PMID: 29267402; PMCID: PMC5739464.

Friedman, J. R., and Nunnari, J. (2014). Mitochondrial form and function. Nature 505, 335–343. doi: 10.1038/nature12985

Frost G, Sleeth ML, Sahuri-Arisoylu M, Lizarbe B, Cerdan S, Brody L, Anastasovska J, Ghourab S, Hankir M, Zhang S, Carling D, Swann JR, Gibson G, Viardot A, Morrison D, Louise Thomas E, Bell JD. The short-chain fatty acid acetate reduces appetite via a central homeostatic mechanism. Nat Commun. 2014 Apr 29;5:3611. doi: 10.1038/ncomms4611. PMID: 24781306; PMCID: PMC4015327.

Fülling C, Dinan TG, Cryan JF. 2019. Gut microbe to brain signaling: what happens in vagus. Neuron 101:998–1002. https://doi.org/10.1016/j.neuron .2019.02.008.

Fulop T, Witkowski JM, Bourgade K, Khalil A, Zerif E, Larbi A, Hirokawa K, Pawelec G, Bocti C, Lacombe G, Dupuis G, Frost EH. Can an Infection Hypothesis Explain the Beta Amyloid Hypothesis of Alzheimer's Disease? Front Aging Neurosci. 2018 Jul 24;10:224.

Furusawa Y, Obata Y, Fukuda S, Endo TA, Nakato G, Takahashi D, Nakanishi Y, Uetake C, Kato K, Kato T, Takahashi M, Fukuda NN, Murakami S, Miyauchi E, Hino S, Atarashi K, Onawa S, Fujimura Y, Lockett T, Clarke JM, Topping DL, Tomita M, Hori S, Ohara O, Morita T, Koseki H, Kikuchi J, Honda K, Hase K, Ohno H. 2013. Commensal microbe-derived butyrate induces the differentiation of colonic regulatory T cells. Nature 504:446–450. https://doi.org/10.1038/nature12721.

Fuso, A., Nicolia, V., Cavallaro, R. A., and Scarpa, S. (2011). DNA methylase and demethylase activities are modulated by one-carbon metabolism in Alzheimer's disease models. J. Nutr. Biochem. 22, 242–251. doi: 10.1016/j.jnutbio.2010. 01.010

Fuso A, Nicolia V, Cavallaro RA, Ricceri L, D'Anselmi F, Coluccia P, Calamandrei G, Scarpa S. B-vitamin deprivation induces hyperhomocysteinemia and brain S-adenosylhomocysteine, depletes brain S-adenosylmethionine, and enhances PS1 and BACE expression and amyloid-beta deposition in mice. Mol Cell Neurosci. 2008 Apr;37(4):731-46. doi: 10.1016/j.mcn.2007.12.018. Epub 2008 Jan 3. PMID: 18243734.

Gabaldon, T., Snel, B., van Zimmeren, F., Hemrika, W., Tabak, H., and Huynen, M.A. (2006). Origin and evolution of the peroxisomal proteome. Biol. Direct 1, 8.

Galea, E., Launay, N., Portero-Otin, M., Ruiz, M., Pamplona, R., Aubourg, P., Ferrer, I., and Pujol, A. (2012). Oxidative stress underlying axonal degeneration in adrenoleukodystrophy: a paradigm for multifactorial neurodegenerative diseases? Biochim. Biophys. Acta 1822, 1475- 1488.

Galino, J., Ruiz, M., Fourcade, S., Schluter, A., Lopez-Erauskin, J., Guilera, C., Jove, M., Naudi, A., Garcia-Arumi, E., Andreu, A.L., et al. (2011). Oxidative damage compromises energy metabolism in the axonal degeneration mouse model of X-adrenoleukodystrophy. Antioxid Redox Signal 15, 2095-2107.

Gambardella S, Limanaqi F, Ferese R, Biagioni F, Campopiano R, Centonze D, et al. ccf-mtDNA as a Potential Link Between the Brain and Immune System in Neuro-Immunological Disorders. Front Immunol. 2019;10:1064.

Gao X, Lee K, Reid MA, Sanderson SM, Qiu C, Li S, Liu J, Locasale JW. Serine Availability Influences Mitochondrial Dynamics and Function through Lipid Metabolism. Cell Rep. 2018 Mar 27;22(13):3507-3520. doi: 10.1016/j.celrep.2018.03.017. PMID: 29590619; PMCID: PMC6054483.

Geldon S, Fernández-Vizarra E, Tokatlidis K. Redox-Mediated Regulation of Mitochondrial Biogenesis, Dynamics, and Respiratory Chain Assembly in Yeast and Human Cells. Front Cell Dev Biol. 2021 Sep 7;9:720656. doi: 10.3389/fcell.2021.720656. PMID: 34557489; PMCID: PMC8452992.

Geva-Zatorsky N, Sefik E, Kua L, Pasman L, Tan TG, Ortiz-Lopez A, Yanortsang TB, Yang L, Jupp R, Mathis D, Benoist C, Kasper DL. Mining the Human Gut Microbiota for Immunomodulatory Organisms. Cell. 2017 Feb 23;168(5):928-943.e11. doi: 10.1016/j.cell.2017.01.022. Epub 2017 Feb 16. PMID: 28215708; PMCID: PMC7774263.

Gibson GE, Starkov A, Blass JP, Ratan RR, Beal MF. Cause and consequence: mitochondrial dysfunction initiates and propagates neuronal dysfunction, neuronal death and behavioral abnormalities in age-associated neurodegenerative diseases. Biochim Biophys Acta. 2010;1802:122–34.

Gibson GR, Hutkins R, Sanders ME, Prescott SL, Reimer RA, Salminen SJ, Scott K, Stanton C, Swanson KS, Cani PD, Verbeke K, Reid G. Expert consensus document: The International Scientific Association for Probiotics and Prebiotics (ISAPP) consensus statement on the definition and scope of prebiotics. Nat Rev Gastroenterol Hepatol. 2017 Aug;14(8):491-502.

Gibson SA, McFarlan C, Hay S, MacFarlane GT (1989) Significance of microflora in proteolysis in the colon. Appl Environ Microbiol 55:679–683

Gilbert JA, Blaser MJ, Caporaso JG, Jansson JK, Lynch SV, Knight R. Current understanding of the human microbiome. Nat Med. 2018 Apr 10;24(4):392-400. doi: 10.1038/nm.4517. PMID: 29634682; PMCID: PMC7043356.

Gilchrist KW, Gilbert EF, Goldfarb S, Goll U, Spranger JW, Opitz JM. Studies of malformation syndromes of man XIB: the cerebro-hepato-renal syndrome of Zellweger: comparative pathology. Eur J Pediatr 121: 99–118, 1976. doi:10.1007/BF00443065.

Gilg, A.G., Singh, A.K., and Singh, I. (2000). Inducible nitric oxide synthase in the central nervous system of patients with X-adrenoleukodystrophy. J. Neuropathol. Exp. Neurol. 59, 1063-1069.

Glancy B, Kim Y, Katti P, Willingham TB. The Functional Impact of Mitochondrial Structure Across Subcellular Scales. Front Physiol. 2020 Nov 11;11:541040. doi:10.3389/fphys.2020.541040. PMID: 33262702; PMCID: PMC7686514.

Gocan AG, Bachg D, Schindler AE, Rohr UD. 2012. Balancing steroidal hormone cascade in treatment-resistant veteran soldiers with PTSD using a fermented soy product (FSWW08): a pilot study. Hormone Mol Biol Clin Invest 10:301–314. https://doi.org/10.1515/hmbci-2011-0135.

Golbabapour S, Abdulla MA, Hajrezaei M. A concise review on epigenetic regulation: insight into molecular mechanisms. Int J Mol Sci. 2011;12(12):8661-94. doi: 10.3390/ijms12128661. Epub 2011 Nov 30. PMID: 22272098; PMCID: PMC3257095.

Goldfischer, S., Moore, C.L., Johnson, A.B., Spiro, A.J., Valsamis, M.P., Wisniewski, H.K., Ritch, R.H., Norton, W.T., Rapin, I., and Gartner, L.M. (1973). Peroxisomal and mitochondrial defects in the cerebro-hepato-renal syndrome. Science 182, 62-64.

Goldman, W. E., Klapper, D. G., and Baseman, J. B. (1982). Detection, isolation, and analysis of a released Bordetella pertussis product toxic to cultured tracheal cells. Infect. Immun. 36, 782–794.

Gómez Morillas A, Besson VC, Lerouet D. Microglia and Neuroinflammation: What Place for P2RY12? Int J Mol Sci. 2021 Feb 6;22(4):1636. doi: 10.3390/ijms22041636. PMID: 33561958; PMCID: PMC7915979.

Goncalves, R. L., Quinlan, C. L., Perevoshchikova, I. V., Hey-Mogensen, M., and Brand, M. D. (2015). Sites of superoxide and hydrogen peroxide production by muscle mitochondria assessed ex vivo under conditions mimicking rest and exercise. J. Biol. Chem. 290, 209–227. doi: 10.1074/jbc.m114.619072

Gong T, Liu L, Jiang W, Zhou R (2019) DAMP-sensing receptors in sterile inflammation and inflammatory diseases. Nat Rev Immunol 20: 95 – 112

Gong Y, Sasidharan N, Laheji F, Frosch M, Musolino P, Tanzi R, Kim DY, Biffi A, El Khoury J, Eichler F. Microglial dysfunction as a key pathological change in adrenomyeloneuropathy. Ann Neurol. 2017 Nov;82(5):813-827. doi: 10.1002/ana.25085. Epub 2017 Nov 11. PMID: 29059709; PMCID: PMC5725816.

Gonzalez-Perez, G., Hicks, A. L., Tekieli, T. M., Radens, C. M., Williams, B. L., and Lamousé-Smith, E. S. N. (2016). Maternal antibiotic treatment impacts development of the neonatal intestinal microbiome and antiviral immunity. J. Immunol. 196, 3768–3779. doi: 10.4049/jimmunol.1502322

Goodwin B, Jones SA, Price RR, Watson MA, McKee DD, Moore LB, Galardi C, Wilson JG, Lewis MC, Roth ME, Maloney PR, Willson TM, Kliewer SA. A regulatory cascade of the nuclear receptors FXR, SHP-1, and LRH-1 represses bile acid biosynthesis. Mol Cell. 2000 Sep;6(3):517-26. doi: 10.1016/s1097-2765(00)00051-4. PMID: 11030332.

Griffin, J.W., Goren, E., Schaumburg, H., Engel, W.K., and Loriaux, L. (1977). Adrenomyeloneuropathy: a probable variant of adrenoleukodystrophy. I. Clinical and endocrinologic aspects. Neurology 27, 1107-1113.

Guda, P., Guda, C., and Subramaniam, S. (2007). Reconstruction of pathways associated with amino acid metabolism in human mitochondria. Genom Proteom Bioinform 5, 166–176. doi:10.1016/s1672-0229(08)60004-2

Guinane CM, Tadrous A, Fouhy F, Ryan CA, Dempsey EM, Murphy B, Andrews E, Cotter PD, Stanton C, Ross RP. Microbial composition of human appendices from patients following appendectomy. mBio. 2013 Jan 15;4(1):e00366-12. doi: 10.1128/mBio.00366-12. PMID: 23322636; PMCID: PMC3551545.

Guo R, Gu J, Zong S, Wu M, Yang M. Structure and mechanism of mitochondrial electron transport chain. Biomed J. 2018;41:9–20.

Guo, Y., Huang, Z., Sang, D., Gao, Q., and Li, Q. (2020). The Role of Nutrition in the Prevention and Intervention of Type 2 Diabetes. Front. Bioeng. Biotechnol. 8, 575442.

Greub G. Culturomics: a new approach to study the human microbiome. Clin Microbiol Infect. 2012 Dec;18(12):1157-9. doi: 10.1111/1469-0691.12032. PMID: 23148445.

Gustafsson BE, Daft FS, Mcdaniel EG, Smith JC, Fitzgerald RJ. Effects of vitamin K-active compounds and intestinal microorganisms in vitamin K-deficient germfree rats. J Nutr. 1962 Dec;78(4):461-8. doi: 10.1093/jn/78.4.461. PMID: 13951405.

Gustafsson BE, Angelin B, Einarsson K, Gustafsson JA (1977) Effects of cholesterol feeding on synthesis and metabolism of cholesterol and bile acids in germfree rats. J Lipid Res 18:717–721

Häberle J, Pauli S, Berning C, Koch HG, Linnebank M. TC II deficiency: avoidance of false-negative molecular genetics by RNA-based investigations. J Hum Genet. 2009 Jun;54(6):331-4. doi: 10.1038/jhg.2009.34. Epub 2009 Apr 17. PMID: 19373259.

Haghikia A, Jörg S, Duscha A, Berg J, Manzel A, Waschbisch A, Hammer A, Lee D-H, May C, Wilck N, Balogh A, Ostermann AI, Schebb NH, Akkad DA, Grohme DA, Kleinewietfeld M, Kempa S, Thöne J, Demir S, Müller DN, Gold R, Linker RA. 2015. Dietary fatty acids directly impact central nervous system autoimmunity via the small intestine. Immunity 43: 817–829. https://doi.org/10.1016/j.immuni.2015.09.007

Haikal C, Chen Q-Q, Li J-Y. 2019. Microbiome changes: an indicator of Parkinson's disease? Transl Neurodegener 8:1–9. https://doi.org/10.1186/ s40035-019-0175-7.

Hajra, A.K., and Bishop, J.E. (1982). Glycerolipid biosynthesis in peroxisomes via the acyl dihydroxyacetone phosphate pathway. Ann. N. Y. Acad. Sci. 386, 170-182.

Halliwell, B., and Whiteman, M. (2004). Measuring reactive species and oxidative damage in vivo and in cell culture: how should you do it and what do the results mean? Br. J. Pharmacol. 142, 231-255.

Halliwell, B. Oxidative Stress and Neurodegeneration: Where Are We Now? J. Neurochem. 2006, 97, 1634–1658.

Halliwell, B. (2007). Biochemistry of oxidative stress. Biochem. Soc. Trans. 35, 1147-1150.

Hamamah S, Gheorghita R, Lobiuc A, Sirbu IO, Covasa M. Fecal microbiota transplantation in non-communicable diseases: Recent advances and protocols. Front Med (Lausanne). 2022 Dec 8;9:1060581. doi: 10.3389/fmed.2022.1060581. PMID: 36569149; PMCID: PMC9773399.

Hampl V, Cepicka I, EliásM(2019) Was the mitochondrion necessary to start eukaryogenesis? Trends Microbiol 27: 96 – 104

Han D, Walsh MC, Cejas PJ, Dang NN, Kim YF, Kim J, Charrier-Hisamuddin L, Chau L, Zhang Q, Bittinger K, Bushman FD, Turka LA, Shen H, Reizis B, Defranco AL, Wu GD, Choi Y. Dendritic cell expression of the signaling molecule TRAF6 is critical for gut microbiota-dependent immune tolerance. Immunity. 2013 Jun 27;38(6):1211-22. doi: 10.1016/j.immuni.2013.05.012. Epub 2013 Jun 20. PMID: 23791643; PMCID: PMC3715143.

Han D, Walsh MC, Kim KS, Hong SW, Lee J, Yi J, Rivas G, Surh CD, Choi Y. Microbiota-Independent Ameliorative Effects of Antibiotics on Spontaneous Th2-Associated Pathology of the Small Intestine. PLoS One. 2015 Feb 17;10(2):e0118795. doi: 10.1371/journal.pone.0118795. Erratum in: PLoS One. 2015 Jul 20;10(7):e0133787. doi: 10.1371/journal.pone.0133787. PMID: 25689829; PMCID: PMC4331505.

Han, S., Van Treuren, W., Fischer, C.R., Merrill, B.D., DeFelice, B.C., Sanchez, J.M., Higginbottom, S.K., Guthrie, L., Fall, L.A., Dodd, D., et al. (2021). A metabolomics pipeline for the mechanistic interrogation of the gut microbiome. Nature 595, 415–420. https://doi.org/10.1038/s41586- 021-03707-9.

Hapfelmeier S, Lawson MA, Slack E, Kirundi JK, Stoel M, Heikenwalder M, Cahenzli J, Velykoredko Y, Balmer ML, Endt K, Geuking MB, Curtiss R 3rd, McCoy KD, Macpherson AJ. Reversible microbial colonization of germ-free mice reveals the dynamics of IgA immune responses. Science. 2010 Jun 25;328(5986):1705-9. doi: 10.1126/science.1188454. PMID: 20576892; PMCID: PMC3923373.

Haran JP, Bhattarai SK, Foley SE, Dutta P, Ward DV, Bucci V, McCormick BA. Alzheimer's Disease Microbiome Is Associated with Dysregulation of the Anti-Inflammatory P-Glycoprotein Pathway. mBio. 2019 May 7;10(3):e00632-19. doi: 10.1128/mBio.00632-19. PMID: 31064831; PMCID: PMC6509190.

Harrington JS, Ryter SW, Plataki M, Price DR, Choi AMK. Mitochondria in health, disease, and aging. Physiol Rev. 2023 Oct 1;103(4):2349-2422. doi: 10.1152/physrev.00058.2021. Epub 2023 Apr 6. PMID: 37021870; PMCID: PMC10393386.

Hart ML, Quon E, Vigil ABG, Engstrom IA, Newsom OJ, Davidsen K, Hoellerbauer P, Carlisle SM, Sullivan LB. Mitochondrial redox adaptations enable alternative aspartate synthesis in SDH-deficient cells. Elife. 2023 Mar 8;12:e78654. doi: 10.7554/eLife.78654. PMID: 36883551; PMCID: PMC10027318.

Hashemi E, Narain Srivastava I, Aguirre A, Tilahan Yoseph E, Kaushal E, Awani A, Kyu Ryu J, Akassoglou K, Talebian S, Chu P, Pisani L, Musolino P, Steinman L, Doyle K, Robinson WH, Sharpe O, Cayrol R, Orchard P, Lund T, Vogel H, Lenail M, Han MH, Bonkowsky JL, Van Haren KP. A novel mouse model of cerebral adrenoleukodystrophy highlights NLRP3 activity in lesion pathogenesis. bioRxiv [Preprint]. 2023 Nov 10:2023.11.07.564025. doi: 10.1101/2023.11.07.564025. PMID: 37986739; PMCID: PMC10659266.

Hegelmaier T, Lebbing M, Duscha A, Tomaske L, Tönges L, Holm JB, Bjørn Nielsen H, Gatermann SG, Przuntek H, Haghikia A. 2020. Interventional influence of the intestinal microbiome through dietary intervention and bowel cleansing might improve motor symptoms in Parkinson’s disease. Cells 9:376. https://doi.org/10.3390/cells9020376.

Hein S, Schönfeld P, Kahlert S, Reiser G. Toxic effects of X-linked adrenoleukodystrophy-associated, very long chain fatty acids on glial cells and neurons from rat hippocampus in culture. Hum Mol Genet. 2008 Jun 15;17(12):1750-61. doi: 10.1093/hmg/ddn066. Epub 2008 Mar 14. PMID: 18344355.

Helgeland L, Dissen E, Dai KZ, Midtvedt T, Brandtzaeg P, Vaage JT. Microbial colonization induces oligoclonal expansions of intraepithelial CD8 T cells in the gut. Eur J Immunol. 2004 Dec;34(12):3389-400. doi: 10.1002/eji.200425122. PMID: 15517613.

Heneka, M.T.; McManus, R.M.; Latz, E. Inflammasome Signalling in Brain Function and Neurodegenerative Disease. Nat. Rev. Neurosci. 2018, 19, 610–621.

Hermanussen M, Gonder U, Jakobs C, Stegemann D, Hoffmann G. Patterns of free amino acids in German convenience food products: marked mismatch between label information and composition. Eur J Clin Nutr. 2010 Jan;64(1):88-98. doi: 10.1038/ejcn.2009.116. Epub 2009 Sep 23. PMID: 19773804.

Hervé C. Gérard, Ute Dreses-Werringloer, Kristin S. Wildt, Srilekha Deka, Cynthia Oszust, Brian J. Balin, William H. Frey, Elizabeth Z. Bordayo, Judith A. Whittum-Hudson, Alan P. Hudson, Chlamydophila (Chlamydia) pneumoniae in the Alzheimer's brain, FEMS Immunology & Medical Microbiology, Volume 48, Issue 3, December 2006, Pages 355–366.

Hill C, Guarner F, Reid G, Gibson GR, Merenstein DJ, Pot B, Morelli L, Canani RB, Flint HJ, Salminen S, Calder PC, Sanders ME. 2014. The International Scientific Association for Probiotics and Prebiotics consensus statement on the scope and appropriate use of the term probiotic. Nat Rev Gastroenterol Hepatol 11:506–514. https://doi.org/10.1038/nrgastro.2014.66.

Hill MJ (1997) Intestinal flora and endogenous vitamin synthesis. Eur J Cancer Prev 6:S43–S45

Hirabayashi Y, Furuya S. Roles of l-serine and sphingolipid synthesis in brain development and neuronal survival. Prog Lipid Res. 2008 May;47(3):188-203. doi: 10.1016/j.plipres.2008.01.003. Epub 2008 Feb 15. PMID: 18319065.

Hirayama D, Iida T, Nakase H. The Phagocytic Function of Macrophage-Enforcing Innate Immunity and Tissue Homeostasis. Int J Mol Sci. 2017 Dec 29;19(1):92. doi: 10.3390/ijms19010092. PMID: 29286292; PMCID: PMC5796042.

Hirokane H, Nakahara M, Tachibana S, Shimizu M, Sato R. Bile acid reduces the secretion of very low density lipoprotein by repressing microsomal triglyceride transfer protein gene expression mediated by hepatocyte nuclear factor-4. J Biol Chem. 2004 Oct 29;279(44):45685-92. doi: 10.1074/jbc.M404255200. Epub 2004 Aug 26. PMID: 15337761.

Höftberger R, Kunze M, Weinhofer I, Aboul-Enein F, Voigtländer T, Oezen I, Amann G, Bernheimer H, Budka H, Berger J. Distribution and cellular localization of adrenoleukodystrophy protein in human tissues: implications for X-linked adrenoleukodystrophy. Neurobiol Dis. 2007 Nov;28(2):165-74. doi: 10.1016/j.nbd.2007.07.007. Epub 2007 Aug 29. PMID: 17761426.

Höftberger R, Kunze M, Voigtländer T, Unterberger U, Regelsberger G, Bauer J, Aboul-Enein F, Garzuly F, Forss-Petter S, Bernheimer H, Berger J, Budka H. Peroxisomal localization of the proopiomelanocortin-derived peptides beta-lipotropin and beta-endorphin. Endocrinology. 2010 Oct;151(10):4801-10. doi: 10.1210/en.2010-0249. Epub 2010 Sep 1. PMID: 20810565

Hollister EB, Gao C, Versalovic J (2014) Compositional and functional features of the gastrointestinal microbiome and their efects on human health. Gastroenterology 146(6):1449–1458. https://doi.org/10.1053/j.gastro.2014.01.052

Holzer P, Farzi A. 2014. Neuropeptides and the microbiota-gut-brain axis, p 195–219. In Microbial endocrinology: the microbiota-gut-brain axis in health and disease. Springer, New York, NY.

Hou K, Wu ZX, Chen XY, Wang JQ, Zhang D, Xiao C, Zhu D, Koya JB, Wei L, Li J, Chen ZS. Microbiota in health and diseases. Signal Transduct Target Ther. 2022 Apr 23;7(1):135. doi: 10.1038/s41392-022-00974-4. PMID: 35461318; PMCID: PMC9034083.

Houten SM, Watanabe M, Auwerx J (2006) Endocrine functions of bile acids. EMBO J 25:1419–1425

Hsieh, S.L., Liu, R.W., Wu, C.H., Cheng, W.T., and Kuo, C.M. (2003). cDNA nucleotide sequence coding for stearoyl-CoA desaturase and its expression in the zebrafish (Danio rerio) embryo. Mol. Reprod. Dev. 66, 325-333.

Hsieh T-H, Kuo C-W, Hsieh K-H, Shieh M-J, Peng C-W, Chen Y-C, Chang Y-L, Huang Y-Z, Chen C-C, Chang P-K, Chen K-Y, Chen H-Y. 2020. Probiotics alleviate the progressive deterioration of motor functions in a mouse model of Parkinson's disease. Brain Sci 10:206.

Hu, X., and Guo, F. (2021). Amino Acid Sensing in Metabolic Homeostasis and Health. Endocr. Rev. 42, 56–76. https://doi.org/10.1210/endrev/ bnaa026.

Hubbard TD, Murray IA, Perdew GH. 2015. Indole and tryptophan metabolism: endogenous and dietary routes to Ah receptor activation. Drug Metab Dispos 43:1522–1535. https://doi.org/10.1124/dmd.115.064246

Hussaini SH, Pereira SP, Murphy GM, Dowling RH (1995) Deoxycholic acid influences cholesterol solubilization and microcrystal nucleation time in gallbladder bile. Hepatology 22:1735–1744

Igarashi, M., Schaumburg, H.H., Powers, J., Kishmoto, Y., Kolodny, E., and Suzuki, K. (1976). Fatty acid abnormality in adrenoleukodystrophy. J. Neurochem. 26, 851-860.

Ito, M., Blumberg, B.M., Mock, D.J., Goodman, A.D., Moser, A.B., Moser, H.W., Smith, K.D., and Powers, J.M. (2001). Potential environmental and host participants in the early white matter lesion of adreno-leukodystrophy: morphologic evidence for CD8 cytotoxic T cells, cytolysis of oligodendrocytes, and CD1-mediated lipid antigen presentation. J. Neuropathol. Exp. Neurol. 60, 1004-1019.

Jaglin M, Rhimi M, Philippe C, Pons N, Bruneau A, Goustard B, Daugé V, Maguin E, Naudon L, Rabot S. Indole, a Signaling Molecule Produced by the Gut Microbiota, Negatively Impacts Emotional Behaviors in Rats. Front Neurosci. 2018 Apr 9;12:216. doi: 10.3389/fnins.2018.00216. PMID: 29686603; PMCID: PMC5900047.

Jandhyala SM, Talukdar R, Subramanyam C, Vuyyuru H, Sasikala M, Nageshwar Reddy D. Role of the normal gut microbiota. World J Gastroenterol. 2015 Aug 7;21(29):8787-803. doi: 10.3748/wjg.v21.i29.8787. PMID: 26269668; PMCID: PMC4528021.

Jang J., Kang H.C., Kim H.S., Kim J.Y., Huh Y.J., Kim D.S., Yoo J.E., Lee J.A., Lim B., Lee J., et al. Induced pluripotent stem cell models from X-linked adrenoleukodystrophy patients. Ann. Neurol. 2011;70:402–409. doi: 10.1002/ana.22486.

Jang J., Park S., Jin Hur H., Cho H.J., Hwang I., Pyo Kang Y., Im I., Lee H., Lee E., Yang W., et al. 25-hydroxycholesterol contributes to cerebral inflammation of X-linked adrenoleukodystrophy through activation of the NLRP3 inflammasome. Nat. Commun. 2016;7:13129. doi: 10.1038/ncomms13129.

Jankute, M., Cox, J. A., Harrison, J., and Besra, G. S. (2015). Assembly of the mycobacterial cell wall. Annu. Rev. Microbiol. 69, 405–423. doi: 10.1146/annurev-micro-091014-104121

Jari Oksanen, F. Guillaume Blanchet, Michael Friendly, Roeland Kindt, Pierre Legendre, Dan McGlinn, Peter R. Minchin, R. B. O'Hara, Gavin L. Simpson, Peter Solymos, M. Henry H. Stevens, Eduard Szoecs and Helene Wagner (2019). vegan: Community Ecology Package. R package version 2.5-6. https://CRAN.R-project.org/package=vegan

Jeffrey H. Meyer, Molecular imaging findings in bipolar disorder, Neurobiology of bypolar disorders, road to novel therapeutics, chapter 16, Pages 183-195, 2021, Academic Press.

Jena AB, Samal RR, Bhol NK, Duttaroy AK. Cellular Red-Ox system in health and disease: The latest update. Biomed Pharmacother. 2023 Jun;162:114606. doi: 10.1016/j.biopha.2023.114606. Epub 2023 Mar 28. PMID: 36989716.

Jensen, P.K. (1966). Antimycin-insensitive oxidation of succinate and reduced nicotinamide- adenine dinucleotide in electron-transport particles. I. pH dependency and hydrogen peroxide formation. Biochim. Biophys. Acta 122, 157-166.

Ježek J, Cooper KF, Strich R. Reactive Oxygen Species and Mitochondrial Dynamics: The Yin and Yang of Mitochondrial Dysfunction and Cancer Progression. Antioxidants (Basel). 2018 Jan 16;7(1):13. doi: 10.3390/antiox7010013. PMID: 29337889; PMCID: PMC5789323.

Jiang W, Li R, Zhang Y, Wang P, Wu T, Lin J, Yu J, Gu M (2017) Mitochondrial DNA mutations associated with type 2 diabetes mellitus in Chinese Uyghur population. Sci Rep 7: 16989

Johnson, J. W., Fisher, J. F., and Mobashery, S. (2013). Bacterial cell-wall recycling. Ann. N. Y. Acad. Sci. 1277, 54–75. doi: 10.1111/j.1749-6632.2012.06813.x

Jong CJ, Sandal P, Schaffer SW. The Role of Taurine in Mitochondria Health: More Than Just an Antioxidant. Molecules. 2021 Aug 13;26(16):4913. doi: 10.3390/molecules26164913. PMID: 34443494; PMCID: PMC8400259.

Joseph H. Neale, Tatsuo Yamamoto, N-acetylaspartylglutamate (NAAG) and glutamate carboxypeptidase II: An abundant peptide neurotransmitter-enzyme system with multiple clinical applications,Progress in Neurobiology, Volume 184,2020,101722,ISSN 0301-0082,https://doi.org/10.1016/j.pneurobio.2019.101722.

Jutras, B. L., Lochhead, R. B., Kloos, Z. A., Biboy, J., Strle, K., Booth, C. J., et al. (2019). Borrelia burgdorferi peptidoglycan is a persistent antigen in patients with Lyme arthritis. Proc. Natl. Acad. Sci. U.S.A. 116, 13498–13507. doi: 10.1073/pnas.1904170116

Kadowaki A, Miyake S, Saga R, Chiba A, Mochizuki H, Yamamura T. 2016. Gut environment-induced intraepithelial autoreactive CD41 T cells suppress central nervous system autoimmunity via LAG-3. Nat Commun 7: 1–16. https://doi.org/10.1038/ncomms11639.

Kalghatgi S, Spina CS, Costello JC, Liesa M, Morones-Ramirez JR, Slomovic S, Molina A, Shirihai OS, Collins JJ. Bactericidal antibiotics induce mitochondrial dysfunction and oxidative damage in Mammalian cells. Sci Transl Med. 2013 Jul 3;5(192):192ra85. doi: 10.1126/scitranslmed.3006055. PMID: 23825301; PMCID: PMC3760005.

Kandell RL, Bernstein C (1991) Bile salt/acid induction of DNA damage in bacterial and mammalian cells: implications for colon cancer. Nutr Cancer 16:227–238

Karau A, Grayson I (2014) Amino acids in human and animal nutrition. Adv Biochem Eng Biotechnol 143:189–228

Kashiwayama Y., Seki M., Yasui A., Murasaki Y., Morita M., Yamashita Y., Sakaguchi M., Tanaka Y., Imanaka T. 70-kDa peroxisomal membrane protein related protein (P70R/ABCD4) localizes to endoplasmic reticulum not peroxisomes, and NH2-terminal hydrophobic property determines the subcellular localization of ABC subfamily D proteins. Exp. Cell Res. 2009;315:190–205. doi: 10.1016/j.yexcr.2008.10.031.

Kathryn C. Fitzgerald, Matthew D. Smith, Sol Kim, Elias S. Sotirchos, Michael D. Kornberg, Morgan Douglas, Bardia Nourbakhsh, Jennifer Graves, Ramandeep Rattan, Laila Poisson, Mirela Cerghet, Ellen M. Mowry, Emmanuelle Waubant, Shailendra Giri, Peter A. Calabresi, Pavan Bhargava, Multi-omic evaluation of metabolic alterations in multiple sclerosis identifies shifts in aromatic amino acid metabolism,Cell Reports Medicine,Volume 2, Issue 10, 2021,100424, ISSN 2666-3791,https://doi.org/10.1016/j.xcrm.2021.100424.

Katsuma S, Hirasawa A, Tsujimoto G (2005) Bile acids promote glucagon-like peptide-1 secretion through TGR5 in a murine enteroendocrine cell line STC-1. Biochem Biophys Res Commun 329:386–390

Kawaguchi K., Morita M. ABC Transporter Subfamily D: Distinct Differences in Behavior between ABCD1-3 and ABCD4 in Subcellular Localization, Function, and Human Disease. BioMed Res. Int. 2016;2016:6786245. doi: 10.1155/2016/6786245.

Kawata, K., Liu, C.Y., Merkel, S.F., Ramirez, S.H., Tierney, R.T. and Langford, D. (2016) Blood biomarkers for brain injury: What are we measuring? Neurosci. Biobehav. Rev., 68, 460-473.

Kayo Ikeda, Makoto Kinoshita, Hisako Kayama, Shushi Nagamori, Pornparn Kongpracha, Eiji Umemoto, Ryu Okumura, Takashi Kurakawa, Mari Murakami, Norihisa Mikami, Yasunori Shintani, Satoko Ueno, Ayatoshi Andou, Morihiro Ito, Hideki Tsumura, Koji Yasutomo, Keiichi Ozono, Seiji Takashima, Shimon Sakaguchi, Yoshikatsu Kanai, Kiyoshi Takeda,Slc3a2 Mediates Branched-Chain Amino-Acid-Dependent Maintenance of Regulatory T Cells, Cell Reports, Volume 21, Issue 7,2017,Pages 1824-1838, ISSN 2211-1247,https://doi.org/10.1016/j.celrep.2017.10.082.

Kazemi A, Noorbala AA, Azam K, Eskandari MH, Djafarian K. 2019. Effect of probiotic and prebiotic versus placebo on psychological outcomes in patients with major depressive disorder: a randomized clinical trial. Clin Nutr 38:522–528. https://doi.org/10.1016/j.clnu.2018.04.010.

Kazor CE, Mitchell PM, Lee AM, Stokes LN, Loesche WJ, Dewhirst FE et al (2003) Diversity of bacterial populations on the tongue dorsa of patients with halitosis and healthy patients. J Clin Microbiol 41(2):558–563

Kemp S., Valianpour F., Denis S., Ofman R., Sanders R.J., Mooyer P., Barth P.G., Wanders R.J. Elongation of very long-chain fatty acids is enhanced in X-linked adrenoleukodystrophy. Mol. Genet. Metab. 2005;84:144–151.

Kemp S, Berger J, Aubourg P. X-linked adrenoleukodystrophy: clinical, metabolic, genetic and pathophysiological aspects. Biochim Biophys Acta. 2012 Sep;1822(9):1465-74. doi: 10.1016/j.bbadis.2012.03.012. Epub 2012 Mar 28. PMID: 22483867.

Kemp S, Huffnagel IC, Linthorst GE, Wanders RJ, Engelen M. Adrenoleukodystrophy - neuroendocrine pathogenesis and redefinition of natural history. Nat Rev Endocrinol. 2016 Oct;12(10):606-15. doi: 10.1038/nrendo.2016.90. Epub 2016 Jun 17. PMID: 27312864.

Kennedy EA, King KY, Baldridge MT. Mouse Microbiota Models: Comparing Germ-Free Mice and Antibiotics Treatment as Tools for Modifying Gut Bacteria. Front Physiol. 2018 Oct 31;9:1534. doi: 10.3389/fphys.2018.01534. PMID: 30429801; PMCID: PMC6220354.

Khalil M, Teunissen CE, Otto M, Piehl F, Sormani MP, Gattringer T, Barro C, Kappos L, Comabella M, Fazekas F, Petzold A, Blennow K, Zetterberg H, Kuhle J. Neurofilaments as biomarkers in neurological disorders. Nat Rev Neurol. 2018 Oct;14(10):577-589. doi: 10.1038/s41582-018-0058-z. PMID: 30171200.

Kheriji, N., Boukhalfa, W., Mahjoub, F., Hechmi, M., Dakhlaoui, T., Mrad, M., Hadj Salah Bahlous, A.H.S., Ben Amor, N., Jamoussi, H., and Kefi, R. (2022). The Role of Dietary Intake in Type 2 Diabetes Mellitus: Importance of Macro and Micronutrients in Glucose Homeostasis. Nutrients 14, 2132. https://doi.org/10.3390/nu14102132.

Kiecker C. 2018. The origins of the circumventricular organs. J Anat 232: 540–553.

Kim J, Lei Y, Guo J, Kim SE, Wlodarczyk BJ, Cabrera RM, Lin YL, Nilsson TK, Zhang T, Ren A, Wang L, Yuan Z, Zheng YF, Wang HY, Finnell RH. Formate rescues neural tube defects caused by mutations in Slc25a32. Proc Natl Acad Sci U S A. 2018 May 1;115(18):4690-4695. doi: 10.1073/pnas.1800138115. Epub 2018 Apr 16. PMID: 29666258; PMCID: PMC5939102.

Kim Y-K. 2020. Method for diagnosing parkinson's disease through bacterial metagenome analysis. Google Patents.

Kirmse B., Barron S., "Overview of Peroxisomal Disorders", Dynamed plus database, article last update at 24/03/2022

Kitada, T.; Asakawa, S.; Hattori, N.; Matsumine, H.; Yamamura, Y.; Minoshima, S.; Yokochi, M.; Mizuno, Y.; Shimizu, N. Mutations in the Parkin Gene Cause Autosomal Recessive Juvenile Parkinsonism. Nature 1998, 392, 605–608.

Knight R, Callewaert C, Marotz C, Hyde ER, Debelius JW, McDonald D, Sogin ML. The Microbiome and Human Biology. Annu Rev Genomics Hum Genet. 2017 Aug 31;18:65-86. doi: 10.1146/annurev-genom-083115-022438. Epub 2017 Mar 20. PMID: 28375652.

Kobayashi, T., Shinnoh, N., Kondo, A., and Yamada, T. (1997). Adrenoleukodystrophy protein- deficient mice represent abnormality of very long chain fatty acid metabolism. Biochem.Biophys.Res.Commun. 232, 631-636.

Köhler W, Engelen M, Eichler F, Lachmann R, Fatemi A, Sampson J, Salsano E, Gamez J, Molnar MJ, Pascual S, Rovira M, Vilà A, Pina G, Martín-Ugarte I, Mantilla A, Pizcueta P, Rodríguez-Pascau L, Traver E, Vilalta A, Pascual M, Martinell M, Meya U, Mochel F; ADVANCE Study Group. Safety and efficacy of leriglitazone for preventing disease progression in men with adrenomyeloneuropathy (ADVANCE): a randomised, double-blind, multi-centre, placebo-controlled phase 2-3 trial. Lancet Neurol. 2023 Feb;22(2):127-136. doi: 10.1016/S1474-4422(22)00495-1. PMID: 36681445.

Korhonen, J.A., Pham, X.H., Pellegrini, M., and Falkenberg, M. (2004). Reconstitution of a minimal mtDNA replisome in vitro. EMBO J. 23, 2423-2429.

Korley, F.K., Yue, J.K., Wilson, D.H., Hrusovsky, K., Diaz-Arrastia, R., Ferguson, A.R., Yuh, E.L., Mukherjee, P., Wang, K.K.W., Valadka, A.B. et al. (2018) Performance Evaluation of a Multiplex Assay for Simultaneous Detection of Four Clinically Relevant Traumatic Brain Injury Biomarkers. J. Neurotrauma, 36, 182-187.

Koshiba, T., Detmer, S. A., Kaiser, J. T., Chen, H., McCaffery, J. M., and Chan, D. C. (2004). Structural basis of mitochondrial tethering by mitofusin complexes. Science 305, 858–862. doi: 10.1126/science.1099793

Krumbeck JA, Rasmussen HE, Hutkins RW, Clarke J, Shawron K, Keshavarzian A, Walter J. 2018. Probiotic Bifidobacterium strains and galactooligosaccharides improve intestinal barrier function in obese adults but show no synergism when used together as synbiotics. Microbiome 6:1–16. https://doi.org/10 .1186/s40168-018-0494-4.

Kruska, N., Schonfeld, P., Pujol, A., and Reiser, G. (2015). Astrocytes and mitochondria from adrenoleukodystrophy protein (ABCD1)-deficient mice reveal that the adrenoleukodystrophy-associated very long-chain fatty acids target several cellular energy-dependent functions. Biochim. Biophys. Acta 1852, 925-936.

Krych, L., Hansen, C. H. F., Hansen, A. K., van den Berg, F. W. J. & Nielsen, D. S. Quantitatively different, yet qualitatively alike: a meta-analysis of the mouse core gut microbiome with a view towards the human gut microbiome. PloS ONE 8, e62578 (2013).

Kumar R, Islinger M, Worthy H, Carmichael R, Schrader M. The peroxisome: an update on mysteries 3.0. Histochem Cell Biol. 2024 Feb;161(2):99-132. doi: 10.1007/s00418-023-02259-5. Epub 2024 Jan 20. PMID: 38244103; PMCID: PMC10822820.

Kurdi P, Kawanishi K, Mizutani K, Yokota A (2006) Mechanism of growth inhibition by free bile acids in lactobacilli and bifidobacteria. J Bacteriol 188:1979–1986

Kurland CG, Andersson SG. Origin and evolution of the mitochondrial proteome. Microbiol Mol Biol Rev. 2000 Dec;64(4):786-820. doi: 10.1128/MMBR.64.4.786-820.2000. PMID: 11104819; PMCID: PMC99014.

Kurlawala, Z., McMillan, J.D., Singhal, R.A. et al. Mutant and curli-producing E. coli enhance the disease phenotype in a hSOD1-G93A mouse model of ALS. Sci Rep 13, 5945 (2023). https://doi.org/10.1038/s41598-023-32594-5

Kuru, E., Hughes, H. V., Brown, P. J., Hall, E., Tekkam, S., Cava, F., et al. (2012). In situ probing of newly synthesized peptidoglycan in live bacteria with fluorescent D-amino acids. Angew. Chem. Int. Ed Engl. 51, 12519–12523. doi: 10.1002/anie.201206749

Kwon SE, Chapman ER. 2011. Synaptophysin regulates the kinetics of synaptic vesicle endocytosis in central neurons. Neuron 70:847–854.

Lagier JC, Khelaifa S, Alou MT, Ndongo S, Dione N, Hugon P et al (2016) Culture of previously uncultured members of the human gut microbiota by culturomics. Nat Microbiol 1:16203. https://doi.org/10.1038/nmicrobiol.2016.203

Lagier JC, Hugon P, Khelaifa S, Fournier PE, La Scola B, Raoult D (2015) The rebirth of culture in microbiology through the example of culturomics to study human gut microbiota. Clin Microbiol Rev 28(1):237–264. https://doi.org/10.1128/ CMR.00014-14

Lambert IH, Kristensen DM, Holm JB, Mortensen OH. Physiological role of taurine-from organism to organelle. Acta Physiol (Oxf). 2015 Jan;213(1):191-212. doi: 10.1111/apha.12365. Epub 2014 Sep 12. PMID: 25142161.

Lamousé-Smith, E. S., Tzeng, A., and Starnbach, M. N. (2011). The intestinal flora is required to support antibody responses to systemic immunization in infant and germ-free mice. PLoS ONE 6:e27662. doi: 10.1371/journal.pone.0027662

Larsson, N.G., Wang, J., Wilhelmsson, H., Oldfors, A., Rustin, P., Lewandoski, M., Barsh, G.S., and Clayton, D.A. (1998). Mitochondrial transcription factor A is necessary for mtDNA maintenance and embryogenesis in mice. Nat. Genet. 18, 231-236.

Larsson N-G (2010) Somatic mitochondrial DNA mutations in mammalian aging. Annu Rev Biochem 79: 683 – 706

Lau JT, Whelan FJ, Herath I, Lee CH, Collins SM, Bercik P et al (2016) Capturing the diversity of the human gut microbiota through culture-enriched molecular profling. Genome Med 8(1):72. https://doi.org/10.1186/s13073-016-0327-7

Launay, N., Ruiz, M., Fourcade, S., Schluter, A., Guilera, C., Ferrer, I., Knecht, E., and Pujol A. (2013). Oxidative stress regulates the ubiquitin-proteasome system and immunoproteasome functioning in a mouse model of X-adrenoleukodystrophy. Brain 136, 891-904.

Launay, N., Aguado, C., Fourcade, S., Ruiz, M., Grau, L., Riera, J., Guilera, C., Giros, M., Ferrer, I., Knecht, E., et al. (2015). Autophagy induction halts axonal degeneration in a mouse model of X-adrenoleukodystrophy. Acta Neuropathol. 129, 399-415.

Launay, N., Ruiz, M., Grau, L., Ortega, F.J., Ilieva, E.V., Martinez, J.J., Galea, E., Ferrer, I., Knecht, E., Pujol, A., et al. (2017). Tauroursodeoxycholic bile acid arrests axonal degeneration by inhibiting the unfolded protein response in X-linked adrenoleukodystrophy. Acta Neuropathol. 133, 283-301

Launay N, Lopez-Erauskin J, Bianchi P, Guha S, Parameswaran J, Coppa A, Torreni L, Schlüter A, Fourcade S, Paredes-Fuentes AJ, Artuch R, Casasnovas C, Ruiz M, Pujol A. Imbalanced mitochondrial dynamics contributes to the pathogenesis of X-linked adrenoleukodystrophy. Brain. 2024 May 20:awae038. doi: 10.1093/brain/awae038. Epub ahead of print. PMID: 38763511.

Lazarow, P.B., and De Duve, C. (1976). A fatty acyl-CoA oxidizing system in rat liver peroxisomes; enhancement by clofibrate, a hypolipidemic drug. Proc. Natl. Acad. Sci. U. S. A. 73, 2043-2046.

Le Chatelier E, Nielsen T, Qin J, Prifti E, Hildebrand F, Falony G et al (2013) Richness of human gut microbiome correlates with metabolic markers. Nature 500(7464):541–546. https:// doi.org/10.1038/nature12506

Lee C.A.A., Seo H.S., Armien A.G., Bates F.S., Tolar J., Azarin S.M. Modeling and rescue of defective blood-brain barrier function of induced brain microvascular endothelial cells from childhood cerebral adrenoleukodystrophy patients. Fluids Barriers CNS. 2018;15:9. doi: 10.1186/s12987-018-0094-5.

Lee, J., Giordano, S., and Zhang, J. (2012). Autophagy, mitochondria and oxidative stress: cross-talk and redox signalling. Biochem. J. 441, 523-540.

Lee KH, Cha M, Lee BH. Neuroprotective effect of antioxidants in the brain. Int J Mol Sci. (2020) 21:21197152. doi: 10.3390/ijms21197152

Lee, Y.S., Kennedy, W.D., and Yin, Y.W. (2009). Structural insight into processive human mitochondrial DNA synthesis and disease-related polymerase mutations. Cell 139, 312-324.

Lee Y-S, Lai D-M, Huang H-J, Lee-Chen G-J, Chang C-H, Hsieh-Li HM, Lee G-C. 2021. Prebiotic lactulose ameliorates the cognitive deficit in Alzheimer's disease mouse model through macroautophagy and chaperone-mediated autophagy pathways. J Agric Food Chem 69:2422–2437.

Lenth, R.V. (2021), In R package version 1.5.4, https://CRAN.R-project.org/package=emmeans).

Levitt MD, Bond JH Jr (1970) Volume, composition, and source of intestinal gas. Gastroenterology 59:921–929

Ley RE, Bäckhed F, Turnbaugh P, Lozupone CA, Knight RD, Gordon JI. Obesity alters gut microbial ecology. Proc Natl Acad Sci U S A. 2005 Aug 2;102(31):11070-5. doi: 10.1073/pnas.0504978102. Epub 2005 Jul 20. PMID: 16033867; PMCID: PMC1176910.

Li D, Wu M. Pattern recognition receptors in health and diseases. Signal Transduct Target Ther. 2021 Aug 4;6(1):291. doi: 10.1038/s41392-021-00687-0. PMID: 34344870; PMCID: PMC8333067.

Li, F., Hao, X., Chen, Y., Bai, L., Gao, X., Lian, Z., et al. (2017). The microbiota maintain homeostasis of liver-resident γδ T-17 cells in a lipid antigen/CD1ddependent manner. Nat. Commun. 7:13839. doi: 10.1038/ncomms13839

Li J, Jia H, Cai X, Zhong H, Feng Q, Sunagawa S et al (2014) An integrated catalog of reference genes in the human gut microbiome. Nat Biotechnol 32(8):834–841. https://doi.org/10.1038/ nbt.2942

Li J, Pora BLR, Dong K, Hasjim J. Health benefits of docosahexaenoic acid and its bioavailability: A review. Food Sci Nutr. 2021 Jul 23;9(9):5229-5243. doi: 10.1002/fsn3.2299. PMID: 34532031; PMCID: PMC8441440.

Li P, Wang X, Zhao M, Song R, Zhao KS. Polydatin protects hepatocytes against mitochondrial injury in acute severe hemorrhagic shock via SIRT1-SOD2 pathway. Expert Opin Therap Targets. 2015;19:997–1010.

Li Q, Barres BA. Microglia and macrophages in brain homeostasis and disease. Nat Rev Immunol. 2018 Apr;18(4):225-242. doi: 10.1038/nri.2017.125. Epub 2017 Nov 20. PMID: 29151590.

Li Q, Hoppe T. Role of amino acid metabolism in mitochondrial homeostasis. Front Cell Dev Biol. 2023 Feb 27;11:1127618. doi: 10.3389/fcell.2023.1127618. PMID: 36923249; PMCID: PMC10008872.

Li S, Wu Z, Li Y, Tantray I, De Stefani D, Mattarei A, Krishnan G, Gao FB, Vogel H, Lu B. Altered MICOS morphology and mitochondrial ion homeostasis contribute to poly(GR) toxicity associated with C9-ALS/FTD. Cell Rep. 2020;32:107989.

Li TT, Chen X, Huo D, Arifuzzaman M, Qiao S, Jin WB, Shi H, Li XV; JRI Live Cell Bank Consortium; Iliev ID, Artis D, Guo CJ. Microbiota metabolism of intestinal amino acids impacts host nutrient homeostasis and physiology. Cell Host Microbe. 2024 May 8;32(5):661-675.e10. doi: 10.1016/j.chom.2024.04.004. Epub 2024 Apr 23. PMID: 38657606.

Li Z., H. Jin, S.Y. Oh, G.E. Ji. Anti-obese effects of two lactobacilli and two Bifidobacteria on ICR mice fed on a high fat diet. Biochemical and Biophysical Research Communications, 480 (2) (2016), pp. 222-227

Li, Y., Watanabe, E., Kawashima, Y., Plichta, D.R., Wang, Z., Ujike, M., Ang, Q.Y., Wu, R., Furuichi, M., Takeshita, K., et al. (2022). Identification of trypsin-degrading commensals in the large intestine. Nature 609, 582–589.

Lin MM, Liu N, Qin ZH, Wang Y. Mitochondrial-derived damage-associated molecular patterns amplify neuroinflammation in neurodegenerative diseases. Acta Pharmacol Sin. 2022 Oct;43(10):2439-2447. doi: 10.1038/s41401-022-00879-6. Epub 2022 Mar 1. PMID: 35233090; PMCID: PMC9525705.

Lin, M.T.; Beal, M.F. Mitochondrial Dysfunction and Oxidative Stress in Neurodegenerative Diseases. Nature 2006, 443, 787–795.

Lin R, Liu W, Piao M, Zhu H. A review of the relationship between the gut microbiota and amino acid metabolism. Amino Acids. 2017 Dec;49(12):2083-2090. doi: 10.1007/s00726-017-2493-3. Epub 2017 Sep 20. PMID: 28932911

Lindahl B. The story of growth differentiation factor 15: another piece of the puzzle. Clin Chem. 2013 Nov;59(11):1550-2. doi: 10.1373/clinchem.2013.212811. Epub 2013 Sep 3. PMID: 24003064.

Lionaki E, Ploumi C, Tavernarakis N. One-Carbon Metabolism: Pulling the Strings behind Aging and Neurodegeneration. Cells. 2022 Jan 9;11(2):214. doi: 10.3390/cells11020214. PMID: 35053330; PMCID: PMC8773781.

Lisi, Ilaria & Moro, Federico & Mazzone, Edoardo & Marklund, Niklas & Pischiutta, Francesca & Kobeissy, Firas & Mao, Xiang & Corrigan, Frances & Helmy, Adel & Nasrallah, Fatima & Di Pietro, Valentina & Ngwenya, Laura & Portela, Luis & Semple, Bridgette & Smith, Douglas & Wellington, Cheryl & Loane, David & Wang, Kevin & Zanier, Elisa. (2023). Translating from mice to humans: using preclinical blood-based biomarkers for the prognosis and treatment of traumatic brain injury. 10.1101/2023.12.01.569152.

Liu B, Li A, Liu Y, Zhou X, Xu J, Zuo X, Xue K, Cui Y. Transcobalamin 2 orchestrates monocyte proliferation and TLR4-driven inflammation in systemic lupus erythematosus via folate one-carbon metabolism. Front Immunol. 2024 May 31;15:1339680. doi: 10.3389/fimmu.2024.1339680. PMID: 38881906; PMCID: PMC11176449.

Liu L, Li Y, Li S, Hu N, He Y, Pong R et al (2012) Comparison of next-generation sequencing systems. J Biomed Biotechnol 2012:251364.

Liu Y, Hou Y, Wang G, Zheng X, Hao H. Gut Microbial Metabolites of Aromatic Amino Acids as Signals in Host-Microbe Interplay. Trends Endocrinol Metab. 2020 Nov;31(11):818-834. doi: 10.1016/j.tem.2020.02.012. Epub 2020 Apr 10. PMID: 32284282.

Loes, D.J., Hite, S., Moser, H., Stillman, A.E., Shapiro, E., Lockman, L., Latchaw, R.E., and Krivit, W. (1994). Adrenoleukodystrophy: a scoring method for brain MR observations. AJNR Am. J. Neuroradiol. 15, 1761-1766.

Long PM, Moffett JR, Namboodiri AMA, Viapiano MS, Lawler SE, Jaworski DM. N-acetylaspartate (NAA) and N-acetylaspartylglutamate (NAAG) promote growth and inhibit differentiation of glioma stem-like cells. J Biol Chem. 2013 Sep 6;288(36):26188-26200. doi: 10.1074/jbc.M113.487553. Epub 2013 Jul 24. Erratum in: J Biol Chem. 2013 Nov 1;288(44):31916-7. PMID: 23884408; PMCID: PMC3764823.

Lopez-Erauskin, J., Fourcade, S., Galino, J., Ruiz, M., Schluter, A., Naudi, A., Jove, M., Portero-Otin, M., Pamplona, R., Ferrer, I., et al. (2011). Antioxidants halt axonal degeneration in a mouse model of X-adrenoleukodystrophy. Ann. Neurol. 70, 84-92.

López-Erauskin J, Galino J, Bianchi P, Fourcade S, Andreu AL, Ferrer I, Muñoz-Pinedo C, Pujol A. Oxidative stress modulates mitochondrial failure and cyclophilin D function in X-linked adrenoleukodystrophy. Brain. 2012 Dec;135(Pt 12):3584-98.

Lopez-Erauskin, J., Ferrer, I., Galea, E., and Pujol, A. (2013a). Cyclophilin D as a potential target for antioxidants in neurodegeneration: the X-ALD case. Biol. Chem. 394, 621-629.

Lopez-Erauskin, J., Galino, J., Ruiz, M., Cuezva, J.M., Fabregat, I., Cacabelos, D., Boada, J., Martinez, J., Ferrer, I., Pamplona, R., et al. (2013b). Impaired mitochondrial oxidative phosphorylation in the peroxisomal disease X-linked adrenoleukodystrophy. Hum. Mol. Genet. 22, 3296-3305.

Lorente-Picón M, Laguna A. 2021. New avenues for Parkinson's disease therapeutics: disease-modifying strategies based on the gut microbiota. Biomolecules 11:433. https://doi.org/10.3390/biom11030433.

Louveau A, Herz J, Alme MN, Salvador AF, Dong MQ, Viar KE, Herod SG, Knopp J, Setliff JC, Lupi AL, Da Mesquita S, Frost EL, Gaultier A, Harris TH, Cao R, Hu S, Lukens JR, Smirnov I, Overall CC, Oliver G, Kipnis J. 2018. CNS lymphatic drainage and neuroinflammation are regulated by meningeal lymphatic vasculature. Nat Neurosci 21:1380–1391. https://doi .org/10.1038/s41593-018-0227-9.

Love MI, Huber W, Anders S (2014). "Moderated estimation of fold change and dispersion for RNA-seq data with DESeq2." Genome Biology, 15, 550. doi: 10.1186/s13059-014-0550-8.

Lovering AL, Lin LYC, Sewell EW, Spreter T, Brown ED, Strynadka NCJ (2010) Structure of the bacterial teichoic acid polymerase TagF provides insights into membrane association and catalysis. Nat Struct Mol Biol 17:582–589.

Lu, J.F., Lawler, A.M., Watkins, P.A., Powers, J.M., Moser, A.B., Moser, H.W., and Smith,K.D. (1997). A mouse model for X-linked adrenoleukodystrophy. Proc.Natl.Acad.Sci.U.S.A 94, 9366-9371.

Luan HH, Wang A, Hilliard BK, Carvalho F, Rosen CE, Ahasic AM, Herzog EL, Kang I, Pisani MA, Yu S, Zhang C, Ring AM, Young LH, Medzhitov R. GDF15 Is an Inflammation-Induced Central Mediator of Tissue Tolerance. Cell. 2019 Aug 22;178(5):1231-1244.e11. doi: 10.1016/j.cell.2019.07.033. Epub 2019 Aug 8. PMID: 31402172; PMCID: PMC6863354.

Lubos, E., Loscalzo, J., and Handy, D. E. (2011). Glutathione peroxidase-1 in health and disease: from molecular mechanisms to therapeutic opportunities. Antioxidants Redox Signal. 15, 1957–1997. doi: 10.1089/ars.2010.3586

Ludwig W, Strunk O, Westram R, Richter L, Meier H, et al. 2004. ARB: a software environment for sequence data. Nucleic Acids Res. 32:1363–71

Lundberg, R., Toft, M. F., August, B., Hansen, A. K. & Hansen, C. H. F. Antibiotic-treated versus germ-free rodents for microbiota transplantation studies. Gut. Microbes. 7, 68–74 (2016).

Lyon P, Strippoli V, Fang B, Cimmino L. B vitamins and one-carbon metabolism: implications in human health and disease. Nutrients. (2020) 12(9):2867. doi: 10.3390/nu12092867

Lyte M. 2013. Microbial endocrinology in the microbiome-gut-brain axis: how bacterial production and utilization of neurochemicals influence behavior. PLoS Pathog 9:e1003726. https://doi.org/10.1371/journal.ppat.1003726

Lyte M. 2014. Microbial endocrinology and the microbiota-gut-brain axis, p 3–24. In Microbial endocrinology: the microbiota-gut-brain axis in health and disease. Springer, New York, NY.

Ma N, Ma X. Dietary Amino Acids and the Gut-Microbiome-Immune Axis: Physiological Metabolism and Therapeutic Prospects. Compr Rev Food Sci Food Saf. 2019 Jan;18(1):221-242. doi: 10.1111/1541-4337.12401. Epub 2018 Dec 18. PMID: 33337014.

Macpherson, A. J. & Uhr, T. Induction of protective IgA by intestinal dendritic cells carrying commensal bacteria. Science 303, 1662–1665 (2004).

Macfarlane GT, Gibson GR, Cummings JH (1992) Comparison of fermentation reactions in different regions of the human colon. J Appl Bacteriol 72:57–64

Magnúsdóttir S, Ravcheev D, de Crécy-Lagard V, Thiele I (2015) Systematic genome assessment of B-vitamin biosynthesis suggests co-operation among gut microbes. Front Genet 6:148

Maier TV, Lucio M, Lee LH, VerBerkmoes NC, Brislawn CJ, Bernhardt J, Lamendella R, McDermott JE, Bergeron N, Heinzmann SS, Morton JT, González A, Ackermann G, Knight R, Riedel K, Krauss RM, Schmitt-Kopplin P, Jansson JK. Impact of Dietary Resistant Starch on the Human Gut Microbiome, Metaproteome, and Metabolome. mBio. 2017 Oct 17;8(5):e01343-17. doi: 10.1128/mBio.01343-17. PMID: 29042495; PMCID: PMC5646248.

Mainardi, J. L., Villet, R., Bugg, T. D., Mayer, C., and Arthur, M. (2008). Evolution of peptidoglycan biosynthesis under the selective pressure of antibiotics in Gram-positive bacteria. FEMS Microbiol. Rev. 32, 386–408. doi: 10.1111/j.1574-6976.2007.00097.x

Mallonee DH, Hylemon PB (1996) Sequencing and expression of a gene encoding a bile acid transporter from Eubacterium sp. strain VPI 12708. J Bacteriol 178:7053–7058

Manach C, Scalbert A, Morand C, Rémésy C, Jiménez L. Polyphenols: food sources and bioavailability. Am J Clin Nutr. 2004 May;79(5):727-47. doi: 10.1093/ajcn/79.5.727. PMID: 15113710.

Mann G, Mora S, Madu G, Adegoke OAJ. Branched-chain Amino Acids: Catabolism in Skeletal Muscle and Implications for Muscle and Whole-body Metabolism. Front Physiol. 2021 Jul 20;12:702826. doi: 10.3389/fphys.2021.702826. PMID: 34354601; PMCID: PMC8329528.

Mardinoglu, A., Shoaie, S., Bergentall, M., Ghaffari, P., Zhang, C., Larsson, E., Backhed, F., and Nielsen, J. (2015). The gut microbiota modulates host € amino acid and glutathione metabolism in mice. Mol. Syst. Biol. 11, 834. https://doi.org/10.15252/msb.20156487.

Mariat D, Firmesse O, Levenez F, Guimaraes V, Sokol H, Dore J et al (2009) The Firmicutes/Bacteroidetes ratio of the human microbiota changes with age. BMC Microbiol 9(1):123. https:// doi.org/10.1186/1471-2180-9-123

Marín L, Miguélez EM, Villar CJ, Lombó F (2015) Bioavailability of dietary polyphenols and gut microbiota metabolism: antimicrobial properties. Biomed Res Int 2015:905215

Marshall BJ, Warren JR. Unidentified curved bacilli in the stomach of patients with gastritis and peptic ulceration. Lancet. 1984 Jun 16;1(8390):1311-5. doi: 10.1016/s0140-6736(84)91816-6. PMID: 6145023.

Martin M., Cutadapt removes adapter sequences from high-throughput sequencing reads. EMBnet J. 2015;17:1–3.

Martínez-Reyes, I., and Chandel, N. S. (2020). Mitochondrial TCA cycle metabolites control physiology and disease. Nat. Commun. 11, 102. doi:10.1038/s41467-019- 13668-3

Martínez Y, Li X, Liu G, Bin P, Yan W, Más D, Valdivié M, Hu CA, Ren W, Yin Y. The role of methionine on metabolism, oxidative stress, and diseases. Amino Acids. 2017 Dec;49(12):2091-2098. doi: 10.1007/s00726-017-2494-2. Epub 2017 Sep 19. PMID: 28929442.

Maslowski KM, Mackay CR. 2011. Diet, gut microbiota and immune responses. Nat Immunol 12:5–9. https://doi.org/10.1038/ni0111-5.

Mastroeni, R., Bensadoun, J.C., Charvin, D., Aebischer, P., Pujol, A., and Raoul, C. (2009). Insulin-like growth factor-1 and neurotrophin-3 gene therapy prevents motor decline in an X- linked adrenoleukodystrophy mouse model. Ann. Neurol. 66, 117-122.

Matcovitch-Natan O, Winter DR, Giladi A, Vargas Aguilar S, Spinrad A, Sarrazin S, Ben-Yehuda H, David E, Zelada González F, Perrin P, Keren Shaul H, Gury M, Lara-Astaiso D, Thaiss CA, Cohen M, Bahar Halpern K, Baruch K, Deczkowska A, Lorenzo-Vivas E, Itzkovitz S, Elinav E, Sieweke MH, Schwartz M, Amit I. 2016. Microglia development follows a stepwise program to regulate brain homeostasis. Science 353:aad8670. https:// doi.org/10.1126/science.aad8670.

Mayer, E. A. The neurobiology of stress and gastrointestinal disease. Gut 47, 861–869 (2000).

Mayer, C., Kluj, R. M., Muhleck, M., Walter, A., Unsleber, S., Hottmann, I., et al. (2019). Bacteria's different ways to recycle their own cell wall. Int. J. Med. Microbiol. doi: 10.1016/j.ijmm.2019.06.006.

Maynard, C. L., Elson, C. O., Hatton, R. D. & Weaver, C. T. Reciprocal interactions of the intestinal microbiota and immune system. Nature 489, 231–241 (2012).

McCaig AE, Glover LA, Prosser JI. 1999. Molecular analysis of bacterial community structure and diversity in unimproved and improved upland grass pastures. Appl. Environ. Microbiol. 65:1721–30

McAllan L., J.R. Speakman, J.F. Cryan, K.N. Nilaweera Whey protein isolate decreases murine stomach weight and intestinal length and alters the expression of Wnt signalling-associated genes British Journal of Nutrition, 113 (2) (2015), pp. 372-379

McCarville JL, Chen GY, Cuevas VD, Troha K, Ayres JS. 2020. Microbiota metabolites in health and disease. Annu Rev Immunol 38:147–170. https://doi.org/10.1146/annurev-immunol-071219-125715.

Macfarlane GT, Cummings JH, Allison C (1986) Protein degradation by human intestinal bacteria. Microbiology 132:1647–1656

Medina, M., Urdiales, J. L., and Amores-Sánchez, M. I. (2001). Roles of homocysteine in cell metabolism: old and new functions. Eur. J. Biochem. 268, 3871–3882. doi: 10.1046/j.1432-1327.2001.02278.x

Meeske, A. J., Sham, L. T., Kimsey, H., Koo, B. M., Gross, C. A., Bernhardt, T. G., et al. (2015). MurJ and a novel lipid II flippase are required for cell wall biogenesis in Bacillus subtilis. Proc. Natl. Acad. Sci. U.S.A. 112, 6437–6442. doi: 10.1073/pnas.1504967112

Meeske, A. J., Riley, E. P., Robins, W. P., Uehara, T., Mekalanos, J. J., Kahne, D., et al. (2016). SEDS proteins are a widespread family of bacterial cell wall polymerases. Nature 537, 634–638. doi: 10.1038/nature19331

Mercer, T. R., Neph, S., Dinger, M. E., Crawford, J., Smith, M. A., Shearwood, A. M. J., et al. (2011). The human mitochondrial transcriptome. Cell 146, 645–658. doi: 10.1016/j.cell.2011.06.051

Messaoudi M, Lalonde R, Violle N, Javelot H, Desor D, Nejdi A, Bisson JF, Rougeot C, Pichelin M, Cazaubiel M, Cazaubiel JM. Assessment of psychotropic-like properties of a probiotic formulation (Lactobacillus helveticus R0052 and Bifidobacterium longum R0175) in rats and human subjects. Br J Nutr. 2011 Mar;105(5):755-64. doi: 10.1017/S0007114510004319. Epub 2010 Oct 26. PMID: 20974015.

Metzker ML (2005) Emerging technologies in DNA sequencing. Genome Res 15(12):1767–1776. https://doi.org/10.1101/ gr.3770505

Migeon, B.R., Moser, H.W., Moser, A.B., Axelman, J., Sillence, D., and Norum, R.A. (1981). Adrenoleukodystrophy: evidence for X linkage, inactivation, and selection favoring the mutant allele in heterozygous cells. Proc. Natl. Acad. Sci. U. S. A. 78, 5066-5070.

Miklossy J. Bacterial Amyloid and DNA are Important Constituents of Senile Plaques: Further Evidence of the Spirochetal and Biofilm Nature of Senile Plaques. J Alzheimers Dis. 2016 Jun 13;53(4):1459-73. doi: 10.3233/JAD-160451. PMID: 27314530; PMCID: PMC4981904.

Milenkovic, D., Matic, S., Kuhl, I., Ruzzenente, B., Freyer, C., Jemt, E., Park, C.B., Falkenberg, M., and Larsson, N.G. (2013). TWINKLE is an essential mitochondrial helicase required for synthesis of nascent D-loop strands and complete mtDNA replication. Hum. Mol. Genet. 22, 1983-1993.

Miller AL, Bessho S, Grando K, Tükel Ç. Microbiome or Infections: Amyloid-Containing Biofilms as a Trigger for Complex Human Diseases. Front Immunol. 2021 Feb 26;12:638867. doi: 10.3389/fimmu.2021.638867. PMID: 33717189; PMCID: PMC7952436.

Moffett JR, Ross B, Arun P, Madhavarao CN, Namboodiri AM. N-Acetylaspartate in the CNS: from neurodiagnostics to neurobiology. Prog Neurobiol. 2007 Feb;81(2):89-131. doi: 10.1016/j.pneurobio.2006.12.003. Epub 2007 Jan 5. PMID: 17275978; PMCID: PMC1919520.

Moir RD, Lathe R, Tanzi RE. The antimicrobial protection hypothesis of Alzheimer's disease. Alzheimers Dement. 2018 Dec;14(12):1602-1614. doi: 10.1016/j.jalz.2018.06.3040. Epub 2018 Oct 9. PMID: 30314800.

Montero R, Yubero D, Villarroya J, Henares D, Jou C, Rodríguez MA, Ramos F, Nascimento A, Ortez CI, Campistol J, Perez-Dueñas B, O'Callaghan M, Pineda M, Garcia-Cazorla A, Oferil JC, Montoya J, Ruiz-Pesini E, Emperador S, Meznaric M, Campderros L, Kalko SG, Villarroya F, Artuch R, Jimenez-Mallebrera C. GDF-15 Is Elevated in Children with Mitochondrial Diseases and Is Induced by Mitochondrial Dysfunction. PLoS One. 2016 Feb 11;11(2):e0148709. doi: 10.1371/journal.pone.0148709. Erratum in: PLoS One. 2016;11(5):e0155172. PMID: 26867126; PMCID: PMC4750949.

Morato, L., Galino, J., Ruiz, M., Calingasan, N.Y., Starkov, A.A., Dumont, M., Naudi, A., Martinez, J.J., Aubourg, P., Portero-Otin, M., et al. (2013). Pioglitazone halts axonal degeneration in a mouse model of X-linked adrenoleukodystrophy. Brain 136, 2432-2443.

Morato, L., Ruiz, M., Boada, J., Calingasan, N.Y., Galino, J., Guilera, C., Jove, M., Naudi, A., Ferrer, I., Pamplona, R., et al. (2015). Activation of sirtuin 1 as therapy for the peroxisomal disease adrenoleukodystrophy. Cell Death Differ. 22, 1742-1753.

Morland C, Nordengen K. N-Acetyl-Aspartyl-Glutamate in Brain Health and Disease. Int J Mol Sci. 2022 Jan 23;23(3):1268. doi: 10.3390/ijms23031268. PMID: 35163193; PMCID: PMC8836185.

Morvay PL, Baes M, Van Veldhoven PP. Differential activities of peroxisomes along the mouse intestinal epithelium. Cell Biochem Funct. 2017 Apr;35(3):144-155. doi: 10.1002/cbf.3255. Epub 2017 Mar 29. PMID: 28370438.

Morita M, Imanaka T. Peroxisomal ABC transporters: structure, function and role in disease. Biochim Biophys Acta. 2012 Sep;1822(9):1387-96. doi: 10.1016/j.bbadis.2012.02.009. Epub 2012 Feb 17. PMID: 22366764.

Moser, A.B., and Moser, H.W. (1999). The prenatal diagnosis of X-linked adrenoleukodystrophy. Prenat. Diagn. 19, 46-48.

Moser, A.B. & Fatemi, A. (2018). Newborn Screening and Emerging Therapies for X-Linked Adrenoleukodystrophy. JAMA Neurology, 75(10), 1175-1176.

Moser H.W., Moser A.B., Kawamura N., Murphy J., Suzuki K., Schaumburg H., Kishimoto Y. Adrenoleukodystrophy: Elevated C26 fatty acid in cultured skin fibroblasts. Ann. Neurol. 1980;7:542–549. doi: 10.1002/ana.410070607

Moser, H.W., Moser, A.B., Frayer, K.K., Chen, W., Schulman, J.D., O'Neill, B.P., and Kishimoto, Y. (1981). Adrenoleukodystrophy: increased plasma content of saturated very long chain fatty acids. Neurology 31, 1241-1249

Moser H.W., K.D. Smith, P.A. Watkins, J. Powers, A.B. Moser. X-linked Adrenoleukodystrophy The Metabolic & Molecular Bases of Inherited Disease (eighth ed.), McGraw-Hill Book Co., New York (2001), pp. 3257-3301

Mosser J, Douar AM, Sarde CO, Kioschis P, Feil R, Moser H, Poustka AM, Mandel JL, Aubourg P. Putative X-linked adrenoleukodystrophy gene shares unexpected homology with ABC transporters. Nature. 1993 Feb 25;361(6414):726-30. doi: 10.1038/361726a0. PMID: 8441467.

Mottis, A., Herzig, S., and Auwerx, J. (2019). Mitocellular communication: shaping health and disease. Science 366, 827–832. doi: 10.1126/science.aax3768

Moynihan, P. J., and Clarke, A. J. (2011). O-Acetylated peptidoglycan: controlling the activity of bacterial autolysins and lytic enzymes of innate immune systems. Int. J. Biochem. Cell Biol. 43, 1655–1659. doi: 10.1016/j.biocel.2011.08.007

Mu C, Yang Y, Zhu W. 2016. Gut microbiota: the brain peacekeeper. Front Microbiol 7:345. https://doi.org/10.3389/fmicb.2016.00345.

Muffat J., Li Y., Yuan B., Mitalipova M., Omer A., Corcoran S., Bakiasi G., Tsai L.H., Aubourg P., Ransohoff R.M., et al. Efficient derivation of microglia-like cells from human pluripotent stem cells. Nat. Med. 2016;22:1358–1367. doi: 10.1038/nm.4189.

Murphy, M. P. (2009). How mitochondria produce reactive oxygen species. Biochem. J. 417, 1–13. doi: 10.1042/BJ20081386

Murphy MP, Hartley RC. Mitochondria as a therapeutic target for common pathologies. Nat Rev Drug Discov. 2018 Dec;17(12):865-886. doi: 10.1038/nrd.2018.174. Epub 2018 Nov 5. PMID: 30393373.

Nagpal R, Wang S, Solberg Woods LC, Seshie O, Chung ST, Shively CA, Register TC, Craft S, McClain DA, Yadav H. Comparative Microbiome Signatures and Short-Chain Fatty Acids in Mouse, Rat, Non-human Primate, and Human Feces. Front Microbiol. 2018 Nov 30;9:2897. doi: 10.3389/fmicb.2018.02897. PMID: 30555441; PMCID: PMC6283898.

Nakayasu ES, Syed F, Tersey SA, Gritsenko MA, Mitchell HD, Chan CY, Dirice E, Turatsinze JV, Cui Y, Kulkarni RN, Eizirik DL, Qian WJ, Webb-Robertson BM, Evans-Molina C, Mirmira RG, Metz TO. Comprehensive Proteomics Analysis of Stressed Human Islets Identifies GDF15 as a Target for Type 1 Diabetes Intervention. Cell Metab. 2020 Feb 4;31(2):363-374.e6. doi: 10.1016/j.cmet.2019.12.005. Epub 2020 Jan 9. PMID: 31928885; PMCID: PMC7319177.

Nardone G, Compare D (2015) The human gastric microbiota: Is it time to rethink the pathogenesis of stomach diseases? United Eur Gastroenterol J 3(3):255–260

Nath S, Villadsen J. Oxidative phosphorylation revisited. Biotechnol Bioeng. 2015;112:429–37

Nayeri Chegeni T, Sarvi S, Moosazadeh M, Sharif M, Aghayan SA, Amouei A, Hosseininejad Z, Daryani A. Is Toxoplasma gondii a potential risk factor for Alzheimer's disease? A systematic review and meta-analysis. Microb Pathog. 2019 Dec;137:103751. doi: 10.1016/j.micpath.2019.103751. Epub 2019 Sep 16. PMID: 31536800.

Neinast M, Murashige D, Arany Z. Branched Chain Amino Acids. Annu Rev Physiol. 2019 Feb 10;81:139-164. doi: 10.1146/annurev-physiol-020518-114455. Epub 2018 Nov 28. PMID: 30485760; PMCID: PMC6536377.

Neis, E.P.J.G., Dejong, C.H.C., and Rensen, S.S. (2015). The role of microbial amino acid metabolism in host metabolism. Nutrients 7, 2930–2946. https://doi.org/10.3390/nu7042930.

Newgard C.B., J. An, J.R. Bain, M.J. Muehlbauer, R.D. Stevens, L.F. Lien, L.P. Svetkey. A branched-chain amino acid-related metabolic signature that differentiates obese and lean humans and contributes to insulin resistance Cell Metabolism, 9 (4) (2009), pp. 311-326

Nicklas, W., Keubler, L., and Bleich, A. (2015). Maintaining and monitoring the defined microbiota status of gnotobiotic rodents. ILAR J. 56, 241–249. doi: 10.1093/ilar/ilv029

Nimgampalle M, Kuna Y. 2017. Anti-Alzheimer properties of probiotic, Lactobacillus plantarum MTCC 1325 in Alzheimer's disease-induced albino rats. J Clin Diagn Red 11:KC01. https://doi.org/10.7860/JCDR/2017/26106.10428.

Nisoli, E., Clementi, E., Moncada, S., and Carruba, M.O. (2004). Mitochondrial biogenesis as a cellular signaling framework. Biochem. Pharmacol. 67, 1-15.

Nordengen, K., Heuser, C., Rinholm, J.E. et al. Localisation of N-acetylaspartate in oligodendrocytes/myelin. Brain Struct Funct 220, 899–917 (2015). https://doi.org/10.1007/s00429-013-0691-7

Norris, G.T.; Kipnis, J. Immune Cells and CNS Physiology: Microglia and Beyond. J. Exp. Med. 2019, 216, 60–70.

O'Connor A, McClean S. The Role of Universal Stress Proteins in Bacterial Infections. Curr Med Chem. 2017 Nov 24;24(36):3970-3979. doi: 10.2174/0929867324666170124145543. PMID: 28120710.

Oezen, I., Rossmanith, W., Forss-Petter, S., Kemp, S., Voigtlander, T., Moser-Thier, K., Wanders, R.J., Bittner, R.E., and Berger, J. (2005). Accumulation of very long-chain fatty acids does not affect mitochondrial function in adrenoleukodystrophy protein deficiency. Hum. Mol. Genet. 14, 1127-1137.

Olsen GJ, Overbeek R, Larsen N, Marsh TL, McCaughey MJ, et al. 1992. The ribosomal database project. Nucleic Acids Res. 20(Suppl.):2199–200.

Ormazabal, A., Casado, M., Molero-Luis, M., Montoya, J., Rahman, S., Aylett, S.-B., et al. (2015). Can folic acid have a role in mitochondrial disorders? Drug Discov. Today 20, 1349–1354. doi: 10.1016/j.drudis.2015.07.002

Osellame LD, Blacker TS, Duchen MR. Cellular and molecular mechanisms of mitochondrial function. Best Pract Res Clin Endocrinol Metab. 2012 Dec;26(6):711-23. doi: 10.1016/j.beem.2012.05.003. Epub 2012 Jun 23. PMID: 23168274; PMCID: PMC3513836.

Ouyang Y, Wu Q, Li J, Sun S, Sun S. S-adenosylmethionine: A metabolite critical to the regulation of autophagy. Cell Prolif. 2020 Nov;53(11):e12891. doi: 10.1111/cpr.12891. Epub 2020 Oct 8. PMID: 33030764; PMCID: PMC7653241.

Owaga E, Hsieh RH, Mugendi B, Masuku S, Shih CK, Chang JS. Th17 Cells as Potential Probiotic Therapeutic Targets in Inflammatory Bowel Diseases. Int J Mol Sci. 2015 Sep 1;16(9):20841-58. doi: 10.3390/ijms160920841. PMID: 26340622; PMCID: PMC4613231

Papadopoulos V, Miller WL. Role of mitochondria in steroidogenesis. Best Pract Res Clin Endocrinol Metabol. (2012) 26:771–90. doi: 10.1016/j.beem. 2012.05.002

Parameswaran J, Goicoechea L, Planas-Serra L, Pastor A, Ruiz M, Calingasan NY, Guilera C, Aso E, Boada J, Pamplona R, Portero-Otín M, de la Torre R, Ferrer I, Casasnovas C, Pujol A, Fourcade S. Activating cannabinoid receptor 2 preserves axonal health through GSK-3β/NRF2 axis in adrenoleukodystrophy. Acta Neuropathol. 2022 Aug;144(2):241-258. doi: 10.1007/s00401-022-02451-2. Epub 2022 Jul 1. PMID: 35778568.

Park JC, Im SH. Of men in mice: the development and application of a humanized gnotobiotic mouse model for microbiome therapeutics. Exp Mol Med. 2020 Sep;52(9):1383-1396. doi: 10.1038/s12276-020-0473-2. Epub 2020 Sep 10. PMID: 32908211; PMCID: PMC8080820.

Park, J. T., and Uehara, T. (2008). How bacteria consume their own exoskeletons (turnover and recycling of cell wall peptidoglycan). Microbiol. Mol. Biol. Rev. 72, 211–227. doi: 10.1128/MMBR.00027-07

Parkhitko AA, Jouandin P, Mohr SE, Perrimon N. Methionine metabolism and methyltransferases in the regulation of aging and lifespan extension across species. Aging Cell. 2019 Dec;18(6):e13034. doi: 10.1111/acel.13034. Epub 2019 Aug 28. PMID: 31460700; PMCID: PMC6826121.

Pärtty A, Kalliomäki M, Wacklin P, Salminen S, Isolauri E. 2015. A possible link between early probiotic intervention and the risk of neuropsychiatric disorders later in childhood: a randomized trial. Pediatr Res 77: 823–828.

Patel AR, Frikke-Schmidt H, Bezy O, Sabatini PV, Rittig N, Jessen N, Myers MG Jr, Seeley RJ. LPS induces rapid increase in GDF15 levels in mice, rats, and humans but is not required for anorexia in mice. Am J Physiol Gastrointest Liver Physiol. 2022 Feb 1;322(2):G247-G255. doi: 10.1152/ajpgi.00146.2021. Epub 2021 Dec 22. PMID: 34935522; PMCID: PMC8799390.

Patrick KL, Bell SL, Weindel CG, Watson RO. Exploring the "Multiple-Hit Hypothesis" of Neurodegenerative Disease: Bacterial Infection Comes Up to Bat. Front Cell Infect Microbiol. 2019 May 28;9:138. doi: 10.3389/fcimb.2019.00138. PMID: 31192157; PMCID: PMC6546885.

Patrick S, Blakely GW. Crossing the eukaryote-prokaryote divide: A ubiquitin homolog in the human commensal bacterium Bacteroides fragilis. Mob Genet Elements. 2012 May 1;2(3):149-151. doi: 10.4161/mge.21191. PMID: 23061022; PMCID: PMC3463472.

Pedersen HK, Gudmundsdottir V, Nielsen HB, Hyotylainen T, Nielsen T, Jensen BA, et al. Human gut microbes impact host serum metabolome and insulin sensitivity. Nature. (2016) 535:376–81. doi: 10.1038/nature 18646

Peeters, A., Shinde, A.B., Dirkx, R., Smet, J., De Bock, K., Espeel, M., Vanhorebeek, I., Vanlander, A., Van Coster, R., Carmeliet, P., et al. (2015). Mitochondria in peroxisome- deficient hepatocytes exhibit impaired respiration, depleted DNA, and PGC-1alpha independent proliferation. Biochim. Biophys. Acta 1853, 285-298.

Peggion C, Calì T, Brini M. Mitochondria Dysfunction and Neuroinflammation in Neurodegeneration: Who Comes First? Antioxidants (Basel). 2024 Feb 16;13(2):240. doi: 10.3390/antiox13020240. PMID: 38397838; PMCID: PMC10885966.

Pérez-Jiménez J, Fezeu L, Touvier M, Arnault N, Manach C, Hercberg S, Galan P, Scalbert A. Dietary intake of 337 polyphenols in French adults. Am J Clin Nutr. 2011 Jun;93(6):1220-8. doi: 10.3945/ajcn.110.007096. Epub 2011 Apr 13. PMID: 21490142.

Perino A, Demagny H, Velazquez-Villegas L, Schoonjans K. Molecular Physiology of Bile Acid Signaling in Health, Disease, and Aging. Physiol Rev. 2021 Apr 1;101(2):683-731. doi: 10.1152/physrev.00049.2019. Epub 2020 Aug 13. PMID: 32790577.

Peters A, Krumbholz P, Jäger E, Heintz-Buschart A, Çakir MV, Rothemund S, Gaudl A, Ceglarek U, Schöneberg T, Stäubert C. Metabolites of lactic acid bacteria present in fermented foods are highly potent agonists of human hydroxycarboxylic acid receptor 3. PLoS Genet. 2019 May 23;15(5):e1008145. doi: 10.1371/journal.pgen.1008145. Erratum in: PLoS Genet. 2019 Jul 19;15(7):e1008283. PMID: 31120900; PMCID: PMC6532841.

Petrillo, S., Piemonte, F., Pastore, A., Tozzi, G., Aiello, C., Pujol, A., Cappa, M., and Bertini, E. (2013). Glutathione imbalance in patients with X-linked adrenoleukodystrophy. Mol. Genet. Metab. 109, 366-370.

Picard, M.; Taivassalo, T.; Gouspillou, G.; Hepple, R.T. Mitochondria: Isolation, Structure and Function. J. Physiol. 2011, 589, 4413–4421.

Pickrell, A. M., and Youle, R. J. (2015). The roles of PINK1, parkin, and mitochondrial fidelity in Parkinson’s disease. Neuron 85, 257–273. doi: 10.1016/ j.neuron.2014.12.007

Pinheiro, J., Bates, D., DebRoy, S., Sarkar, D. and Team, R.C. (2021), In R package version 3.1-152, https://CRAN.R-project.org/package=nlme).

Pircher PC, Kitto JL, Petrowski ML, Tangirala RK, Bischoff ED, Schulman IG, Westin SK. Farnesoid X receptor regulates bile acid-amino acid conjugation. J Biol Chem. 2003 Jul 25;278(30):27703-11. doi: 10.1074/jbc.M302128200. Epub 2003 May 16. PMID: 12754200.

Pizcueta P, Vergara C, Emanuele M, Vilalta A, Rodríguez-Pascau L, Martinell M. Development of PPARγ Agonists for the Treatment of Neuroinflammatory and Neurodegenerative Diseases: Leriglitazone as a Promising Candidate. Int J Mol Sci. 2023 Feb 6;24(4):3201. doi: 10.3390/ijms24043201. PMID: 36834611; PMCID: PMC9961553.

Poirier Y, Antonenkov VD, Glumoff T, Hiltunen JK. Peroxisomal beta-oxidation--a metabolic pathway with multiple functions. Biochim Biophys Acta. 2006 Dec;1763(12):1413-26. doi: 10.1016/j.bbamcr.2006.08.034. Epub 2006 Aug 30. PMID: 17028011.

Portune, K.J., Beaumont, M., Davila, A.M., Tome´, D., Blachier, F., and Sanz, Y. (2016). Gut microbiota role in dietary protein metabolism and health-related outcomes: The two sides of the coin. Trends Food Sci. Technol. 57, 213–232. https://doi.org/10.1016/J.TIFS.2016.08.011

Powers, J.M., and Schaumberg, H.H. (1974). Adreno-leukodystrophy. Similar ultrastructural changes in adrenal cortical and Schwann cells. Arch. Neurol. 30, 406-408.

Powers JM, DeCiero DP, Ito M, Moser AB, Moser HW. Adrenomyeloneuropathy: a neuropathologic review featuring its noninflammatory myelopathy. J Neuropathol Exp Neurol. 2000 Feb;59(2):89-102. doi: 10.1093/jnen/59.2.89. PMID: 10749098.

Powers, J.M., DeCiero, D.P., Cox, C., Richfield, E.K., Ito, M., Moser, A.B., and Moser, H.W. (2001). The dorsal root ganglia in adrenomyeloneuropathy: neuronal atrophy and abnormal mitochondria. J. Neuropathol. Exp. Neurol. 60, 493-501.

Powers JM, Pei ZT, Heinzer AK, Deering R, Moser AB, Moser HW, et al. Adreno-leukodystrophy: oxidative stress of mice and men. J Neuropath Exp Neur. (2005) 64:1067–79. doi: 10.1097/01.jnen.0000190064.28559.a4

Pradhan, S., Bacolla, A., Wells, R. D., and Roberts, R. J. (1999). Recombinant human DNA (cytosine-5) methyltransferase. I. Expression, purification, and comparison of novo and maintenance methylation. J. Biol. Chem. 274, 33002– 33010. doi: 10.1074/jbc.274.46.33002

Pujol A., Hindelang C., Callizot N., Bartsch U., Schachner M., Mandel J.L. Late onset neurological phenotype of the X-ALD gene inactivation in mice: A mouse model for adrenomyeloneuropathy. Hum. Mol. Genet. 2002;11:499–505. doi: 10.1093/hmg/11.5.499.

Pujol A., Ferrer I., Camps C., Metzger E., Hindelang C., Callizot N., Ruiz M., Pampols T., Giros M., Mandel J.L. Functional overlap between ABCD1 (ALD) and ABCD2 (ALDR) transporters: A therapeutic target for X-adrenoleukodystrophy. Hum. Mol. Genet. 2004;13:2997–3006. doi: 10.1093/hmg/ddh323.

Qin J, Li R, Raes J, Arumugam M, Burgdorf KS, Manichanh C et al (2010) A human gut microbial gene catalogue established by metagenomic sequencing. Nature 464(7285):59–65. https://doi.org/10.1038/nature0882

Quince C, Walker AW, Simpson JT, Loman NJ, Segata N. Shotgun metagenomics, from sampling to analysis. Nat Biotechnol. 2017 Sep 12;35(9):833-844. doi: 10.1038/nbt.3935. Erratum in: Nat Biotechnol. 2017 Dec 8;35(12):1211. PMID: 28898207.

Quinn, R.A., Melnik, A.V., Vrbanac, A., Fu, T., Patras, K.A., Christy, M.P., Bodai, Z., Belda-Ferre, P., Tripathi, A., Chung, L.K., et al. (2020). Global chemical effects of the microbiome include new bile-acid conjugations. Nature 579, 123–129. https://doi.org/10.1038/s41586-020-2047-9.

Quirós, P. M., Mottis, A., and Auwerx, J. (2016). Mitonuclear communication in homeostasis and stress. Nat. Rev. Mol. Cell Biol. 17, 213–226. doi: 10.1038/nrm. 2016.23

R Core Team (2022). R: A Language and Environment for Statistical Computing. R Foundation for Statistical Computing, Vienna, Austria. https://www.R-project.org/.

Raas Q., Gondcaille C., Hamon Y., Leoni V., Caccia C., Ménétrier F., Lizard G., Trompier D., Savary S. CRISPR/Cas9-mediated knockout of Abcd1 and Abcd2 genes in BV-2 cells: Novel microglial models for X-linked Adrenoleukodystrophy. Biochim. Biophys. Acta Mol. Cell. Biol. Lipids. 2019;1864:704–714. doi: 10.1016/j.bbalip.2019.02.006

Rackham, O., Shearwood, A. M. J., Mercer, T. R., Davies, S. M. K., Mattick, J. S., and Filipovska, A. (2011). Long noncoding RNAs are generated from the mitochondrial genome and regulated by nuclear-encoded proteins. RNA 17, 2085–2093. doi: 10.1261/rna.029405.111

Rajagopal, M., and Walker, S. (2017). Envelope structures of gram-positive bacteria. Curr. Top. Microbiol. Immunol. 404, 1–44. doi: 10.1007/82_2015_5021

Ramsahoye, B. H., Biniszkiewicz, D., Lyko, F., Clark, V., Bird, A. P., and Jaenisch, R. (2000). Non-CpG methylation is prevalent in embryonic stem cells and may be mediated by DNA methyltransferase 3a. Proc. Natl. Acad. Sci. U.S.A. 97, 5237–5242. doi: 10.1073/pnas.97.10.5237

Ranea-Robles, P., Launay, N., Ruiz, M., Calingasan, N.Y., Dumont, M., Naudi, A., Portero- Otin, M., Pamplona, R., Ferrer, I., Beal, M.F., et al. (2018). Aberrant regulation of the GSK- 3beta/NRF2 axis unveils a novel therapy for adrenoleukodystrophy. EMBO Mol. Med. 10.

Rasmussen KD, Helin K. Role of TET enzymes in DNA methylation, development, and cancer. Genes Dev. 2016 Apr 1;30(7):733-50. doi: 10.1101/gad.276568.115. PMID: 27036965; PMCID: PMC4826392.

Raymond GV, Moser AB, Fatemi A. X-Linked Adrenoleukodystrophy. 1999 Mar 26 [Updated 2023 Apr 6]. In: Adam MP, Feldman J, Mirzaa GM, et al., editors. GeneReviews® [Internet]. Seattle (WA): University of Washington, Seattle; 1993-2024.

Reith, J., and Mayer, C. (2011). Peptidoglycan turnover and recycling in Gram-positive bacteria. Appl. Microbiol. Biotechnol. 92, 1–11. doi: 10.1007/s00253-011-3486-x

Reitz C. 2012. Alzheimer's disease and the amyloid cascade hypothesis: a critical review. Int J Alzheimer's Dis 2012:1–11. https://doi.org/10.1155/2012/ 369808.

Reynolds EH. The neurology of folic acid deficiency. Handb Clin Neurol. 2014;120:927-43. doi: 10.1016/B978-0-7020-4087-0.00061-9. PMID: 24365361.

Rezaeiasl Z, Salami M, Sepehri G. 2019. The effects of probiotic Lactobacillus and Bifidobacterium strains on memory and learning behavior, long-term potentiation (ltp), and some biochemical parameters in b-amyloid-induced rat's model of alzheimer's disease. Prev Nutr Food Sci 24:265–273. https://doi.org/10.3746/pnf.2019.24.3.265.

Rhodin J (1954) Correlation of ultrastructural organization and function in normal and experimentally changed proximal convoluted tubule cells of the mouse kidney. Karolinska Institutet, Stockholm

Ridlon JM, Kang D-J, Hylemon PB (2006) Bile salt biotransformations by human intestinal bacteria. J Lipid Res 47:241–259

Ridlon JM, Wolf PG, Gaskins R (2016) Taurocholic acid metabolism by gut microbes and colon cancer. Gut Microbes 7:201–215

Riley JS, Tait SW. Mitochondrial DNA in inflammation and immunity. EMBO Rep. 2020 Apr 3;21(4):e49799. doi: 10.15252/embr.201949799. Epub 2020 Mar 23. PMID: 32202065; PMCID: PMC7132203.

Rinninella E, Raoul P, Cintoni M, Franceschi F, Miggiano GAD, Gasbarrini A, Mele MC. What is the Healthy Gut Microbiota Composition? A Changing Ecosystem across Age, Environment, Diet, and Diseases. Microorganisms. 2019 Jan 10;7(1):14.

Ríos-Covián D, Ruas-Madiedo P, Margolles A, Gueimonde M, de los Reyes-Gavilán CG, Salazar N. 2016. Intestinal short chain fatty acids and their link with diet and human health. Front Microbiol 7:185. https://doi .org/10.3389/fmicb.2016.00185.

Ritchie ME, Phipson B, Wu D, Hu Y, Law CW, Shi W, Smyth GK. limma powers differential expression analyses for RNA-sequencing and microarray studies. Nucleic Acids Res. 2015 Apr 20;43(7):e47. doi: 10.1093/nar/gkv007. Epub 2015 Jan 20. PMID: 25605792; PMCID: PMC4402510.

Rizzo Gianluca, Laganà Antonio Simone ,Chapter 6 - A review of vitamin B12,Editor(s): Vinood B. Patel, Molecular Nutrition, Academic Press,2020, Pages 105-129, ISBN 9780128119075.

Roager HM, Licht TR. 2018. Microbial tryptophan catabolites in health and disease. Nat Commun 9:1–10.

Rocco A, Sgamato C, Compare D, Coccoli P, Nardone OM, Nardone G. Gut Microbes and Hepatic Encephalopathy: From the Old Concepts to New Perspectives. Front Cell Dev Biol. 2021 Nov 26;9:748253. doi: 10.3389/fcell.2021.748253. PMID: 34900994; PMCID: PMC8662376.

Rodríguez-Pascau L, Vilalta A, Cerrada M, Traver E, Forss-Petter S, Weinhofer I, Bauer J, Kemp S, Pina G, Pascual S, Meya U, Musolino PL, Berger J, Martinell M, Pizcueta P. The brain penetrant PPARγ agonist leriglitazone restores multiple altered pathways in models of X-linked adrenoleukodystrophy. Sci Transl Med. 2021 Jun 2;13(596):eabc0555. doi: 10.1126/scitranslmed.abc0555. PMID: 34078742.

Roger AJ, Muñoz-Gómez SA, Kamikawa R (2017) The origin and diversification of mitochondria. Curr Biol 27: R1177 – R1192

Rogers G, Keating D, Young R, Wong M, Licinio J, Wesselingh S. 2016. From gut dysbiosis to altered brain function and mental illness: mechanisms and pathways. Mol Psychiatry 21:738–748. https://doi.org/10.1038/mp.2016.50

Rowland I, Gibson G, Heinken A, Scott K, Swann J, Thiele I, Tuohy K. Gut microbiota functions: metabolism of nutrients and other food components. Eur J Nutr. 2018 Feb;57(1):1-24. doi: 10.1007/s00394-017-1445-8. Epub 2017 Apr 9. PMID: 28393285; PMCID: PMC5847071.

Royet, J., Gupta, D., and Dziarski, R. (2011). Peptidoglycan recognition proteins: modulators of the microbiome and inflammation. Nat. Rev. Immunol. 11, 837–851. doi: 10.1038/nri3089

Ruan C, Elyaman W. A New Understanding of TMEM119 as a Marker of Microglia. Front Cell Neurosci. 2022 Jun 13;16:902372. doi: 10.3389/fncel.2022.902372. PMID: 35769325; PMCID: PMC9234454.

Ruiz, N. (2008). Bioinformatics identification of MurJ (MviN) as the peptidoglycan lipid II flippase in Escherichia coli. Proc. Natl. Acad. Sci. U.S.A. 105, 15553–15557. doi: 10.1073/pnas.0808352105

Russell WR, Duncan SH, Scobbie L, Duncan G, Cantlay L, Calder AG, Anderson SE, Flint HJ (2013) Major phenylpropanoidderived metabolites in the human gut can arise from microbial fermentation of protein. Mol Nutr Food Res 57:523–535

Russell WR, Scobbie L, Chesson A, Richardson AJ, Stewart CS, Duncan SH, Drew JE, Duthie GG. Anti-inflammatory implications of the microbial transformation of dietary phenolic compounds. Nutr Cancer. 2008;60(5):636-42. doi: 10.1080/01635580801987498. PMID: 18791927.

Rutsch A, Kantsjö JB, Ronchi F. The Gut-Brain Axis: How Microbiota and Host Inflammasome Influence Brain Physiology and Pathology. Front Immunol. 2020 Dec 10;11:604179. doi: 10.3389/fimmu.2020.604179. PMID: 33362788; PMCID: PMC7758428.

Sagan L. On the origin of mitosing cells. J Theor Biol. 1967 Mar;14(3):255-74. doi: 10.1016/0022-5193(67)90079-3. PMID: 11541392.

Salcedo C, Andersen JV, Vinten KT, Pinborg LH, Waagepetersen HS, Freude KK, Aldana BI. Functional Metabolic Mapping Reveals Highly Active Branched-Chain Amino Acid Metabolism in Human Astrocytes, Which Is Impaired in iPSC-Derived Astrocytes in Alzheimer's Disease. Front Aging Neurosci. 2021 Sep 17;13:736580. doi: 10.3389/fnagi.2021.736580. PMID: 34603012; PMCID: PMC8484639.

Salim S. Oxidative stress and the central nervous system. J Pharmacol Exp Therapeut. (2017) 360:201–5. doi: 10.1124/jpet.116.237503

Salton MRJ, Kim KS. Structure. In: Baron S, editor. Medical Microbiology. 4th edition. Galveston (TX): University of Texas Medical Branch at Galveston; 1996. Chapter 2. Available from: https://www.ncbi.nlm.nih.gov/books/NBK8477

Salzman NH, Hung K, Haribhai D, Chu H, Karlsson-Sjöberg J, Amir E, Teggatz P, Barman M, Hayward M, Eastwood D, Stoel M, Zhou Y, Sodergren E, Weinstock GM, Bevins CL, Williams CB, Bos NA. Enteric defensins are essential regulators of intestinal microbial ecology. Nat Immunol. 2010 Jan;11(1):76-83. doi: 10.1038/ni.1825. Epub 2009 Oct 22. PMID: 19855381; PMCID: PMC2795796.

Salzman R., Kemp S., www.x-ald.nl, last update at 02/05/2024

Sampson TR, Mazmanian SK. Control of brain development, function, and behavior by the microbiome. Cell Host Microbe. 2015 May 13;17(5):565-76. doi: 10.1016/j.chom.2015.04.011. PMID: 25974299; PMCID: PMC4442490.

Sampson TR, Debelius JW, Thron T, Janssen S, Shastri GG, Ilhan ZE, Challis C, Schretter CE, Rocha S, Gradinaru V, Chesselet MF, Keshavarzian A, Shannon KM, Krajmalnik-Brown R, Wittung-Stafshede P, Knight R, Mazmanian SK. Gut Microbiota Regulate Motor Deficits and Neuroinflammation in a Model of Parkinson's Disease. Cell. 2016 Dec 1;167(6):1469-1480.e12. doi: 10.1016/j.cell.2016.11.018. PMID: 27912057; PMCID: PMC5718049.

Sanderson SM, Gao X, Dai Z, Locasale JW. Methionine metabolism in health and cancer: a nexus of diet and precision medicine. Nat Rev Cancer. 2019 Nov;19(11):625-637.

Sanger F, Nicklen S, Coulson AR (1977) DNA sequencing with chain-terminating inhibitors. Proc Natl Acad Sci USA 74(12):5463–5467

Santhakumar A.B., M. Battino, J.M. Alvarez-Suarez. Dietary polyphenols: Structures, bioavailability and protective effects against atherosclerosis Food and Chemical Toxicology, 113 (2018), pp. 49-65

Sasso JM, Ammar RM, Tenchov R, Lemmel S, Kelber O, Grieswelle M, Zhou QA. Gut Microbiome-Brain Alliance: A Landscape View into Mental and Gastrointestinal Health and Disorders. ACS Chem Neurosci. 2023 May 17;14(10):1717-1763.

Sato H, Takado Y, Toyoda S, Tsukamoto-Yasui M, Minatohara K, Takuwa H, Urushihata T, Takahashi M, Shimojo M, Ono M, Maeda J, Orihara A, Sahara N, Aoki I, Karakawa S, Isokawa M, Kawasaki N, Kawasaki M, Ueno S, Kanda M, Nishimura M, Suzuki K, Mitsui A, Nagao K, Kitamura A, Higuchi M. Neurodegenerative processes accelerated by protein malnutrition and decelerated by essential amino acids in a tauopathy mouse model. Sci Adv. 2021 Oct 22;7(43):eabd5046. doi: 10.1126/sciadv.abd5046. Epub 2021 Oct 22. PMID: 34678069; PMCID: PMC8535828.

Savage DC, Siegel JE, Snellen JE, Whitt DD. Transit time of epithelial cells in the small intestines of germfree mice and ex-germfree mice associated with indigenous microorganisms. Appl Environ Microbiol. 1981 Dec;42(6):996-1001. doi: 10.1128/aem.42.6.996-1001.1981. PMID: 7198427; PMCID: PMC244145.

Scalise M, Galluccio M, Console L, Pochini L, Indiveri C. The Human SLC7A5 (LAT1): The Intriguing Histidine/Large Neutral Amino Acid Transporter and Its Relevance to Human Health. Front Chem. 2018 Jun 22;6:243. doi: 10.3389/fchem.2018.00243. PMID: 29988369; PMCID: PMC6023973.

Schaumburg H.H., Powers J.M., Suzuki K., Raine C.S. Adreno-leukodystrophy (sex-linked Schilder disease). Ultrastructural demonstration of specific cytoplasmic inclusions in the central nervous system. Arch. Neurol. 1974;31:210–213. doi: 10.1001/archneur.1974.00490390092013.

Scheurwater, E., Reid, C. W., and Clarke, A. J. (2008). Lytic transglycosylases: bacterial space-making autolysins. Int. J. Biochem. Cell Biol. 40, 586–591. doi: 10.1016/j.biocel.2007.03.018

Scheurwater, E. M., and Burrows, L. L. (2011). Maintaining network security: how macromolecular structures cross the peptidoglycan layer. FEMS Microbiol. Lett. 318, 1–9. doi: 10.1111/j.1574-6968.2011.02228.x

Schiering C, Wincent E, Metidji A, Iseppon A, Li Y, Potocnik AJ, Omenetti S, Henderson CJ, Wolf CR, Nebert DW, Stockinger B. 2017. Feedback control of AHR signalling regulates intestinal immunity. Nature 542:242–245. https://doi .org/10.1038/nature21080.

Schilder, P. (1924). Die Encephalitis periaxialis diffusa. Arch Psychiatr. Nervenkr. 71, 327–356.

Schloss PD, Handelsman J. 2005. Introducing DOTUR, a computer program for defining operational taxonomic units and estimating species richness. Appl. Environ. Microbiol. 71:1501–6

Schluter, A., Fourcade, S., Ripp, R., Mandel, J.L., Poch, O., and Pujol, A. (2006). The evolutionary origin of peroxisomes: an ER-peroxisome connection. Mol. Biol. Evol. 23, 838- 845.

Schluter, A., Real-Chicharro, A., Gabaldon, T., Sanchez-Jimenez, F., and Pujol, A. (2010). PeroxisomeDB 2.0: an integrative view of the global peroxisomal metabolome. Nucleic Acids Res. 38, D800-805.

Schluter, A., Espinosa, L., Fourcade, S., Galino, J., Lopez, E., Ilieva, E., Morato, L., Asheuer, M., Cook, T., McLaren, A., et al. (2012). Functional genomic analysis unravels a metabolic- inflammatory interplay in adrenoleukodystrophy. Hum. Mol. Genet. 21, 1062-1077.

Schmit KJ, Garcia P, Sciortino A, Aho VTE, Pardo Rodriguez B, Thomas MH, Gérardy JJ, Bastero Acha I, Halder R, Cialini C, Heurtaux T, Ostahi I, Busi SB, Grandmougin L, Lowndes T, Singh Y, Martens EC, Mittelbronn M, Buttini M, Wilmes P. Fiber deprivation and microbiome-borne curli shift gut bacterial populations and accelerate disease in a mouse model of Parkinson's disease. Cell Rep. 2023 Sep 26;42(9):113071. doi: 10.1016/j.celrep.2023.113071. Epub 2023 Sep 8. PMID: 37676767; PMCID: PMC10548091.

Schneider, T., and Sahl, H. G. (2010). An oldie but a goodie—cell wall biosynthesis as antibiotic target pathway. Int. J. Med. Microbiol. 300, 161–169. doi: 10.1016/j.ijmm.2009.10.005

Schober FA, Tang JX, Sergeant K, Moedas MF, Zierz CM, Moore D, Smith C, Lewis D, Guha N, Hopton S, Falkous G, Lam A, Pyle A, Poulton J, Gorman GS, Taylor RW, Freyer C, Wredenberg A. Pathogenic SLC25A26 variants impair SAH transport activity causing mitochondrial disease. Hum Mol Genet. 2022 Jun 22;31(12):2049-2062. doi: 10.1093/hmg/ddac002. PMID: 35024855; PMCID: PMC9239748.

Schoenfeld, R., Wong, A., Silva, J., Li, M., Itoh, A., Horiuchi, M., Itoh, T., Pleasure, D., and Cortopassi, G. (2010). Oligodendroglial differentiation induces mitochondrial genes and inhibition of mitochondrial function represses oligodendroglial differentiation. Mitochondrion 10, 143-150.

Schön M, Mousa A, Berk M, Chia WL, Ukropec J, Majid A, Ukropcová B, de Courten B. The Potential of Carnosine in Brain-Related Disorders: A Comprehensive Review of Current Evidence. Nutrients. 2019 May 28;11(6):1196. doi: 10.3390/nu11061196. PMID: 31141890; PMCID: PMC6627134.

Schrader M, Costello J, Godinho LF, Islinger M. Peroxisome-mitochondria interplay and disease. J Inherit Metab Dis. 2015 Jul;38(4):681-702. doi: 10.1007/s10545-015-9819-7. Epub 2015 Feb 17. PMID: 25687155.

Schroder, J.M., Mayer, M., and Weis, J. (1996). Mitochondrial abnormalities and intrafamilial variability of sural nerve biopsy findings in adrenomyeloneuropathy. Acta Neuropathol. 92, 64- 69.

Schubert, A. M., Sinani, H., and Schloss, P. D. (2015). Antibiotic-induced alterations of the murine gut microbiota and subsequent effects on colonization resistance against clostridium difficile. mBio 6:e00974-15. doi: 10.1128/mBio.00974-15

Seckler JM, Lewis SJ. Advances in D-Amino Acids in Neurological Research. Int J Mol Sci. 2020 Oct 3;21(19):7325. doi: 10.3390/ijms21197325. PMID: 33023061; PMCID: PMC7582301.

Sekirov, I., Russell, S. L., Antunes, L. C. M. & Finlay, B. B. Gut microbiota in health and disease. Physiol. Rev. 90, 859–904 (2010).

Segal R, Baumoehl Y, Elkayam O, Levartovsky D, Litinsky I, Paran D, et al. Anemia, serum vitamin B12, and folic acid in patients with rheumatoid arthritis, psoriatic arthritis, and systemic lupus erythematosus. Rheumatol Int. (2004) 24:14–9. doi: 10.1007/s00296-003-0323-2

Selma M.V, J.C. Espin, F.A. Tomas-Barberan. Interaction between phenolics and gut microbiota: role in human health. Journal of Agricultural and Food Chemistry, 57 (15) (2009), pp. 6485-6501

Sena, L. A., and Chandel, N. S. (2012). Physiological roles of mitochondrial reactive oxygen species. Mol. Cell. 48, 158–167. doi: 10.1016/j.molcel.2012.09.025

Shai N, Schuldiner M, Zalckvar E. No peroxisome is an island - Peroxisome contact sites. Biochim Biophys Acta. 2016 May;1863(5):1061-9. doi: 10.1016/j.bbamcr.2015.09.016. Epub 2015 Sep 16. PMID: 26384874; PMCID: PMC4869879.

Shanahan F, Ghosh TS, O'Toole PW. The Healthy Microbiome-What Is the Definition of a Healthy Gut Microbiome? Gastroenterology. 2021 Jan;160(2):483-494. doi: 10.1053/j.gastro.2020.09.057. Epub 2020 Nov 27. PMID: 33253682.

Shani N., Jimenez-Sanchez G., Steel G., Dean M., Valle D. Identification of a fourth half ABC transporter in the human peroxisomal membrane. Hum. Mol. Genet. 1997;6:1925–1931. doi: 10.1093/hmg/6.11.1925.

Sharon G, Sampson TR, Geschwind DH, Mazmanian SK. 2016. The central nervous system and the gut microbiome. Cell 167:915–932. https://doi .org/10.1016/j.cell.2016.10.027.

Shin N.R., J.C. Lee, H.Y. Lee, M.S. Kim, T.W. Whon, M.S. Lee, J.W. Bae. An increase in the Akkermansia spp. population induced by metformin treatment improves glucose homeostasis in diet-induced obese mice Gut, 63 (5) (2014), pp. 727-735

Shinomoto M, Kasai T, Tatebe H, Kitani-Morii F, Ohmichi T, Fujino Y, Allsop D, Mizuno T, Tokuda T. Cerebral spinal fluid biomarker profiles in CNS infection associated with HSV and VZV mimic patterns in Alzheimer's disease. Transl Neurodegener. 2021 Jan 4;10(1):2. doi: 10.1186/s40035-020-00227-w. PMID: 33397456; PMCID: PMC7780670.

Siemerling, E., and Creutzfeldt, H.G. (1923). Bronzekrankheit und sklerosierende encephalomyelitis. Arch. Psychiatr Nervenkr. 68, 217-244.

Sies H., Berndt C., Jones D.P. Oxidative stress. Annu. Rev. Biochem. 2017;86:715–748. doi: 10.1146/annurev-biochem-061516-045037.

Sies H, Jones DP. Reactive oxygen species (ROS) as pleiotropic physiological signalling agents. Nat Rev Mol Cell Biol. 2020 Jul;21(7):363-383. doi: 10.1038/s41580-020-0230-3. Epub 2020 Mar 30. PMID: 32231263.

Silva, G. G. Z., Green K., B. E. Dutilh, and R. A. Edwards: SUPER-FOCUS: A tool for agile functional analysis of shotgun metagenomic data. Bioinformatics. 2015 Oct 9. pii: btv584. Website: https://edwards.sdsu.edu/SUPERFOCUS

Silva, J.M., Wong, A., Carelli, V., and Cortopassi, G.A. (2009). Inhibition of mitochondrial function induces an integrated stress response in oligodendroglia. Neurobiol. Dis. 34, 357-365

Silva YP, Bernardi A, Frozza RL. 2020. The role of short-chain fatty acids from gut microbiota in gut-brain communication. Front Endocrinol (Lausanne) 11:25.

Sinenko SA, Starkova TY, Kuzmin AA, Tomilin AN. Physiological Signaling Functions of Reactive Oxygen Species in Stem Cells: From Flies to Man. Front Cell Dev Biol. 2021 Aug 6;9:714370. doi: 10.3389/fcell.2021.714370. PMID: 34422833; PMCID: PMC8377544.

Singh, I., Moser, A.E., Moser, H.W., and Kishimoto, Y. (1984b). Adrenoleukodystrophy: impaired oxidation of very long chain fatty acids in white blood cells, cultured skin fibroblasts, and amniocytes. Pediatr. Res. 18, 286-290.

Singh, I., and Pujol, A. (2010). Pathomechanisms underlying X-adrenoleukodystrophy: a three- hit hypothesis. Brain Pathol. 20, 838-844.

Singh P, Gollapalli K, Mangiola S, Schranner D, Yusuf MA, Chamoli M, Shi SL, Lopes Bastos B, Nair T, Riermeier A, Vayndorf EM, Wu JZ, Nilakhe A, Nguyen CQ, Muir M, Kiflezghi MG, Foulger A, Junker A, Devine J, Sharan K, Chinta SJ, Rajput S, Rane A, Baumert P, Schönfelder M, Iavarone F, di Lorenzo G, Kumari S, Gupta A, Sarkar R, Khyriem C, Chawla AS, Sharma A, Sarper N, Chattopadhyay N, Biswal BK, Settembre C, Nagarajan P, Targoff KL, Picard M, Gupta S, Velagapudi V, Papenfuss AT, Kaya A, Ferreira MG, Kennedy BK, Andersen JK, Lithgow GJ, Ali AM, Mukhopadhyay A, Palotie A, Kastenmüller G, Kaeberlein M, Wackerhage H, Pal B, Yadav VK. Taurine deficiency as a driver of aging. Science. 2023 Jun 9;380(6649):eabn9257. doi: 10.1126/science.abn9257. Epub 2023 Jun 9. PMID: 37289866; PMCID: PMC10630957.

Smith EA, Macfarlane GT (1996) Enumeration of human colonic bacteria producing phenolic and indolic compounds: effects of pH, carbohydrate availability and retention time on dissimilatory aromatic amino acid metabolism. J Appl Bacteriol 81:288–302

Smith JJ, Aitchison JD. Peroxisomes take shape. Nat Rev Mol Cell Biol. 2013 Dec;14(12):803-17. doi: 10.1038/nrm3700. PMID: 24263361; PMCID: PMC4060825.

Smith PM, Howitt MR, Panikov N, Michaud M, Gallini CA, Bohlooly-Y M, Glickman JN, Garrett WS. 2013. The microbial metabolites, short-chain fatty acids, regulate colonic Treg cell homeostasis. Science 341:569–573.

Sochocka M, Donskow-Łysoniewska K, Diniz BS, Kurpas D, Brzozowska E, Leszek J. The Gut Microbiome Alterations and Inflammation-Driven Pathogenesis of Alzheimer's Disease-a Critical Review. Mol Neurobiol. 2019 Mar;56(3):1841-1851. doi: 10.1007/s12035-018-1188-4. Epub 2018 Jun 23. PMID: 29936690; PMCID: PMC6394610.

Solana-Manrique C, Sanz FJ, Martínez-Carrión G, Paricio N. Antioxidant and Neuroprotective Effects of Carnosine: Therapeutic Implications in Neurodegenerative Diseases. Antioxidants (Basel). 2022 Apr 26;11(5):848. doi: 10.3390/antiox11050848. PMID: 35624713; PMCID: PMC9137727.

Son D., Quan Z., Kang P.J., Park G., Kang H.C., You S. Generation of two induced pluripotent stem cell (iPSC) lines from X-linked adrenoleukodystrophy (X-ALD) patients with adrenomyeloneuropathy (AMN) Stem Cell Res. 2017;25:46–49. doi: 10.1016/j.scr.2017.10.003.

Song CS, Echchgadda I, Baek BS, Ahn SC, Oh T, Roy AK, Chatterjee B. Dehydroepiandrosterone sulfotransferase gene induction by bile acid activated farnesoid X receptor. J Biol Chem. 2001 Nov 9;276(45):42549-56. doi: 10.1074/jbc.M107557200. Epub 2001 Aug 30. PMID: 11533040.

Sorbara, M. T., and Philpott, D. J. (2011). Peptidoglycan: a critical activator of the mammalian immune system during infection and homeostasis. Immunol. Rev. 243, 40–60. doi: 10.1111/j.1600-065X.2011.01047.x

Sorboni SG, Moghaddam HS, Jafarzadeh-Esfehani R, Soleimanpour S. A Comprehensive Review on the Role of the Gut Microbiome in Human Neurological Disorders. Clin Microbiol Rev. 2022 Jan 19;35(1):e0033820. doi: 10.1128/CMR.00338-20. Epub 2022 Jan 5. PMID: 34985325; PMCID: PMC8729913.

Sperandeo P, Martorana AM, Polissi A. Lipopolysaccharide Biosynthesis and Transport to the Outer Membrane of Gram-Negative Bacteria. Subcell Biochem. 2019;92:9-37. doi: 10.1007/978-3-030-18768-2_2. PMID: 31214983.

Stanley L. Hazen,A Cardiovascular Disease-Linked Gut Microbial Metabolite Acts via Adrenergic Receptors,Cell, Volume 180, Issue 5,2020,Pages 862-877.e22, ISSN 0092-8674,https://doi.org/10.1016/j.cell.2020.02.016.

Stayrook KR, Bramlett KS, Savkur RS, Ficorilli J, Cook T, Christe ME, Michael LF, Burris TP. Regulation of carbohydrate metabolism by the farnesoid X receptor. Endocrinology. 2005 Mar;146(3):984-91. doi: 10.1210/en.2004-0965. Epub 2004 Nov 24. PMID: 15564327.

Steimle A, Autenrieth IB, Frick JS. Structure and function: Lipid A modifications in commensals and pathogens. Int J Med Microbiol. 2016 Aug;306(5):290-301. doi: 10.1016/j.ijmm.2016.03.001. Epub 2016 Mar 5. PMID: 27009633.

Stein MM, Hrusch CL, Gozdz J, Igartua C, Pivniouk V, Murray SE, Ledford JG, Marques Dos Santos M, Anderson RL, Metwali N, Neilson JW, Maier RM, Gilbert JA, Holbreich M, Thorne PS, Martinez FD, von Mutius E, Vercelli D, Ober C, Sperling AI. Innate Immunity and Asthma Risk in Amish and Hutterite Farm Children. N Engl J Med. 2016 Aug 4;375(5):411-421. doi: 10.1056/NEJMoa1508749. PMID: 27518660; PMCID: PMC5137793.

Steliou K, Boosalis MS, Perrine SP et al (2012) Butyrate histone deacetylase inhibitors. Biores Open Access 1:192–198

Stewart L, D M Edgar J, Blakely G, Patrick S. Antigenic mimicry of ubiquitin by the gut bacterium Bacteroides fragilis: a potential link with autoimmune disease. Clin Exp Immunol. 2018 Nov;194(2):153-165. doi: 10.1111/cei.13195. Epub 2018 Sep 17. PMID: 30076785; PMCID: PMC6194340.

Strachan, L.R., Stevenson, T.J., Freshner, B., Keefe, M.D., Miranda Bowles, D., and Bonkowsky, J.L. (2017). A zebrafish model of X-linked adrenoleukodystrophy recapitulates key disease features and demonstrates a developmental requirement for abcd1 in oligodendrocyte patterning and myelination. Hum. Mol. Genet. 26, 3600-3614.

Strandwitz P. 2018. Neurotransmitter modulation by the gut microbiota. Brain Res 1693:128–133. https://doi.org/10.1016/j.brainres.2018.03.015.

Suarez F, Furne J, Springfield J, Levitt M (1997) Insights into human colonic physiology obtained from the study of flatus composition. Am J Physiol 272:G1028–G1033

Sudo N, Chida Y, Aiba Y, Sonoda J, Oyama N, Yu XN, Kubo C, Koga Y. Postnatal microbial colonization programs the hypothalamic-pituitary-adrenal system for stress response in mice. J Physiol. 2004 Jul 1;558(Pt 1):263-75. doi: 10.1113/jphysiol.2004.063388. Epub 2004 May 7. PMID: 15133062; PMCID: PMC1664925.

Sugihara, K., Morhardt, T.L., and Kamada, N. (2018). The role of dietary nutrients in inflammatory bowel disease. Front. Immunol. 9, 3183.

Sugiura, A., Mattie, S., Prudent, J., and McBride, H.M. (2017). Newly born peroxisomes are a hybrid of mitochondrial and ER-derived pre-peroxisomes. Nature 542, 251-254.

Sullivan, L. B., Gui, D. Y., Hosios, A. M., Bush, L. N., Freinkman, E., and Vander Heiden, M. G. (2015). Supporting aspartate biosynthesis is an essential function of respiration in proliferating cells. Cell 162, 552–563. doi:10.1016/j.cell.2015.07.017

Surtees R, Leonard J, Austin S. Association of demyelination with deficiency of cerebrospinal-fluid S-adenosylmethionine in inborn errors of methyl-transfer pathway. Lancet. 1991 Dec 21-28;338(8782-8783):1550-4. doi: 10.1016/0140-6736(91)92373-a. PMID: 1683972.

Taguchi, A., Welsh, M. A., Marmont, L. S., Lee, W., Sjodt, M., Kruse, A. C., et al. (2019). FtsW is a peptidoglycan polymerase that is functional only in complex with its cognate penicillin-binding protein. Nat. Microbiol. 4, 587–594. doi: 10.1038/s41564-018-0345-x

Takeda K, Akira S. Microbial recognition by Toll-like receptors. J Dermatol Sci 34: 73– 82, 2004. doi:10.1016/j.jdermsci.2003.10.002

Tamtaji OR, Taghizadeh M, Daneshvar Kakhaki R, Kouchaki E, Bahmani F, Borzabadi S, Oryan S, Mafi A, Asemi Z. Clinical and metabolic response to probiotic administration in people with Parkinson's disease: A randomized, double-blind, placebo-controlled trial. Clin Nutr. 2019 Jun;38(3):1031-1035. doi: 10.1016/j.clnu.2018.05.018. Epub 2018 Jun 1. PMID: 29891223.

Tapias, V. Editorial: Mitochondrial Dysfunction and Neurodegeneration. Front. Neurosci. 2019, 13, 1372.

Tarsa L, Goda Y. 2002. Synaptophysin regulates activity-dependent synapse formation in cultured hippocampal neurons. Proc Natl Acad Sci U S A 99:1012–1016.

Tau GZ, Peterson BS. 2010. Normal development of brain circuits. Neuropsychopharmacology 35:147–168. https://doi.org/10.1038/npp.2009.115

Tawbeh A, Gondcaille C, Trompier D, Savary S. Peroxisomal ABC Transporters: An Update. Int J Mol Sci. 2021 Jun 5;22(11):6093. doi: 10.3390/ijms22116093. PMID: 34198763; PMCID: PMC8201181.

Tazoe H, Otomo Y, Kaji I, Tanaka R, Karaki SI, Kuwahara A. Roles of short-chain fatty acids receptors, GPR41 and GPR43 on colonic functions. J Physiol Pharmacol. 2008 Aug;59 Suppl 2:251-62. PMID: 18812643.

The MetaHIT Consortium. (2011). MetaHIT: The European Union Project on Metagenomics of the Human Intestinal Tract. In: Nelson, K. (eds) Metagenomics of the Human Body. Springer, New York, NY.

The Human Microbiome Project Consortium. Structure, function and diversity of the healthy human microbiome. Nature. 2012 Jun 13;486(7402):207-14. doi: 10.1038/nature11234. PMID: 22699609; PMCID: PMC3564958.

Theiss AL, Idell RD, Srinivasan S, Klapproth JM, Jones DP, Merlin D, Sitaraman SV. Prohibitin protects against oxidative stress in intestinal epithelial cells. FASEB J. 2007 Jan;21(1):197-206. doi: 10.1096/fj.06-6801com. Epub 2006 Nov 29. PMID: 17135366.

Thion MS, Low D, Silvin A, Chen J, Grisel P, Schulte-Schrepping J, Blecher R, Ulas T, Squarzoni P, Hoeffel G, Coulpier F, Siopi E, David FS, Scholz C, Shihui F, Lum J, Amoyo AA, Larbi A, Poidinger M, Buttgereit A, Lledo P-M, Greter M, Chan JKY, Amit I, Beyer M, Schultze JL, Schlitzer A, Pettersson S, Ginhoux F, Garel S. 2018. Microbiome influences prenatal and adult microglia in a sex-specific manner. Cell 172:500–516. https://doi.org/10.1016/j.cell.2017.11.042.

Thorburn AN, Macia L, Mackay CR. 2014. Diet, metabolites, and “western-lifestyle” inflammatory diseases. Immunity 40:833–842. https://doi .org/10.1016/j.immuni.2014.05.014.

Thomson, A. W. & Knolle, P. A. Antigen-presenting cell function in the tolerogenic liver environment. Nat. Rev. Immunol. 10, 753–766 (2010).

Thul PJ, Åkesson L, Wiking M, Mahdessian D, Geladaki A, Ait Blal H, Alm T, Asplund A, Björk L, Breckels LM, Bäckström A, Danielsson F, Fagerberg L, Fall J, Gatto L, Gnann C, Hober S, Hjelmare M, Johansson F, Lee S, Lindskog C, Mulder J, Mulvey CM, Nilsson P, Oksvold P, Rockberg J, Schutten R, Schwenk JM, Sivertsson Å, Sjöstedt E, Skogs M, Stadler C, Sullivan DP, Tegel H, Winsnes C, Zhang C, Zwahlen M, Mardinoglu A, Pontén F, von Feilitzen K, Lilley KS, Uhlén M, Lundberg E. A subcellular map of the human proteome. Science. 2017 May 26;356(6340):eaal3321. doi: 10.1126/science.aal3321. Epub 2017 May 11. PMID: 28495876.

Tibbetts, A. S., and Appling, D. R. (2010). Compartmentalization of Mammalian folate-mediated one-carbon metabolism. Annu. Rev. Nutr. 30, 57–81. doi: 10. 1146/annurev.nutr.012809.104810

Tomas J, Wrzosek L, Bouznad N, Bouet S, Mayeur C, Noordine ML, Honvo-Houeto E, Langella P, Thomas M, Cherbuy C. Primocolonization is associated with colonic epithelial maturation during conventionalization. FASEB J. 2013 Feb;27(2):645-55. doi: 10.1096/fj.12-216861. Epub 2012 Nov 1. PMID: 23118025.

Torres L, Robinson SA, Kim DG, Yan A, Cleland TA, Bynoe MS. Toxoplasma gondii alters NMDAR signaling and induces signs of Alzheimer's disease in wild-type, C57BL/6 mice. J Neuroinflammation. 2018 Feb 23;15(1):57. doi: 10.1186/s12974-018-1086-8. PMID: 29471842; PMCID: PMC5824585.

Tranberg B., A.N. Madsen, A.K. Hansen, L.I. Hellgren. Whey-reduced weight gain is associated with a temporary growth reduction in young mice fed a high-fat diet Journal of Nutritional Biochemistry, 26 (1) (2015), pp. 9-15

Trifunov S, Paredes-Fuentes AJ, Badosa C, et al. Circulating cellfree mitochondrial DNA in cerebrospinal fluid as a biomarker for mitochondrial diseases. Clin Chem. 2021;67:1113-1121.

Trigo, D.; Avelar, C.; Fernandes, M.; Sá, J.; Cruz e Silva, O. Mitochondria, Energy, and Metabolism in Neuronal Health and Disease. FEBS Lett. 2022, 596, 1095–1110.

Trudler D, Ghatak S, Lipton SA. Emerging hiPSC Models for Drug Discovery in Neurodegenerative Diseases. Int J Mol Sci. 2021 Jul 30;22(15):8196. doi: 10.3390/ijms22158196. PMID: 34360966; PMCID: PMC8347370

Tsai TY, Lee TH, Wang HH, Yang TH, Chang IJ, Huang YC. Serum homocysteine, folate, and vitamin B(12) levels in patients with systemic lupus erythematosus: A meta-analysis and meta-regression. J Am Coll Nutr. (2021) 40:443– 53. doi: 10.1080/07315724.2020.1788472

Tükel C, Wilson RP, Nishimori JH, Pezeshki M, Chromy BA, Bäumler AJ. Responses to amyloids of microbial and host origin are mediated through toll-like receptor 2. Cell Host Microbe. 2009 Jul 23;6(1):45-53. doi: 10.1016/j.chom.2009.05.020. PMID: 19616765; PMCID: PMC2745191.

Tükel C, Nishimori JH, Wilson RP, Winter MG, Keestra AM, van Putten JP, Bäumler AJ. Toll-like receptors 1 and 2 cooperatively mediate immune responses to curli, a common amyloid from enterobacterial biofilms. Cell Microbiol. 2010 Oct;12(10):1495-505. doi: 10.1111/j.1462-5822.2010.01485.x. PMID: 20497180; PMCID: PMC3869100.

Turk BR, Theda C, Fatemi A, Moser AB. X-linked adrenoleukodystrophy: Pathology, pathophysiology, diagnostic testing, newborn screening and therapies. Int J Dev Neurosci. 2020 Feb;80(1):52-72. doi: 10.1002/jdn.10003. Epub 2020 Jan 26. PMID: 31909500; PMCID: PMC7041623.

Typas, A., Banzhaf, M. B., van den Berg van Saparoea, B, Verheul, J., Biboy, J., Nichols, R. J., et al. (2010). Regulation of peptidoglycan synthesis by outer-membrane proteins. Cell 143, 1097–1109. doi: 10.1016/j.cell.2010.11.038

Ueland PM, Ulvik A, Rios-Avila L, Midttun Ø, Gregory JF. Direct and Functional Biomarkers of Vitamin B6 Status. Annu Rev Nutr. 2015;35:33-70. doi: 10.1146/annurev-nutr-071714-034330. Epub 2015 May 13. PMID: 25974692; PMCID: PMC5988249.

Ullah H, Arbab S, Tian Y, Liu CQ, Chen Y, Qijie L, Khan MIU, Hassan IU, Li K. The gut microbiota-brain axis in neurological disorder. Front Neurosci. 2023 Aug 4;17:1225875. doi: 10.3389/fnins.2023.1225875. PMID: 37600019; PMCID: PMC10436500.

US Preventive Services Task Force. Folic Acid Supplementation to Prevent Neural Tube Defects: US Preventive Services Task Force Reaffirmation Recommendation Statement. JAMA. 2023;330(5):454–459. doi:10.1001/jama.2023.12876

Uto, T., Contreras, M.A., Gilg, A.G., and Singh, I. (2008). Oxidative imbalance in nonstimulated X-adrenoleukodystrophy-derived lymphoblasts. Dev. Neurosci. 30, 410-418.

Vaishnava S, Behrendt CL, Hooper LV. Innate immune responses to commensal bacteria in the gut epithelium. J Pediatr Gastroenterol Nutr. 2008 Apr;46 Suppl 1:E10-1. doi: 10.1097/01.mpg.0000313823.93841.65. PMID: 18354312.

Valencia EM, Maki KA, Dootz JN, Barb JJ. Mock community taxonomic classification performance of publicly available shotgun metagenomics pipelines. Sci Data. 2024 Jan 17;11(1):81. doi: 10.1038/s41597-023-02877-7. PMID: 38233447; PMCID: PMC10794705.

Valente, E.M.; Abou-Sleiman, P.M.; Caputo, V.; Muqit, M.M.K.; Harvey, K.; Gispert, S.; Ali, Z.; Del Turco, D.; Bentivoglio, A.R.; Healy, D.G.; et al. Hereditary Early-Onset Parkinson's Disease Caused by Mutations in PINK1. Science 2004, 304, 1158–1160.

Van Ballegoij WJC, van de Stadt SIW, Huffnagel IC, Kemp S, Willemse EAJ, Teunissen CE, Engelen M. Plasma NfL and GFAP as biomarkers of spinal cord degeneration in adrenoleukodystrophy. Ann Clin Transl Neurol. 2020 Nov;7(11):2127-2136. doi: 10.1002/acn3.51188. Epub 2020 Oct 13. PMID: 33047897; PMCID: PMC7664277.

Van der Zand, A., Gent, J., Braakman, I., and Tabak, H.F. (2012). Biochemically distinct vesicles from the endoplasmic reticulum fuse to form peroxisomes. Cell 149, 397-409.

Van Geel BM, Poll-The BT, Verrips A, Boelens JJ, Kemp S, Engelen M. Hematopoietic cell transplantation does not prevent myelopathy in X-linked adrenoleukodystrophy: a retrospective study. J Inherit Metab Dis. 2015 Mar;38(2):359-61. doi: 10.1007/s10545-014-9797-1. Epub 2014 Dec 9. PMID: 25488625.

Vanderver A., Wolf Nicole, Genetic and Metabolic Disorders of the White Matter, Swaiman's Pediatric Neurology (Sixth Edition), 2017, Pages 747-758

Vargas CR, Wajner M, Sirtori LR, Goulart L, Chiochetta M, Coelho D, et al. Evidence that oxidative stress is increased in patients with X-linked adrenoleukodystrophy. Biochim Biophys Acta. (2004) 1688:26–32. doi: 10. 1016/j.bbadis.2003.10.004

Vatanen T, Kostic AD, d'Hennezel E, Siljander H, Franzosa EA, Yassour M, Kolde R, Vlamakis H, Arthur TD, Hämäläinen AM, Peet A, Tillmann V, Uibo R, Mokurov S, Dorshakova N, Ilonen J, Virtanen SM, Szabo SJ, Porter JA, Lähdesmäki H, Huttenhower C, Gevers D, Cullen TW, Knip M; DIABIMMUNE Study Group; Xavier RJ. Variation in Microbiome LPS Immunogenicity Contributes to Autoimmunity in Humans. Cell. 2016 May 5;165(4):842-53. doi: 10.1016/j.cell.2016.04.007. Epub 2016 Apr 28. Erratum in: Cell. 2016 Jun 2;165(6):1551. doi: 10.1016/j.cell.2016.05.056. PMID: 27133167; PMCID: PMC4950857.

Vercellino, I., and Sazanov, L. A. (2022). The assembly, regulation and function of the mitochondrial respiratory chain. Nat. Rev. Mol. Cell Bio 23, 141–161. doi:10.1038/ s41580-021-00415-0

Viader, A., Sasaki, Y., Kim, S., Strickland, A., Workman, C.S., Yang, K., Gross, R.W., and Milbrandt, J. (2013). Aberrant Schwann cell lipid metabolism linked to mitochondrial deficits leads to axon degeneration and neuropathy. Neuron 77, 886-898.

Visconti, A., Le Roy, C.I., Rosa, F. et al. Interplay between the human gut microbiome and host metabolism. Nat Commun 10, 4505 (2019). https://doi.org/10.1038/s41467-019-12476-z

Vollmer, W., Joris, B., Charlier, P., and Foster, S. (2008b). Bacterial peptidoglycan (murein) hydrolases. FEMS Microbiol. Rev. 32, 259–286. doi: 10.1111/j.1574-6976.2007.00099.x

Vollmer, W. (2012). Bacterial growth does require peptidoglycan hydrolases. Mol. Microbiol. 86, 1031–1035. doi: 10.1111/mmi.12059

Walker AW, Hoyles L. Human microbiome myths and misconceptions. Nat Microbiol. 2023 Aug;8(8):1392-1396. doi: 10.1038/s41564-023-01426-7. Epub 2023 Jul 31. PMID: 37524974.

Wall, R. et al. in Microbial Endocrinology: The Microbiota-Gut-Brain Axis in Health and Disease Vol. 817 (eds Mark Lyte & John F. Cryan) 221–239 (Springer New York, 2014).

Walsh CJ, Guinane CM, O'Toole PW, Cotter PD. Beneficial modulation of the gut microbiota. FEBS Lett. 2014 Nov 17;588(22):4120-30. doi: 10.1016/j.febslet.2014.03.035. Epub 2014 Mar 26. PMID: 24681100.

Wanders RJA, Waterham HR, Ferdinandusse S. Metabolic Interplay between Peroxisomes and Other Subcellular Organelles Including Mitochondria and the Endoplasmic Reticulum. Front Cell Dev Biol. 2016 Jan 28;3:83. doi: 10.3389/fcell.2015.00083. PMID: 26858947; PMCID: PMC4729952.

Wanders RJA, Baes M, Ribeiro D, Ferdinandusse S, Waterham HR. The physiological functions of human peroxisomes. Physiol Rev. 2023 Jan 1;103(1):957-1024. doi: 10.1152/physrev.00051.2021. Epub 2022 Aug 11. PMID: 35951481.

Wang H-X, Wang Y-P. 2016. Gut microbiota-brain axis. Chin Med J (Engl) 129:2373–2380.

Wang J., H. Tang, C. Zhang, Y. Zhao, M. Derrien, E. Rocher, J. Shen Modulation of gut microbiota during probiotic-mediated attenuation of metabolic syndrome in high fat diet-fed mice. The ISME Journal, 9 (1) (2015), pp. 1-15

Wang S, Ju D, Zeng X. Mechanisms and Clinical Implications of Human Gut Microbiota-Drug Interactions in the Precision Medicine Era. Biomedicines. 2024 Jan 16;12(1):194. doi: 10.3390/biomedicines12010194. PMID: 38255298; PMCID: PMC10813426.

Wang Z, Wu M. An integrated phylogenomic approach toward pinpointing the origin of mitochondria. Sci Rep. 2015 Jan 22;5:7949. doi: 10.1038/srep07949. PMID: 25609566; PMCID: PMC4302308.

Wang X.M., Yik W.Y., Zhang P., Lu W., Dranchak P.K., Shibata D., Steinberg S.J., Hacia J.G. The gene expression profiles of induced pluripotent stem cells from individuals with childhood cerebral adrenoleukodystrophy are consistent with proposed mechanisms of pathogenesis. Stem. Cell. Res. Ther. 2012;3:39. doi: 10.1186/scrt130

Wang Y, Wang Z, Wang Y, Li F, Jia J, Song X, Qin S, Wang R, Jin F, Kitazato K, Wang Y. 2018. The gut-microglia connection: implications for central nervous system diseases. Front Immunol 9:2325. https://doi.org/ 10.3389/fimmu.2018.02325.

Wang Y, Xu E, Musich PR, Lin F. Mitochondrial dysfunction in neurodegenerative diseases and the potential countermeasure. CNS Neurosci Therap. 2019;25:816–24.

Ward JPT. From Physiological Redox Signalling to Oxidant Stress. Adv Exp Med Biol. 2017;967:335-342. doi: 10.1007/978-3-319-63245-2_21. PMID: 29047097.

Wasser CI, Mercieca EC, Kong G, Hannan AJ, McKeown SJ, Glikmann-Johnston Y, Stout JC. Gut dysbiosis in Huntington's disease: associations among gut microbiota, cognitive performance and clinical outcomes. Brain Commun. 2020 Jul 24;2(2):fcaa110. doi: 10.1093/braincomms/fcaa110. PMID: 33005892; PMCID: PMC7519724.

Watanabe M, Houten SM, Wang L, Moschetta A, Mangelsdorf DJ, Heyman RA, Moore DD, Auwerx J. Bile acids lower triglyceride levels via a pathway involving FXR, SHP, and SREBP-1c. J Clin Invest. 2004 May;113(10):1408-18. doi: 10.1172/JCI21025. PMID: 15146238; PMCID: PMC406532.

Watanabe M, Houten SM, Mataki C, Christoffolete MA, Kim BW, Sato H, Messaddeq N, Harney JW, Ezaki O, Kodama T, Schoonjans K, Bianco AC, Auwerx J. Bile acids induce energy expenditure by promoting intracellular thyroid hormone activation. Nature. 2006 Jan 26;439(7075):484-9. doi: 10.1038/nature04330. Epub 2006 Jan 8. PMID: 16400329.

Waterham HR, Ferdinandusse S, Wanders RJ. Human disorders of peroxisome metabolism and biogenesis. Biochim Biophys Acta. 2016 May;1863(5):922-33. doi: 10.1016/j.bbamcr.2015.11.015. Epub 2015 Nov 22. PMID: 26611709.

Weinhofer I, Zierfuss B, Hametner S, Wagner M, Popitsch N, Machacek C, Bartolini B, Zlabinger G, Ohradanova-Repic A, Stockinger H, Köhler W, Höftberger R, Regelsberger G, Forss-Petter S, Lassmann H, Berger J. Impaired plasticity of macrophages in X-linked adrenoleukodystrophy. Brain. 2018 Aug 1;141(8):2329-2342. doi: 10.1093/brain/awy127. PMID: 29860501; PMCID: PMC6061697.

Weinhofer I, Rommer P, Zierfuss B, Altmann P, Foiani M, Heslegrave A, Zetterberg H, Gleiss A, Musolino PL, Gong Y, Forss-Petter S, Berger T, Eichler F, Aubourg P, Köhler W, Berger J. Neurofilament light chain as a potential biomarker for monitoring neurodegeneration in X-linked adrenoleukodystrophy. Nat Commun. 2021 Mar 22;12(1):1816. doi: 10.1038/s41467-021-22114-2. PMID: 33753741; PMCID: PMC7985512.

West AP, Khoury-Hanold W, Staron M, Tal MC, Pineda CM, Lang SM, et al. Mitochondrial DNA stress primes the antiviral innate immune response. Nature. 2015;520:553–7.

White PJ, McGarrah RW, Herman MA, Bain JR, Shah SH, Newgard CB. Insulin action, type 2 diabetes, and branched-chain amino acids: A two-way street. Mol Metab. 2021 Oct;52:101261. doi: 10.1016/j.molmet.2021.101261. Epub 2021 May 24. PMID: 34044180; PMCID: PMC8513145.

Winter SE, Lopez CA, Bäumler AJ. The dynamics of gut-associated microbial communities during inflammation. EMBO Rep. (2013) 14:319–27. doi: 10.1038/embor.2013.27

Wischhusen J, Melero I, Fridman WH. Growth/Differentiation Factor-15 (GDF-15): From Biomarker to Novel Targetable Immune Checkpoint. Front Immunol. 2020 May 19;11:951. doi: 10.3389/fimmu.2020.00951. PMID: 32508832; PMCID: PMC7248355.

Whitcomb, R.W., Linehan, W.M., and Knazek, R.A. (1988). Effects of long-chain, saturated fatty acids on membrane microviscosity and adrenocorticotropin responsiveness of human adrenocortical cells in vitro. J. Clin. Invest. 81, 185-188.

Whiten, D.R.; Cox, D.; Sue, C.M. PINK1 Signalling in Neurodegenerative Disease. Essays Biochem. 2021, 65, 913–923.

Whitt, D.D., and Demoss, R.D. (1975). Effect of Microflora on the Free Amino Acid Distribution in Various Regions of the Mouse Gastrointestinal Tract. Appl. Microbiol. 30, 609–615. https://doi.org/10. 1128/am.30.4.609-615.1975.

Wiedemann N, Pfanner N. Mitochondrial machineries for protein import and assembly. Annu Rev Biochem. 2017;86:685–714.

Wiese M, Bannister AJ. Two genomes, one cell: Mitochondrial-nuclear coordination via epigenetic pathways. Mol Metab. 2020 Aug;38:100942. doi: 10.1016/j.molmet.2020.01.006. Epub 2020 Feb 15. PMID: 32217072; PMCID: PMC7300384.

Wiesinger C., Kunze M., Regelsberger G., Forss-Petter S., Berger J. Impaired very long-chain acyl-CoA beta-oxidation in human X-linked adrenoleukodystrophy fibroblasts is a direct consequence of ABCD1 transporter dysfunction. J. Biol. Chem. 2013;288:19269–19279.

Willems PH, Rossignol R, Dieteren CE, Murphy MP, Koopman WJ. Redox Homeostasis and Mitochondrial Dynamics. Cell Metab. 2015 Aug 4;22(2):207-18. doi: 10.1016/j.cmet.2015.06.006. Epub 2015 Jul 9. PMID: 26166745.

Williams HR, Cox IJ, Walker DG, Cobbold JF, Taylor-Robinson SD, Marshall SE, Orchard TR. Differences in gut microbial metabolism are responsible for reduced hippurate synthesis in Crohn's disease. BMC Gastroenterol. 2010 Sep 17;10:108. doi: 10.1186/1471-230X-10-108. PMID: 20849615; PMCID: PMC2954941.

Wimo A, Guerchet M, Ali G-C, Wu Y-T, Prina AM, Winblad B, Jönsson L, Liu Z, Prince M. 2017. The worldwide costs of dementia 2015 and comparisons with 2010. Alzheimers Dement 13:1–7. https://doi.org/10.1016/ j.jalz.2016.07.150.

Wood, D.E., Lu, J. & Langmead, B. Improved metagenomic analysis with Kraken 2. Genome Biol 20, 257 (2019). https://doi.org/10.1186/s13059-019-1891-0

Woollett LA, Buckley DD, Yao L, Jones PJ, Granholm NA, Tolley EA, Heubi JE. Effect of ursodeoxycholic acid on cholesterol absorption and metabolism in humans. J Lipid Res. 2003 May;44(5):935-42. doi: 10.1194/jlr.M200478-JLR200. Epub 2003 Mar 1. PMID: 12611908.

Wu G, Wu Z, Dai Z, Yang Y, Wang W, Liu C, Wang B, Wang J, Yin Y. Dietary requirements of "nutritionally non-essential amino acids" by animals and humans. Amino Acids. 2013 Apr;44(4):1107-13. doi: 10.1007/s00726-012-1444-2. Epub 2012 Dec 18. PMID: 23247926.

Wu GD, Chen J, Hoffmann C, Bittinger K, Chen YY, Keilbaugh SA, Bewtra M, Knights D, Walters WA, Knight R, Sinha R, Gilroy E, Gupta K, Baldassano R, Nessel L, Li H, Bushman FD, Lewis JD. Linking long-term dietary patterns with gut microbial enterotypes. Science. 2011 Oct 7;334(6052):105-8. doi: 10.1126/science.1208344. Epub 2011 Sep 1. PMID: 21885731; PMCID: PMC3368382.

Wu HJ, Wu E. The role of gut microbiota in immune homeostasis and autoimmunity. Gut Microbes. 2012 Jan-Feb;3(1):4-14. doi: 10.4161/gmic.19320. Epub 2012 Jan 1. PMID: 22356853; PMCID: PMC3337124.

Xu H, Liu M, Cao J, Li X, Fan D, Xia Y, Lu X, Li J, Ju D, Zhao H. The Dynamic Interplay between the Gut Microbiota and Autoimmune Diseases. J Immunol Res. 2019 Oct 27;2019:7546047. doi: 10.1155/2019/7546047. PMID: 31772949; PMCID: PMC6854958.

Xu S, Zhang X, Liu C, Liu Q, Chai H, Luo Y, Li S. Role of Mitochondria in Neurodegenerative Diseases: From an Epigenetic Perspective. Front Cell Dev Biol. 2021 Aug 27;9:688789. doi: 10.3389/fcell.2021.688789. PMID: 34513831; PMCID: PMC8429841.

Xu, W., Yang, H., Liu, Y., Yang, Y., Wang, P., Kim, S. H., et al. (2011). Oncometabolite 2-hydroxyglutarate is a competitive inhibitor of α-ketoglutarate-dependent dioxygenases. Cancer Cell 19, 17–30. doi: 10.1016/j.ccr.2010.12.014

Xue RQ, Zhao M, Wu Q, Yang S, Cui YL, Yu XJ, Liu J, Zang WJ. Regulation of mitochondrial cristae remodelling by acetylcholine alleviates palmitate-induced cardiomyocyte hypertrophy. Free Radic Biol Med. 2019;145:103–17.

Yamamoto Y, Nakanishi Y, Murakami S, Aw W, Tsukimi T, Nozu R, Ueno M, Hioki K, Nakahigashi K, Hirayama A, Sugimoto M, Soga T, Ito M, Tomita M, Fukuda S. A Metabolomic-Based Evaluation of the Role of Commensal Microbiota throughout the Gastrointestinal Tract in Mice. Microorganisms 6: E101, 2018. doi:10.3390/ microorganisms6040101.

Yang D, Zhao D, Ali Shah SZ, Wu W, Lai M, Zhang X, Li J, Guan Z, Zhao H, Li W, Gao H, Zhou X, Yang L. 2019. The role of the gut microbiota in the pathogenesis of Parkinson's disease. Front Neurol 10.

Yang, L., Chu, Z., Liu, M. et al. Amino acid metabolism in immune cells: essential regulators of the effector functions, and promising opportunities to enhance cancer immunotherapy. J Hematol Oncol 16, 59 (2023).

Yang Z, Wang KK. Glial fibrillary acidic protein: from intermediate filament assembly and gliosis to neurobiomarker. Trends Neurosci. 2015 Jun;38(6):364-74. doi: 10.1016/j.tins.2015.04.003. Epub 2015 May 11. PMID: 25975510; PMCID: PMC4559283

Yang Z., S. Huang, D. Zou, D. Dong, X. He, N. Liu, L. Huang.Metabolic shifts and structural changes in the gut microbiota upon branched-chain amino acid supplementation in middle-aged mice Amino Acids, 48 (12) (2016), pp. 2731-2745

Yao, J., Irwin, R. W., Zhao, L., Nilsen, J., Hamilton, R. T., and Brinton, R. D. (2009). Mitochondrial bioenergetic deficit precedes Alzheimer's pathology in female mouse model of Alzheimer's disease. Proc. Natl. Acad. Sci. U.S.A. 106, 14670–14675. doi: 10.1073/pnas.0903563106

Yatsuga S, Fujita Y, Ishii A, Fukumoto Y, Arahata H, Kakuma T, Kojima T, Ito M, Tanaka M, Saiki R, Koga Y. Growth differentiation factor 15 as a useful biomarker for mitochondrial disorders. Ann Neurol. 2015 Nov;78(5):814-23. doi: 10.1002/ana.24506. Epub 2015 Oct 14. PMID: 26463265; PMCID: PMC5057301.

Yi, P., and Li, L. J. (2012). The germfree murine animal: an important animal model for research on the relationship between gut microbiota and the host. Vet. Microbiol. 157, 1–7. doi: 10.1016/j.vetmic.2011. 10.024

Yin W, Wang Y, Liu L, He J. Biofilms: The Microbial "Protective Clothing" in Extreme Environments. Int J Mol Sci. 2019 Jul 12;20(14):3423. doi: 10.3390/ijms20143423. PMID: 31336824; PMCID: PMC6679078.

Yi-Wei Tang, Musa Y. Hindiyeh, Dongyou Liu, Andrew Sails, Paul Spearman, Jing-Ren Zhang,Chapter 1 - Molecular medical microbiology—from bench to bedside, Pages 1-6; Chapter 2- Classification of medically important bacteria, Pages 9-21; Chapter 3 - Bacterial ultrastructure,Pages 23-43; Editor(s): Yi-Wei Tang, Musa Y. Hindiyeh, Dongyou Liu, Andrew Sails, Paul Spearman, Jing-Ren Zhang, Molecular Medical Microbiology (Third Edition), Academic Press, 2024, ISBN 9780128186190, https://doi.org/10.1016/B978-0-12-818619-0.00027-7.

Yu J, Chen T, Guo X, Zafar MI, Li H, Wang Z, Zheng J. The Role of Oxidative Stress and Inflammation in X-Link Adrenoleukodystrophy. Front Nutr. 2022 Apr 8;9:864358. doi: 10.3389/fnut.2022.864358. PMID: 35463999; PMCID: PMC9024313.

Yudkoff M., Brain metabolism of branched-chain amino acids. Glia. 1997 Sep;21(1):92-8. doi: 10.1002/(sici)1098-1136(199709)21:1<92::aid-glia10>3.0.co;2-w. PMID: 9298851.

Zackular, J. P., Baxter, N. T., Chen, G. Y., and Schloss, P. D. (2016). Manipulation of the gut microbiota reveals role in colon tumorigenesis. mSphere 1, e00001–15. doi: 10.1128/mSphere.00001-15

Zarrouk, A., Vejux, A., Nury, T., El Hajj, H.I., Haddad, M., Cherkaoui-Malki, M., Riedinger, J.M., Hammami, M., and Lizard, G. (2012). Induction of mitochondrial changes associated with oxidative stress on very long chain fatty acids (C22:0, C24:0, or C26:0)-treated human neuronal cells (SK-NB-E). Oxid. Med. Cell. Longev. 2012, 623257.

Zeevi D, Korem T, Zmora N, Israeli D, Rothschild D, Weinberger A, Ben-Yacov O, Lador D, Avnit-Sagi T, Lotan-Pompan M, Suez J, Mahdi JA, Matot E, Malka G, Kosower N, Rein M, Zilberman-Schapira G, Dohnalová L, Pevsner-Fischer M, Bikovsky R, Halpern Z, Elinav E, Segal E. Personalized Nutrition by Prediction of Glycemic Responses. Cell. 2015 Nov 19;163(5):1079-1094. doi: 10.1016/j.cell.2015.11.001. PMID: 26590418.

Zeng, X., Xing, X., Gupta, M., Keber, F.C., Lopez, J.G., Lee, Y.J., Roichman, A., Wang, L., Neinast, M.D., Donia, M.S., et al. (2022). Gut bacterial nutrient preferences quantified in vivo. Cell 185, 3441–3456.e19. https://doi.org/10.1016/J.CELL.2022.07.020.

Zernike F., Phase contrast, a new method for the microscopic observation of transparent objects, part I. Phys 9, 9 (1942), pp. 686-698

Zhang H, Chen Y, Wang Z, Xie G, Liu M, Yuan B, Chai H, Wang W, Cheng P. Implications of Gut Microbiota in Neurodegenerative Diseases. Front Immunol. 2022 Feb 14;13:785644. doi: 10.3389/fimmu.2022.785644. PMID: 35237258; PMCID: PMC8882587.

Zhang X, Wu X, Hu Q, Wu J, Wang G, Hong Z, et al. Mitochondrial DNA in liver inflammation and oxidative stress. Life Sci. 2019;236:116464.

Zhang X, Wang L, Li B, Shi J, Xu J, Yuan M. Targeting Mitochondrial Dysfunction in Neurodegenerative Diseases: Expanding the Therapeutic Approaches by Plant-Derived Natural Products. Pharmaceuticals (Basel). 2023 Feb 13;16(2):277. doi: 10.3390/ph16020277. PMID: 37259422; PMCID: PMC9961467.

Zhao G, Nyman M, Jönsson JA. Rapid determination of short-chain fatty acids in colonic contents and faeces of humans and rats by acidified water-extraction and direct-injection gas chromatography. Biomed Chromatogr. 2006 Aug;20(8):674-82. doi: 10.1002/bmc.580. PMID: 16206138.

Zhao H, Gao X, Xi L, Shi Y, Peng L, Wang C, Zou L, Yang Y. 2019. Mo1667 fecal microbiota transplantation for children with autism spectrum disorder. Gastrointest Endoscopy 89:AB512–AB513. https://doi.org/10 .1016/j.gie.2019.03.857

Zhao, H., Patel, V., Helmann, J. D., and Dorr, T. (2017). Don't let sleeping dogmas lie: new views of peptidoglycan synthesis and its regulation. Mol. Microbiol. 106, 847–860. doi: 10.1111/mmi.13853

Zhao, Q. & Elson, C. O. Adaptive immune education by gut microbiota antigens. Immunology 154, 28–37 (2018).

Zhao Y, Cong L, Jaber V, Lukiw WJ. 2017. Microbiome-derived lipopolysaccharide enriched in the perinuclear region of Alzheimer's disease brain. Front Immunol 8:1064.

Zhong F, Liang S, Zhong Z. Emerging role of mitochondrial DNA as a major driver of inflammation and disease progression. Trends Immunol. 2019;40:1120–33

Zhou X, Zhang H, He L, Wu X, Yin Y. Long-Term l-Serine Administration Reduces Food Intake and Improves Oxidative Stress and Sirt1/NFκB Signaling in the Hypothalamus of Aging Mice. Front Endocrinol (Lausanne). 2018 Aug 23;9:476. doi: 10.3389/fendo.2018.00476. PMID: 30190704; PMCID: PMC6115525.

Zhou Y, Smith D, Leong BJ, Brännström K, Almqvist F, Chapman MR. Promiscuous cross-seeding between bacterial amyloids promotes interspecies biofilms. J Biol Chem. 2012 Oct 12;287(42):35092-35103. doi: 10.1074/jbc.M112.383737. Epub 2012 Aug 13. PMID: 22891247; PMCID: PMC3471717.

Zhu Y, Li Y, Zhang Q, Song Y, Wang L, Zhu Z. Interactions Between Intestinal Microbiota and Neural Mitochondria: A New Perspective on Communicating Pathway From Gut to Brain. Front Microbiol. 2022 Feb 24;13:798917. doi: 10.3389/fmicb.2022.798917. PMID: 35283843; PMCID: PMC8908256.

Zhu J, Eichler F, Biffi A, Duncan CN, Williams DA, Majzoub JA. The Changing Face of Adrenoleukodystrophy. Endocr Rev. 2020 Aug 1;41(4):577–93. doi: 10.1210/endrev/bnaa013. PMID: 32364223; PMCID: PMC7286618.

Zhu Y, Li Y, Zhang Q, Song Y, Wang L, Zhu Z. Interactions Between Intestinal Microbiota and Neural Mitochondria: A New Perspective on Communicating Pathway From Gut to Brain. Front Microbiol. 2022 Feb 24;13:798917. doi: 10.3389/fmicb.2022.798917. PMID: 35283843; PMCID: PMC8908256.

Ziabreva, I., Campbell, G., Rist, J., Zambonin, J., Rorbach, J., Wydro, M.M., Lassmann, H., Franklin, R.J., and Mahad, D. (2010). Injury and differentiation following inhibition of mitochondrial respiratory chain complex IV in rat oligodendrocytes. Glia 58, 1827-1837.

APPENDIX 1 – List of significantly different abundant taxa between X-ALD patients and controls

log2 Fold Change	pvalue	padj	Genus	Species
0,518789768	0,00041059	0,02729738	Gordonia	Gordonia iterans
-0,6771453	0,00033782	0,02540983	Shewanella	Shewanella aestuarii
-1,185068615	2,56E-05	0,00653558	Otariodibacter	Otariodibacter oris
-1,113422707	0,00045854	0,02776174	Methylotenera	Methylotenera versatilis
0,656620209	0,00021984	0,01994188	Thioalkalivibrio	Thioalkalivibrio versutus
0,412988575	0,00053788	0,02868873	Opitutus	Opitutus terrae
-1,079275937	0,00010441	0,01405622	Acinetobacter	Acinetobacter ursingii
-0,749024082	0,00026692	0,02226013	Chryseobacterium	Chryseobacterium joostei
0,509392323	0,00033513	0,02540983	Kyrpidia	NA
-0,709243012	0,00081306	0,03492186	Chryseobacterium	Chryseobacterium taihuense
-0,805247892	0,00039513	0,02729738	Kangiella	Kangiella sediminilitoris
-0,776912725	0,00092186	0,03662211	Sulfurimonas	Sulfurimonas gotlandica
-0,5420428	0,0018322	0,04954334	Nostoc	NA
0,356819943	0,00078365	0,03486539	Propionibacterium	Propionibacterium australiense
-0,80225158	5,13E-05	0,01038049	Kordia	Kordia antarctica
-0,487091763	0,00167445	0,04669	Caldicellulosiruptor	Caldicellulosiruptor changbaiensis
-0,726022848	0,00053601	0,02868873	Weissella	Weissella paramesenteroides
-0,69692762	0,00167879	0,04669	Gramella	Gramella sp. MAR_2010_147
-0,796792498	0,00126624	0,04166486	Providencia	Providencia alcalifaciens
-0,537974301	0,00077633	0,03486539	Staphylococcus	Staphylococcus haemolyticus
0,78129225	0,00030013	0,02379541	Streptococcus	NA
1,973013984	4,19E-05	0,00909498	Streptococcus	Streptococcus salivarius
0,663386774	0,0010465	0,03910728	Streptococcus	Streptococcus mutans
2,439585642	4,00E-05	0,00901827	Streptococcus	Streptococcus sp. HSISS1
2,230996406	5,17E-08	0,00010104	Streptococcus	Streptococcus sp. HSISS2
2,06048486	2,60E-07	0,00030522	Streptococcus	Streptococcus sp. HSISS3
-0,979527207	8,32E-05	0,01272219	Chryseobacterium	Chryseobacterium gallinarum
1,255618724	1,99E-05	0,00649035	Streptococcus	Streptococcus equinus
1,16201984	9,54E-07	0,00093289	Gordonibacter	Gordonibacter urolithinfaciens
-0,616425896	0,00157948	0,04564925	Polaribacter	Polaribacter sp. Hel1_33_78
2,77147411	4,24E-11	2,49E-07	Streptococcus	Streptococcus vestibularis
-0,952221719	0,00042931	0,02764147	Planococcus	Planococcus kocurii
-0,383512105	0,00093007	0,03662211	Bacillus	Bacillus circulans
1,407498406	0,00016397	0,01738733	Anaplasma	Anaplasma ovis

log2 Fold Change	pvalue	padj	Genus	Species
-0,470422043	0,00166649	0,04669	Hyphomicrobium	Hyphomicrobium nitrativorans
-0,877703298	0,00135666	0,04243813	Mannheimia	Mannheimia sp. USDA-ARS-USMARC-1261
-0,998370148	1,73E-05	0,0059586	Salegentibacter	Salegentibacter salegens
0,867629407	0,00141577	0,04326196	Streptococcus	Streptococcus gwangjuense
-1,367705075	0,00082729	0,03492186	Myroides	Myroides sp. ZB35
-0,930992263	0,00027881	0,02240831	Basilea	Basilea psittacipulmonis
-0,708101839	0,00186078	0,04954334	Candidatus Izimaplasma	Candidatus Izimaplasma sp. HR1
-0,934901616	2,19E-05	0,00653558	Mucilaginibacter	Mucilaginibacter gotjawali
0,370339956	0,00011611	0,01405622	Desulfotomaculum	Desulfotomaculum ruminis
-0,778488392	0,00150579	0,04520592	Neptunomonas	Neptunomonas phycophila
-0,80576964	0,00016018	0,01738733	Pseudomonas	Pseudomonas sp. S35
-0,925422287	4,76E-05	0,00997937	Sulfurospirillum	Sulfurospirillum sp. UCH001
0,659674138	0,00156387	0,04564925	Ligilactobacillus	Ligilactobacillus agilis
0,495422591	0,00126418	0,04166486	Novosphingobium	Novosphingobium sp. P6W
-1,138047211	0,00062796	0,03019847	Mycoplasma	Mycoplasma tullyi
-0,554835918	7,78E-05	0,01234248	Listeria	Listeria grayi
-0,682220661	0,00016596	0,01738733	Weissella	Weissella koreensis
0,371486562	0,00078842	0,03486539	Actinomyces	NA
0,880519456	8,89E-05	0,01288499	Schaalia	Schaalia odontolytica
0,496057431	0,00089029	0,03652675	Mycobacterium	Mycobacterium sp. YC-RL4
-0,650512899	4,81E-06	0,00224757	Paenibacillus	Paenibacillus crassostreae
-1,405256385	0,00090407	0,03658074	Candidatus Hoaglandella	Candidatus Hoaglandella endobia
0,701529517	0,00022093	0,01994188	Mycobacterium	Mycobacterium xenopi
-0,769423798	0,00152334	0,04520592	Formosa	Formosa sp. Hel1_31_208
-0,614543746	0,00136822	0,04247276	Campylobacter	Campylobacter hepaticus
0,52107013	0,00027364	0,02229805	Streptomyces	Streptomyces nigra
2,155438683	1,58E-05	0,00581195	Streptococcus	Streptococcus sp. FDAARGOS_192
-0,490995795	0,00162274	0,04634931	Anaerocolumna	NA
0,425174713	0,00104503	0,03910728	Desulfovibrio	Desulfovibrio magneticus
-0,63880096	0,00052797	0,02868169	Pseudobutyrivibrio	Pseudobutyrivibrio xylanivorans
-0,534133508	0,00056523	0,02960917	Butyrivibrio	Butyrivibrio hungatei
-0,574487268	0,00087479	0,03639992	Sneathia	Sneathia amnii
0,316812413	0,00154555	0,04556661	Micromonospora	NA
0,477598433	0,00024399	0,0210515	Halomonas	Halomonas sp. 1513
-0,887329382	0,00131559	0,04207271	Bacillus	Bacillus wiedmannii

log2 Fold Change	pvalue	padj	Genus	Species
-0,957550662	0,00035331	0,02607178	Vibrio	Vibrio aphrogenes
-0,542145599	0,00046041	0,02776174	Macrococcus	Macrococcus sp. IME1552
0,813827359	0,00098584	0,03804725	Plantibacter	NA
-0,91340368	0,00092924	0,03662211	Staphylococcus	Staphylococcus sp. MI 10-1553
-0,79487516	0,0019003	0,04954334	Gramella	Gramella salexigens
0,307504825	0,0005553	0,02935091	Azospirillum	Azospirillum brasilense
-1,31436667	0,00011157	0,01405622	Candidatus Mancarchaeum	Candidatus Mancarchaeum acidiphilum
0,550679848	0,00082736	0,03492186	Streptomyces	Streptomyces vinaceus
-0,505180589	0,00135987	0,04243813	Calothrix	Calothrix parasitica
0,520503525	0,00017683	0,01820114	Cryobacterium	Cryobacterium sp. LW097
-0,565879736	0,00088645	0,03652675	Sulfurimonas	Sulfurimonas autotrophica
-0,722448786	0,00127726	0,04166486	Acinetobacter	Acinetobacter baylyi
0,422812841	0,00127828	0,04166486	Eubacterium	Eubacterium maltosivorans
-0,733759028	0,00185486	0,04954334	Changchengzhania	Changchengzhania lutea
1,190780184	0,0001245	0,01405622	Citrobacter	Citrobacter freundii complex sp. CFNIH2
-0,815027918	7,76E-05	0,01234248	Aureitalea	Aureitalea sp. RR4-38
0,423379762	0,00086767	0,03636143	Nissabacter	Nissabacter sp. SGAir0207
0,664856809	0,00108756	0,03963171	Klebsiella	Klebsiella huaxiensis
-0,449288546	0,00132319	0,04207271	Lysinibacillus	Lysinibacillus sp. 2017
-0,392985574	0,00078453	0,03486539	Clostridium	Clostridium carboxidivorans
-0,595548394	0,00121195	0,04162997	Flavobacterium	Flavobacterium pallidum
-0,747927835	0,00045603	0,02776174	Flavobacterium	Flavobacterium crocinum
0,499639733	0,00043338	0,02764147	Streptomyces	Streptomyces sp. WAC 01438
0,521618223	0,0012891	0,04169082	Cryobacterium	Cryobacterium soli
-0,640851951	0,00189287	0,04954334	Runella	Runella sp. SP2
-0,592087478	0,00050196	0,02778298	Lactobacillus	Lactobacillus terrae
-1,128267698	0,00126638	0,04166486	Saccharolobus	Saccharolobus solfataricus
-1,598173741	0,00060167	0,0299638	Candidatus Phytoplasma	Candidatus Phytoplasma Aster yellows witches'-broom phytoplasma
-0,704949659	0,00111752	0,04006754	Arachidicoccus	Arachidicoccus soli
-0,858070761	0,00138774	0,0428519	Tenacibaculum	Tenacibaculum sp. DSM 106434
-0,593227909	0,00129329	0,04169082	Flavobacterium	NA
-0,685947867	0,00062344	0,03019847	Cloacibacterium	Cloacibacterium normanense
0,374382293	0,0009922	0,03804725	Pseudonocardia	Pseudonocardia dioxanivorans
0,905060552	3,78E-05	0,0088788	Serratia	Serratia sp. FDAARGOS_506
-1,253492124	2,12E-06	0,00143774	Ichthyobacterium	Ichthyobacterium seriolicida

log2 Fold Change	pvalue	padj	Genus	Species
-1,560382301	0,00039354	0,02729738	Serratia	Serratia sp. 3ACOL1
-0,884931471	0,00113149	0,04006754	Vibrio	Vibrio sp. HBUAS61001
-0,830762299	6,90E-05	0,01234248	Chryseobacterium	Chryseobacterium gleum
-0,59384858	0,00167915	0,04669	Apibacter	Apibacter raozihei
0,304271145	0,00179593	0,04946812	Caproiciproducens	Caproiciproducens sp. NJN-50
-0,693286786	0,00049211	0,02776174	Muriicola	Muriicola sp. MMS17-SY002
-0,699771282	0,00107509	0,03963171	Arachidicoccus	Arachidicoccus sp. B3-10
-0,702262657	0,00156848	0,04564925	Acinetobacter	Acinetobacter sp. 10FS3-1
0,990065378	0,00079037	0,03486539	Brevundimonas	Brevundimonas sp. SGAir0440
0,7375128	0,0003216	0,02482632	Plantibacter	Plantibacter sp. M259
1,299061086	0,00185446	0,04954334	Sutterella	Sutterella faecalis
0,524839324	0,00045039	0,02776174	Georgenia	Georgenia sp. Z294
0,409477082	0,00189845	0,04954334	Paracoccus	Paracoccus sp. AK26
1,177389899	0,00117018	0,04095892	Streptococcus	Streptococcus sp. KS 6
0,442949786	0,00010565	0,01405622	Hypericibacter	Hypericibacter terrae
0,509016601	0,00026938	0,02226013	Flintibacter	Flintibacter sp. KGMB00164
-0,846550357	2,61E-06	0,00152975	Francisella	Francisella tularensis
0,450772893	0,00133382	0,04207271	Hydrogenophaga	Hydrogenophaga sp. BPS33
0,473165578	0,00122754	0,04162997	Paracoccus	Paracoccus denitrificans
0,54317505	0,00038074	0,02729738	Streptomyces	Streptomyces sp. SYP-A7193
-1,041370443	2,21E-06	0,00143774	Sphingobacterium	Sphingobacterium sp. dk4302
-0,459302019	0,00082414	0,03492186	Gracilibacillus	Gracilibacillus sp. SCU50
0,837222572	1,33E-05	0,00521387	Corynebacterium	Corynebacterium sp. 2019
-0,72771751	0,00104096	0,03910728	Winogradskyella	Winogradskyella schleiferi
-1,28015048	1,23E-06	0,00102887	Algibacter	Algibacter sp. L3A6
0,435688255	0,00026619	0,02226013	Eggerthella	Eggerthella sp. HF-1101
0,562988232	0,0004866	0,02776174	Lysobacter	Lysobacter oculi
0,454363007	0,00044077	0,02776174	Thermus	NA
-0,812984853	0,00022792	0,02026095	Legionella	Legionella sp. TUM19329
0,418422695	0,00157881	0,04564925	Salinibacterium	Salinibacterium sp. ZJ450
0,729909463	0,00019006	0,01872191	Saccharopolyspora	Saccharopolyspora sp. ASAGF58
0,597202691	2,43E-05	0,00653558	Trueperella	Trueperella sp. 19M2397
-1,035694018	6,59E-06	0,00276323	Flavobacterium	Flavobacterium sp. I3-2
-0,96858295	0,00068426	0,03237545	Bdellovibrio	Bdellovibrio sp. KM01
1,0567734	7,27E-05	0,01234248	Streptomyces	Streptomyces sp. CB00271

log2 Fold Change	pvalue	padj	Genus	Species
-0,916827485	0,00047829	0,02776174	Mannheimia	Mannheimia sp. ZY190616
1,673985593	3,26E-06	0,00173706	Bifidobacterium	Bifidobacterium animalis
-0,694722659	0,0004643	0,02776174	Candidatus Amoebophilus	Candidatus Amoebophilus asiaticus
-0,778692237	0,00125733	0,04166486	Vibrio	Vibrio metschnikovii
-0,720047927	0,00031312	0,02449418	Arcobacter	Arcobacter nitrofigilis
-2,211734882	1,39E-08	4,07E-05	Pseudomonas	Pseudomonas aeruginosa
-0,811087691	0,0004735	0,02776174	Hydrogenovibrio	Hydrogenovibrio marinus
-0,406784222	0,00052769	0,02868169	Dolosigranulum	Dolosigranulum pigrum
-1,801158047	0,00162327	0,04634931	Moraxella	Moraxella ovis
0,368788956	0,00060736	0,0299638	Desulfovibrio	Desulfovibrio carbinolicus
-1,441039369	2,39E-07	0,00030522	Pseudoalteromonas	Pseudoalteromonas spongiae
-0,650425236	6,79E-05	0,01234248	Alkalihalobacillus	Alkalihalobacillus lehensis
-0,663269665	0,00100729	0,038375	Staphylococcus	Staphylococcus simiae
-0,843725422	0,00019146	0,01872191	Croceibacter	Croceibacter atlanticus
-1,348557103	2,68E-05	0,00654051	Dokdonia	Dokdonia sp. MED134
-0,783207953	0,00122405	0,04162997	Maribacter	Maribacter sp. HTCC2170
-0,782454242	0,00081403	0,03492186	Sulfurimonas	Sulfurimonas paralvinellae
-1,054263627	0,00048893	0,02776174	Dokdonia	NA
-0,760214303	0,0012483	0,04166486	Nonlabens	Nonlabens dokdonensis
1,393906722	0,00096857	0,03788395	Alistipes	Alistipes onderdonkii
-0,794885528	0,00057153	0,02967429	Desulfurella	Desulfurella acetivorans
-0,776178219	0,00092079	0,03662211	Providencia	Providencia vermicola
-0,696381466	0,00140706	0,04322095	Candidatus Sulcia	Candidatus Sulcia muelleri
0,585079311	0,00178265	0,04933405	Streptomyces	Streptomyces subrutilus
-1,252126002	7,78E-05	0,01234248	Phocaeicola	Phocaeicola salanitronis
-0,680583815	0,00106366	0,03949689	Marinomonas	Marinomonas arctica
0,674071454	0,00132744	0,04207271	Coraliomargarita	Coraliomargarita akajimensis
0,433211401	0,00190844	0,04954334	Mycolicibacterium	Mycolicibacterium duvalii
-1,183824149	0,00112651	0,04006754	Methylacidiphilum	Methylacidiphilum kamchatkense
0,312478678	0,0016686	0,04669	Aminipila	Aminipila butyrica
-0,687497952	0,00081493	0,03492186	Pseudoalteromonas	Pseudoalteromonas piscicida
1,12225789	0,00043344	0,02764147	Rothia	Rothia mucilaginosa
-0,527369583	0,00152561	0,04520592	Nitrosomonas	Nitrosomonas communis
-0,81065574	0,00117361	0,04095892	Capnocytophaga	Capnocytophaga haemolytica
-0,803798364	0,00144637	0,04396811	Borrelia	Borrelia miyamotoi

log2 Fold Change	pvalue	padj	Genus	Species
-0,843469822	0,00020363	0,01926885	Calditerrivibrio	Calditerrivibrio nitroreducens
0,450067237	0,00023404	0,02049459	Micromonospora	Micromonospora carbonacea
-1,166294966	4,98E-06	0,00224757	Myroides	Myroides profundi
-0,788574507	0,00011097	0,01405622	Zygosaccharomyces	Zygosaccharomyces rouxii
-1,800920309	0,00072752	0,03412254	Sphingobium	Sphingobium sp. RSMS
-0,911093969	0,00018232	0,01844307	Vibrio	Vibrio tapetis
0,575944295	0,00108519	0,03963171	Schaalia	Schaalia meyeri
-0,583301258	0,00183205	0,04954334	Planobacterium	Planobacterium Chryseobacterium taklimakanense
0,810118548	0,0016274	0,04634931	Actinomyces	Actinomyces oris
1,163823082	2,40E-05	0,00653558	Citrobacter	Citrobacter koseri
1,98373788	9,00E-05	0,01288499	Escherichia	NA
2,103600991	2,45E-05	0,00653558	Escherichia	Escherichia coli
-0,821411135	0,00041409	0,02729738	Candidatus Planktophila	Candidatus Planktophila limnetica
-0,669866926	0,00090262	0,03658074	Proteus	NA
-0,500503918	0,00190407	0,04954334	Plasmodium	Plasmodium vivax
0,587346976	0,00012153	0,01405622	Sanguibacter	Sanguibacter keddieii
-0,705951471	0,00050068	0,02778298	Staphylococcus	Staphylococcus succinus
0,642710297	0,00016055	0,01738733	Dehalococcoides	Dehalococcoides mccartyi
2,189444541	0,00012458	0,01405622	Shigella	NA
-0,799202746	0,00040362	0,02729738	Xenorhabdus	Xenorhabdus nematophila
0,994417906	0,00012402	0,01405622	Desulfovibrio	Desulfovibrio sp. G11
0,465392284	0,00060775	0,0299638	Altererythrobacter	Altererythrobacter namhicola
-0,539681682	0,00065005	0,03100707	Aliivibrio	Aliivibrio fischeri
-0,656770906	0,00059856	0,0299638	Vibrio	Vibrio mimicus
0,53058609	0,00040966	0,02729738	Streptomyces	Streptomyces katrae
-1,701758124	0,00111762	0,04006754	Cyclobacterium	NA
-0,577366618	0,0018675	0,04954334	Flavobacterium	Flavobacterium haoranii
-0,349077804	0,00117983	0,04095892	Cellulosilyticum	NA
-0,729452095	7,34E-05	0,01234248	Macrococcus	Macrococcus caseolyticus
0,730469422	0,00184647	0,04954334	Actinomyces	Actinomyces sp. oral taxon 169
0,411130268	0,00152407	0,04520592	Actinomyces	Actinomyces sp. oral taxon 414
1,028233093	0,00073637	0,03412254	Streptococcus	Streptococcus sp. oral taxon 061
1,108496445	0,00074445	0,03412254	Streptococcus	Streptococcus sp. oral taxon 431
-0,905314474	0,00020783	0,01935476	Candidatus Atelocyanobacterium	Candidatus Atelocyanobacterium thalassa
-0,75879845	0,00074175	0,03412254	Rodentibacter	Rodentibacter pneumotropicus

log2 Fold Change	pvalue	padj	Genus	Species
0,432066514	0,0003555	0,02607178	Mycolicibacterium	Mycolicibacterium litorale
-0,692796492	0,00098388	0,03804725	Siansivirga	Siansivirga zeaxanthinifaciens
-0,830909388	0,00020341	0,01926885	Cellulophaga	Cellulophaga baltica
1,109059454	0,00059587	0,0299638	Rickettsia	Rickettsia prowazekii
0,750104817	0,00059891	0,0299638	Pseudomonas	Pseudomonas migulae
0,51544897	0,00047393	0,02776174	Thermanaerovibrio	Thermanaerovibrio acidaminovorans
0,980624513	0,00011068	0,01405622	Campylobacter	Campylobacter gracilis
-0,519539097	0,00113366	0,04006754	Butyrivibrio	NA
1,263612896	7,11E-05	0,01234248	Eggerthella	Eggerthella lenta
-0,426166655	0,00121345	0,04162997	Plasmodium	Plasmodium relictum
-0,557858927	0,00185768	0,04954334	Microbacterium	Microbacterium sp. LKL04
-0,737014049	0,0001216	0,01405622	Flavobacterium	Flavobacterium sp. Sr18
-1,022950444	0,000622	0,03019847	Halobacteriovorax	Halobacteriovorax marinus
-1,634267614	8,46E-05	0,01272219	Ferroplasma	Ferroplasma acidarmanus
-0,510443847	0,00151105	0,04520592	Cytophaga	Cytophaga hutchinsonii
-0,688338564	0,00040997	0,02729738	Staphylococcus	Staphylococcus agnetis
-0,729321161	0,00038451	0,02729738	Flavobacterium	Flavobacterium columnare

APPENDIX 2 – List of significantly different abundant functions between X-ALD patients and controls

log2 Fold Change	pvalue	padj	Subsystem3
2,221068885	1,06E-08	9,66E-06	Mediator of hyperadherence YidE in Enterobacteria and its conserved region
3,859631018	3,00E-08	1,37E-05	Colonization factor antigen I fimbriae
1,136160537	5,78E-08	1,75E-05	D-Sorbitol(D-Glucitol) and L-Sorbose Utilization
2,300518878	1,10E-07	2,51E-05	Commensurate regulon activation
-0,249887655	1,64E-07	2,99E-05	At3g21300
1,72674433	1,20E-06	0,00013698	Type 4 secretion and conjugative transfer
1,149806949	9,33E-07	0,00013698	Unknown carbohydrate utilization (cluster Yeg)
1,541781063	1,12E-06	0,00013698	Glyoxylate bypass
2,020771208	1,78E-06	0,00018004	Biogenesis of cytochrome c oxidases
1,507639414	2,11E-06	0,00019232	Siderophore assembly kit
0,979118811	2,66E-06	0,00022016	Orphan regulatory proteins
1,573848375	3,76E-06	0,00028562	Ferrous iron transporter EfeUOB, low-pH-induced
1,497565258	4,27E-06	0,00029937	Small multidrug resistance strays
0,959363778	5,18E-06	0,00033688	Unknown carbohydrate utilization (cluster Ydj)
1,048746414	5,59E-06	0,00033954	Regulation of Oxidative Stress Response
1,876742653	6,04E-06	0,00034376	D-galactonate catabolism
1,81614149	7,47E-06	0,00037795	Two partner secretion pathway (TPS)
1,342867001	7,30E-06	0,00037795	Putrescine utilization pathways
1,297900859	9,90E-06	0,00047476	Universal stress protein family
2,040591733	1,12E-05	0,00050922	Carnitine Metabolism in Microorganisms
0,47254288	1,26E-05	0,0005475	Mannitol Utilization
1,245875783	1,36E-05	0,0005648	A Gammaproteobacteria Cluster Relating to Translation
1,271193934	2,04E-05	0,00079275	Lipid A modifications
2,195103692	2,09E-05	0,00079275	Siderophore Yersiniabactin Biosynthesis
1,259901892	2,51E-05	0,00091641	Phosphoglycerate transport system
0,853533614	2,66E-05	0,00093242	Tolerance to colicin E2
1,242884446	3,02E-05	0,00101945	Late competence
-0,138219912	3,14E-05	0,00102209	Translation termination factors bacterial
-0,188420088	3,75E-05	0,00114579	Glycine cleavage system
1,635596273	3,77E-05	0,00114579	Single-Rhodanese-domain proteins
1,919287498	4,64E-05	0,00136288	Tellurite resistance: Chromosomal determinants
2,454342841	5,52E-05	0,00156871	Type 1 pili (mannose-sensitive fimbriae)
1,615629971	5,68E-05	0,00156871	CBSS-211586.1.peg.3133
1,954309346	6,57E-05	0,00176122	CytR regulation

log2 Fold Change	pvalue	padj	Subsystem3
2,514322191	6,89E-05	0,00179325	CBSS-194948.1.peg.143
-0,145425069	8,06E-05	0,00204057	Ribosomal protein S12p Asp methylthiotransferase
0,668668289	9,52E-05	0,00234448	Putative sugar ABC transporter (ytf cluster)
1,960020107	0,00010568	0,00252037	Intracellular septation in Enterobacteria
0,92850287	0,0001079	0,00252037	Molybdopterin cytosine dinucleotide
1,112013775	0,00012755	0,00290485	Streptococcus pyogenes Virulome
2,143614166	0,00013253	0,00294478	Biofilm Adhesin Biosynthesis
1,804889246	0,00014175	0,00305951	CBSS-196620.1.peg.2477
0,676395956	0,00014467	0,00305951	RNA 3'-terminal phosphate cyclase
2,024777019	0,00014777	0,00305951	RNA processing orphans
0,704253214	0,00015579	0,00315385	Putative oxidase COG2907
1,838575728	0,00018865	0,00369251	CBSS-269801.1.peg.2186
1,363862348	0,0001905	0,00369251	Formate dehydrogenase
-0,216895277	0,00020272	0,00384739	Cysteine Biosynthesis, MCB 432
1,489172435	0,00022149	0,00411797	carbazol degradation cluster
-0,173876385	0,00022979	0,00418684	TenI-like tautomerase
-0,095693891	0,00023655	0,00422552	Heat shock dnaK gene cluster extended
-0,12205966	0,00024543	0,00429979	tRNA aminoacylation, Phe
-0,13666459	0,00027355	0,00470197	Bacterial Cell Division
2,066176537	0,00029634	0,0049744	Unknown carbohydrate utilization containing Fructose-bisphosphate aldolase
0,810175052	0,00030032	0,0049744	CBSS-211586.1.peg.2357
-0,125606872	0,00031722	0,00516052	RP Bacterial Cell Division
1,085971	0,00034218	0,0054689	Beta-lactamase cluster in Streptococcus
-0,130363001	0,00036148	0,00558153	tRNA aminoacylation, Glu and Gln
-0,218859074	0,00035867	0,00558153	Mycobacterium virulence operon possibly involved in quinolinate biosynthesis
2,018302422	0,00037843	0,00571769	Capsular Polysaccharide (CPS) of Campylobacter
0,559121857	0,00038285	0,00571769	Adaptation to d-cysteine
0,369712515	0,00041017	0,00598215	Type VI secretion systems
-0,474128327	0,00041369	0,00598215	Flagellar motility
-0,157839005	0,0004305	0,00612788	Serine Biosynthesis
-0,16928254	0,00046754	0,0065528	F0F1-type ATP synthase
0,609470179	0,00053603	0,00739888	Ubiquinone Biosynthesis
1,192377131	0,00060551	0,00823311	SeqA and Co-occurring Genes
1,037190321	0,00062503	0,0083735	Coenzyme PQQ synthesis
2,185842809	0,000637	0,00841027	The fimbrial Stf cluster
1,182866647	0,00073658	0,00958604	Competence in Streptococci

log2 Fold Change	pvalue	padj	Subsystem3
0,629586261	0,00077209	0,00990666	Lipopolysaccharide assembly
1,096269591	0,00079435	0,01005072	Phospholipid and Fatty acid biosynthesis related cluster
-0,121457417	0,00081124	0,01012388	Single-copy ribosomal proteins
-0,088032669	0,00083545	0,01028501	Competence or DNA damage-inducible protein CinA and related protein families
3,571801853	0,0009314	0,01116449	β-Fimbriae
2,375375637	0,00092029	0,01116449	Lysozyme inhibitors
0,862982111	0,00104126	0,01231938	Phd-Doc, YdcE-YdcD toxin-antitoxin (programmed cell death) systems
-0,113338735	0,00106098	0,01239168	UDP-N-acetylmuramate from Fructose-6-phosphate Biosynthesis
0,831817325	0,0011818	0,01362816	Benzoate degradation
-0,105932213	0,0012206	0,01389953	DNA repair, UvrABC system
-0,165755597	0,00130989	0,01473218	Methylthiotransferases
-0,103866839	0,00133958	0,01488236	Glutamine, Glutamate, Aspartate and Asparagine Biosynthesis
1,670496491	0,00148816	0,01613943	Iron acquisition in Vibrio
0,727054973	0,00147493	0,01613943	Tagatose utilization
1,582459687	0,00154333	0,0165409	Curli production
-0,128188303	0,00156962	0,01662701	tRNA aminoacylation, Ile
-0,176006351	0,00164234	0,01707944	Glycogen metabolism
-0,117948484	0,00164983	0,01707944	Methionine Biosynthesis
0,489459501	0,00167685	0,01716421	Autoinducer 2 (AI-2) transport and processing (lsrACDBFGE operon)
-0,18859898	0,00184865	0,01850681	Adenosyl nucleosidases
0,469978912	0,00183773	0,01850681	Lysine degradation
2,462962835	0,0019614	0,01900887	P uptake (cyanobacteria)
-0,06789874	0,00193625	0,01900887	Pyridoxin (Vitamin B6) Biosynthesis
1,258951122	0,00194875	0,01900887	Quorum sensing in Yersinia
-0,165565509	0,00221791	0,02126855	CarD
0,536626113	0,00224574	0,02131112	Khodge314 Isoleucine Biosynthesis
-0,088564905	0,00247967	0,02305082	Transcription factors bacterial
0,773167638	0,00246237	0,02305082	Integrons
-0,141408325	0,00253018	0,02328281	coA-FolK
-0,118705165	0,0025644	0,02336172	Universal GTPases
0,863334013	0,00289988	0,02615637	trimethylamine N-oxide (TMAO) reductase
-0,141230959	0,00324751	0,02892173	Leucine Biosynthesis
0,831878668	0,00326996	0,02892173	Nitric oxide synthase
0,529308383	0,00333179	0,02918522	Fructose and Mannose Inducible PTS
0,885150621	0,00345016	0,02993427	Sulfur oxidation
-0,076284514	0,00362831	0,03118297	Protein chaperones
-0,145127037	0,00366498	0,03120368	tRNA aminoacylation, Arg

log2 Fold Change	pvalue	padj	Subsystem3
0,321280882	0,00387035	0,03234759	EC 3.4.19.- Omega peptidases
-0,143935025	0,00386658	0,03234759	Glycolysis and Gluconeogenesis
-0,088144289	0,00408005	0,03379026	Glutamine synthetases
-0,138814207	0,00439109	0,03450977	Branched-Chain Amino Acid Biosynthesis
0,617734841	0,00440719	0,03450977	Citrate Metabolism KE2
-0,112137736	0,00441621	0,03450977	De Novo Purine Biosynthesis
0,467393665	0,00427854	0,03450977	Homogentisate pathway of aromatic compound degradation
0,353760516	0,00430628	0,03450977	L-Cystine Uptake and Metabolism
-0,111358639	0,0044321	0,03450977	Ribonuclease H
1,455584782	0,00422592	0,03450977	Streptococcal Mga Regulon
-0,114776959	0,00454965	0,03482964	Ribosome biogenesis bacterial
-0,256248984	0,00452019	0,03482964	Sporulation-associated proteins with broader functions
-0,144766266	0,0046349	0,03518664	t(6)A synthesis in bacteria
1,118060949	0,00510611	0,03844352	Alpha-acetolactate operon
-0,18420901	0,00623387	0,04423664	dcernst CoA Salvage
-0,125343678	0,00596788	0,04423664	tRNA aminoacylation, Asp and Asn
0,522197668	0,00616666	0,04423664	Carotenoids
-0,094081113	0,00614307	0,04423664	Folate Biosynthesis
0,535084501	0,00602275	0,04423664	Osmotic stress cluster
-0,09361276	0,00600264	0,04423664	Polyadenylation bacterial
-0,146917951	0,00626403	0,04423664	Proline Synthesis
-0,094477313	0,00622914	0,04423664	Proteolysis in bacteria, ATP-dependent
-0,114677466	0,00645873	0,04440552	tRNA aminoacylation, Trp
1,301897086	0,00653166	0,04440552	Chlorobenzoate degradation
0,331296576	0,00649192	0,04440552	Dissimilatory nitrite reductase
1,448349615	0,00648884	0,04440552	Selenoprotein O
-0,128137709	0,00643088	0,04440552	At5g63290
0,3885961	0,00682304	0,04537072	Transport of Nickel and Cobalt
0,38367684	0,00676993	0,04537072	Nitrate and nitrite ammonification
-0,128143245	0,00682092	0,04537072	NusA-TFII Cluster
0,399532141	0,0068899	0,04548332	Bacterial hemoglobins
-0,122466914	0,007032	0,04608744	tRNA processing
-0,10440731	0,00728299	0,04739146	Alanine biosynthesis
-0,14709649	0,00743995	0,0480695	tRNA nucleotidyltransferase
0,48214664	0,0074931	0,04807195	Glycerol fermentation to 1,3-propanediol
-0,087263525	0,00757727	0,04827199	Translation initiation factors bacterial
-0,100312564	0,00778307	0,04923874	Threonine and Homoserine Biosynthesis

APPENDIX 3 – Related academic work

Launay N, Lopez-Erauskin J, Bianchi P, Guha S, Parameswaran J, Coppa A, **Torreni L**, Schlüter A, Fourcade S, Paredes-Fuentes AJ, Artuch R, Casasnovas C, Ruiz M, Pujol A. **Imbalanced mitochondrial dynamics contributes to the pathogenesis of X-linked adrenoleukodystrophy.** Brain. 2024 Jun 3;147(6):2069-2084. doi: 10.1093/brain/awae038. PMID: 38763511.